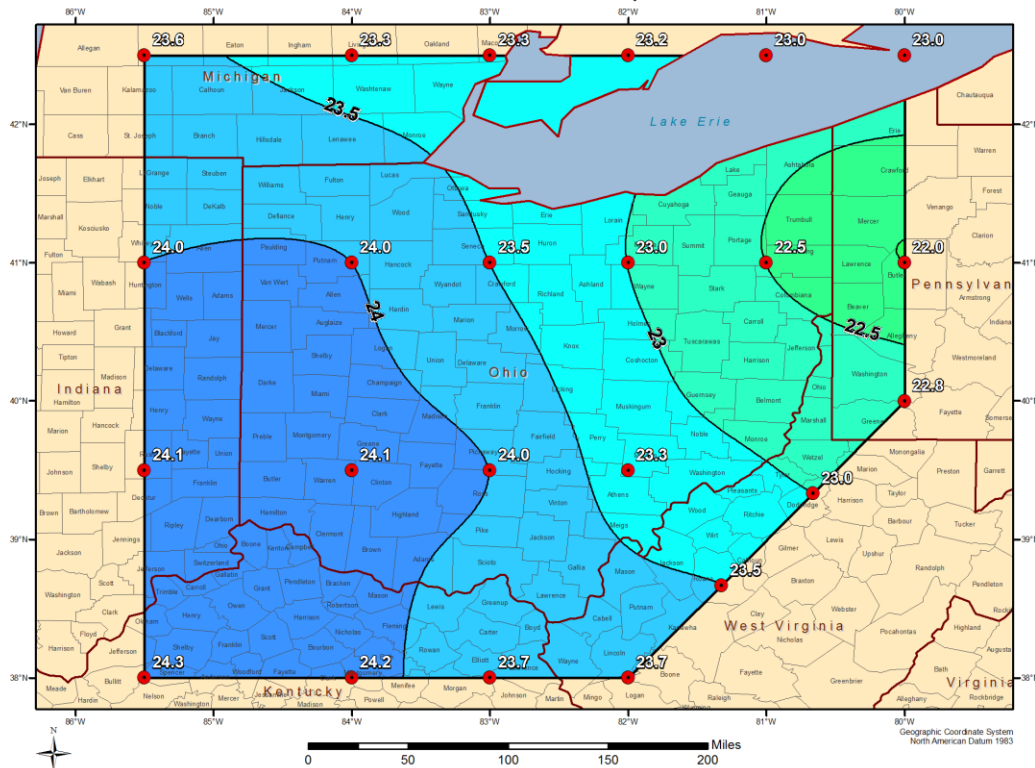




PO Box 680
Monument, Co 80132
(719) 488-9117
<http://www.appliedweatherassociates.com>

Probable Maximum Precipitation Study for the State of Ohio

All-Season PMP - 24-hour 10 mi² (inches)
Ohio Statewide PMP Study



Prepared for
Ohio Dept. of Natural Resources
2050 East Wheeling Ave
Cambridge, OH 43725

Prepared by
Applied Weather Associates, LLC
Monument, Colorado

Ed Tomlinson, PhD, Chief Meteorologist/Project Manager
Bill Kappel, Senior Meteorologist
Doug Hultstrand, Hydrometeorologist
Geoff Muhlestein, GIS/Staff Scientist
Steve Lovisone, Staff Meteorologist

February 2013

NOTICE

This report was prepared by Applied Weather Associates, LLC (AWA). The results and conclusions in this report are based upon our best professional judgment using currently available data. Therefore, neither AWA nor any person acting on behalf of AWA can (a) make any warranty, express or implied, regarding future use of any information or method shown in the report or (b) assume any future liability regarding use of any information or method contained in the report.

Table of Contents

Table of Contents	iii
List of Figures	v
List of Tables	ix
Executive Summary	x
Glossary	xiii
1. Introduction	1
1.1 Background	1
1.2 Objectives	4
1.3 Approach	5
1.4 Ohio Location and Description	8
2. Weather and Climate of Ohio	10
2.1 Ohio PMP Storm Type Climatology	10
2.2 Ohio Area General Weather Patterns	12
3. Extreme Storm types	14
3.1 Synoptic Fronts	14
3.2 Mesoscale Convective Systems	15
4. Extreme Storm Identification	18
4.1 Storm Search Area	18
4.2 Data Sources	19
4.3 Storm Search Method	19
4.4 Developing the Intermediate Short List of Extreme Storms	23
4.5 Short Storm List Derivation	23
4.5.1 New SPAS Storm Analyses	25
5. Storm Depth-Area-Duration Analyses for New Storms	26
5.1 Data Collection	27
5.2 Mass Curves	27
5.3 Hourly or Sub-hourly Precipitation Maps	27
5.4 Depth-Area-Duration Program	28
6. Updated Data Sets Used in this Study	29
6.1 Development of the Updated Dew Point Climatology	29
6.1.1 Dew Point Temperature Interpolation Methodology	29
6.1.2 Dew Point Adjustments to 1000mb and to Mid-Month	34
6.2 HYSPLIT Trajectory Model	35
6.3 Use of Grid Points to Spatially Distribute PMP Values	38

7.	Storm Maximization	41
7.1	Use of Dew Point Temperatures for Storm Maximization	41
7.1.1	Rationale for Using Average Dew Point Climatology	43
7.1.2	Rationale for Adjusting HMR 51 Persisting Dew Point Values	44
8.	Storm Transpositioning	46
8.1	Storm Transposition Calculations	46
8.2	Storm Spreadsheet Development Process	48
9.	Development of PMP Values for Ohio	50
9.1	Envelopment Procedures and DAD Derivation	50
10.	Storm Orientation and Timing	53
10.1	PMP Design Storm Shape and Orientation	53
10.1.1	Storm Ratio Estimation Procedures	53
10.2	PMP Design Storm Timing	56
10.3	Ohio Standardized Timing Distributions by Storm Type	64
10.3.1	Results of the Analysis	65
11.	Results	78
11.1	Ohio Statewide PMP Values	78
11.2	Comparison of the All-season PMP Values with HMR 51 PMP	130
11.3	Comparison of the Ohio Study PMP Values with 6-, 12-, and 24-Hour 100-Year Return Frequency Rainfall Values	132
11.4	Reasons for Reductions of PMP versus HMR 51	133
12.	Sensitivity Analysis	135
12.1	Assumptions	135
12.1.1	Saturated Storm Atmospheres	135
12.1.2	Maximum Storm Efficiency	135
12.2	Parameters	136
12.2.1	Storm Representative Dew Point and Maximum Dew Point	136
12.2.2	Sensitivity of the Elevation Adjustment Factor	137
13.	Recommendations for Application	138
13.1	PMP Application	138
13.2	Discussion on the Spatial Limits of the PMP Values	138
13.3	Climate Change Assumptions	138
	REFERENCES	140
Appendix A	Dew Point Climatology Maps Used in the Storm Maximization and Transposition Processes	A-1
Appendix B	Procedure for using Dew Point Temperatures for Storm Maximization and Transposition	B -1
Appendix C	Procedure for Deriving PMP Values from Storm Depth-Area-Duration (DAD) Analyses	C-1

Appendix D	Depth-Area-Duration Comparison Tables Ohio Statewide PMP vs. HMR 51 PMP	D-1
Appendix E	Depth-Area-Duration Comparison Tables Ohio Statewide PMP vs. FERC Michigan/Wisconsin PMP	E-1
Appendix F	Short Storm List Storm Analysis	Separate Binding
Appendix G	Storm Precipitation Analysis System (SPAS) Description	G-1
Appendix H	Smethport, PA 1942 Extreme Rainfall Event Transposition Limitations Memo	H-1

LIST OF FIGURES

Figure 1.1	Example of HMR 51 all-season PMP map; 24-hour 1,000-square mile (Schreiner and Riedel 1978)	2
Figure 1.2	Locations of AWA PMP studies as of February 2013	4
Figure 1.3	Flow chart showing the major steps involved in PMP development	6
Figure 1.4	Grid points used in the study	8
Figure 1.5	Elevations contours across Ohio at 200 foot intervals	9
Figure 2.1	Locations of surface features associated with a strong flow of moisture from the Gulf of Mexico into the upper Midwest (from https://www.meted.ucar.edu/ , accessed September 2012)	10
Figure 2.2	Locations of surface features and air masses associated with a common synoptic storm pattern across the United States (from http://www.nc-climate.ncsu.edu/edu/k12/.JetStreams , accessed September 2012)	11
Figure 2.3	General polar front positions over the United States during winter and summer (from http://earth.usc.edu/~stott/Catalina/WeatherPatterns.html , accessed September 2012)	11
Figure 2.4	Air masses which affect Ohio (from http://www.geography.hunter.cuny.edu/~tbw/wc.notes/ , accessed September 2012)	12
Figure 3.1	Typical Bermuda High circulation and its relation to Ohio (from http://www.meted.ucar.edu/refra/seconus/summer/reg_1_1.htm , accessed October 2012)	14
Figure 3.2	Bermuda High interaction with the Jet Stream and frontal boundaries over Ohio (from http://www.meted.ucar.edu/refra/seconus/summer/reg_1_1.htm , accessed October 2012)	15
Figure 3.3	Color enhanced infrared satellite image of an MCS from August 8, 2010. (from http://cimss.ssec.wisc.edu/goes/blog/archives/6337 , accessed September 2012)	16
Figure 4.1	Storm search domain used for Ohio	18
Figure 4.2	Ohio long list storm locations at the 6-hour duration	20
Figure 4.3	Ohio long list storm locations at the 1-day duration	21
Figure 4.4	Ohio long list storm locations at the 3-day duration	22

Figure 4.5	Ohio statewide PMP short storm list locations	25
Figure 6.1	Hourly dew point temperature station locations used for the maximum dew point return frequency analysis	31
Figure 6.2	June 100-year 24-hour average maximum dew point map	35
Figure 6.3	HYSPLIT trajectory model results for Fall River, KS, June 2007 (AWA Storm Number 120)	37
Figure 6.4	HMR 51 PMP contours, 24-hour 10-square miles (Schreiner and Riedel 1978)	39
Figure 6.5	Ohio statewide PMP contours for 24-hour 10-square miles	40
Figure 7.1	Dew point climatology development dates and regions	42
Figure 8.1	Inflow wind vector transpositioning for Warner Park, TN. The storm representative dew point location is 360 miles south/southwest of the storm location.	47
Figure 8.2	Example of the storm spreadsheet for Warner Park, TN, May, 2010 storm (AWA Storm Number 126) transpositioned to grid point 15	49
Figure 9.1	24-hour DA curves for grid point 15	51
Figure 9.2	DD curves for grid point 15	52
Figure 10.1	Schematic example of problem in averaging isohyetal orientations (reproduced from HMR 52 Figure 6, page 26)	54
Figure 10.2	Example storm ratio analysis from the Dubuque, OH, July 2011 (AWA Storm Number 127)	55
Figure 10.4	Example of 6-hour incremental precipitation timing for AWA Storm Number 2010	59
Figure 10.5	Example of hourly incremental precipitation timing for AWA Storm Number 2010	59
Figure 10.6	Average 6-hour incremental precipitation for Synoptic storm events	60
Figure 10.7	Example of average hourly incremental precipitation for Synoptic storm events	60
Figure 10.8	Ohio 6-hour incremental temporal distributions based on SPAS storm centers	62
Figure 10.9	Example of one potential temporal timing sequence based on HMR 52 recommendations (image from HMR 52, Figure 3)	63
Figure 10.10	Rand SPAS rainfall for Minneapolis, MN July 1987, AWA Storm Number 102	65
Figure 10.11	Rainfall R versus Time for SPAS MCS storms	66
Figure 10.12	Normalized R versus Time for SPAS MCS storms	67
Figure 10.13	Normalized R versus shifted time for SPAS MCS storms	68
Figure 10.14	Rainfall R versus Time for SPAS Hybrid storms	69
Figure 10.15	Normalized R versus Time for SPAS Hybrid storms	70
Figure 10.16	Normalized R versus shifted time for SPAS Hybrid storms	71
Figure 10.17	Rainfall R versus Time for SPAS Synoptic storms	72
Figure 10.18	Normalized R versus Time for SPAS Synoptic storms	73
Figure 10.19	Normalized R versus shifted time for SPAS Synoptic storms	74
Figure 10.20	Rainfall R versus Time for all SPAS storms	75
Figure 10.21	Normalized R versus Time for all SPAS storms	76
Figure 10.22	Normalized R versus shifted time for all SPAS storms	77
Figure 11.1	All-season PMP (inches) for 6-hour, 1-square mile	80
Figure 11.2	All-season PMP (inches) for 12-hour, 1-square mile	81
Figure 11.3	All-season PMP (inches) for 24-hour, 1-square mile	82
Figure 11.4	All-season PMP (inches) for 48-hour, 1-square mile	83
Figure 11.5	All-season PMP (inches) for 72-hour, 1-square mile	84
Figure 11.6	All-season PMP (inches) for 6-hour, 10-square mile	85
Figure 11.7	All-season PMP (inches) for 12-hour, 10-square mile	86

Figure 11.8	All-season PMP (inches) for 24-hour, 10-square mile	87
Figure 11.9	All-season PMP (inches) for 48-hour, 10-square mile	88
Figure 11.10	All-season PMP (inches) for 72-hour, 10-square mile	89
Figure 11.11	All-season PMP (inches) for 6-hour, 100-square mile	90
Figure 11.12	All-season PMP (inches) for 12-hour, 100-square mile	91
Figure 11.13	All-season PMP (inches) for 24-hour, 100-square mile	92
Figure 11.14	All-season PMP (inches) for 48-hour, 100-square mile	93
Figure 11.15	All-season PMP (inches) for 72-hour, 100-square mile	94
Figure 11.16	All-season PMP (inches) for 6-hour, 200-square mile	95
Figure 11.17	All-season PMP (inches) for 12-hour, 200-square mile	96
Figure 11.18	All-season PMP (inches) for 24-hour, 200-square mile	97
Figure 11.19	All-season PMP (inches) for 48-hour, 200-square mile	98
Figure 11.20	All-season PMP (inches) for 72-hour, 200-square mile	99
Figure 11.21	All-season PMP (inches) for 6-hour, 500-square mile	100
Figure 11.22	All-season PMP (inches) for 12-hour, 500-square mile	101
Figure 11.23	All-season PMP (inches) for 24-hour, 500-square mile	102
Figure 11.24	All-season PMP (inches) for 48-hour, 500-square mile	103
Figure 11.25	All-season PMP (inches) for 72-hour, 500-square mile	104
Figure 11.26	All-season PMP (inches) for 6-hour, 1,000-square mile	105
Figure 11.27	All-season PMP (inches) for 12-hour, 1,000-square mile	106
Figure 11.28	All-season PMP (inches) for 24-hour, 1,000-square mile	107
Figure 11.29	All-season PMP (inches) for 48-hour, 1,000-square mile	108
Figure 11.30	All-season PMP (inches) for 72-hour, 1,000-square mile	109
Figure 11.31	All-season PMP (inches) for 6-hour, 2,000-square mile	110
Figure 11.32	All-season PMP (inches) for 12-hour, 2,000-square mile	111
Figure 11.33	All-season PMP (inches) for 24-hour, 2,000-square mile	112
Figure 11.34	All-season PMP (inches) for 48-hour, 2,000-square mile	113
Figure 11.35	All-season PMP (inches) for 72-hour, 2,000-square mile	114
Figure 11.36	All-season PMP (inches) for 6-hour, 5,000-square mile	115
Figure 11.37	All-season PMP (inches) for 12-hour, 5,000-square mile	116
Figure 11.38	All-season PMP (inches) for 24-hour, 5,000-square mile	117
Figure 11.39	All-season PMP (inches) for 48-hour, 5,000-square mile	118
Figure 11.40	All-season PMP (inches) for 72-hour, 5,000-square mile	119
Figure 11.41	All-season PMP (inches) for 6-hour, 10,000-square mile	120
Figure 11.42	All-season PMP (inches) for 12-hour, 10,000-square mile	121
Figure 11.43	All-season PMP (inches) for 24-hour, 10,000-square mile	122
Figure 11.44	All-season PMP (inches) for 48-hour, 10,000-square mile	123
Figure 11.45	All-season PMP (inches) for 72-hour, 10,000-square mile	124
Figure 11.46	All-season PMP (inches) for 6-hour, 20,000-square mile	125
Figure 11.47	All-season PMP (inches) for 12-hour, 20,000-square mile	126
Figure 11.48	All-season PMP (inches) for 24-hour, 20,000-square mile	127
Figure 11.49	All-season PMP (inches) for 48-hour, 20,000-square mile	128
Figure 11.50	All-season PMP (inches) for 72-hour, 20,000-square mile	129
Figure B.1	HYSPLIT trajectory model results for Fall River, KS, June 2007, AWA Storm Number 120	B-4
Figure G.1	SPAS flow chart	G-3

Figure G.2	Sample SPAS “basemaps” (a) A pre-existing (USGS) isohyetal pattern across flat terrain (SPAS 1209), (b) PRISM mean monthly (October) precipitation (SPAS 1192) and (c) A 100-year 24-hour precipitation grid from NOAA Atlas 14 (SPAS 1138)	G-7
Figure G.3	U.S. radar locations and their radial extents of coverage below 10,000 feet above ground level (AGL). Each U.S. radar covers an approximate 285 mile radial extent over which the radar can detect precipitation.	G-8
Figure G.4	(a) Level-II radar mosaic of CONUS radar with no quality control, (b) WDT quality controlled Level-II radar mosaic	G-9
Figure G.5	Illustration of SPAS-beam blockage infilling where (a) is raw, blocked radar and (b) is filled for a 42-hour storm event	G-10
Figure G.6	Example of disaggregation of daily precipitation into estimated hourly precipitation based on three (3) surrounding hourly recording gauges	G-12
Figure G.7	Sample mass curve plot depicting a precipitation gauge with an erroneous observation time (blue line). X-axis is the SPAS index hour and the y-axis is inches. The statistics in the upper left denote gauge type, distance from target gauge (in km), and gauge ID. In this example, the center gauge (blue line) was found to have an observation error/shift of 1 day.	G-13
Figure G.8	Depictions of total storm precipitation based on the three SPAS interpolation methodologies for a storm (SPAS #1177, Vanguard, Canada) across flat terrain: (a) no basemap, (b) basemap-aided and (3) radar	G-14
Figure G.9	Example SPAS (denoted as “Exponential”) vs. default Z-R relationship (SPAS #1218, Georgia September 2009)	G-15
Figure G.10	Commonly used Z-R algorithms used by the NWS	G-16
Figure G.11	Comparison of the SPAS optimized hourly Z-R relationships (black lines) versus a default $Z=75R^{2.0}$ Z-R relationship (red line) for a period of 99 hours for a storm over southern California	G-16
Figure G.12	A series of maps depicting 1-hour of precipitation utilizing (a) inverse distance weighting of gauge precipitation, (b) gauge data together with a climatologically-aided interpolation scheme, (c) default Z-R radar-estimated interpolation (no gauge correction) and (d) SPAS precipitation for a January 2005 storm in southern California	G-18
Figure G.13	Z-R plot (a), where the blue line is the SPAS derived Z-R and the black line is the default Z-R, and the (b) associated observed versus SPAS scatter plot at gauge locations	G-19
Figure G.14	Depiction of radar artifacts (Source: Wikipedia)	G-21
Figure G.15	“Pyramidville” Total precipitation. Center = 1.00”, Outside edge = 0.10”	G-22
Figure G.16	10-hour DA results for “Pyramidville”; truth vs. output from DAD software	G-23
Figure G.17	Various examples of SPAS output, including (a) total storm map and its associated (b) basin average precipitation time series, (c) total storm precipitation map, (d) depth-area-duration (DAD) table and plot, and (e) precipitation gauge catalog with total storm statistics.	G-26

LIST OF TABLES

Table 4.1	Ohio statewide PMP short storm list in chronological order	24
Table 5.1	SPAS storms used in this study	26
Table 6.1	Stations used in the maximum dew point climatology development	32
Table 6.2	Original station dew point data (°F), the adjusted 15 th data, and the 1,000mb data for the 20-yr, 50-yr, and 100-yr frequencies	34
Table 7.1	Comparison of 6-hour average storm representative dew point vs. 12-hour persisting storm representative dew point for the David City, NE, 1963 storm	43
Table 7.2	Storms used to evaluate average vs. persisting dew point values specific to Ohio. The tables is separated by MCS storms and synoptic storm types.	45
Table 10.1	SPAS storms used in the evaluation of storm orientation and ellipse ratios	55
Table 10.2	SPAS storm events used in Ohio PMP temporal distribution	58
Table 10.3	Example of 6-hour incremental precipitation timing for Warner Park, TN, May 2010 (AWA Storm Number 126) storm center	58
Table 11.1	Percent difference between the Ohio statewide PMP values at grid point 15 and the HMR 51 PMP values at that location. Values represent reductions from HMR 51. Rainfall values are in inches.	130
Table 11.2	Controlling storms of the PMP values. The number designates the AWA storm numbers assigned to each storm on the short storm list.	131
Table 11.3	Percent difference between Ohio statewide PMP values at grid point 15 and FERC Michigan/Wisconsin regional PMP study values at the same location. Positive values represent reductions from the FERC Michigan/Wisconsin regional PMP study values. Rainfall values are in inches.	132
Table 11.4	Comparison of the 10-square mile PMP value against the x-hour 100-year precipitation frequency from NOAA Atlas 14 for grid point 15	133
Table G.1	Different precipitation gauge types used by SPAS	G-5
Table G.2	The percent difference [(AWA-NWS)/NWS] between the AWA DA results and those published by the NWS for the 1953 Ritter, Iowa storm	G-24
Table G.3	The percent difference [(AWA-NWS)/NWS] between the AWA DA results and those published by the NWS for the 1955 Westfield, Massachusetts storm	G-24

Executive Summary

Applied Weather Associates (AWA) has completed a statewide Probable Maximum Precipitation (PMP) study for the state of Ohio. The purpose of the study was to determine PMP values for any point or basin within the state boundaries. This study took into account topography, climate and storm types that affect Ohio to produce the PMP values, for use in producing estimates of the Probable Maximum Flood (PMF) for drainage basins across the state. This study builds on previous site-specific studies completed by AWA in the region (e.g., Tomlinson 1993, Tomlinson et al. 1994, Tomlinson et al. 2008, Tomlinson et al. 2011, Kappel et al. 2012).

Ohio lies within the domain of National Weather Service (NWS) Hydrometeorological Report No. 51 (HMR 51). The methods and procedures used to derive the PMP values are similar to other site-specific PMP studies conducted by AWA within the HMR 51 domain. These include the Upper and Middle Dams drainage basins in Maine (Tomlinson 2002), the Stewarts Bridge drainage basin in New York (Tomlinson et al. 2003), the Woodcliff Lake drainage basin study in New Jersey (Tomlinson et al. 2006), the Wanahoo drainage basin study in Nebraska (Tomlinson et al. 2008), the Nebraska statewide PMP study (Tomlinson et al. 2008), the Blenheim Gilboa drainage basin in New York (Tomlinson et al. 2008), the Tuxedo Lake drainage basin in New York (Tomlinson et al. 2009), the Tarrant Regional Water District studies in Texas (Tomlinson et al. 2011, Kappel et al. 2012), the Brassua Dam basin, Maine (Tomlinson et al. 2012), and the Quad Cities Nuclear Generating Station (Kappel et al. 2012). Additionally, a regional study managed by the Electric Power Research Institute (EPRI) and accepted by the Federal Energy Regulatory Commission (FERC) for the states of Michigan and Wisconsin was completed in 1993 (Tomlinson 1993) and a site-specific PMP study was completed for the Miami Conservancy District in 1994 (Tomlinson et al. 1994). Those studies have been accepted by appropriate regulators, such as the FERC, Natural Resources Conservation Services (NRCS), and state dam regulators, for use in computing the PMF.

The approach used in this study is a storm-based approach which utilizes many of the procedures used by the National Weather Service (NWS) in the development of the HMRS. These same procedures are recommended by the World Meteorological Organization (WMO) for PMP determination (WMO 1986, 2009). This approach identifies extreme rainfall events that have occurred in regions that have meteorological and topographical characteristics similar to extreme rain storms that could occur over any point within the state of Ohio. The largest of these rainfall events are selected for detailed analyses and many are used to compute the PMP values within Ohio.

Forty-five extreme rainfall events were identified as relevant storms, having similar characteristics to extreme rainfall events that could potentially occur over some location within Ohio. This assemblage of storms is used to produce PMP values at one or more of the drainage area sizes and/or durations analyzed. These storms are listed on the short storm list. The NWS and/or US Army Corps of Engineers (USACE) previously analyzed 26 of these storms; two storms were analyzed as part of the FERC Michigan/Wisconsin regional PMP study; and the remaining 17 storms were analyzed by AWA using the Storm Precipitation Analysis System (SPAS). Seven of these SPAS storms were analyzed in previous PMP studies, with 10 analyzed for this study. For the SPAS analyzed storms, standard Depth-Area-Duration (DAD)

tables, total storm isohyetal maps, and mass curve plots were produced for each storm similar to the storm analysis results produced by the NWS, USACE, and FERC Michigan/Wisconsin storm analyses.

HMR procedures for maximization, transposition, and elevation moisture adjustments were used with minor changes (e.g., average dew points for specified durations instead of 12-hour persisting dew points, no 1,000 foot exemption for moisture adjustments, and +/-1,000 foot vertical transposition limitations for individual storms). Updated techniques (i.e., use of GIS, and extreme value statistics) and databases (i.e., average dew point values that match the duration of a storm) are used in the study to increase accuracy and reliability, while adhering to the basic procedures in the HMRs and WMO Manuals. An updated maximum dew point climatology was developed during this study and was used in the storm maximization and storm transpositioning processes.

With the exception of the 10 new SPAS storms analyzed during this study, all other storms have previously had storm maximization factors determined by AWA during previous PMP work. For the newly analyzed storms, maximization factors were determined using the updated climatologies and storm representative dew point data. A parcel trajectory model called HYSPLIT (Draxler and Rolph 2003, 2010) was used along with the National Center for Environmental Prediction (NCEP) Reanalysis (Mesinger 2006) database to assist in the determination of inflow moisture vectors.

Each storm on the short storm list was maximized, transpositioned, and elevation adjusted to each of the 23 grid points used to distribute PMP across Ohio and its margins as appropriate, based on guidelines associated with transpositionability. Depth-Area (DA) plots were made for durations of 6-, 12-, 24-, 48-, and 72-hour for area sizes of 1-, 10-, 200-, 500-, 1,000-, 2,000-, 5,000-, 10,000-, and 20,000-square miles. Enveloping curves were constructed using adjusted storm rainfall values at each grid point. Depth-Duration (DD) plots were plotted and envelope curves constructed. These envelop curves provide PMP values for each grid point. The final step was to spatially interpolate the resulting values using a Geographic Information System (GIS) and manual adjustments to ensure continuity in space and time across the 23 grid point domain. Results of this final step allow PMP values for standard durations and area sizes to be determined for any location within the state. These values can be used in modeling efforts to produce estimates of PMF.

GLOSSARY

Adiabat: Curve of thermodynamic change taking place without addition or subtraction of heat. On an adiabatic chart or pseudo-adiabatic diagram, a line showing pressure and temperature changes undergone by air rising or condensation of its water vapor; a line, thus, of constant potential temperature.

Adiabatic: Referring to the process described by adiabat.

Advection: The process of transfer (of an air mass property) by virtue of motion. In particular cases, advection may be confined to either the horizontal or vertical components of the motion. However, the term is often used to signify horizontal transfer only.

Air mass: Extensive body of air approximating horizontal homogeneity, identified as to source region and subsequent modifications.

Barrier: A mountain range or region of elevated terrain which partially blocks the flow of low level moisture from a source of moisture to the basin or region under study.

Cirrus shield: In this study, the area of cirrus cloud that covers a mesoscale convective complex.

Cold front: The type of front where relatively colder air displaces warmer air.

Convective rain: Rainfall caused by the vertical motion of an ascending mass of air that is warmer than the environment and typically forms a cumulonimbus cloud. The horizontal dimension of such a mass of air is generally of the order of 12 miles or less. Convective rain is typically of greater intensity than either of the other two main classes of rainfall (cyclonic and orographic) and is often accompanied by thunder.

Convergence: Horizontal shrinking and vertical stretching of a volume of air, accompanied by net inflow horizontally and internal upward motion.

Cooperative station: A weather observation site where an unpaid observer maintains a climatological station for the National Weather Service.

Cyclone: A distribution of atmospheric pressure in which there is a low central pressure relative to the surroundings. On large-scale weather charts, cyclones are characterized by a system of closed constant pressure lines (isobars), generally approximately circular or oval in form, enclosing a central low-pressure area. Cyclonic circulation is counterclockwise in the northern hemisphere and clockwise in the southern. (That is, the sense of rotation about the local vertical is the same as that of the earth's rotation.)

Depth-Area curve: Curve showing, for a given duration, the relation of maximum average depth to size of area within a storm or storms.

Depth-Area-Duration: The precipitation values derived from Depth-Area and Depth-Duration curves at each time and area size increment analyzed for a PMP evaluation.

Depth-Area-Duration curve: A curve showing the relation between an averaged areal rainfall depth and the area over which it occurs, for a specified time interval, during a specific rainfall event.

Depth-Duration curve: Curve showing, for a given area size, the relation of maximum average depth of precipitation to duration periods within a storm or storms.

Dew point: The temperature to which a given parcel of air must be cooled at constant pressure and constant water vapor content for saturation to occur.

Effective Barrier Height: The barrier height determined from elevation analysis that reflects the effect of the barrier on the precipitation process for a storm event. The actual barrier height may be either higher or lower than the effective barrier height.

Envelopment: A process for selecting the largest value from any set of data. In estimating PMP, the maximum and transposed rainfall data are plotted on graph paper, and a smooth curve is drawn through the largest values.

Explicit Transposition: The movement of the rainfall amounts associated with a storm within boundaries of a region throughout which a storm may be transposed with only relatively minor modifications of the observed storm rainfall amounts. The area within the transposition limits has similar, but not identical, climatic and topographic characteristics throughout.

First-order NWS station: A weather station that is either automated, or staffed by employees of the National Weather Service and records observations on a continuous basis.

Front: The interface or transition zone between two air masses of different parameters. The parameters describing the air masses are temperature and dew point.

General storm: A storm event, that produces precipitation over areas in excess of 500-square miles, has a duration longer than 6 hours, and is associated with a major synoptic weather feature.

Gulf Stream Current: A warm, well-defined, swift, relatively narrow, ocean current in the western North Atlantic that originates where the Florida Current and the Antilles Current begin to curve eastward from the continental slope of Cape Hatteras, North Carolina. East of the Grand Banks, the Gulf Stream meets the cold Labrador Current, and the two flow eastward separated by the cold wall.

HYSPLIT: HYbrid Single-Particle Lagrangian Integrated Trajectory. A complete system for computing parcel trajectories to complex dispersion and deposition simulations using either puff or particle approaches.

Implicit Transposition: The process of applying regional, areal, or durational smoothing to eliminate discontinuities resulting from the application of explicit transposition limits for various storms.

Isohyets: Lines of equal value of precipitation for a given time interval.

Isohyetal Pattern: The pattern formed by the isohyets of an individual storm.

Isohyetal orientation: The term used to define the orientation of precipitation patterns of major storms when approximated by elliptical patterns of best fit. It is also the orientation (direction from north) of the major axis through the elliptical PMP storm pattern.

Jet Stream: A strong, narrow current concentrated along a quasi-horizontal axis (with respect to the earth's surface) in the upper troposphere or in the lower stratosphere, characterized by strong vertical and lateral wind shears. Along this axis it features at least one velocity maximum (jet streak). Typical jet streams are thousands of miles long, hundreds of miles wide, and several miles deep.

Local storm: A storm event that occurs over a small area in a short time period. Precipitation rarely exceeds 6 hours in duration and the area covered by precipitation is less than 500-square miles. Frequently, local storms will last only 1 or 2 hours and precipitation will occur over areas of up to 200-square miles. Precipitation from local storms will be isolated from general-storm rainfall. Often these storms are thunderstorms.

Low-level jet: A region of relatively strong winds in the lower part of the atmosphere. Specifically, it often refers to a southerly wind maximum in the boundary layer, common over the Plains states at night during the warm season (spring and summer).

Mass curve: Curve of cumulative values of precipitation through time.

Mesoscale Convective Complex: For the purposes of this study, a heavy rain-producing storm with horizontal scales of 10 to 1000 kilometers (6 to 625 miles) which includes significant, heavy convective precipitation over short periods of time (hours) during some part of its lifetime.

Mesoscale Convective System: A complex of thunderstorms which becomes organized on a scale larger than the individual thunderstorms, and normally persists for several hours or more. MCSs may be round or linear in shape, and include systems such as tropical cyclones, squall lines, and MCCs (among others). MCS often is used to describe a cluster of thunderstorms that does not satisfy the size, shape, or duration criteria of an MCC.

Mid-latitude frontal system: An assemblage of fronts as they appear on a synoptic chart north of the tropics and south of the polar latitudes. This term is used for a continuous front and its characteristics along its entire extent, its variations of intensity, and any frontal cyclones along it.

Moisture maximization: The process of adjusting observed precipitation amounts upward based upon the hypothesis of increased moisture inflow to the storm.

Observational day: The 24-hour time period between daily observation times for two consecutive days at cooperative stations, e.g., 6:00PM to 6:00PM.

One-hundred year rainfall event: The point rainfall amount that has a one-percent probability of occurrence in any year. Also referred to as the rainfall amount that on the

average occurs once in a hundred years or has a 1 percent chance of occurring in any single year.

Polar front: A semi-permanent, semi-continuous front that separates tropical air masses from polar air masses.

Precipitable water: The total atmospheric water vapor contained in a vertical column of unit cross-sectional area extending between any two specified levels in the atmosphere; commonly expressed in terms of the height to which the liquid water would stand if the vapor were completely condensed and collected in a vessel of the same unit cross-section. The total precipitable water in the atmosphere at a location is that contained in a column or unit cross-section extending from the earth's surface all the way to the "top" of the atmosphere. The 30,000 foot level (approximately 300mb) is considered the top of the atmosphere in this study.

Persisting dew point: The dew point value at a station that has been equaled or exceeded throughout a period. Commonly durations of 12 or 24 hours are used, though other durations may be used at times.

Probable Maximum Flood: The flood that may be expected from the most severe combination of critical meteorological and hydrologic conditions that are reasonably possible in a particular drainage area.

Probable Maximum Precipitation: Theoretically, the greatest depth of precipitation for a given duration that is physically possible over a given size storm area at a particular geographic location at a certain time of the year.

Pseudo-adiabat: Line on thermodynamic diagram showing the pressure and temperature changes undergone by saturated air rising in the atmosphere, without ice-crystal formation and without exchange of heat with its environment, other than that involved in removal of any liquid water formed by condensation.

Pseudo-adiabatic: Referring to the process described by the pseudo-adiabat.

Probable Maximum Precipitation storm pattern: The isohyetal pattern that encloses the PMP area, plus the isohyets of residual precipitation outside the PMP portion of the pattern.

Saturation: Upper limit of water-vapor content in a given space; solely a function of temperature.

Short storm list: The final list of storms used to derive the Probable Maximum Precipitation values.

Shortwave: Also referred to as a shortwave trough, is an embedded kink in the trough / ridge pattern. This is the opposite of longwaves, which are responsible for synoptic scale systems, although shortwaves may be contained within or found ahead of longwaves and range from the mesoscale to the synoptic scale.

Spatial distribution: The geographic distribution of precipitation over a drainage according to an idealized storm pattern of the PMP for the storm area.

Storm transposition: The hypothetical transfer, or relocation of storms, from the location where they occurred to other areas where they could occur. The transfer and the mathematical adjustment of storm rainfall amounts from the storm site to another location is termed "explicit transposition." The areal, durational, and regional smoothing done to obtain comprehensive individual drainage estimates and generalized PMP studies is termed "implicit transposition" (WMO, 1986).

Synoptic: Showing the distribution of meteorological elements over an area at a given time, e.g., a synoptic chart. Use in this report also means a weather system that is large enough to be a major feature on large-scale maps (e.g., of the continental U.S.).

Temporal distribution: The time order in which incremental PMP amounts are arranged within a PMP storm.

Tropical Storm: A cyclone of tropical origin that derives its energy from the ocean surface.

Total storm area and total storm duration: The largest area size and longest duration for which depth-area-duration data are available in the records of a major storm rainfall.

Transposition limits: The limits in the region surrounding an actual storm location where similar, but not identical, meteorological and topographic characteristics occur, and therefore the given storm event can be relocated. The storm can be transpositioned within the transposition limits without modification of the expected storm dynamics and adjustments can be applied to the difference in elevation and moisture availability between the two locations.

Undercutting: The process of placing an envelopment curve somewhat lower than the highest rainfall amounts on depth-area and depth-duration plots.

Warm front: Front where relatively warmer air replaces colder air.

Warm sector: Sector of warm air bounded on two sides by the cold and warm fronts extending from a center of low pressure.

Acronyms and Abbreviations used in the report

ALERT: Automated Local Evaluation in Real Time

AMS: Annual Maximum Series

AWA: Applied Weather Associates, LLC

COCORAHS: Community Collaborative Rain, Hail, and Snow Network

COOP: Cooperative Observer Program

DA: Depth-Area

DAD: Depth-Area-Duration

DD: Depth-Duration

dd: decimal degrees

DND: drop number distribution

DSD: drop size distribution

EPRI: Electric Power Research Institute

F: Fahrenheit

FERC: Federal Energy Regulatory Commission

GEV: General Extreme Value

GIS: Geographical Information System

GRASS: Geographic Resource Analysis Support System

HMR: Hydrometeorological Report

HOUR: Hour

HYSPLIT: Hybrid Single Particle Lagrangian Integrated Trajectory Model

IPCC: Intergovernmental Panel on Climate Change

km: kilometer

MADIS: Meteorological Assimilation Data Ingest System

mb: millibar

MCC: Mesoscale Convective Complex

MCS: Mesoscale Convective System

mph: miles per hour

NCAR: National Center for Atmospheric Research

NCDC: National Climatic Data Center

NCEP: National Centers for Environmental Prediction

NEXRAD: Next Generation Radar

NOAA: National Oceanic and Atmospheric Association

NWS: National Weather Service

PMF: Probable Maximum Flood

PMP: Probable Maximum Precipitation

PW: Precipitable water

R: Accumulated Rainfall at the storm center during the SSP

R_n: Normalized R

RNT: Adjusted SPAS accumulated rainfall

RAWS: Remote Automatic Weather Stations

SMC: spatially based mass curve

SPAS: Storm Precipitation and Analysis System

SPP: Significant Precipitation Period when the majority of the rainfall occurred

T: Time when R occurred

T₅₀: Time when R_n = 0.5

T_S: Shifted Time

USACE: US Army Corps of Engineers

USGS: United States Geological Survey

WMO: World Meteorological Organization

1. Introduction

This study provides Probable Maximum Precipitation (PMP) values for use in the computation of the Probable Maximum Flood (PMF) for watersheds within the state of Ohio. The study builds on the previous PMP studies completed by AWA in the region (e.g., Tomlinson 1993, Tomlinson et al. 2002-2012, Kappel et al. 2012).

1.1 Background

Definitions of PMP are found in most Hydrometeorological Reports (HMRs) published by the National Weather Service (NWS). The definition used in the most recently published HMR (HMR 59, 1999, p. 5) is *"theoretically, the greatest depth of precipitation for a given duration that is physically possible over a given storm area at a particular geographical location at a certain time of the year."* Since the mid-1940s, several government agencies have been developing methods to calculate PMP in various regions of the United States. The NWS (formerly the U.S. Weather Bureau) and the Bureau of Reclamation have been the primary agencies involved in this activity. PMP values from their reports are used to calculate the PMF which, in turn, is often used in the design of significant hydraulic structures.

The generalized PMP studies currently in use in the conterminous United States include HMR 49 (1977) for the Colorado River and Great Basin drainage; HMRs 51 (1978), 52 (1982) and 53 (1980) for the U.S. east of the 105th meridian; HMR 55A (1988) for the area between the Continental Divide and the 103rd meridian; HMR 57 (1994) for the Columbia River Drainage; and HMRs 58 (1998) and 59 (1999) for California. The region covered by HMR 51 constitutes the largest generalized region addressed by a single HMR. Figure 1.1 shows an example of a HMR 51 PMP map. In addition to these HMRs, numerous Technical Papers and Reports deal with specific subjects concerning precipitation. Examples are NOAA Technical Report NWS 25 (1980) and NOAA Technical Memorandum NWS HYDRO 45 (1995). Topics include maximum observed rainfall amounts; return periods for various rainfall amounts, and specific storm studies. Climatological atlases (Technical Paper No. 40, 1961; NOAA Atlas 2, 1973; and NOAA Atlas 14, 2003-2012) are available for use in determining point rainfall amounts for specified return periods for selected regions of the U.S.

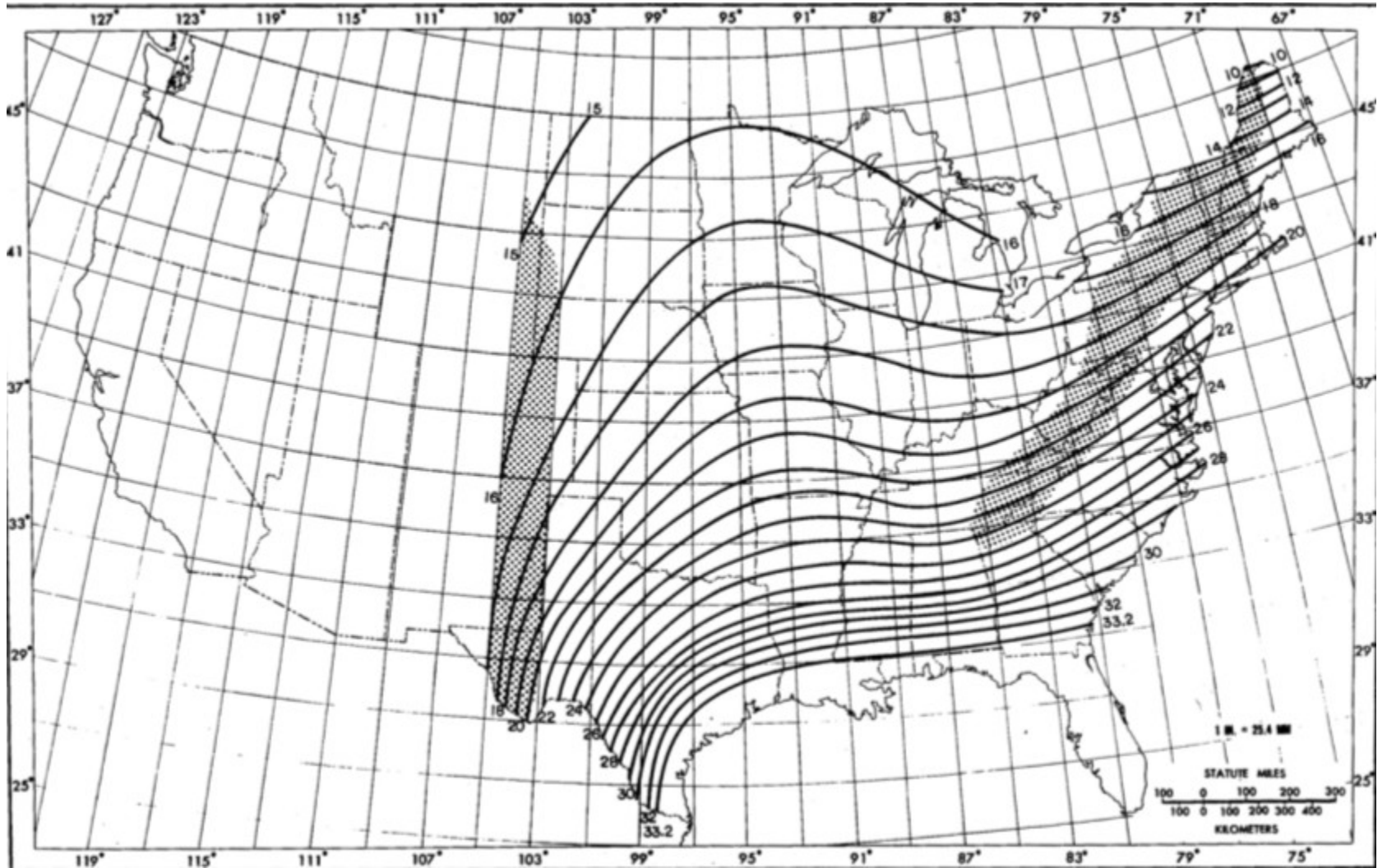


Figure 1.1 Example of HMR 51 all-season PMP map; 24-hour 1,000-square mile (Schreiner and Riedel 1978)

A number of specialized and regional PMP studies augment generalized HMRs. These studies are for specific regions or drainage basins within the large area addressed by HMR 51 (over half of the contiguous United States). The meteorological conditions producing extreme rainfall events vary significantly in different regions within this large geographic area. Along the Gulf Coast and much of the eastern seaboard, hurricanes are a major contributor. In much of the Midwest, extreme events are usually linked to either Mesoscale Convective Systems (MCSs) or synoptic storms with embedded convection. For Ohio, the main storm type leading to PMF level flooding for small basins (i.e., less than 500-square miles) are the MCS events, while for larger basins (i.e., larger than 500-square miles) the synoptic event with embedded convection is the controlling storm type.

Although HMR 51 provides generalized estimates of PMP values for a large, climatologically diverse area, it recognizes that studies addressing PMP over specific regions can incorporate more site-specific considerations and provide improved PMP estimates. By periodically reviewing storm data and advances in meteorological concepts, PMP analysts can identify relevant new data and approaches for use in determining PMP estimates (HMR 51, Section 1.4.1).

As described previously, several site-specific PMP studies have been completed by AWA within the region covered by HMR 51 (Figure 1.2). Each of these studies provided PMP values which could be used in place of PMP values from HMR 51. These are good examples of PMP studies that explicitly consider the meteorology and topography of the study location along with characteristics of historic extreme storms over climatically similar regions. These regional and site-specific PMP studies have received extensive review and been accepted by the appropriate regulatory agencies. Results have been used in computing the PMF for individual watersheds.

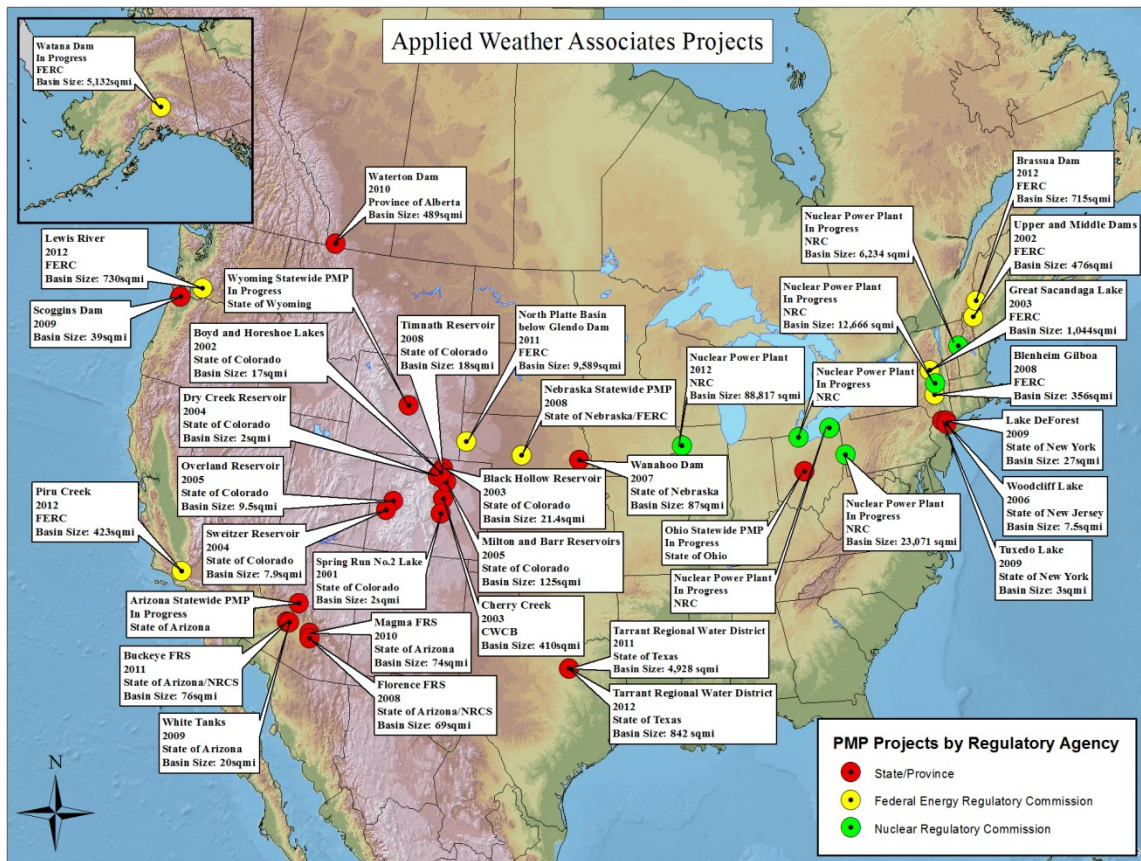


Figure 1.2 Locations of AWA PMP studies as of February 2013

This report presents details of the Ohio statewide PMP study. Section 1 provides an overview of the study. The weather and climate of the upper Midwest and northern Great Plains are discussed in Section 2. Section 3 details the storm types important for PMP development for the basin. The steps involved with identifying extreme storms are discussed in Section 4 and procedures used to analyze these storms are discussed in Section 5. Development of the maximum dew point climatology is provided in Section 6. Adjustments for storm maximization, storm transpositioning, and elevation adjustments are presented in Sections 7 and 8. The final procedure of developing PMP values from the adjusted rainfall amounts is provided in Section 9. Section 10 provides information on PMP storm orientation and timing. Results are discussed in Section 11. Section 12 provides discussions related to the sensitivity analysis of the parameters used in the study. The recommended application of results is given in Section 13.

1.2 Objectives

The objective of this study was to perform a statewide PMP analysis to determine reliable estimates of PMP values for any location within the state of Ohio. The most reliable methods

and data currently available have been used, with updated methods, techniques, and data compared to HMR 51 and 52 used where appropriate.

1.3 Approach

The approach used in this study follows the same basic procedures that were used in the development of the HMRS. These procedures were applied considering the meteorological and topographic characteristics across the state.

The study maintains as much consistency as possible with the general method used in HMR 51 and the numerous site-specific, statewide, and regional PMP studies AWA has completed over the past 15 years. Deviations are incorporated where justified by developments in meteorological analyses and available data. The basic approach identifies PMP-type storms that occurred within the following bounds of approximately 49.0°N 102.0°W to 33.0° N 75.0°W. Elevation was also an important consideration, where storm centers which occurred at elevations greater than 3,000 feet were not considered transpositionable to any location within the state. This relatively large domain ensured that several transpositionable storms of each area size and duration were included in the storm list development to produce the most robust PMP values for Ohio. Results of this storm search led to the production of a short list of storms used to determine the PMP values.

The moisture content of each of these storms is maximized to provide an estimate of the maximum rainfall that could have been produced by each storm at the location where it occurred. This is accomplished by computing the ratio of the *maximum* amount of atmospheric moisture that could have been entrained into the storm at that time of year to the *actual* atmospheric moisture entrained into the storm as it occurred in-place. The difference between the *maximum* and *actual* is converted into a percent and the storm rainfall totals are enhanced – maximized – by this value - called a maximization factor. After maximization, the storms are transpositioned to each grid point to the extent supportable by similarity of meteorological conditions and topography. Maximized and transpositioned-adjusted rainfall values are plotted and enveloped at each grid point and values contoured to ensure continuity in time and space to provide PMP estimates for various area sizes and durations. Figure 1.3 shows the flow chart of the major steps in the PMP development process.

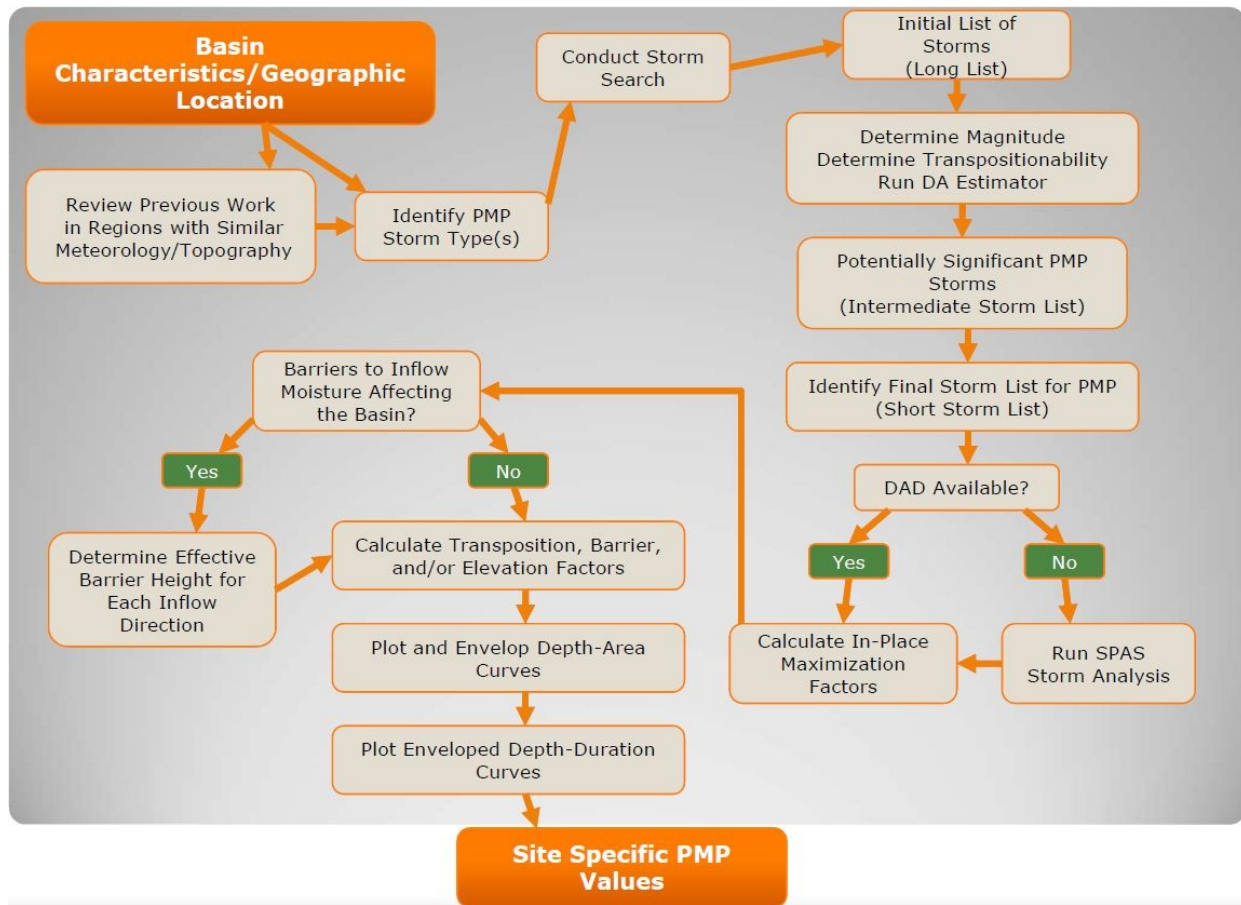


Figure 1.3 Flow chart showing the major steps involved in PMP development

For some applications, this study applied standard methods (e.g., WMO Operational Hydrology Report No. 1, 1986), while for other applications, improved techniques were developed. Advanced computer-based technologies together with Weather Service Radar WSR-88D NEXt generation RADar (NEXRAD) data were used for storm analyses along with updated meteorological data sources. The Hybrid Single Particle Lagrangian Integrated Trajectory Model (HYSPLIT) model trajectories were used as guidance to determine moisture inflow vectors. Improved technology and data were incorporated into the study when they provided improved reliability, while maintaining as much consistency as possible with previous studies. This approach provides the most complete scientific application compatible with the engineering requirements of consistency and reliability for credible PMP determination.

Moisture analyses in HMR 51 used monthly maximum observed 12-hour persisting dew points to quantify atmospheric moisture. Maximum dew point values are provided by *Climatic Atlas of the United States*, published by the Environmental Data Services, Department of Commerce (1968). This Ohio statewide PMP study, however, used an updated maximum dew point return frequency analysis that was developed as part of this study. This maximum dew point analysis incorporated data sets with longer periods of record than were available for use in HMR 51 and the FERC Michigan/Wisconsin PMP study. This updated climatology produced 20-, 50-, and 100-year return frequencies for maximum average dew point values for 6-, 12-, and

24-hour duration periods. GIS was used extensively in the development of the updated maximum dew point climatology.

A reanalysis of transposition limits was completed that evaluated the elevation of each storm's isohyetal pattern versus the elevation of each grid point used in this study. It was determined from this analysis that storms should not be transpositioned more than approximately +/- 1,000 feet in elevation from their original storm elevations and/or approximately +/- six degrees in latitude, as empirical data indicate that storms display different characteristics over these elevations changes and distances. This follows similar guidelines provided in HMRs 51, 55A, 57, and 59 and in previous PMP studies completed by AWA (e.g., Tomlinson et al. 2008). This procedure provided explicit guidance and constraints on the regions of influence for individual storms. Appendix F details which storms were ultimately transpositioned to which grid point(s).

As mentioned previously, a set of 23 grid points (Figure 1.4) were placed over the region. The grid not only covers the entire state of Ohio but also extends into bordering regions to ensure continuity across the state boundaries. The adjusted storm rainfall amounts were determined at each grid point. PMP values were analyzed at each grid point using standard procedures. Envelopment of the largest rainfall totals ensured spatial and temporal continuity of the final PMP values. Once values were derived for each area size and duration, the PMP values were spatially and temporally distributed using GIS technologies and manual adjustments. The interpolation allows PMP values to be determined for any location within the state. This complete process produced the final set of PMP maps for the study.

As was completed in HMR 51 and the FERC Michigan/Wisconsin regional PMP study, a preferred storm orientation analysis was completed using storm isohyetal patterns from the storms used to determine PMP values. In addition, a similar analysis was completed to determine the timing of the PMP design storm rainfall on an incremental basis. Actual storm events used to provide PMP for this study were used to determine both of these PMP design storm components. Recommendations for the PMP design storm orientation and timing were made as part of this study.

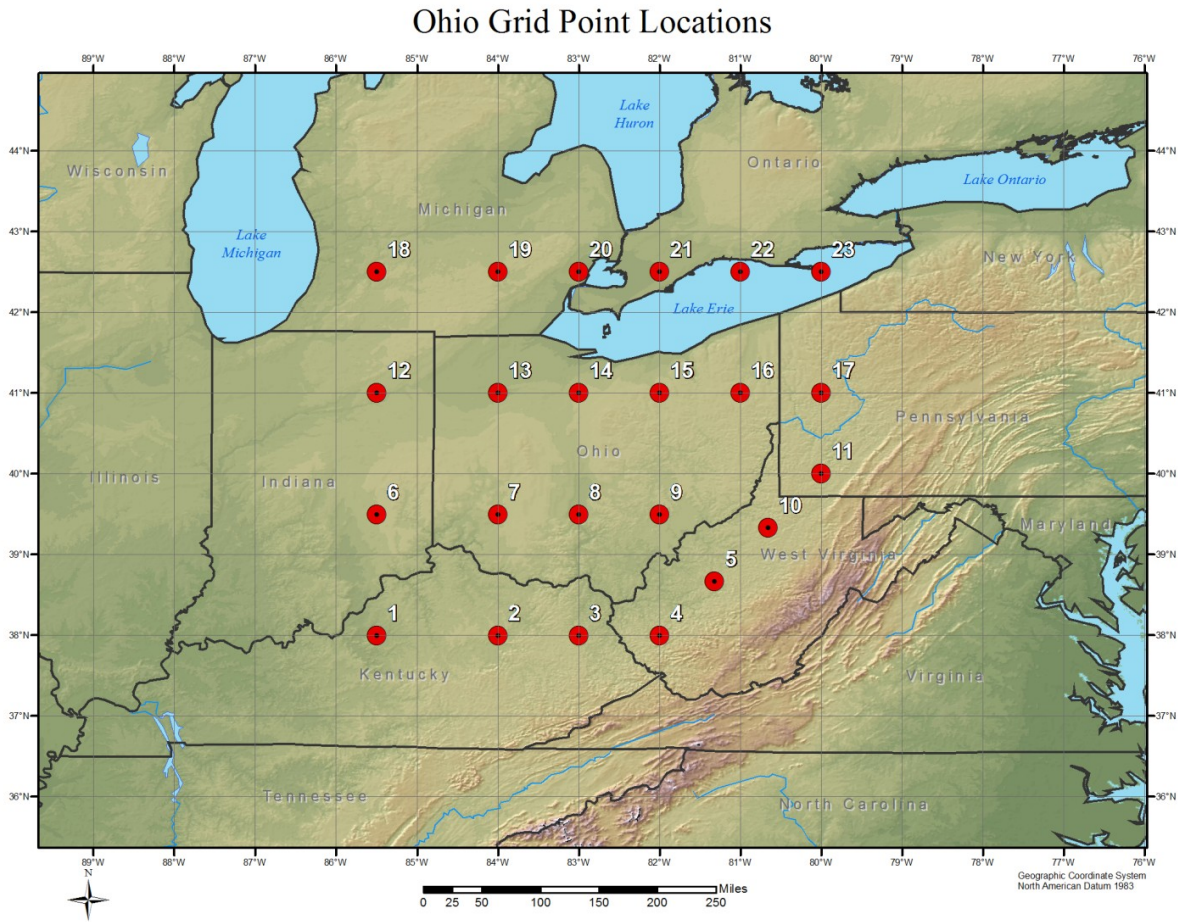


Figure 1.4 Grid points used in the study

1.4 Ohio Location and Description

Many of the watersheds of Ohio lie within the Ohio River basin, extending from near Lake Erie on the north to the Ohio River on the south. Because Ohio extends across a large latitudinal extent, PMP-type storm events can vary across the state, and any given storm event will not be affecting the entire state at one time. In addition, the western and northern portions of the state lack upwind barriers that limit atmospheric moisture in the PMP/PMF scenarios. The various storm types that can produce PMP within Ohio have been explicitly evaluated during the study to ensure appropriate PMP development.

Elevations across the state range from 455 feet along the Ohio River state boundary with Kentucky to 1,549 feet in west central Ohio (Figure 1.5). Overall relief within the state is very benign (compared with neighboring Pennsylvania, for example) and most often occurs with relatively shallow elevation gradients. Extensive discussions with the Board of Consultants along with ground reconnaissance led to the conclusion that orographic enhancement or depletion of rainfall is not a major factor in Ohio. Therefore, storms that were influenced by orographics were not considered transpositionable in this study (e.g., Smethport 1942). Further, limits of transpositionability were mainly controlled by the moisture source for the original storm event and how that would be affected if the storm were transpositioned to and within Ohio.

Ohio Elevation Contours 200' Intervals

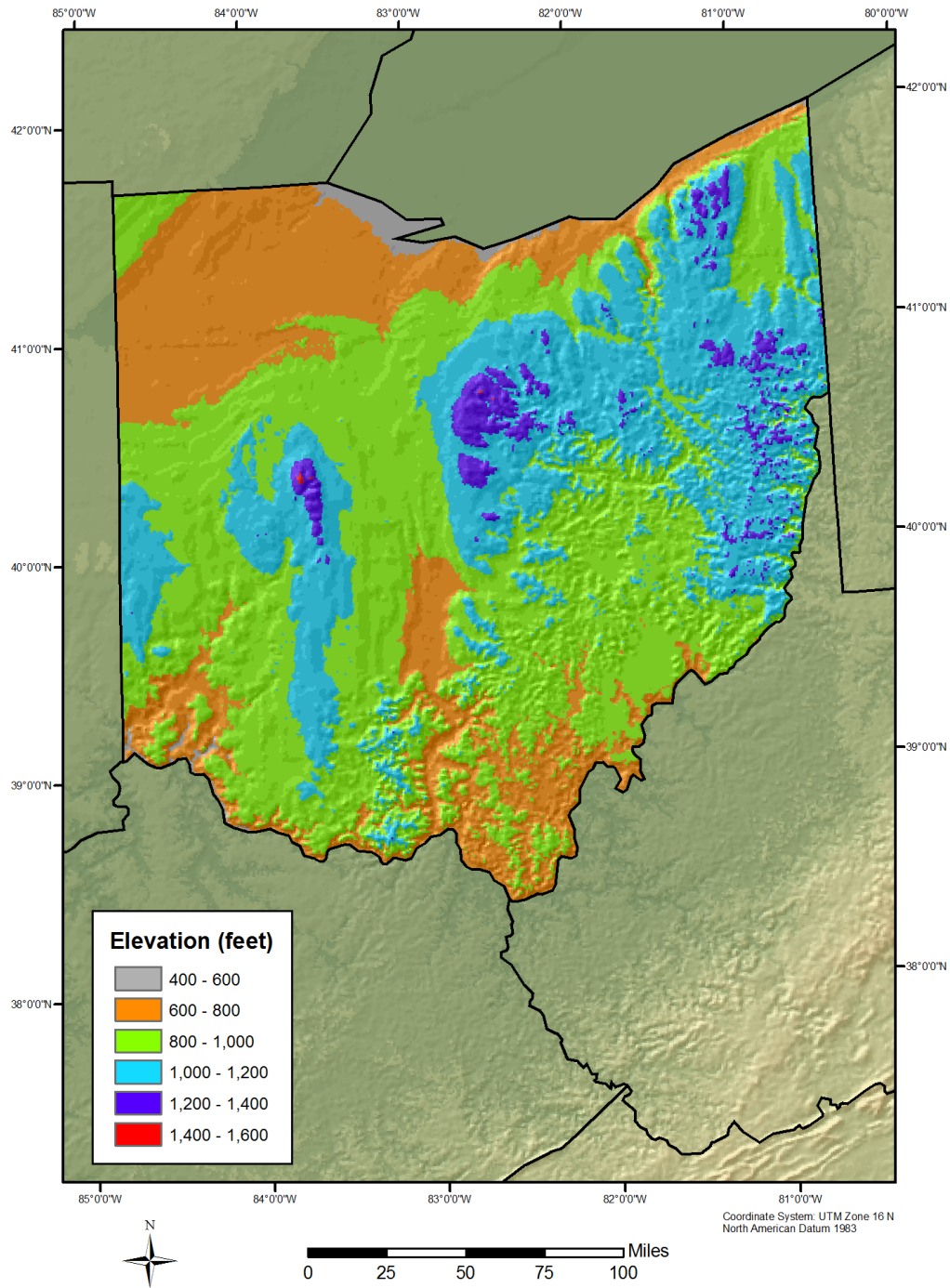


Figure 1.5 Elevations contours across Ohio at 200 foot intervals

2. Weather and Climate of Ohio

2.1 Ohio PMP Storm Type Climatology

The region around Ohio is influenced by several factors that can contribute to the production of extreme rainfall. First is the proximity to the Gulf of Mexico with no intervening barrier to limit moisture from moving north (Figure 2.1). This opens the door to allow high amounts of atmospheric moisture to flow directly into the region. The limiting factor is the duration that these high levels of moisture are able to feed into storms in the region. Because of the state's northerly location and distance from the Gulf of Mexico, storm patterns generally do not stay fixed in one location for long periods. Therefore, the synoptic situations which lead to high levels of Gulf moisture moving into the region are transient and limit the magnitude and duration of PMP rainfall as well as limiting the spatial extent of such storms. This lack of consistent moisture is somewhat compensated for by strong storm dynamics associated with synoptic weather systems which move through the region.



Figure 2.1 Locations of surface features associated with a strong flow of moisture from the Gulf of Mexico into the upper Midwest
(from <https://www.meted.ucar.edu/>, accessed September 2012)

But atmospheric moisture alone does not produce rainfall. A mechanism to lift and condense that moisture is required. The lift required to convert high levels of atmospheric moisture into rainfall on the ground is provided in several ways in and around Ohio. Synoptic storm dynamics are very effective in converting atmospheric moisture into rainfall. These are most often associated with fronts (boundaries between two different air masses) which affect the region (Figure 2.2). Numerous large scale weather systems with their associated fronts traverse the region during the year, with the fewest and weakest occurring in summer. The fronts can be a

focusing mechanism, thereby providing upward motion in the atmosphere. These frontal systems are associated with the jet stream which varies seasonally (Figure 2.3). These are often locations where heavy rainfall is produced. Normally a front will move through with enough speed that no one area receives excessive amounts of rainfall. However, in extreme instances the pattern can become blocked and some of these fronts will stall or move very slowly across the region. This allows heavy amounts of rainfall to continue for several days in the same general area, which can lead to extreme widespread flooding.

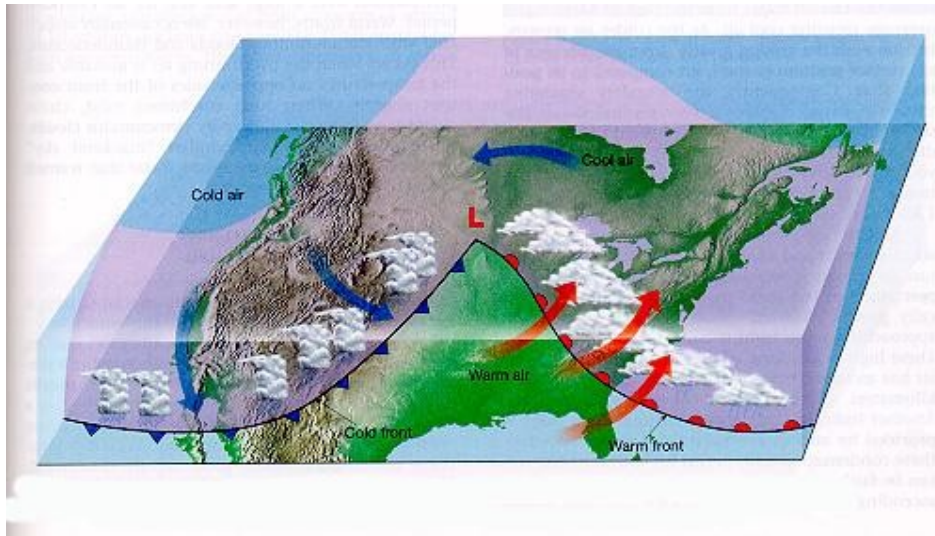


Figure 2.2 Locations of surface features and air masses associated with a common synoptic storm pattern across the United States
(from <http://www.nc-climate.ncsu.edu/edu/k12/.JetStreams>, accessed September 2012)

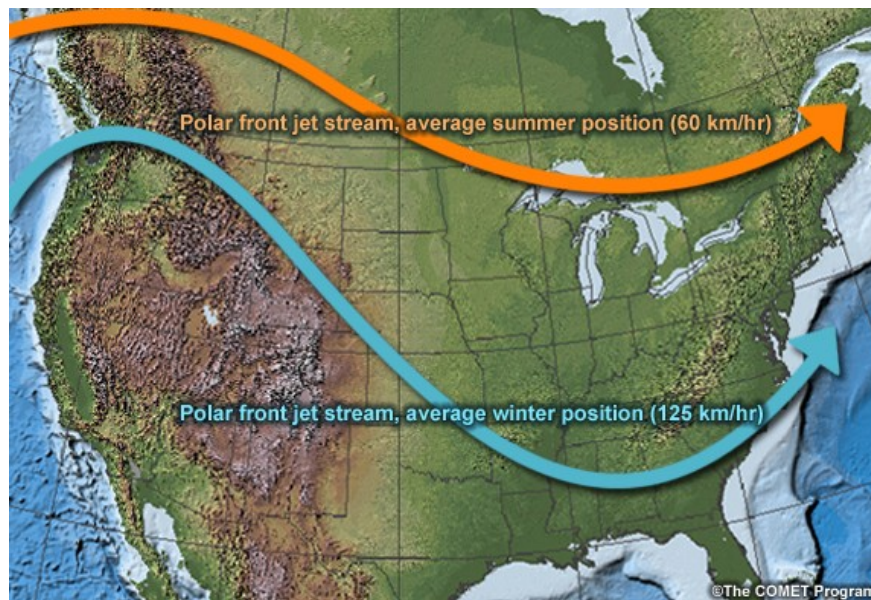


Figure 2.3 General polar front positions over the United States during winter and summer
(from <http://earth.usc.edu/~stott/Catalina/WeatherPatterns.html>, accessed September 2012)

Another mechanism which creates lift in the region is heating of the surface and lower atmosphere by the solar radiation. This produces warmer air below colder air resulting in atmospheric instability and leads to buoyancy (i.e., rising motions). This will often form ordinary afternoon and evening thunderstorms. However, in unique circumstances the instability and moisture levels in the atmosphere can reach very high levels and stay over the same region for an extended period of time, leading to intense thunderstorms and very heavy rainfall. If these storms are focused over the same area for a long period, flooding rains can be produced. This type of storm produces some of the largest point rainfall amounts recorded, but often do not affect larger areas with extreme rainfall amounts. More details on the PMP storm types which have produced extreme rainfall in and around Ohio are given in Section 3.

2.2 Ohio Area General Weather Patterns

Weather patterns in the region are characterized by passages of fronts with differing air masses that lead to large ranges in temperatures and rainfall (Figure 2.4). Fronts are most prevalent in the fall, winter, and spring, with more stagnant patterns common from late spring through early fall.

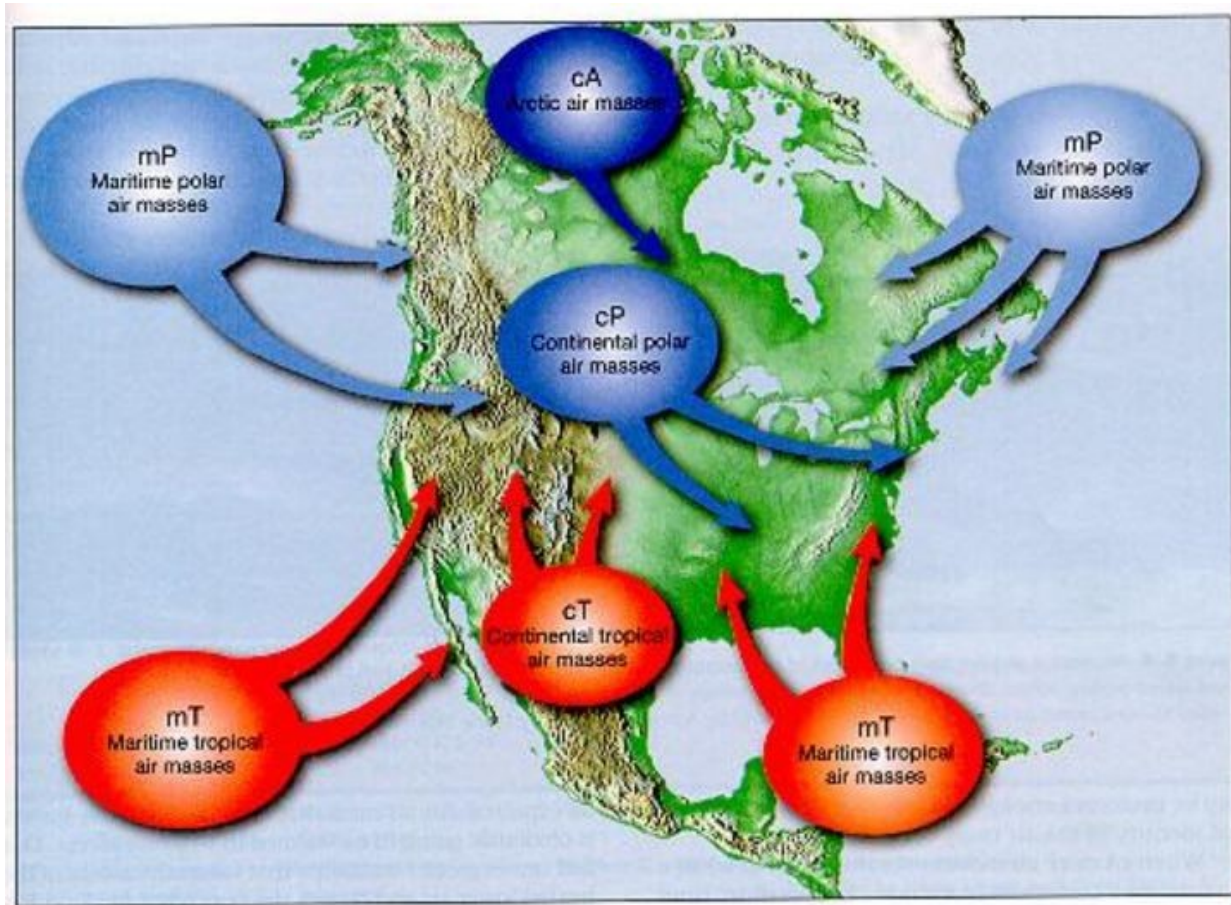


Figure 2.4 Air masses which affect Ohio
(from <http://www.geography.hunter.cuny.edu/~tbw/wc.notes/>, accessed September 2012)

There are several air mass types that affect the weather and climate of the region and produce heavy rainfall. The continental polar (cP) air mass, with origins from the arctic regions of Canada, is most common during winter. This air mass is often associated with a strong cold front passage and stratiform snowfall events. When this air mass type arrives, it often collides with a more humid air mass from warmer regions to the south. Low pressure (rising air) often results, and when combined with strong winds aloft, can produce heavy rainfall. As the cold air following this frontal passage affects the region during the cool season, widespread snowfall along with lake-effect snow events can occur.

The second type of air mass observed in the region is maritime polar (mP) which originates in the Gulf of Alaska and Pacific Ocean. This air mass often arrives on strong winds from the west and northwest, but is usually devoid of significant amounts of low-level moisture because its source region is relatively cool, hence it carries less moisture than warmer source regions, and it has traveled across several mountain ranges. This storm type often produces precipitation (rain and snow) at upstream locations, losing much of its low-level moisture on its way to the northern and central Plains. However, in extreme cases, moisture flowing north from the Gulf of Mexico can replenish low-level atmospheric moisture enough to produce heavy rainfall. If the storm system stalls over the region, flood producing rains can result. This storm type can occur anytime of the year, but is most common from fall through late spring.

Another type of air mass that affects the region and produces rainfall originates from the Gulf of Mexico and can contain copious amounts of atmospheric moisture in a conditionally unstable atmosphere. This type of air mass is called maritime tropical (mT). This type of air mass is most directly responsible for producing heavy rainfall in the region when interacting with a front and/or air mass of polar origins moving from the north. Generally, the frontal boundary is located just to the south or within the southern portions of Ohio, allowing high amounts of atmospheric moisture to stream in from the south, ascending over the frontal boundary. The release of the conditional instability in the atmosphere provides a very efficient mechanism to convert atmospheric moisture to rain on the ground. If this pattern is able to remain in place for an extended period and continue to tap into Gulf of Mexico moisture, flooding can result. This storm type is most common in summer to early fall.

3. Extreme Storm types

Ohio and the surrounding region have very active and varied weather patterns throughout the year. Consequently heavy rainfall events at both short and long durations are common. By far, the largest amount of moisture available for rainfall over the region comes from the Gulf of Mexico. The major types of extreme rainfall events in the region are produced by Mesoscale Convective Systems (MCS) (short durations and small area sizes) and synoptic events/fronts (large areas sizes and longer durations), and/or a combination of these.

3.1 Synoptic Fronts

The polar front and jet stream, which separate cool, relatively dry Canadian air to the north from warm, moist air to the south, is often a cause of heavy rainfall over large areas for long durations. This boundary provides large amounts of energy and strong storm dynamics as fronts move through the region. These features are strongest and most active over the area during fall, winter, and spring. A common type of storm occurrence with the polar front is an overrunning event. Frontal overrunning occurs when warm, humid air carried northward around the western edge of the Bermuda High circulation encounters the frontal zone and is forced to rise over the cooler, drier air mass to the north of the front (Figures 3.1 and 3.2). This forced ascent condenses atmospheric moisture in the warm air mass, forming clouds and producing precipitation while releasing latent heat. This process most often produces widespread rainfall over longer durations, but can also help enhance convection. Air that arrives at the frontal location is conditionally unstable, where the lower layers are much warmer and more humid than the air above. This conditionally unstable air mass needs a mechanism to initiate lift to begin energy release, leading to more instability and further up-lift. The forced ascent over the polar front initiates the lifting of the moist air mass, releasing its energy in the form of latent heat, and initiates the conversion of the atmospheric moisture to rainfall.



Figure 3.1 Typical Bermuda High circulation and its relation to Ohio (from http://www.meted.ucar.edu/reftra/seconus/summer/reg_1_1.htm, accessed October 2012)

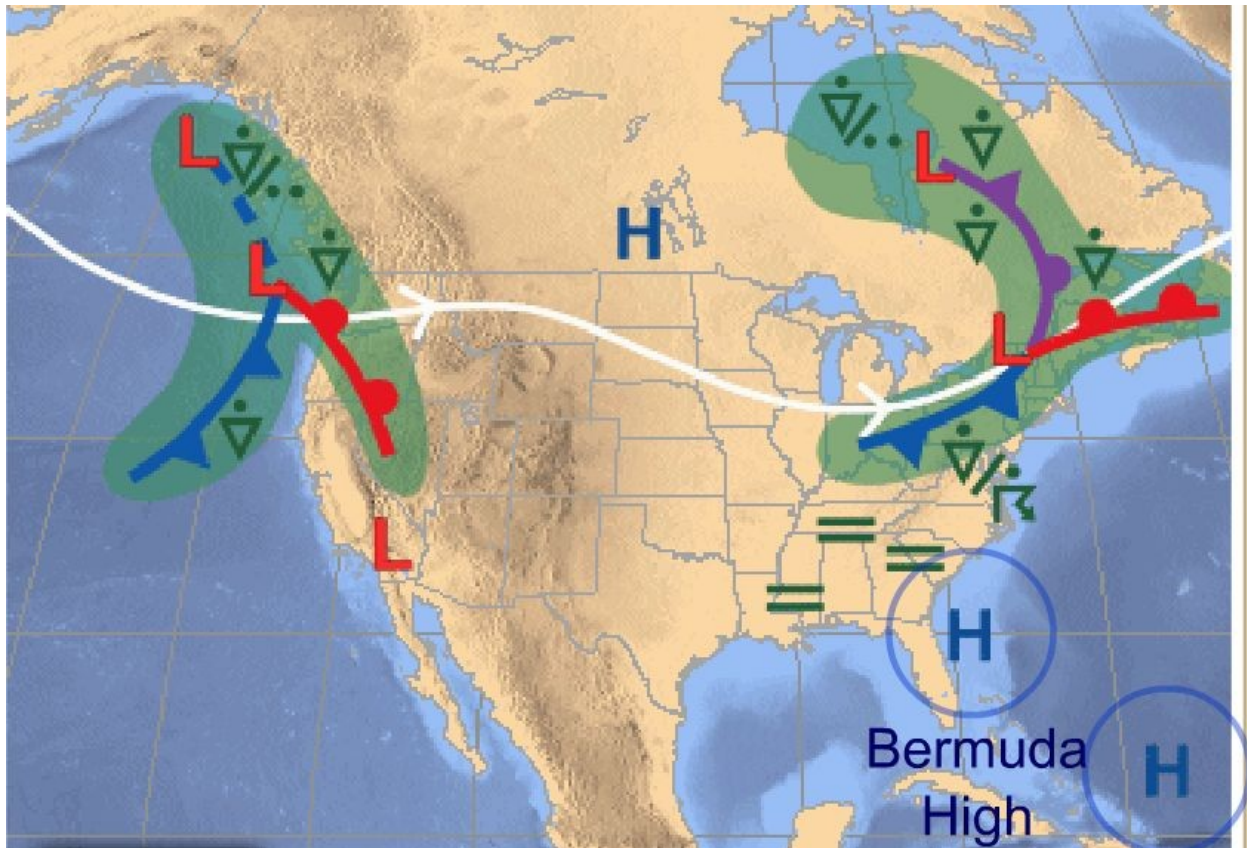


Figure 3.2 Bermuda High interaction with the Jet Stream and frontal boundaries over Ohio (from http://www.meted.ucar.edu/reftra/seconus/summer/reg_1_1.htm, accessed October 2012)

A stationary or slow moving cold or warm front located near Ohio will often provide the mechanism necessary for this warm, humid air mass to release its convective potential. When this occurs, rainfall is produced, sometimes associated with pockets of convection and extremely heavy rainfall. The pockets of heavy rain are usually associated with a minor wave riding along the frontal boundary, called a shortwave. These are not strong enough to move the overall large scale pattern, but instead add to the storm dynamics and energy available for producing rainfall within the storm area.

This type of storm environment (synoptic frontal) will usually not produce the highest rainfall rates over short durations, but instead leads to flooding situations as moderate to heavy rain continues to fall over the same regions for an extended period of time.

3.2 Mesoscale Convective Systems

Mesoscale Convective Systems (MCSs) are capable of producing extreme amounts of rainfall for short durations over small area sizes, generally 12 hours or less over area sizes of 500 square miles or less. The current understanding of MCS type storms has progressed tremendously with the advent of satellite technology starting in the 1970s and early 1980s. The current name of MCS was first applied in the late 1970s to this type of “flood producing”, strong

thunderstorm complexes (Maddox 1980). MCSs are so named because they are small in areal extent (10's to 100's of square miles), whereas synoptic storm events generally cover areas 100's to 1000's of square miles. MCSs also exhibit a distinctive signature on satellite imagery where they show rapidly growing cirrus clouds shields with very high cloud tops. Furthermore, the high level cloud shield associated with MCSs usually take on a nearly circular pattern about the size of the state of Ohio with constantly regenerating thunderstorms fed by a low-level jet bringing an inflow of atmospheric moisture from the Gulf of Mexico (Figure 3.3).

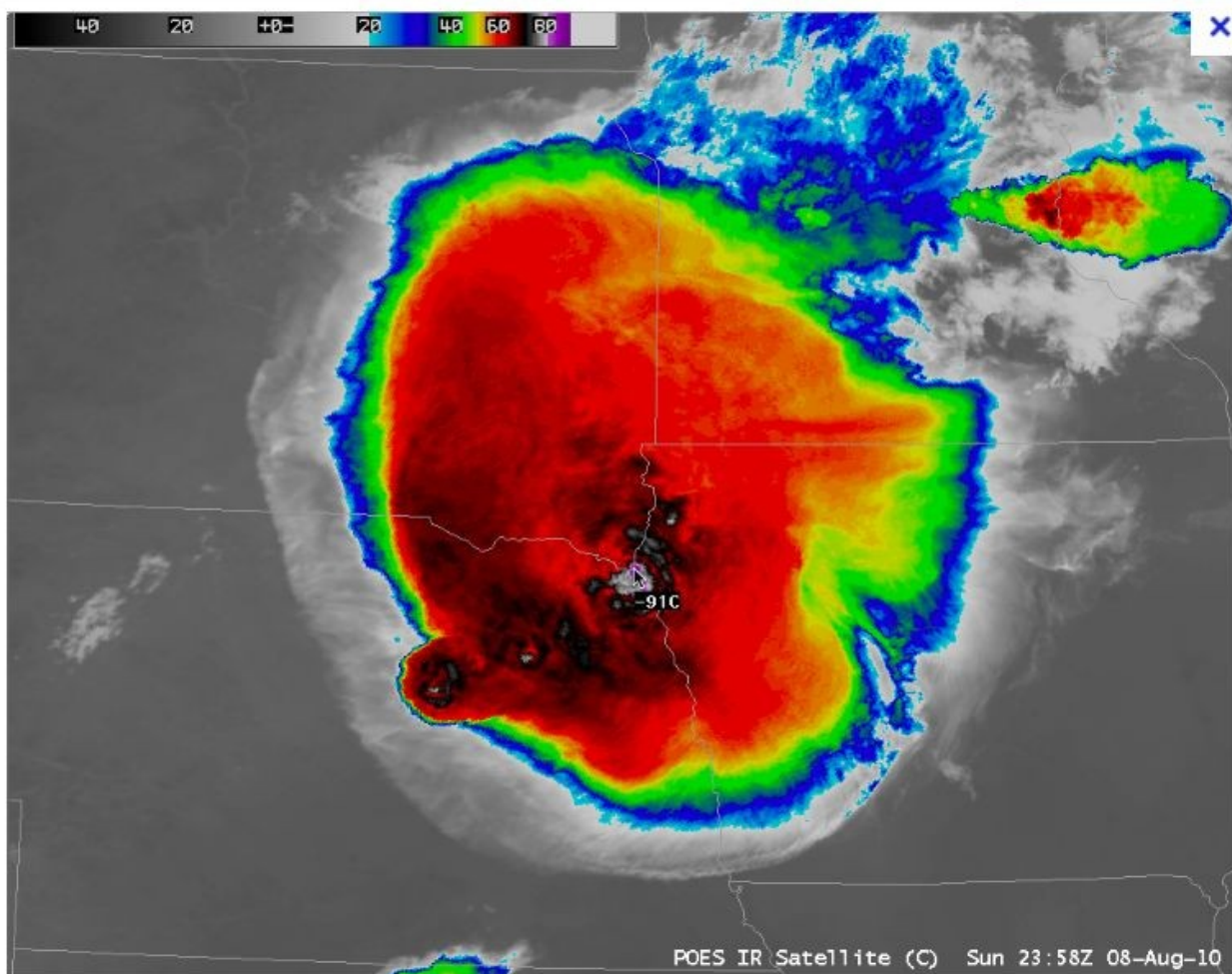


Figure 3.3 Color enhanced infrared satellite image of an MCS from August 8, 2010. Note the nearly circular structure, very cold cloud tops at the center (red, black, and center white colors), and a size similar to the state of Ohio.

(from <http://cimss.ssec.wisc.edu/goes/blog/archives/6337>, accessed September 2012)

The vast majority of MCSs have distinctive features and evolve in a standard pattern. A typical MCS begins as an area of thunderstorms over the Front Range of the Rocky Mountains or western High Plains. As these storms begin to form early in the day, the predominantly westerly winds aloft move them in a generally eastward direction. As the day progresses, the rain-cooled air below and around the storms begins to form a mesoscale high pressure area. This mesoscale

high moves along with the area of thunderstorms. During nighttime hours, the MCS undergoes rapid development as it encounters increasingly warm and humid air from the Gulf of Mexico, usually associated with the low-level jet 3,000-5,000 feet above the ground. The area of thunderstorms will often form a ring around the leading edge of the mesoscale high and continue to intensify, producing heavy rain, damaging winds, hail, and/or tornadoes. An MCS will often remain at a constant strength as long as the low level moisture transport continues to provide an adequate supply of moisture. Once the mesoscale environment begins to change, the storms weaken, usually around sunrise, but may persist into the early daylight hours.

MCSs are included in the more general definition of Mesoscale Convective Complexes (MCCs), which include a wider variety of mesoscale sized storm systems, such as squall lines and MCSs that do not fit the strict definition of size, duration, and/or appearance on satellite imagery. MCSs primarily form during the warm season (May through September) around the Ohio region.

Many of the storms previously analyzed by the USACE and NWS Hydrometeorological Branch in support of pre-1979 PMP research have features that indicate they were most likely MCCs or MCSs. However, this nomenclature had not yet been introduced into the scientific literature, nor were the events fully understood. For Ohio, the MCS storm type is the controlling storm type for most of the watersheds less than 500-square miles. In addition, intense convection similar to this storm type can occur within an overall synoptic frontal event. This can lead to intense areas of embedded rainfall within the overall lighter rainfall pattern. This combination of synoptic and convective storm types is very important for determining PMP values for larger watersheds in the region.

4. Extreme Storm Identification

4.1 Storm Search Area

A comprehensive storm search covering Ohio and regions surrounding Ohio was conducted as part of this study, which was built extensively off other site-specific and regional PMP studies in the region. This included an analysis of all extreme rainfall storms in meteorological and topographically similar regions, where extreme rainfall storms similar to those that could occur over any part of Ohio were observed. The storm search results were inclusive through the first half of 2012 and include all 12 months of the year. The domain used was contained within the longitude-latitude box approximately from 49.0°N 102.0°W to 33.0°N 75.0°W, with exclusion of orographic regions along the Appalachian Mountains (Figure 4.1). This insured a large enough area was analyzed to capture all significant storms that could potentially influence the final PMP values for the state.

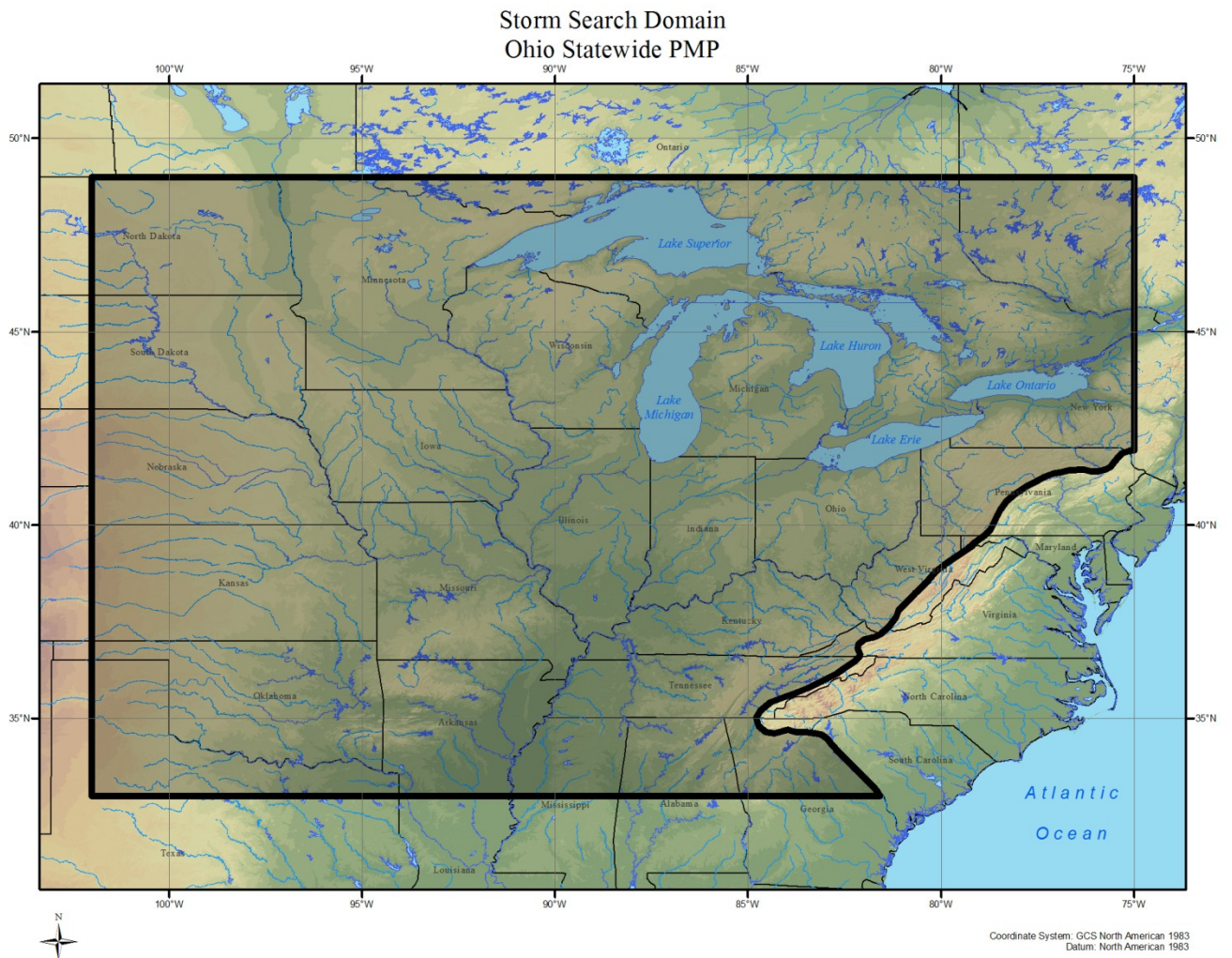


Figure 4.1 Storm search domain used for Ohio

4.2 Data Sources

AWA storm searches were conducted by searching the National Climatic Data Center (NCDC) hourly and daily rainfall records for maximum rainfall amounts that occurred during 6-hour, 24-hour/1-day, and 72-hour/3-day periods within the storm search domain. Further searches were conducted from additional sources listed below:

1. Cooperative Summary of the Day / TD3200 through 2011. These data are published by the National Climatic Data Center (NCDC)
2. Hourly Weather Observations published by NCDC, U.S. Environmental Protection Agency, and Forecast Systems Laboratory (now National Severe Storms Laboratory)
3. NCDC Recovery Disk
4. Hydrometeorological Reports (e.g., USGS, Bureau of Reclamation)
5. Corps of Engineers Storm Studies
6. Other data published by state climate office
7. American Meteorological Society journals
8. Various weather books
9. Data from supplemental sources, such as Community Collaborative Rain, Snow, and Hail Network (COCORAHS), Weather Underground, Forecast Systems Laboratories, Remote Automatic Weather Stations (RAWS), etc.

4.3 Storm Search Method

The primary storm search began with identifying hourly and daily stations that have reliable rainfall data within the storm search area described previously. These stations were evaluated to identify the largest 1-, 6-, 12-hour and 1-, 2-, 3-day precipitation totals. Other reference sources such as HMRS 51 and 55A, USACE storm reports, reference books regarding Ohio weather and flooding, and USGS reports were reviewed to identify other dates with large rainfall amounts and/or large floods for locations within the storm search domain. The initial cut-off criterion for storms to make the list of significant storms (referred to as the long storm list) were events that exceeded the 100-year return frequency value for the specified duration at the storm location.

The resulting long storm list was extensively quality controlled to ensure that only the highest storm rainfall values for each event were selected and that each event was transpositionable to at least one of the grid points in Ohio. Other quality control checks eliminated such things as duplicate storm centers and rainfall amounts which were accumulations. Storms were then grouped by duration for further analysis and comparison by storm type.

Figures 4.2-4.4 display the long storm list locations in relation to the state of Ohio by duration and represents an initial assessment of all the storms found during the initial storm search that were considered in the PMP development. The long storm list included 656 storm events extending from the late 1800s through 2012.

Locations of Major Storm Events - 6 Hour
Ohio Long List

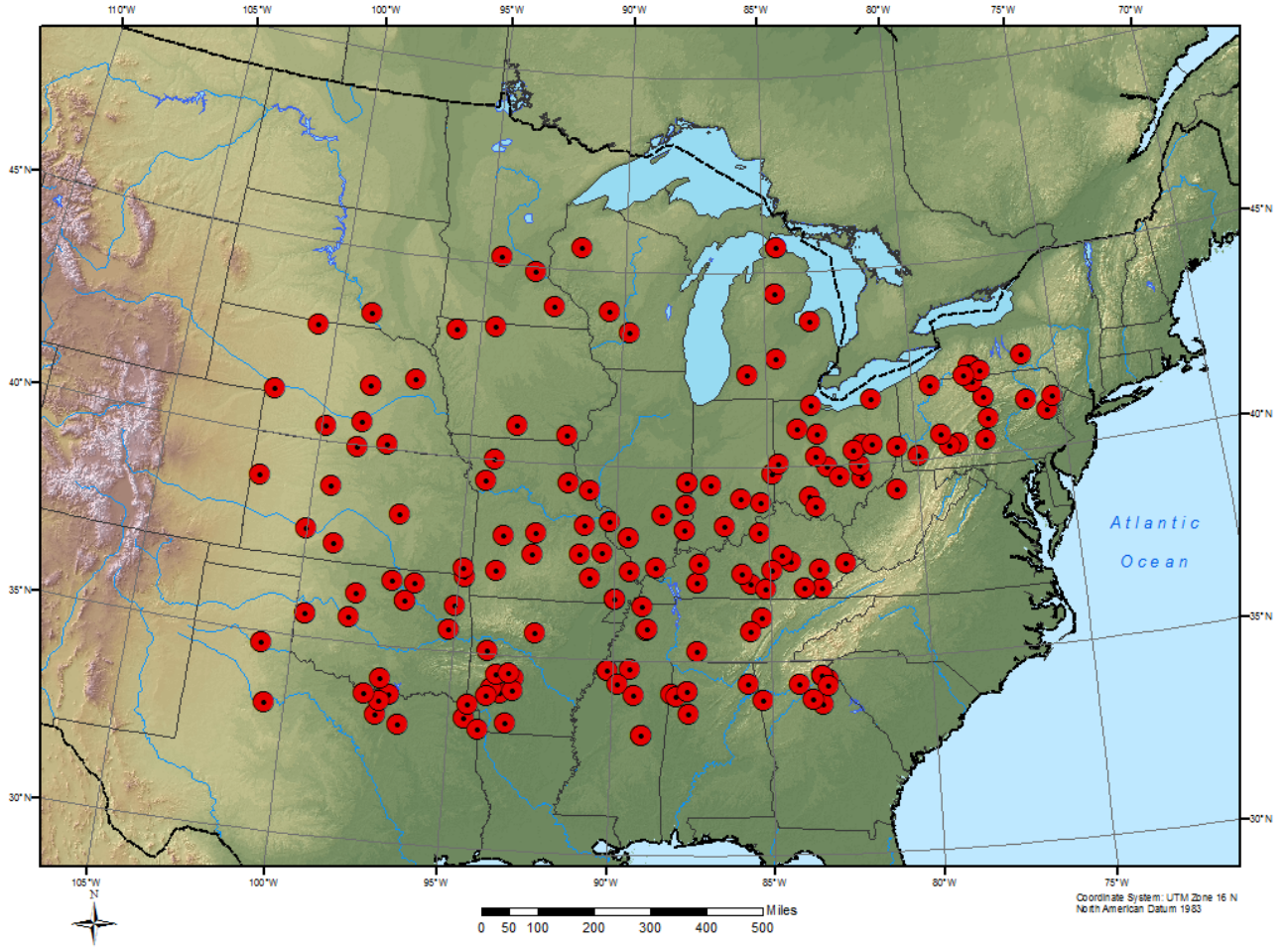


Figure 4.2 Ohio long list storm locations at the 6-hour duration

Locations of Major Storm Events - 1 Day
Ohio Long List

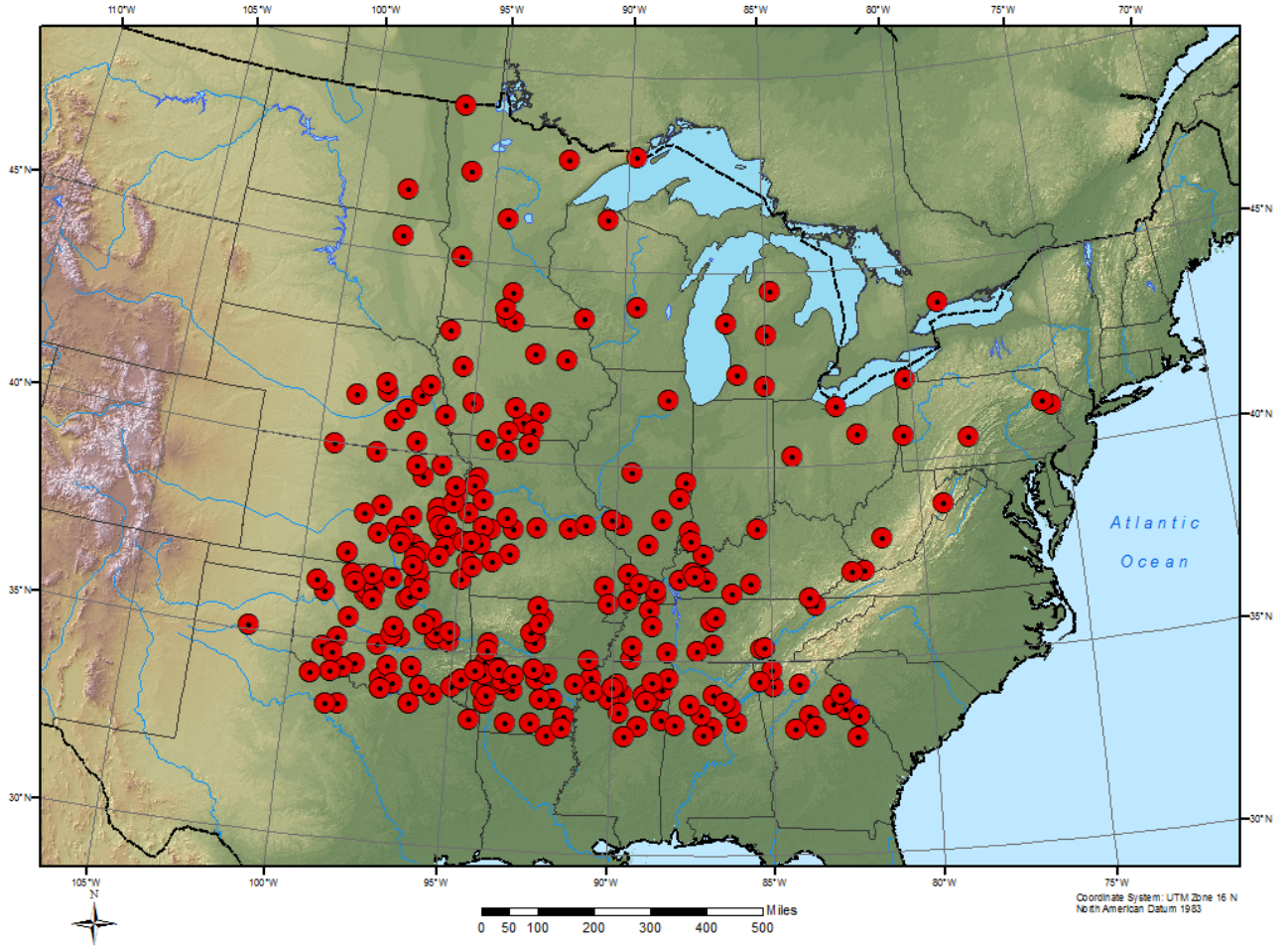


Figure 4.3 Ohio long list storm locations at the 1-day duration

Locations of Major Storm Events - 3 Day
Ohio Long List

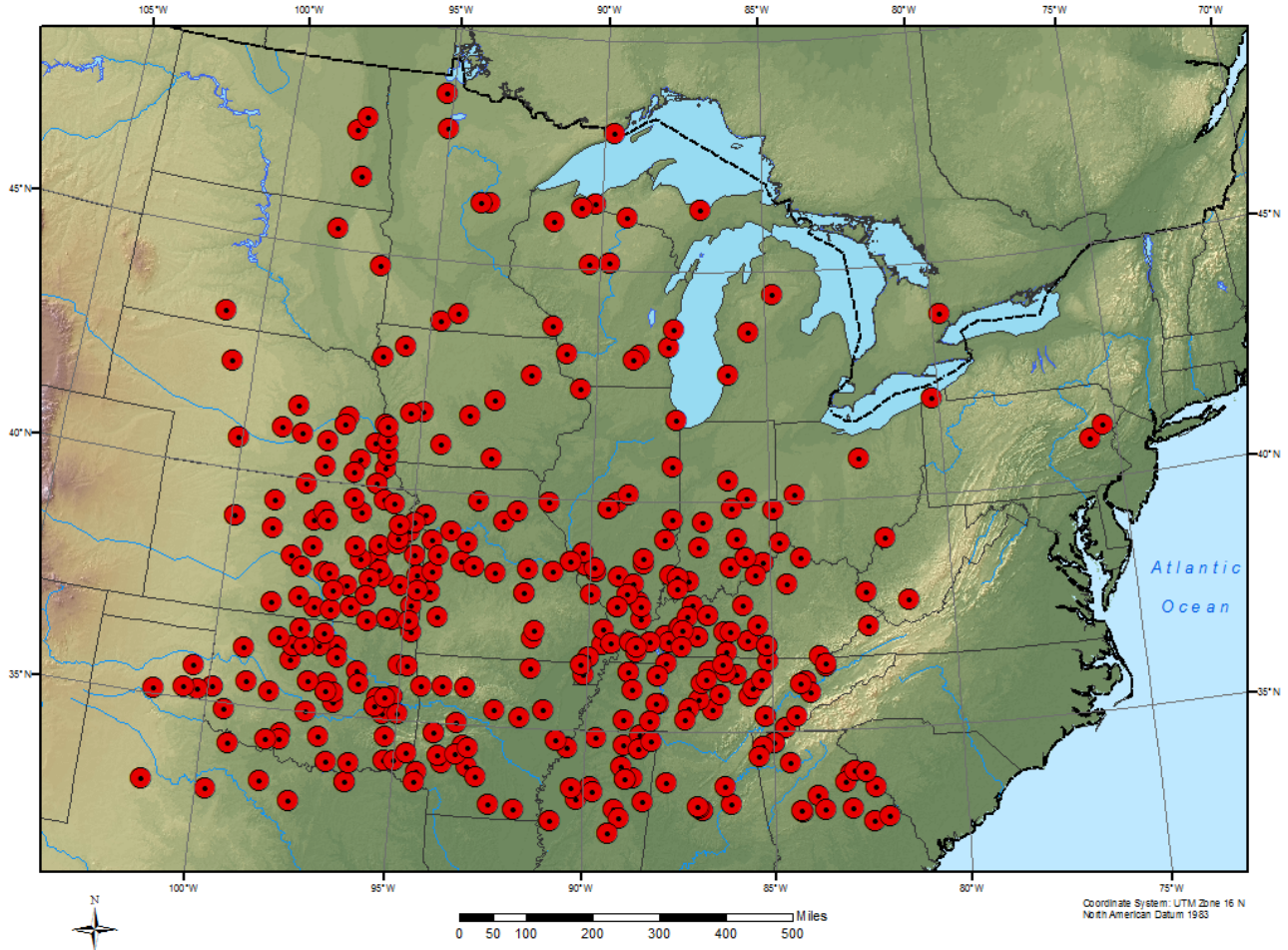


Figure 4.4 Ohio long list storm locations at the 3-day duration

4.4 Developing the Intermediate Short List of Extreme Storms

The long storm list was very extensive, with 656 potentially significant storms identified. A multiple step process was followed to produce a comprehensive list of major storms across the region. The process also eliminated smaller events that would not be significant for determining PMP values at any area size or duration after standard adjustments were applied. Initially, all storms previously analyzed in the HMR reports or by the USACE were placed on an intermediate storm list. The remaining long list storms were sorted by maximum rainfall amount. Of those events with maximum rainfall reported at the same locations, only the largest event was kept. From this list, only storms that were within approximately 65% of the largest events over a given duration were retained, as any storms smaller than that has virtually no chance of driving PMP values, even after standard adjustments. Further analysis was conducted to verify that each storm was transpositionable to one or more grid points, was not orographically influenced, or had other unique factors that would not allow it to be useable in the PMP analysis for Ohio. This list of storms comprised the intermediate storm list. Each storm on this list was then subjected to further analysis and comparison. Each of these storms was compared to the largest events at the appropriate durations (6-, 24-, and 72-hours), not only for point location, but also at the area sizes relevant for Ohio (100-, 200-, 500-, and 1,000-square miles). Storms on this list were subsequently further analyzed and pruned to produce a short list of storms which were used to derive the PMP values for each of the 23 grid points. The winnowing process sometimes eliminates fairly large storms, i.e. storms with extreme rainfall amounts, when there is an even larger one in the database applicable for some area size or specific duration.

4.5 Short Storm List Derivation

The final short storm list used to determine the PMP values for Ohio was derived following the process described above and by analyzing the results of previous PMP studies in regions similar to Ohio. These studies include the following: FERC Michigan/Wisconsin regional PMP study (1993), Nebraska statewide PMP study (2008), Quad Cities regional PMP study (2012), the Tarrant Regional Water District PMP (2011, 2012), and the Wyoming statewide PMP study (in progress as of February 2013).

These analyses resulted in the final short storm list used to derive the PMP values at each of the 23 grid points. Note, not all storms were moved to all 23 grid points. Instead, each storm was assigned individual transposition limits based on its meteorological and topographical characteristics versus each grid point location. Some storms were used at all grid points while others were restricted to a limited number of grid points.

The short storm list evaluations considered all 12 months of the year. However, the final PMP results are considered all-season and are valid for use from May through October and therefore should not be combined with snowpack to produce a cool-season

PMF. Table 4.1 shows the short storm list and Figure 4.5 displays the locations of the storms. The area southwest of Ohio is relatively flat and open to direct moisture flow from the Gulf of Mexico. This region produces the majority of PMP-type storms which are transpositionable to Ohio and Figure 4.5 shows that the majority of the short list storms occurring this region. The AWA Storm Number is used to identify each storm used in this study to derive PMP values.

Table 4.1 Ohio statewide PMP short storm list in chronological order

Storm Name	State	AWA Storm Number	Lat	Lon	Year	Month	Day	Max Rainfall	Precipitation Source
JEFFERSON	OH	1	40.8017	-82.0223	1878	9	10	15.00	OR 9-19
LARRABEE	IA	3	42.8608	-95.5453	1891	6	23	13.00	MR 4-2
GREELEY	NE	5	41.5500	-98.5333	1896	6	4	12.30	MR 4-3
WOODBURN	IA	9	41.0120	-93.5991	1903	8	24	15.50	MR 1-10
BONAPARTE	IA	10	40.7667	-91.7500	1905	6	10	12.10	UMV 2-5
MEEKER	OK	13	35.5034	-96.9028	1908	10	19	16.23	SW 1-11
BEAULIEU	MN	14	47.3000	-95.9000	1909	7	18	10.50	UMV 1-11A
IRONWOOD	MI	15	46.4500	-90.1833	1909	7	21	13.20	UMV 1-11B
COOPER	MI	18	42.3764	-85.6103	1914	8	31	12.60	GL 2-16
NEOSHO FALLS	KS	19	38.0820	-95.7010	1926	9	12	14.00	SW 2-1
BOYDEN	IA	20	43.1900	-96.0100	1926	9	17	24.00	MR 4-24
CHEYENNE	OK	25	35.6100	-99.6700	1934	4	3	23.00	SW 2-11
NEWCOMERSTOWN	OH	29	40.2723	-81.6060	1935	8	6	12.70	OR 9-11
GRANT TOWNSHIP	NE	30	42.2400	-96.5900	1940	6	3	13.00	MR 4-5
INDEX	AR	31	33.5471	-94.0419	1940	6	30	11.50	LMV 4-25
HALLETT	OK	32	36.2000	-96.6000	1940	9	2	24.00	SW 2-18
HAYWARD	WI	34	46.0130	-91.4846	1941	8	28	15.00	UMV 1-22
WARNER	OK	35	35.4900	-95.3100	1943	5	6	25.00	SW 2-20
MOUNDS	OK	37	35.8770	-96.0610	1943	5	16	17.00	SW 2-21
STANTON	NE	40	41.8670	-97.0500	1944	6	10	17.30	MR 6-15
COLLE CAMP	MO	44	38.4600	-93.2027	1946	8	12	19.40	MR 7-2A
COLLINSVILLE	IL	45	38.6717	-89.9800	1946	8	12	18.70	MR 7-2B
HOLT	MO	47	39.4528	-94.3422	1947	6	18	17.60	MR 8-20
DUMONT	IA	57	42.7519	-92.9755	1951	6	25	12.00	UMV 3-29
COUNCIL GROVE	KS	58	38.6600	-96.4900	1951	7	9	18.50	MR 10-2
KELSO	MO	59	37.1906	-89.5495	1952	8	11	13.00	UMV 3-30
PARIS WATERWORK	IN	63	39.0500	-87.7000	1957	6	27	12.40	HMB-V18
IDA GROVE	IA	70	42.3167	-95.4667	1962	8	30	12.85	FERC MI/WI
COLLEGE HILL	OH	71	40.0854	-81.6479	1963	6	3	19.39	SPAS 1226
DAVID CITY	NE	72	41.2132	-97.0710	1963	6	24	15.98	SPAS 1030
EDGERTON	MO	75	40.4125	-95.5125	1965	7	18	20.76	SPAS 1183
WOOSTER	OH	78	40.9146	-81.9729	1969	7	4	14.95	SPAS 1209
ENID	OK	83	36.3805	-97.8683	1973	10	10	19.45	SPAS 1034
LOUISVILLE	MS	88	33.1167	-89.0500	1979	4	12	22.07	SPAS 1227
CLYDE	TX	92	32.4790	-99.4790	1981	10	12	23.00	SPAS 1184
BIG FORK	AR	94	35.8708	-92.1208	1982	12	1	15.92	SPAS 1219
FOREST CITY	MN	96	45.2394	-94.5404	1983	6	20	17.00	SPAS 1035
BIG RAPIDS	MI	100	43.6125	-85.3125	1986	9	9	13.42	SPAS 1206
MINNEAPOLIS	MN	102	44.8890	-93.4021	1987	7	23	11.55	SPAS 1210
AURORA COLLEGE	IL	112	41.7500	-88.3333	1996	7	16	18.24	SPAS 1029
FALL RIVER	KS	120	37.6300	-96.0500	2007	6	30	25.50	SPAS 1228
HOKAH	MN	121	43.8125	-91.3625	2007	8	18	18.32	SPAS 1048
DOUGLASVILLE	GA	125	33.8700	-84.7600	2009	9	19	25.37	SPAS 1218
WARNER PARK	TN	126	36.0611	-86.9056	2010	4	30	19.71	SPAS 1208
DUBUQUE	IA	127	42.4400	90.7500	2011	7	27	15.14	SPAS 1220

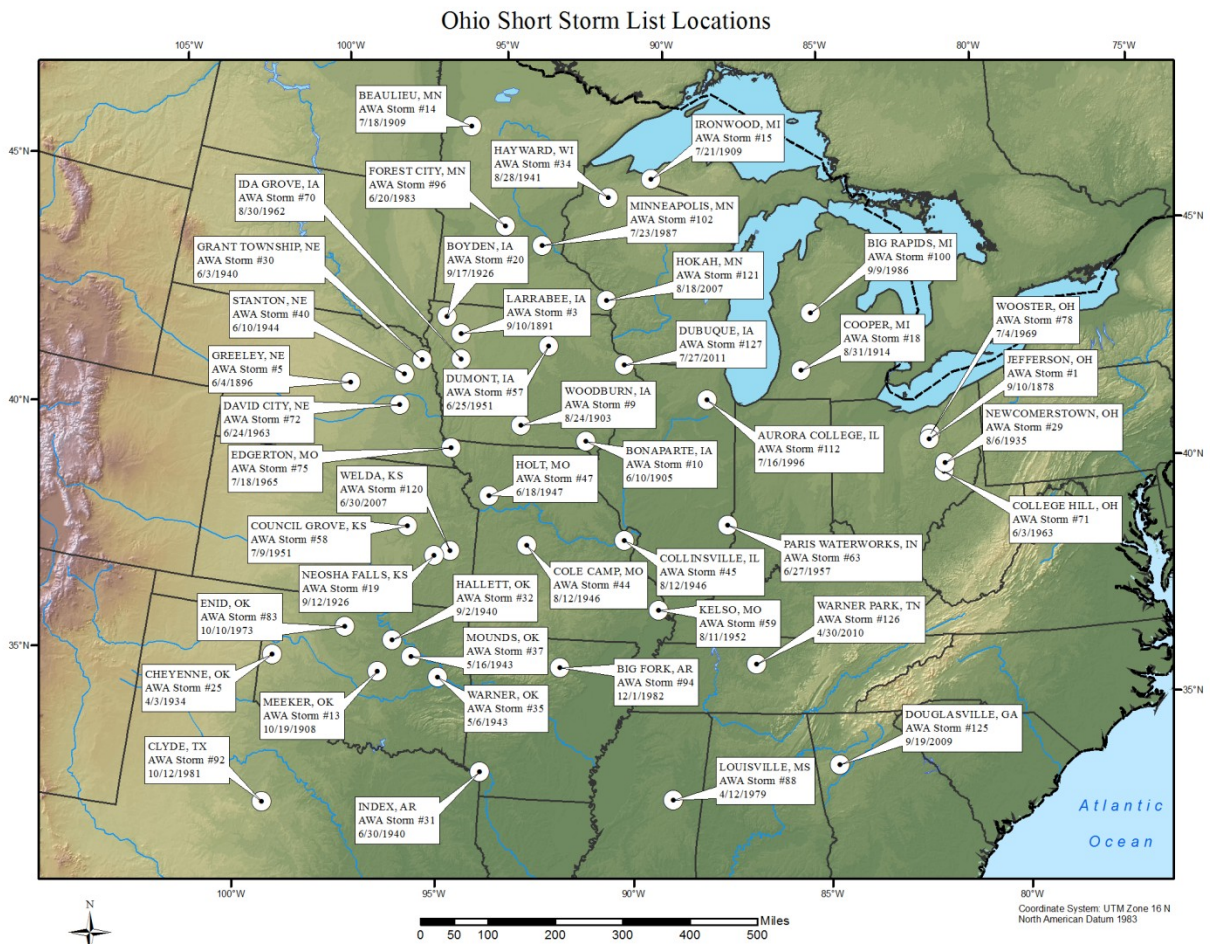


Figure 4.5 Ohio statewide PMP short storm list locations

4.5.1 New SPAS Storm Analyses

Results of the storm search and short storm list development identified 10 storms important for PMP derivation which had not been previously analyzed by the NWS/USACE or AWA, or were in need of re-analysis using SPAS. Seven SPAS storms analyzed in previous AWA PMP studies were included on the short storm list. The last column in Table 4.1 lists the source of the precipitation analysis for each storm event. The seven storms analyzed in previous AWA studies and the 10 newly analyzed SPAS storm events are referenced with a SPAS number (e.g., SPAS 1226)¹. Each SPAS storm analysis produced the required storm Depth-Area-Duration (DAD) values (see Section 5

¹ The precipitation/storm analysis source for each short list storm is listed in Table 4.1. SPAS references a SPAS analysis number, FERC MI/WI refers to the FERC Michigan/Wisconsin regional PMP study, while the remaining are the reference nomenclature from the NWS/USACE storm studies files.

and Appendix G for a full description of the SPAS storm analysis process). In addition, the SPAS analysis produced all the necessary data required to evaluate and utilize the storm in the PMP derivation process.

5. Storm Depth-Area-Duration Analyses for New Storms

Full storm analyses need to be completed for newly identified extreme rainfall events without published DAD analyses. SPAS was used to compute these data. Table 5.1 lists the storms used in this study which were analyzed using the SPAS program.

There are two main steps in a DAD analysis: 1) Creation of high-resolution hourly precipitation grids and 2) computation of Depth-Area (DA) rainfall amounts for various durations. Reliability of results from step 2) depends on the accuracy of step 1). Historically the process has been very labor intensive. SPAS utilizes Geographic Information Systems (GIS) concepts to create more spatially-oriented and accurate results in an efficient manner (step 1). Furthermore, the availability of NEXRAD data allows SPAS to better account for the spatial and temporal variability of storm precipitation among rain gauge locations for events occurring since the early 1990s. Prior to NEXRAD, the NWS developed and used a method based on the research of several scientists (Corps of Engineers, 1936-1973). Because this process has been the standard for many years and holds merit, the DAD analysis process developed within the SPAS program attempts to mimic it as much as possible. By adopting this approach, some level of consistency between the newly analyzed storms and the hundreds of storms already analyzed can be achieved. Comparisons between the NWS DAD results and those computed using the new method for two storms (Westfield, MA, 1955 and Ritter, IA, 1953) indicated very similar results (see Appendix G for complete discussion, comparisons, and results).

Table 5.1 SPAS storms used in this study

Storm Name	State	AWA Storm Number	Lat	Lon	Year	Month	Day	Max Rainfall	SPAS Storm Number
COLLEGE HILL	OH	71	40.0854	-81.6479	1963	6	3	19.39	SPAS 1226
DAVID CITY	NE	72	41.2132	-97.0710	1963	6	24	15.98	SPAS 1030
EDGERTON	MO	75	40.4125	-95.5125	1965	7	18	20.76	SPAS 1183
WOOSTER	OH	78	40.9146	-81.9729	1969	7	4	14.95	SPAS 1209
ENID	OK	83	36.3805	-97.8683	1973	10	10	19.45	SPAS 1034
LOUISVILLE	MS	88	33.1167	-89.0500	1979	4	12	22.07	SPAS 1227
CLYDE	TX	92	32.4790	-99.4790	1981	10	12	23.00	SPAS 1184
BIG FORK	AR	94	35.8708	-92.1208	1982	12	1	15.92	SPAS 1219
FOREST CITY	MN	96	45.2394	-94.5404	1983	6	20	17.00	SPAS 1035
BIG RAPIDS	MI	100	43.6125	-85.3125	1986	9	9	13.42	SPAS 1206
MINNEAPOLIS	MN	102	44.8890	-93.4021	1987	7	23	11.55	SPAS 1210
AURORA COLLEGE	IL	112	41.7500	-88.3333	1996	7	16	18.24	SPAS 1029
FALL RIVER	KS	120	37.6300	-96.0500	2007	6	30	25.50	SPAS 1228
HOKAH	MN	121	43.8125	-91.3625	2007	8	18	18.32	SPAS 1048
DOUGLASVILLE	GA	125	33.8700	-84.7600	2009	9	19	25.37	SPAS 1218
WARNER PARK	TN	126	36.0611	-86.9056	2010	4	30	19.71	SPAS 1208
DUBUQUE	IA	127	42.4400	90.7500	2011	7	27	15.14	SPAS 1220

5.1 Data Collection

The areal extent of a storm's rainfall was evaluated using existing maps and documents along with plots of total storm rainfall. Based on the storm's spatial domain (longitude-latitude box), hourly and daily data were extracted for the specified area, date, and time. To account for the temporal variability in observation times at daily stations, the extracted hourly data must capture the entire observational period of all extracted daily stations. For example, if a station takes daily observations at 8:00 AM local time, then the hourly data needs to be complete from 8:00 AM local time the day prior. As long as the hourly data are sufficient to capture all of the daily station observations, the hourly variability in the daily observations can be properly addressed.

The daily database is comprised of data from NCDC TD-3206 (pre 1948) and TD-3200 (generally 1948 through present). The hourly database is comprised of data from NCDC TD-3240 and NOAAs Meteorological Assimilation Data Ingest System (MADIS). The daily supplemental database is largely comprised of data from "bucket surveys," local rain gauge networks (e.g., ALERT, USGS, COCORAHS, etc.) and daily gauges with accumulated data.

5.2 Mass Curves

The most complete rainfall observational dataset available is compiled for each storm. To obtain an hourly temporal resolution in the DAD results, it is necessary to distribute the daily precipitation observations (at daily stations) into hourly bins. This process has traditionally been accomplished by anchoring each of the daily stations to a single hourly timer station. However, this may introduce biases and may not correctly represent hourly precipitation at locations between hourly reporting stations. A preferred approach is to anchor the daily station to some set of the nearest hourly stations. This is accomplished using a spatially based approach that is called the spatially based mass curve (SMC) process.

5.3 Hourly or Sub-hourly Precipitation Maps

At this point, SPAS can either operate in its standard mode or in NEXRAD-mode to create high resolution hourly or sub-hourly (for NEXRAD storms) grids. In practice both modes are run when NEXRAD data are available so that a comparison can be made between the methods. Regardless of the mode, the resulting rainfall grids serve as the basis for the DAD computations.

5.4 Depth-Area-Duration Program

The DAD extension of SPAS runs from within a Geographic Resource Analysis Support System (GRASS) GIS environment² and utilizes many of the built-in functions for calculation of area sizes and average rainfall depths. The following is the general outline of the procedure:

1. Given a duration (e.g., x-hours) and cumulative precipitation, sum the appropriate hourly or sub-hourly precipitation grids to obtain an x-hour total precipitation grid starting with the first x-hour moving window.
2. Determine the x-hour precipitation total and its associated areal coverage, and then store these values. Repeat for various lower rainfall thresholds. Store the average rainfall depths and area sizes.
3. The result is a table of precipitation depth and associated area sizes for each x-hour window location. Summarize the results by moving through each of the area sizes and choosing the maximum precipitation amount. A log-linear plot of these values provides the DA curve for the x-hour duration.
4. Based on the log-linear plot of the rainfall DA curve for the x-hour duration, determine rainfall amounts for the standard area sizes for the final DAD table. Store these values as the rainfall amounts for the standard sizes for the x-duration period. Determine if the x-hour duration period is the longest duration period being analyzed. If it is not, analyze the next longest duration period by returning to step 1.
5. Construct the final DAD table with the stored rainfall values for each standard area for each duration period.

² Geographic Resource Analysis Support System is commonly referred to as GRASS. This is free Geographic Information System (GIS) software used for geospatial data management and analysis, image processing, graphics/maps production, spatial modeling, and visualization. GRASS is currently used in academic and commercial settings around the world, as well as by many governmental agencies and environmental consulting companies. GRASS is an official project of the [Open Source Geospatial Foundation](#).

6. Updated Data Sets Used in this Study

Several new data sets and technologies not available in the development of HMR 51 were employed as part of this study in the development of the PMP values. These include the updated dew point climatology for use in storm maximization and transposition, as well as the use of the HYSPLIT trajectory model to help in identifying the moisture source region for individual storm events. The identification and use of these provide significant improvements in storm rainfall adjustments, especially relating to the determination of each storm's moisture source and appropriate maximization factors.

6.1 Development of the Updated Dew Point Climatology

As part of previous AWA PMP studies, as well as this study, updated dew point climatologies have been developed. These updated maximum average dew point climatologies provide 20-year, 50-year, and 100-year return frequency values for 6-hour, 12-hour, and 24-hour durations. This process followed the same reasoning and use as described in the FERC Michigan/Wisconsin regional PMP study (1993), the Nebraska statewide PMP study (2008), the Tarrant Regional Water District (2011, 2012), the Wyoming statewide PMP study (in progress as of February 2013), and the Arizona statewide PMP study (in progress as of February 2013). The data used in the HMRs were outdated but more importantly did not adequately represent the atmospheric moisture available in the PMP storm environment. Discussion and analysis from those studies demonstrated that the data used in the HMRs to derive the maximization factors were inadequate³. The 12-hour persisting dew point values often missed or underestimated the atmospheric moisture available and hence led to overly conservative maximization calculations. The updated climatology more accurately represents the atmospheric moisture fueling storms by using average maximum dew point values observed over durations specific to each storm's rainfall duration. The average maximum dew point values for various durations replace the maximum 12-hour persisting dew point values. The process used to develop the climatology is discussed in this section and the final maps used in the maximization and transpositioning processes are provided in Appendix B.

6.1.1 Dew Point Temperature Interpolation Methodology

The updated maximum dew point climatology used here calculated monthly 6-, 12-, and 24-hour maximum average dew point temperatures that are spatially interpolated across the defined domain (Figure 6.1). A sophisticated interpolation procedure, within the GRASS GIS environment, was applied to dew point temperature data to reduce bulls-eye effects created from inverse distance weighting spatial distributions between known

³ Each of those studies has been reviewed by a BOC and accepted by the appropriate regulators or is in process of being completed.

data points and to incorporate terrain characteristics. The final dew point climatology maps and values underwent a manual smoothing process to ensure spatially continuity.

Construction of the maximum dew point climatology began with a search of archived NCDC hourly datasets for the 6-, 12-, and 24-hour maximum dew point temperatures for each reporting station within the defined search box (49°N, -87°W, 35°N, -62°W). A total of 137 hourly stations identified. Initial quality control limited stations to periods of record of 30-years or more. This resulted in 123 hourly stations being used in the development of the maximum dew point temperature analysis (Figure 6.2 and Table 6.1). A program was written to extract the station's monthly maximum dew point temperature for each year, known as the annual maximum series (AMS). The AMS for each month, at each station, served as input for calculating L-moment statistics. Using the generalized-extreme-value (GEV) distribution, the 20-yr, 50-yr, and 100-yr maximum dew point temperature values were calculated for each month for each station. The extracted dew point data were adjusted to represent the 15th of each month and adjusted to represent the 1,000mb dew point values. This was done in order to follow the same process used in the HMRs and allowed the data to represent the middle of the month. This allowed for the temporal movement of a given storm event to be moved two weeks towards the warm season and to normalize all storms to a standard level (i.e., 1,000mb or approximately sea level). Following accepted procedures by the FERC and appropriate state regulators in previous AWA PMP studies, the 100-year return frequency values were used in all storm maximization calculations. This results in the most conservative use of the available data, as they are the highest values of the three return frequencies and therefore result in the largest maximization factors⁴.

⁴ Note that each 1°F change in dew point temperature results in a 4-5% change in the resulting maximization factor. Generally, the difference between the 50-year and 100-year return frequency values is less than 1°F.

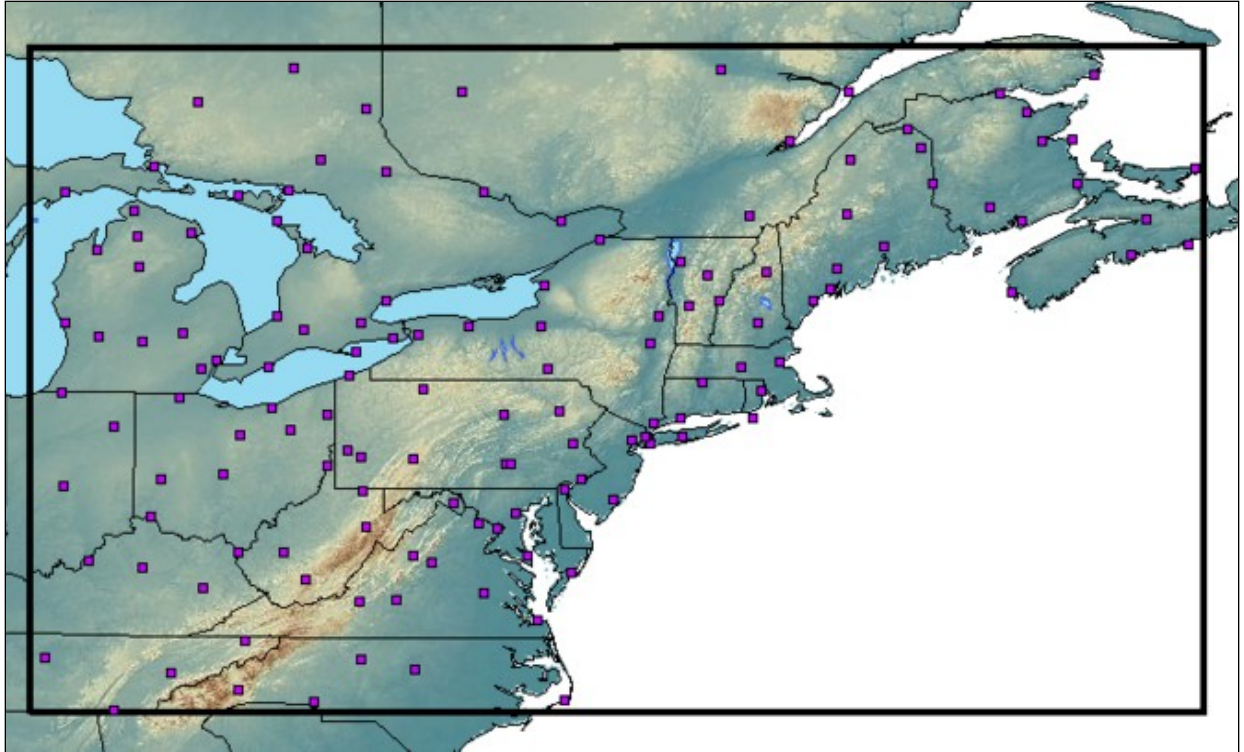


Figure 6.1 Hourly dew point temperature station locations used for the maximum dew point return frequency analysis

Table 6.1 Stations used in the maximum dew point climatology development

Station ID	Station Name	State	Latitude	Longitude	Elevation in Feet	Period of Record
CYCL	CHARLO	CN	48.000	-66.333	125	30
CYWA	PETAWAWA AP	CN	45.950	-77.317	427	36
BDL	HARTFORD	CT	41.933	-72.683	179	60
BDR	BRIDGEPORT	CT	41.167	-73.133	17	62
DCA	WASHINGTON	DC	38.850	-77.033	65	68
ILG	WILMINGTON	DE	39.667	-75.600	80	61
SBN	SOUTH BEND	IN	41.700	-86.317	773	61
FWA	FORT WAYNE	IN	41.000	-85.200	828	61
IND	INDIANAPOLIS	IN	39.733	-86.283	808	61
JKL	JACKSON	KY	37.600	-83.317	1358	28
LEX	LEXINGTON	KY	38.033	-84.600	989	61
SDF	LOUISVILLE	KY	38.183	-85.733	488	61
ORH	WORCESTER	MA	42.267	-71.867	1011	60
BOS	BOSTON	MA	42.367	-71.033	29	64
NHK	PATUXENT R.NAS	MD	38.286	-76.412	39	64
BWI	BALTIMORE	MD	39.183	-76.667	155	60
CAR	CARIBOU	ME	46.867	-68.017	628	61
AUG	AUGUSTA	ME	44.316	-69.797	350	32
NHZ	BRUNSWICK NAS	ME	43.892	-69.939	75	32
PWM	PORTLAND	ME	43.650	-70.317	63	61
GNR	GREENVILLE	ME	45.462	-69.595	1002	11
KFVE	FRENCHVILLE AROOSTOOK AP	ME	47.283	-68.317	988	21
KHUL	HOULTON INTL AP	ME	46.133	-67.783	496	67
BGR	BANGOR	ME	44.800	-68.817	192	37
KPLN	PELLSTON	MI	45.564	-84.793	715	28
APN	ALPENA	MI	45.067	-83.567	693	50
TVC	TRAVERSE CITY	MI	44.737	-85.570	630	61
KP75	MANISTIQUE	MI	45.950	-86.230	584	61
ANJ	SAULT STE MARIE	MI	46.479	-84.357	721	61
MKG	MUSKEGON	MI	43.167	-86.233	633	61
LAN	LANSING	MI	42.783	-84.600	874	61
GRR	GRAND RAPIDS	MI	42.883	-85.517	803	46
HTL	HOUGHTON LAKE	MI	44.367	-84.683	1160	45
DET	DETROIT CITY APRT	MI	42.407	-83.009	626	61
FNT	FLINT	MI	42.967	-83.733	766	61
CYFC	BLISSVILLE	na	45.617	-66.550	73	54
CYCH	CHATHAM	NB	47.017	-65.450	112	51
CYQM	MONCTON	NB	46.117	-64.683	250	67
CYSJ	ST JOHN	NB	45.317	-65.883	352	54
AVL	ASHEVILLE	NC	35.433	-82.550	2170	61
HSE	HATTERAS	NC	35.232	-75.623	11	33
CLT	CHARLOTTE	NC	35.213	-80.949	769	61
GSO	GREENSBORO	NC	36.083	-79.950	886	61
RDU	RALEIGH-DURHAM	NC	35.867	-78.783	441	61
LEB	LEBANON	NH	43.633	-72.317	571	32
CON	CONCORD	NH	43.200	-71.500	346	61
MWN	MT. WASHINGTON	NH	44.267	-71.300	6273	32
ACY	ATLANTIC CITY	NJ	39.450	-74.567	67	51
EWR	NEWARK	NJ	40.700	-74.167	30	61
CWUR	TRURO AUTO	NS	45.367	-63.217	132	28

Table 6.1 Stations used in the maximum dew point climatology development
(continued)

Station ID	Station Name	State	Latitude	Longitude	Elevation in Feet	Period of Record
CWBV	BEAVER ISLAND AUTO	NS	44.817	-62.333	32	24
CWDA	MCNABS ISLAND	NS	44.600	-63.533	56	24
RME	GRIFFISS AFB	NY	43.233	-75.400	505	32
ALB	ALBANY	NY	42.750	-73.800	292	64
ISP	ISLIP	NY	40.795	-73.100	108	32
JFK	NEW YORK-KENNEDY	NY	40.650	-73.783	22	61
HPN	WHITE PLAINS	NY	41.062	-73.704	379	60
GFL	GLENS FALLS	NY	43.338	-73.611	320	32
SYR	SYRACUSE	NY	43.117	-76.117	407	64
ART	WATERTOWN	NY	43.989	-76.026	323	32
BGM	BINGHAMTON	NY	42.217	-75.983	1629	61
BUF	BUFFALO	NY	42.933	-78.733	706	63
ROC	ROCHESTER	NY	43.117	-77.667	555	61
TOL	TOLEDO	OH	41.600	-83.800	692	54
CAK	AKRON CANTON	OH	40.917	-81.433	1236	61
CMH	COLUMBUS	OH	40.000	-82.883	833	61
YNG	YOUNGSTOWN	OH	41.267	-80.667	1186	61
CLE	CLEVELAND	OH	41.400	-81.850	805	61
LUK	CINCINNATI/LUNK	OH	39.100	-84.433	489	61
MFD	MANSFIELD	OH	40.817	-82.517	1296	61
DAY	DAYTON	OH	39.900	-84.200	1003	61
CYVV	WIARTON	ON	44.750	-81.100	728	59
CWAJ	ERIEAU	ON	42.250	-81.900	584	23
CYZE	GORE BAY	ON	45.883	-82.567	633	36
CYTS	TIMMINS	ON	48.567	-81.383	968	36
CYSB	SUDBURY	ON	46.633	-80.800	1142	36
CYHM	HAMILTON	ON	43.167	-79.933	778	36
CYXU	LONDON	ON	43.033	-81.150	912	36
CYYB	NORTH BAY	ON	46.367	-79.417	1214	59
YOW	OTTAWA	ON	45.317	-75.667	374	32
CYXR	EARLTON	ON	47.700	-79.850	797	36
CWBE	KILLARNEY (AUTO)	ON	45.967	-81.483	643	24
CYTZ	TORONTO CITY CENTER	ON	43.633	-79.400	253	36
CYLD	CHAPLEAU	ON	47.833	-83.433	1404	36
IPT	WILLIAMSPORT	PA	41.250	-76.917	525	61
BFD	BRADFORD	PA	41.800	-78.633	2150	52
ABE	ALLENTOWN	PA	40.650	-75.433	385	61
CXY	HARRISBURG	PA	40.218	-76.856	340	61
ERI	ERIE	PA	42.083	-80.183	737	61
PHL	PHILADELPHIA	PA	39.883	-75.250	28	68
AVP	WILKES-BARRE AP	PA	41.333	-75.733	948	60
JST	JOHNSTOWN	PA	40.315	-78.831	2269	32
PIT	PITTSBURGH	PA	40.500	-80.217	1225	57
AGC	ALLEGHENY CO.ARPT	PA	40.350	-79.933	1253	32
MDT	MIDDLETWN/HARRISB	PA	40.196	-76.773	303	32
CWEW	EAST BALTIC AUTO	PE	46.433	-62.167	201	15
CWRZ	CAP D'ESPOIR	PQ	48.417	-64.317	51	24
CYVO	VAL DOR	PQ	48.050	-77.783	1109	52
CYRJ	ROBERVAL	PQ	48.517	-72.267	591	36
YSC	SHERBROOKE	QC	45.433	-71.683	791	32

Table 6.1 Stations used in the maximum dew point climatology development
(continued)

Station ID	Station Name	State	Latitude	Longitude	Elevation in Feet	Period of Record
PVD	PROVIDENCE	RI	41.733	-71.433	62	61
BID	BLOCK ISL.(AMOS)	RI	41.167	-71.583	118	32
TYS	KNOXVILLE	TN	35.817	-83.983	980	61
TRI	BRISTOL	TN	36.483	-82.400	1525	61
CHA	CHATTANOOGA	TN	35.033	-85.200	688	61
BNA	NASHVILLE	TN	36.117	-86.683	605	61
LYH	LYNCHBURG	VA	37.333	-79.200	937	61
IAD	WASH-DULLES	VA	38.950	-77.450	323	61
ORF	NORFOLK	VA	36.900	-76.200	30	61
RIC	RICHMOND	VA	37.500	-77.333	177	61
WAL	WALLOPS ISLAND	VA	37.933	-75.467	15	43
SHD	STAUNTON	VA	38.267	-78.850	1201	14
CHO	CHARLOTTESVILLE	VA	38.133	-78.450	640	32
BTV	BURLINGTON	VT	44.467	-73.150	340	61
MPV	MONTPELIER	VT	44.200	-72.567	1158	32
RUT	RUTLAND (AWOS)	VT	43.533	-72.950	787	32
BKW	BECKLEY	WV	37.783	-81.117	2514	46
EKN	ELKINS	WV	38.883	-79.850	1997	61
HTS	HUNTINGTON	WV	38.367	-82.550	838	48
MRB	MARTINSBURG	WV	39.404	-77.975	531	32
CRW	CHARLESTON	WV	38.367	-81.600	982	60
MGW	MORGANTOWN	WV	39.650	-79.917	1247	32
HLG	WHEELING	WV	40.183	-80.650	1194	32

6.1.2 Dew Point Adjustments to 1000mb and to Mid-Month

Once the dew point station data were collected and organized, the next step reduced all data to a standard level for comparison and analysis purposes. This was done following the accepted methodology of reducing the dew point data following the moist pseudo-adiabatic line to a standard level - in this case 1,000mb. Furthermore, dew point data were adjusted to the 15th of each month so the dew point climatology maps represented mid-month values. An example is shown in Table 6.2. The table shows the original station data, the data adjusted to the 15th, and the data adjusted to 1,000mb.

Table 6.2 Original station dew point data (°F), the adjusted 15th data, and the 1,000mb data for the 20-yr, 50-yr, and 100-yr frequencies

	20-year	50-year	100-year
Station Data	76.13	76.65	76.94
15th Data	76.10	76.62	76.91
1000 mb Data	77.71	78.23	78.52

The final step in the development process was to combine results of this maximum dew point climatology development with the previous climatologies developed for the Nebraska, Arizona, Wyoming statewide studies and Tarrant Regional Water

District study. This allowed for a seamless dew point climatology dataset covering the majority of the contiguous United States. Figure 6.2 shows results of the final maximum dew point map representing the 24-hour duration 100-year return frequency for the month of August⁵.

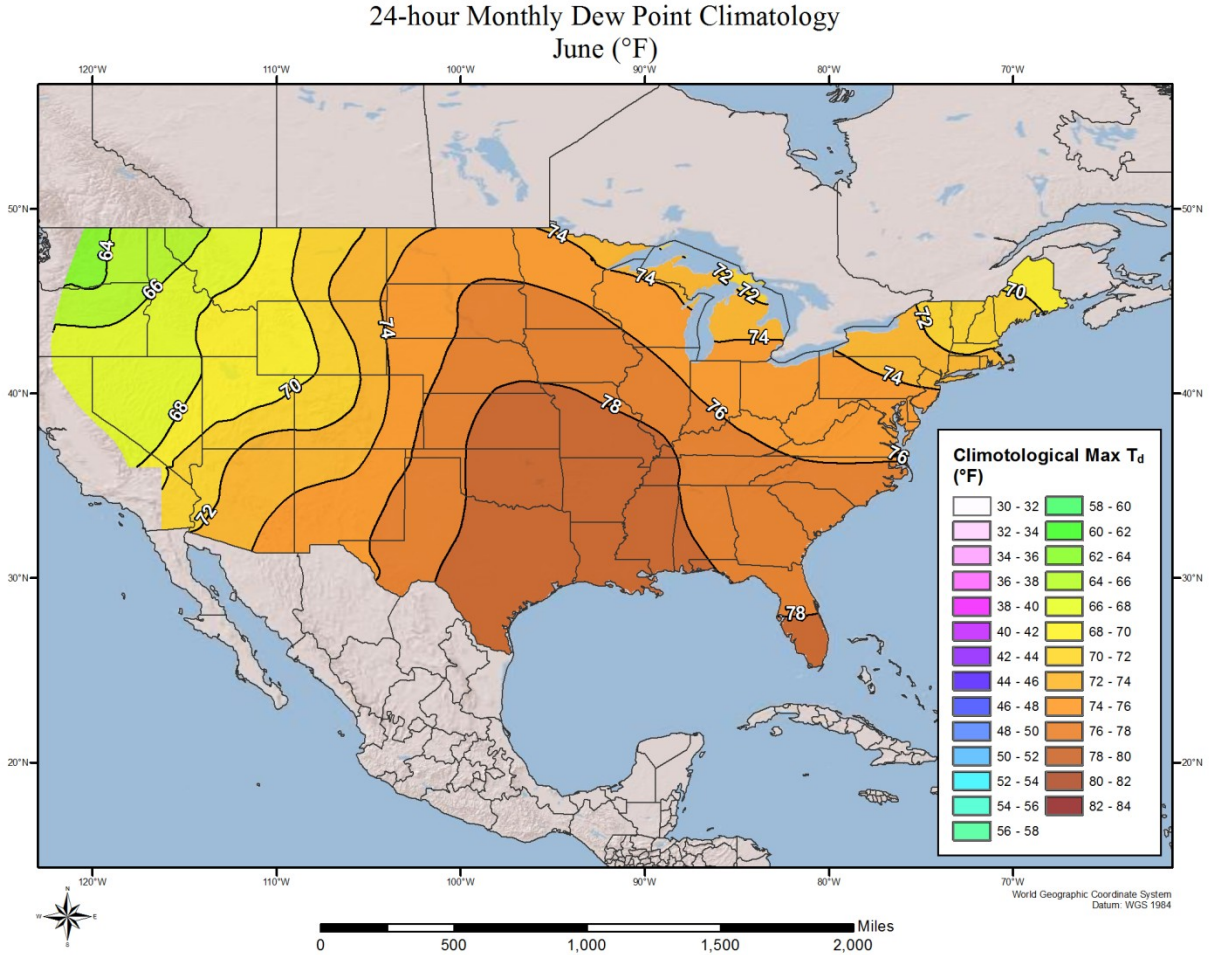


Figure 6.2 June 100-year 24-hour average maximum dew point map

6.2 HYSPLIT Trajectory Model

The HYSPLIT trajectory model developed by the NOAA Air Resources Laboratory (Draxler and Rolph 2003, 2010) was used during the analysis of each of the rainfall events included on the short storm list post 1948 (from the National Centers for Environmental Prediction NCEP Global Reanalysis fields). Use of a trajectory model

⁵ These data are housed in a GIS environment enabling explicit extraction of appropriate values during the storm maximization and transpositioning processes.

provides increased reliability for determining moisture inflow vectors and storm representative dew point values. The HYSPLIT model trajectories have been used to analyze the moisture inflow vectors in other PMP studies completed by AWA over the past several years. During these analyses, the model trajectory results were verified and the utility explicitly evaluated (Tomlinson et al. 2006-2011, Kappel et al. 2012).

Instead of subjectively determining the moisture inflow trajectory, the HYSPLIT software was used to determine the trajectory of the moisture inflow, both location and altitude, for various levels in the atmosphere. The HYSPLIT model was run for trajectories at several levels of the lower atmosphere to capture the moisture source for each storm event. These included 700mb (approximately 10,000 feet), 850mb (approximately 5,000 feet), and storm center surface elevation. For the majority of the analyses a combination of all three levels was determined to be most appropriate for use in evaluation of the upwind moisture source location. It is important to note that the resulting HYSPLIT model trajectories are only used as a general guide for identifying the moisture source for storms in space and time. The final determination of the storm representative dew point and its location is determined following the standard procedures used by AWA in previous PMP studies and as outlined in the HMRs and WMO manuals. Appendix F of this report shows each of the HYSPLIT trajectories analyzed as part of this study for each storm. As an example, Figure 6.3 shows the HYSPLIT trajectory model results used to determine the inflow vector for the Fall River, KS, June 2007 (AWA Storm Number 120).

NOAA HYSPLIT MODEL
 Backward trajectories ending at 1200 UTC 28 Jun 07
 CDC1 Meteorological Data

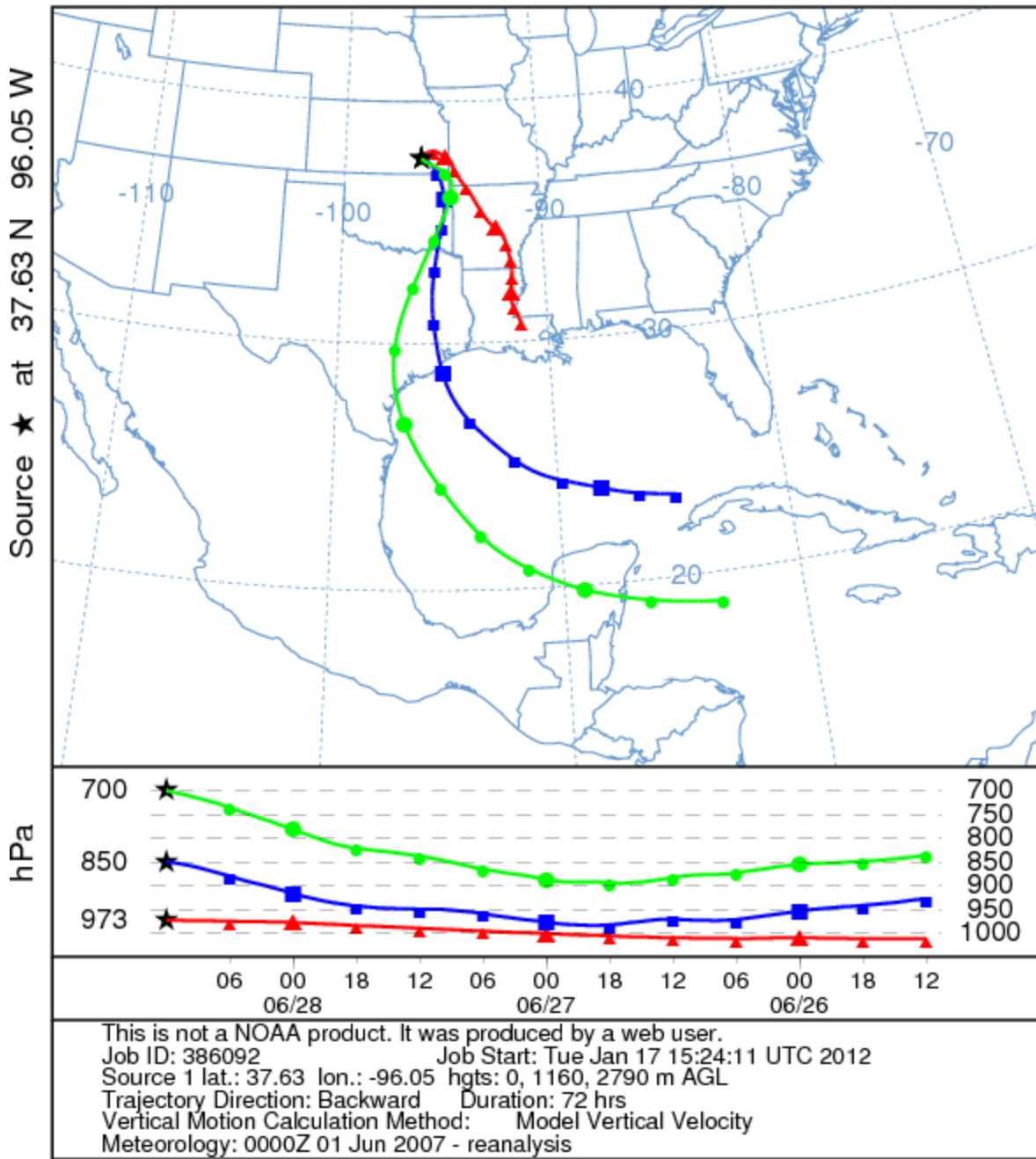


Figure 6.3 HYSPLIT trajectory model results for Fall River, KS, June 2007 (AWA Storm Number 120)

6.3 Use of Grid Points to Spatially Distribute PMP Values

To appropriately distribute rainfall values spatially across the large area covered by the state of Ohio, a series of grid points were used and the gridded data were interpolated among these points. The grid consisted of 23 points and extended outside of the state boundaries over bordering regions (see Figure 1.3). This grid design ensured that no extrapolation of PMP values was required for any location within the state.

All appropriate storm rainfall values were maximized and transpositioned to each of the 23 grid points as appropriate (Appendix F lists the grid point(s) where each storm was transpositioned). DA curves for each duration (6-hours to 72-hours) were plotted for each grid point and envelop curves constructed. Using results from the DA analyses, Depth-Duration (DD) curves were constructed for each grid point (see Section 9 for details). Results from the DD analysis were input into GIS where the values for each duration and area size at each grid point were spatially analyzed. The final PMP maps derived using the grid point methodologies are displayed in Section 11.1 and are available in GIS.

Having the contoured PMP maps to analyze on a regional basis proved to be a valuable asset vs having only rainfall values at single locations. The ability to look at the relationships among grid points at various spatial and temporal scales as a whole proved very insightful and was of great importance in deriving the final PMP values across the large Ohio domain. It should be noted that the general shape of the PMP values across the state show the highest values to the south and west, with lower values to the north and east. This is to be expected based on the location of the moisture source leading to PMP-type rainfalls in the region. This was recognized during previous weather and climate studies as well. For example, the USGS National Water Summary (Paulson et al. 1991), "The spatial distribution of annual precip in Ohio is affected by the proximity to the tropical maritime air masses."

The HMR 51 PMP curves are drawn almost west to east across the major barrier of the Appalachians and inappropriately across the "stippled" region in what appears to be an attempt to provide continuity in space (Figure 6.4). However, this does not take into account the effects of orographics caused by the Appalachians and the fact the storms on the east side of the Appalachians are fed by moisture directly from the Atlantic, while storms on the west side are fed by moisture from the Gulf of Mexico. Low level moisture does not cross the crest of the Appalachians in either direction to feed into PMP-type storms as the low level moisture is "rained out" on the upwind side as the air masses cross the mountains. Although no explicit discussions or working paper exist, it appears that the Smethport 1942 storm improperly influenced PMP values on both sides of the Appalachians and for great distances well beyond where it should have been transpositioned according to our analysis (see Appendix H for a complete discussion on the Smethport storm transposition discussion).

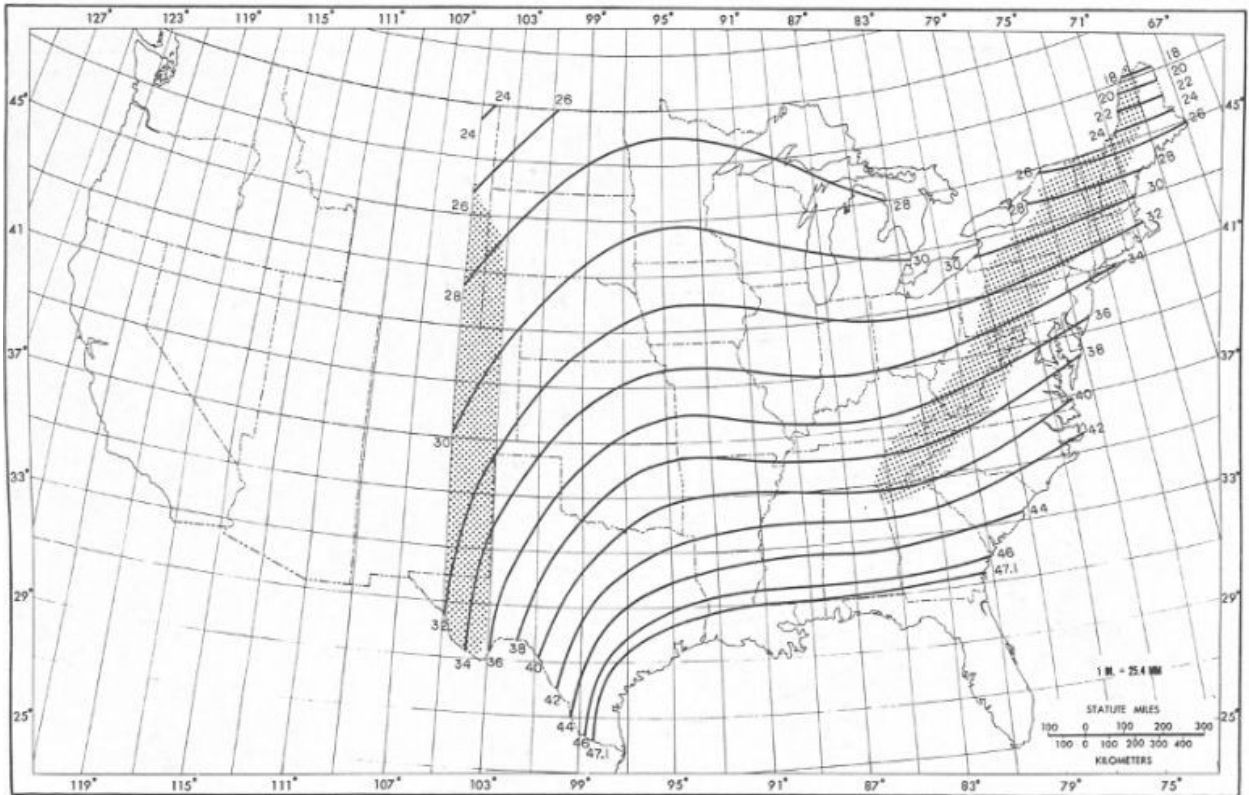


Figure 6.4 HMR 51 PMP contours, 24-hour 10-square miles (Schreiner and Riedel 1978)

The PMP values produced in this study are intended to be used in place of the HMR 51 values. These updated PMP values more appropriately reflect the moisture source region for the PMP-type storms (Figure 6.5). For Ohio, this is the Gulf of Mexico, as warm, moist air flows clockwise around the semi-permanent area of high pressure known as the Bermuda High, generally located over the Atlantic Ocean off the East Coast (see Figures 3.0 and 3.1). This air flow comes around the high over the Gulf of Mexico, northward into the Great Plains and Ohio River valley. This wind pattern supplies moisture for the PMP type storm events in the region. The PMP values in this study reflect this pattern where there is a general decrease from southwest to northeast further from the predominant moisture source.

All-Season PMP - 24-hour 10 mi² (inches)
Ohio Statewide PMP Study

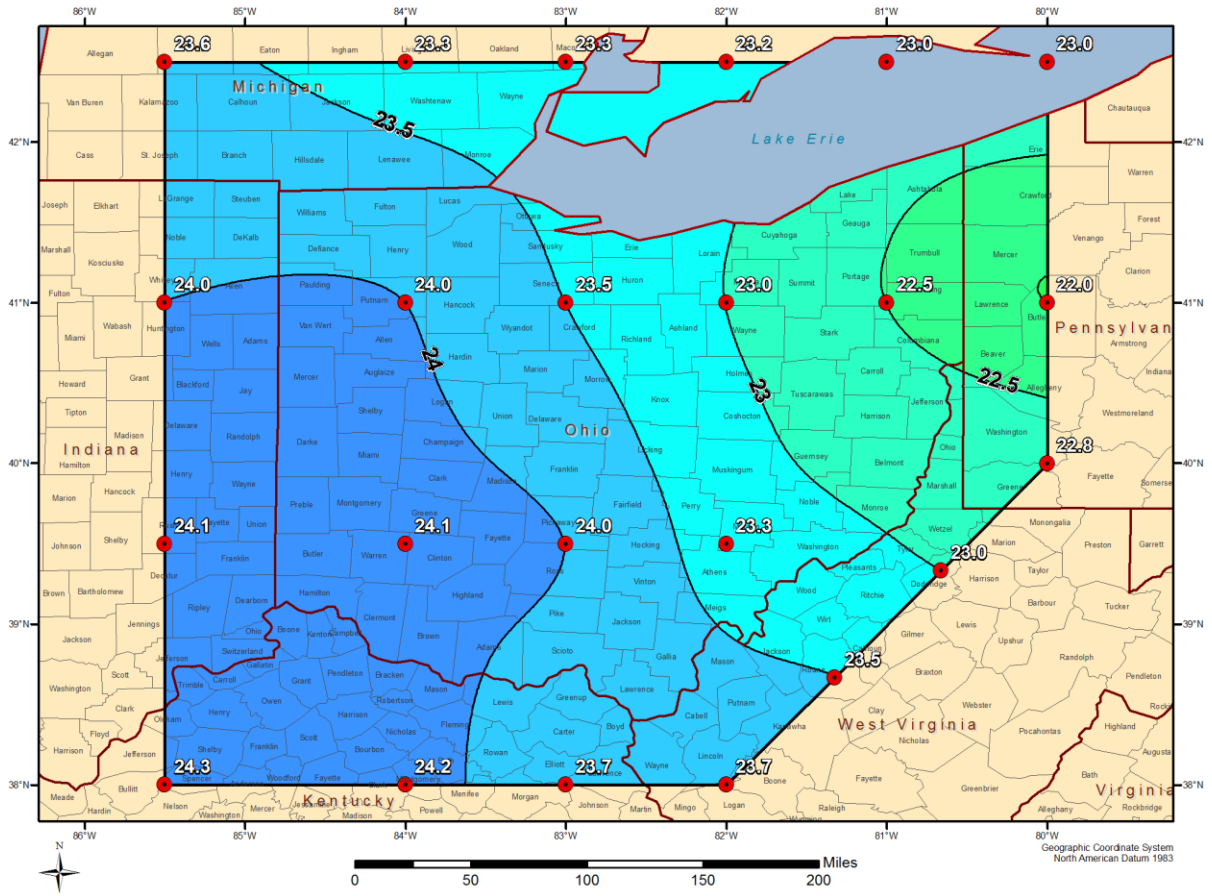


Figure 6.5 Ohio statewide PMP contours for 24-hour 10-square miles

7. Storm Maximization

Storm maximization is the process of increasing rainfall associated with an observed extreme rainfall storm under the potential condition that additional atmospheric moisture could have been available to the storm for rainfall production. Maximization is accomplished by comparing surface dew points associated with a storm event to some climatological maximum and calculating the enhanced rainfall amounts that could potentially be produced. An additional consideration is usually applied that selects the climatological maximum dew point for a date two weeks towards the warm season from the date that the storm actually occurred. This procedure assumes that the storm could have occurred with the same storm dynamics two weeks earlier or later in the year when maximum dew points (and hence moisture levels) could be higher. A more detailed discussion of this procedure and example calculations are provided in Appendix B.

7.1 Use of Dew Point Temperatures for Storm Maximization

HMR and WMO procedures for storm maximization use a storm representative dew point as the parameter to represent available moisture to a storm. Maximum dew point climatologies are used to determine the maximum atmospheric moisture that could have been available. Prior to the mid-1980s, maps of maximum dew point values from the *Climatic Atlas of the United States* (1968) were the source for maximum dew point values. HMR 55A (Hansen 1988) contained updated maximum dew point values for a portion of United States from the Continental Divide eastward into the Central Plains. The regional PMP study for Michigan and Wisconsin produced return frequency maps using the L-moments method. The Review Committee for that study included representatives from NWS, FERC, Bureau of Reclamation, and others. They agreed that the 50-year return frequency values were appropriate for use in PMP calculations. HMR 57 was published in 1994 and HMR 59 in 1999. These more recent NWS publications also updated the maximum dew point climatology, but used maximum observed dew points instead of return frequency values. For the Nebraska statewide study, the Review Committee and FERC Board of Consultants agreed that the 100-year return frequency dew point climatology maps were appropriate because this added a layer of conservatism over 50-year return period. This has subsequently been employed in all PMP studies. This study is again using the 100-year return frequency climatology with data updated through the first half of 2012 (Figure 7.1).

Observed storm rainfall amounts are maximized using the ratio of precipitable water for the maximum dew point to precipitable water for the storm representative dew point, assuming a vertically saturated atmosphere. The difference between the *maximum* precipitable water and *actual* precipitable water is converted into a percent and the storm rainfall totals as they occurred are enhanced – maximized – by this value - called the in-place maximization factor. By definition, maximization factors are always greater than or equal to 1. Following HMR and previous AWA PMP in-place storm maximization

guidance (e.g., Tomlinson et al. 2008), the in-place maximization value is capped at 1.50 (HMR 51 Section 3.2.2 and HMR 55A Section 8.4.1.1). This 1.50 limitation is based on the consideration that if the moisture is increased too much, the assumption that the moisture can be increased without altering the storms dynamics is no longer valid (HMR 55A, Section 8.4.1.1). The assumption is that properly analyzed and maximized storms should be some percent larger than the actual storm, but increases beyond certain limits (e.g., 50%) would begin to change the characteristics of that storm making it no longer useable as adjusted. This procedure was followed in this study using the updated maximum dew point climatology described in Section 6. More detailed discussions, along with examples of this procedure, are provided in Appendices B and C.

For storm maximization, average dew point values for the duration most consistent with the actual rainfall accumulation period for an individual storm (6-, 12-, or 24-hour) were used to determine the storm representative dew point. To determine which time frame was most appropriate, the total rainfall amount was analyzed. The duration (6-, 12- or 24-hour) closest to when approximately 90% of the rainfall had accumulated was used to determine the duration used, i.e. 6-hour, 12-hour, or 24-hour.

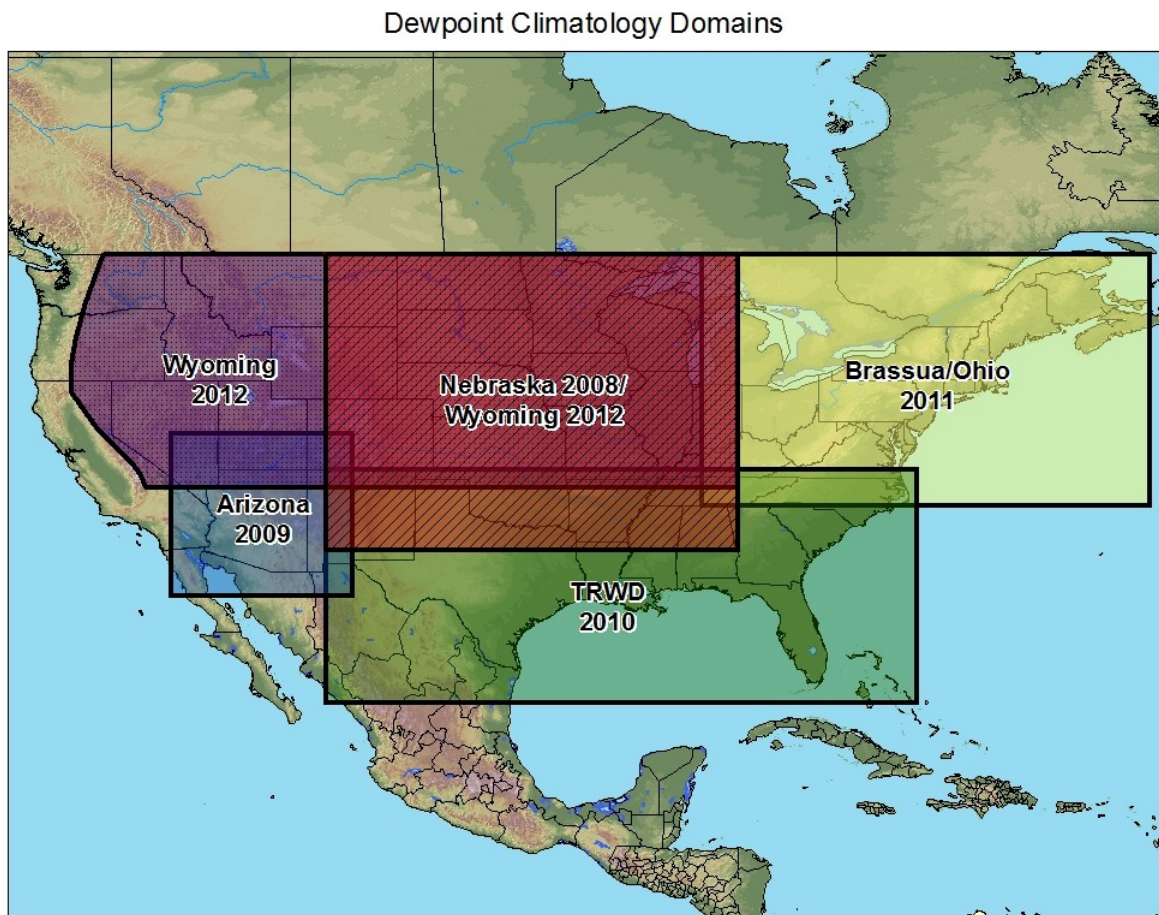


Figure 7.1 Dew point climatology development dates and regions

7.1.1 Rationale for Using Average Dew Point Climatology

In previous storm analyses performed by the NWS and the USACE, a 12-hour persisting dew point was used for both the storm representative and maximum dew points. The 12-hour persisting dew point is the value equaled or exceeded at all observations during the 12-hour period (e.g., WMO 2009). However, as was established in previous and ongoing AWA PMP studies, this dew point methodology tends to underestimate the available atmospheric moisture associated with the rainfall event.

An excellent example of this (from the Nebraska statewide PMP study but relevant for the storm types that affect Ohio) is illustrated by the David City, NE 1963 storm. During this extreme storm event, a narrow tongue of moisture was advected into the region by strong southeasterly flow during a short time period. Most of the rain with this event (approximately 15 inches) accumulated in less than 6 hours. For this storm, hourly dew point data were collected from several locations near the rainfall event. These included Omaha, NE; Des Moines, IA; Topeka, KS; and Kansas City, MO. Following standard procedures for determining storm representative dew point location, it was determined that Topeka, KS and Kansas City, MO were the two stations that best represented the air mass that produced the extreme rainfall. Using hourly dew point data for these two stations clearly showed that use of 6-hour average dew point values better represented the atmospheric moisture available to the storm event than did use of 12-hour persisting dew point values. The 6-hour average dew point representing the moisture in the air mass associated with the rainfall was 71.5°F at Kansas City, MO and 71°F at Topeka, KS. Using these dew point values, a 1,000mb 6-hour average dew point of 73.5°F was determined for Kansas City, MO and a dew point of 73°F was determined for Topeka, KS. Using the NWS approach, the 12-hour persisting dew point is 63°F (65°F at 1,000mb) at Kansas City, MO and 66°F (68°F at 1,000mb) at Topeka, KS for an average 12-hour persisting 1,000mb adjusted value of 66.5°F (Table 7.1).

Table 7.1 Comparison of 6-hour average storm representative dew point vs. 12-hour persisting storm representative dew point for the David City, NE, 1963 storm

Observed Dew Point Values for David City, NE 1963																								
Kansas City, MO																								
Hour	00Z	01Z	02Z	03Z	04Z	05Z	06Z	07Z	08Z	09Z	10Z	11Z	12Z	13Z	14Z	15Z	16Z	17Z	18Z	19Z	20Z	21Z	22Z	23Z
Dew Point	58	61	62	62	63	63	63	64	66	68	69	71	72	72	72	71	71	69	68	67	67	67	67	67
												Air Mass Supplying Rainfall Event												
12-Hour Persisting Td 63 (65 reduced to 1000mb)						12 Hour Persisting Td Timeframe																		
6-Hour Average Td 71.5 (73.5 reduced to 1000mb)						6 Hour Average Td timeframe																		
Topeka, KS																								
Hour	00Z	01Z	02Z	03Z	04Z	05Z	06Z	07Z	08Z	09Z	10Z	11Z	12Z	13Z	14Z	15Z	16Z	17Z	18Z	19Z	20Z	21Z	22Z	23Z
Dew Point	61	62	64	65	65	65	66	66	67	68	69	72	71	71	71	70	70	70	69	70	69	68	66	69
												Air Mass Supplying Rainfall Event												
12-Hour Persisting Td 66 (68 reduced to 1000mb)						12 Hour Persisting Td Timeframe																		
6-Hour Average Td 71 (73 reduced to 1000mb)						6 Hour Average Td timeframe																		

The 12-hour persisting dew point analysis included dew point values from a six hour period not associated with the rainfall. The hourly dew point value that provides the 12-hour persisting dew point occurred outside of the rainfall period after adjustment for advection time from the dew point observing station to the storm location.

7.1.2 Rationale for Adjusting HMR 51 Persisting Dew Point Values

In some cases, e.g., storms on the short storm list previously analyzed in the USACE Storm Studies and used in NWS HMRs, an adjustment factor was applied to provide consistency in storm maximization while utilizing the updated dew point climatology. The adjustment factor was determined using the same procedure used in the FERC Michigan/Wisconsin and subsequent AWA PMP studies.

Results from the dew point analyses showed consistent results for MCS type storms for differences between the older method for determining 12-hour persisting storm representative dew points and the approach using average storm representative dew points. The following discussion from the FERC Michigan/Wisconsin report addresses these differences:

The average difference between dew points for the synoptic storms was five degrees less than that for the MCS storms. This may be attributed to the greater homogeneity of inflow moisture associated with the synoptic events. With most of the modern MCS storms, limited-area, short-duration pockets of relatively moist air were found within the inflow moisture at one or two locations. The analyses may indicate that for MCS events, bubbles of extremely moist air interact with storm catalysts to create extreme rainfall events of short duration. A warm humid air mass over a broad area with small moisture gradients more aptly describes the synoptic inflow moisture. Several stations within the air mass may have the same or similar dew points. Much smaller variations in dew points along the inflow moisture vector are expected.

Large spatial and temporal variations in moisture associated with MCS-type storms are not represented well with 12-hour persisting dew points, especially when only two observations a day are available. Average dew point values, temporally consistent with the duration of the storm event provide a much improved description of the inflow moisture available for conversion to precipitation. The more homogeneous moist air masses associated with synoptic storms result in smaller differences between average and persisting values.

This analysis has provided correlations between 12-hour persisting storm dew points and average storm dew points for both MCS and synoptic storms. Despite the small sample size, the consistent results tend to support the reliability of the analysis. However, the small sample size has been considered in making recommendations for adjusting the old storm representative dew points for use in determining PMP estimations. The eight degree difference for MCS-type storms has been decreased to five degrees to provide a conservative adjustment. A similar consideration is made for synoptic-type storms. The three-degree difference is decreased to two degrees to provide a conservative adjustment. The adjusted representative storm dew points are used with the new maximum average dew point climatology to maximize storms.

Similar analyses were completed in the Nebraska statewide PMP study and in this study. These analyses investigated additional modern storms specifically relevant for Ohio. Results of these analyses of MCS storm data provided an average difference of

7°F between the average and 12-hour persisting dew points. For synoptic storms, the average difference was 3°F (Table 7.2). Results of the more recent analyses were very consistent with the FERC Michigan/Wisconsin regional PMP study. This again validated the process of adjusting the 12-hour persisting dew points to achieve compliance with using the average dew point climatology.

Table 7.2 Storms used to evaluate average vs. persisting dew point values specific to Ohio. The tables is separated by MCS storms and synoptic storm types.

Ohio MCS Storms					
Storm Event	Date	Avg. 12-hr Persisting Td	Avg. Td	Avg. Delta	Duration Analyzed
Aurora College, IL	July 16-18, 1996	68.0	75.0	7.0	6hr
David City, NE	June 22-23, 1963	67.0	73.5	6.5	6hr
Minneapolis, MN	July 21-24, 1987	69.0	76.0	7.0	6hr
Tomah, WI	August 15-17, 1990	72.0	77.5	5.5	6hr
			Average	7.0	
Ohio Synoptic Storms					
Storm Event	Date	Avg. 12-hr Persisting Td	Avg. Td	Avg. Delta	Duration Analyzed
Aurora College, IL	July 16-18, 1996	68.0	70.5	2.5	24hr
Big Rapids, MI	September 9-13, 1986	66.5	70.5	4.0	24hr
Edgerton, MO	July 16-19, 1965	69.5	70.5	1.0	24hr
Ida Grove, IA	August 28-31, 1962	67.0	69.5	2.5	24hr
Paris Waterworks, IL	June 25-28, 1957	66.0	71.0	5.0	12hr
			Average	3.0	

8. Storm Transpositioning

Extreme rain events that occurred over geographically and climatically similar regions surrounding a study area are a very important part of the historical evidence on which PMP estimates are based. Study locations usually have a limited period of record for rainfall data collected at that location and hence have a limited number of extreme storms that have been observed. As such, the storm transpositioning process uses additional space to compensate for the limited time frame of instrumental climate records at any location. Storms observed regionally with similar meteorology and topography are analyzed and adjusted to provide information describing the storm rainfall as if the storm had occurred over the study area. Transfer of a storm from where it occurred to a location that is meteorologically and topographically similar is called *storm transpositioning*. The underlying assumption is that storms transposed to the study area could occur over the study area location under similar meteorological conditions. To properly relocate such storms, it is necessary to address issues of similarity as they relate to topography and atmospheric moisture availability, and make appropriate adjustments.

For this study, the region considered to contain storms which were potentially transpositionable to one or more grid points analyzed as part of this study included most of the Midwest from approximately 102°W longitude eastward to the first upslopes on the west side of the Appalachians, north into southern Canada and south to the southern Plains (see Section 4.1). This region was considered meteorologically homogenous and therefore the climatological settings within Ohio and the locations of each of the transposed storms are similar. Further analysis of storm patterns on both a temporal and spatial scale within this region revealed that only storms that occurred within a +/- 1,000 feet of elevation of a location possessed similar enough storm dynamics to be transpositionable to that location. Further, the limits of transpositionability were refined for specific storms after all adjustments were applied based on meteorological judgment and fit with other similar storms in the region.

8.1 Storm Transposition Calculations

The procedure for in-place storm maximization has been discussed (see Section 7.0). The same maps used for deriving maximum dew points were used in the storm transpositioning procedure. The procedure for deriving the climatological maximum dew points for use in calculating the transposition maximization ratio uses the information derived during the calculation of the in-place maximization factor. The moisture inflow vector connecting the storm location with the storm representative dew point location was transpositioned to each grid point. The value of the maximum dew point at the upwind location provided the transpositioned maximum dew point value used to compute the transposition adjustment factor for relocating the storm to the appropriate grid point. These transposition factors can be greater than or less than 1.0, depending on whether the transpositioned location and inflow vector produced higher or lower maximum dew point

values from the 100-year maximum dew point climatology. Figure 8.1 shows an example inflow vector map and transpositioned vector to grid point 15 for the Warner Park, TN, May, 2010 storm (AWA Storm Number 126). The primary effect of storm transpositioning was to adjust storm rainfall amounts to account for enhanced (or reduced) atmospheric moisture made available to the storm at the transposed location vs. the original storm location. A more detailed discussion of this procedure and example calculations are provided in Appendix C. The inflow vector map and data used to calculate the transposition factor for each storm are included in Appendix F.



Figure 8.1 Inflow wind vector transpositioning for Warner Park, TN. The storm representative dew point location is 360 miles south/southwest of the storm location.

8.2 Storm Spreadsheet Development Process

AWA has developed Excel spreadsheets for each storm on the short storm list which incorporates relevant storm information, automatically calculates appropriate adjustment factors, and computes the adjusted DAD table. These storm spreadsheets used the observed storm DADs, storm representative dew points, maximum dew points (both in-place and transpositioned), storm elevation, and transposition location elevation information either as published in the USACE Storm Studies reports, HMR 51, or as developed by AWA. This information was entered into individual storm spreadsheets, one for each short list storm for each appropriate grid point. Using the storm center location and inflow vector, the in-place maximum dew point was determined. The inflow vector was then moved to each appropriate grid point to determine the transpositioned maximum dew point value and total adjustment factor for that storm at each location. This information was entered into the storm spreadsheet to calculate the in-place maximization factor, the transposition factor, and finally the total adjustment factor. This total adjustment factor was applied to the storm DAD table values to provide the final adjusted DAD table for the maximized and transpositioned storm rainfall values at each appropriate grid point.

Once all the storms were adjusted to each appropriate grid point, DA and DD plots were constructed for each grid point for analysis and envelopment. This ensured spatial and temporal continuity across the grid point locations. The analysis results were subsequently plotted and contoured within GIS to produce the final statewide PMP maps. Appendix F includes the storm spreadsheets developed for each storm. Figure 8.2 displays an example storm spreadsheet for the Warner Park, TN, May, 2010 storm (AWA Storm Number 126) at grid point 15. The information in Appendix F allows a user the opportunity to explicitly evaluate, verify, and recalculate the values derived in this study if desired.

Storm Name:		SPAS 1208 - Warner Park, TN		Storm Adjustment for Grid Point 15							
Storm Date:		5/1-3/2010									
AWA Analysis Date:		2/19/2013									
Temporal Transposition Date		15-May									
		Lat	Long								
Storm center location		36.06 N	86.91 W	Moisture Inflow Direction: SSW @ 360 miles							
Storm Rep Td location		31.50 N	90.00 W	Grid Point Elevation 900 feet							
Transposition Td location		36.44 N	85.09 W	Storm Elevation 600 feet							
Grid point location		41.00 N	82.00 W	Storm Duration 12 hours							
The storm representative Td is		75.0 F	with total precipitable water above sea level of		2.85 inches.						
The in-place maximum Td is		76.5 F	with total precipitable water above sea level of		3.07 inches.						
The transpositioned maximum Td is		74.5 F	with total precipitable water above sea level of		2.79 inches.						
The in-place storm elevation is		600	which subtracts	0.15	inches of precipitable water at	75.0 F					
The in-place storm elevation is		600	which subtracts	0.16	inches of precipitable water at	76.5 F					
The transposition storm elevation at		900	which subtracts	0.23	inches of precipitable water at	74.5 F					
The moisture inflow barrier height is		900	which subtracts	0.23	inches of precipitable water at	74.5 F					
The in-place maximization factor is		1.08		Notes: Storm representative Td value was based on 12-hr surface dewpoint values between on May 1 along with Hysplit backward trajectory. Values were selected in region where temperature did not vary more than a degree over a large area. Used an average of KJAN, KMCB, KHBG, and KASD.							
The transposition/elevation factor is		0.88									
The barrier adjustment factor is		1.00									
The total adjustment factor is		0.95									
Observed Storm Depth-Area-Duration											
		1 Hours	6 Hours	12 Hours	18 Hours	24 Hours	36 Hours	48 Hours	60 Hours	72 Hours	
10 sq miles		4.4	15.0	17.3	18.0	18.1	19.0	19.2	19.4	-	
100 sq miles		3.7	13.2	15.9	16.5	16.6	18.3	18.5	18.7	-	
200 sq miles		3.4	12.2	15.0	15.6	15.8	17.8	18.1	18.3	-	
500 sq miles		2.8	10.6	13.5	14.3	14.6	16.8	17.4	17.7	-	
1000 sq miles		2.3	9.0	12.6	13.3	13.5	16.4	16.9	17.1	-	
2000 sq miles		1.8	7.4	11.1	12.0	12.6	15.7	16.1	16.4	-	
5000 sq miles		1.4	5.2	9.2	10.3	10.9	14.1	14.8	15.0	-	
10000 sq miles		1.0	3.8	7.4	8.4	8.6	12.2	13.0	13.1	-	
20000 sq miles		0.7	2.9	5.4	6.3	7.2	10.2	11.0	11.2	-	
Adjusted Storm Depth-Area-Duration											
		1 Hours	6 Hours	12 Hours	18 Hours	24 Hours	36 Hours	48 Hours	60 Hours	72 Hours	
10 sq miles		4.2	14.2	16.4	17.0	17.1	18.1	18.2	18.4	-	
100 sq miles		3.5	12.5	15.1	15.7	15.8	17.4	17.6	17.7	-	
200 sq miles		3.3	11.5	14.2	14.8	15.0	16.8	17.2	17.4	-	
500 sq miles		2.7	10.1	12.8	13.6	13.9	16.0	16.5	16.8	-	
1000 sq miles		2.2	8.5	11.9	12.6	12.8	15.5	16.0	16.2	-	
2000 sq miles		1.7	7.0	10.5	11.3	12.0	14.9	15.3	15.5	-	
5000 sq miles		1.3	5.0	8.8	9.8	10.4	13.4	14.0	14.2	-	
10000 sq miles		0.9	3.6	7.0	8.0	8.2	11.6	12.3	12.4	-	
20000 sq miles		0.6	2.8	5.2	6.0	6.8	9.7	10.5	10.6	-	
Storm or Storm Center Name		SPAS 1208 - Warner Park, TN									
Storm Date(s)		5/1-3/2010									
Storm Type		Synoptic									
Storm Location		36.06 N		86.91 W							
Storm Center Elevation		600		feet							
Precipitation Total & Duration		19.71 inches in 60 hours									
Storm Representative Td		75.0 F									
Storm Representative Td Location		31.50 N		90.00 W							
In-place Maximum Td		76.5 F									
Moisture Inflow Vector		SSW @ 360									
In-place Maximization Factor		1.08									
Temporal Transposition (Date)		15-May									
Transposition Td Location		36.44 N		85.09 W							
Transposition Maximum Td		74.5 F									
Transposition Adjustment Factor		0.88									
Grid Point 15 Elevation		900		feet							
Inflow Barrier Height		900		feet							
Barrier Adjustment Factor		1.00									
Total Adjustment Factor		0.95									

Figure 8.2 Example of the storm spreadsheet for Warner Park, TN, May, 2010 storm (AWA Storm Number 126) transpositioned to grid point 15

9. Development of PMP Values for Ohio

Storm maximization and transposition factors applied to a storm DAD table provide an indication of the maximum amount of rainfall that a storm could have produced at locations within the region analyzed for Ohio. Use of these values alone does not ensure that PMP values are provided for all area sizes and durations since some of the maximized and transpositioned values could be less than PMP. By enveloping the rainfall amounts from all the major storms, rainfall values indicative of the PMP magnitude are produced (e.g., WMO, 1986 and 2009). Standard processes for deriving DAD values for all grid points were used in the study.

9.1 Envelopment Procedures and DAD Derivation

Enveloping is a process for selecting the largest value from a set of data. This procedure provides continuous smooth curves based on the largest rainfall values from the set of maximized and transpositioned storm rainfall values. The largest rainfall amounts provide guidance for drawing the curves.

During the enveloping process, values which are not consistent (are either high or low) are re-evaluated to insure reliability. High values are enveloped unless an explanation can be provided to justify undercutting the value. No undercutting of rainfall values was done in this study. Low values are also re-evaluated for reliability and then enveloped to maintain consistency with surrounding values. This enveloping procedure addresses the possibility that for certain area sizes and durations, no significantly large storms have been observed that provide large enough values after being maximized and transposed to represent PMP at an area size and/or duration. The result of this procedure is a set of smooth curves that maintain continuity among temporal periods and areal sizes.

The envelopment process was used in PMP determination for this study, following the same procedures used for envelopment in the derivation of PMP in the HMRS, the WMO PMP Manual (2009), and previous AWA PMP studies. Once the total storm adjusted rainfall values for the appropriate storms at each grid point were determined, they were plotted on individual DA charts for each duration for analysis. Envelopment was applied to each DA curve for each duration. The DA envelopment curves were drawn to provide continuity in space. Figure 9.1 is an example of a DA chart with the envelopment curve for the 24-hour duration at grid point 15. Each storm on the short storm list transpositionable to that grid point is plotted individually. The envelopment curve of the data is plotted as the black. The red line is the HMR 51 PMP values at the grid point location for that duration and is provided for comparison purposes.

Twenty-Four Hour Depth-Area Curves
Adjusted to Grid Point 15

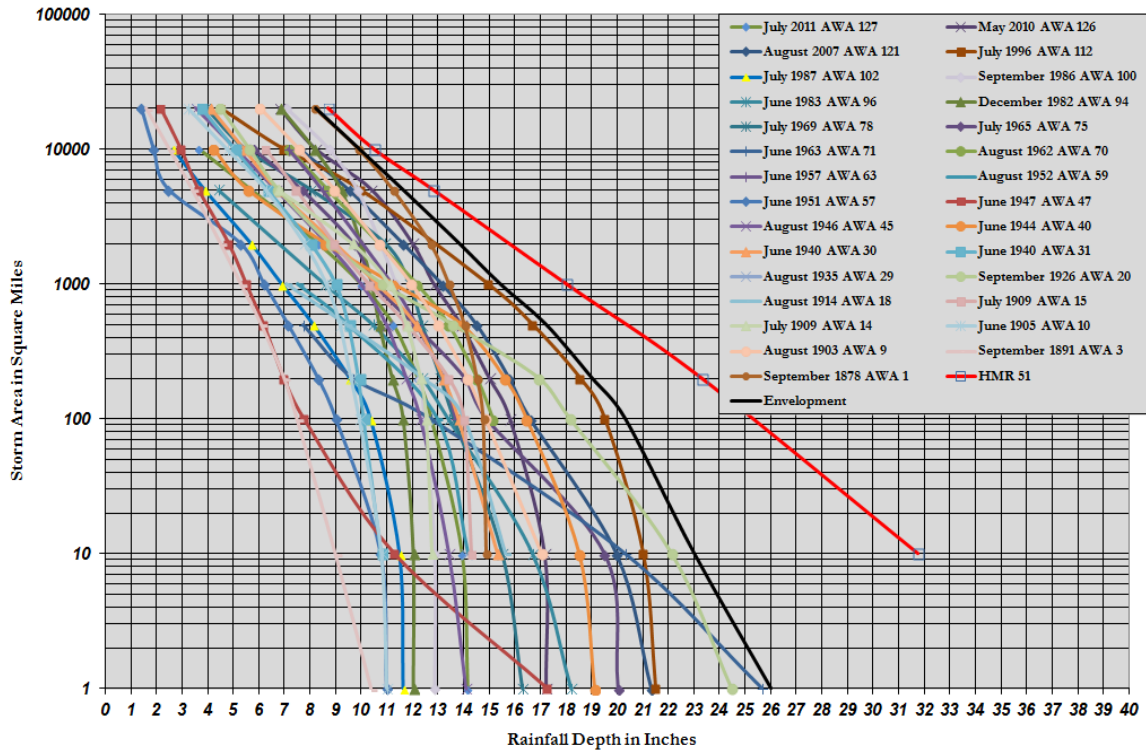


Figure 9.1 24-hour DA curves for grid point 15

The second application of the envelopment process was used with the DD curves at each grid point. Curves for each of the area sizes were constructed using results from the DA envelopment curve at each grid point. The DD curves were drawn to produce smooth curves that provide continuity in time among all durations. Each curve represents the rainfall as it occurs at that grid point for a specific area size over all durations analyzed. The curves insure that continuity of the rainfall at a given area size accumulates appropriately, with the largest 6-hour value contained within the largest 12-hour value and so forth. Figure 9.2 gives an example of the DD curves for grid point 15.

Depth-Duration Chart of Enveloped Storm Data
Grid Point 15

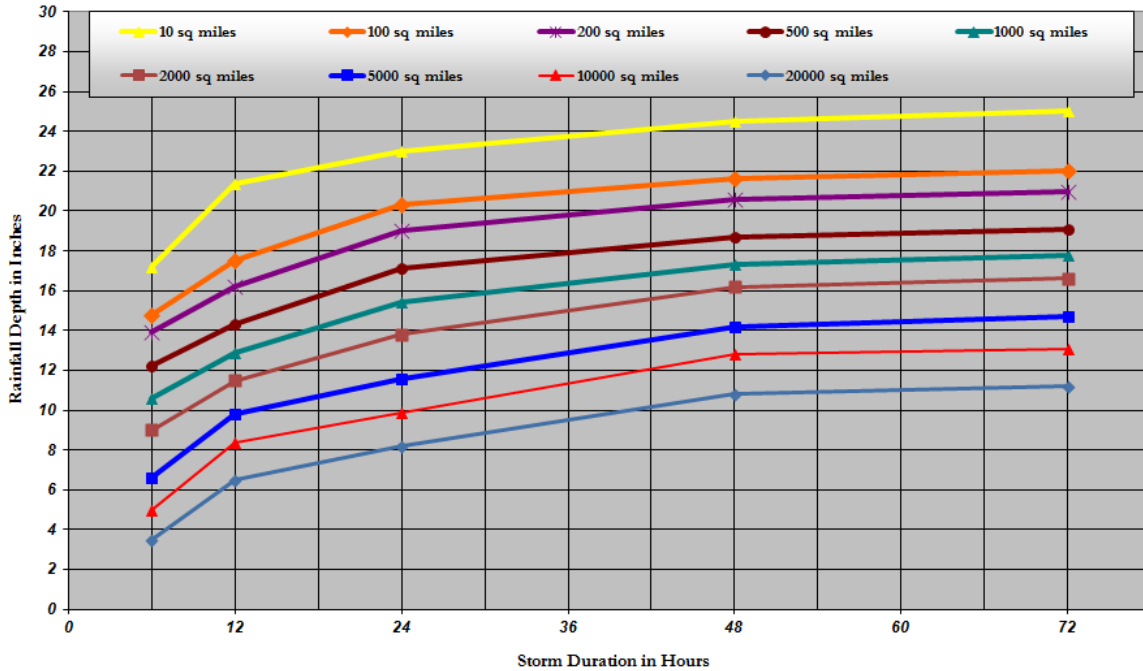


Figure 9.2 DD curves for grid point 15

The final set of DD curves for all durations at each grid point defines the initial set of PMP values for the entire region. Figure 9.1 is for the 24-hour duration, with the same process followed for the 6-, 12-, 48-, and 72-hour durations. The envelopment of the adjusted storms together with the curve smoothing process insured that all storm data were included and that the resulting set of PMP values provides rainfall values that are consistent spatially and temporally over the state. These are the values that were then plotted and contoured in GIS to begin the process of manual smoothing among the grid points. Several smoothing iterations were completed to provide spatial and temporal continuity of the PMP values across all grid points. The final version of this process produced the gridded PMP values.

10. Storm Orientation and Timing

10.1 PMP Design Storm Shape and Orientation

Storm isohyetal patterns for 41 of the short list storms were evaluated to determine whether the PMP design storm parameters for the orientation as given in HMR 52 (Hansen 1982 et al.) are appropriate for storms in Ohio. The purpose of this analysis was to determine whether an update to the guidance provided in HMR 52, detailing how the PMP-design storm shape and orientation, was warranted. Following the same guidance as was used in this study to derive the PMP values, a storm-based investigation was completed using the short list of storms from this study. When available, the SPAS total storm isohyetal patterns were used to estimate the orientation while non-SPAS storms relied on the isohyetal pattern images found in the supplemental sheets for USACE Storm Rainfall in the United States (1973) report.

The orientation and major/minor axis ratio was estimated for each storm using a carefully drawn ellipse to approximate the general shape of isohyetal pattern (Table 10.1). Each ellipse was drawn to envelop the majority of the storm's precipitation with the orientation axis drawn through the location of highest precipitation.

The azimuth of the major axis of each ellipse was measured and recorded for each storm ellipse. The orientations were averaged using the same process described in HMR 52. Each axis has two azimuthal measurements from north (e.g., 115° and 295°). The average orientation for all storms was obtained by using the appropriate value for each two-value axis orientation resulting in a minimum range for all values. HMR 52 describes the problem and solution of determining the minimum range of multiple major axis orientations. An example illustration from HMR 52 is shown in Figure 10.1.

The minimum range for the Ohio storms spanned 150° (180° to 330°). The ratio of the major to minor axis was 2.63. These values were similar to those derived in HMR 52 and therefore the results of this analysis led to the recommendation that the parameters given in HMR 52 be used in Ohio.

10.1.1 Storm Ratio Estimation Procedures

The storm shape can be represented by a family of ellipses with some ratio of the length of the major axis to the length of the semi-major axis.

In the example shown in Figure 10.2, Dubuque, OH, July 2011 (AWA Storm Number 127), the orientation of the major axis is measured at 105°/285° and minor axis is 15°/195°. The orientation value of 285° is the value used in the orientation average since it falls within the minimum range described in the previous section. The length of the major axis is 5 times the length of the minor axis yielding a ratio of 5.

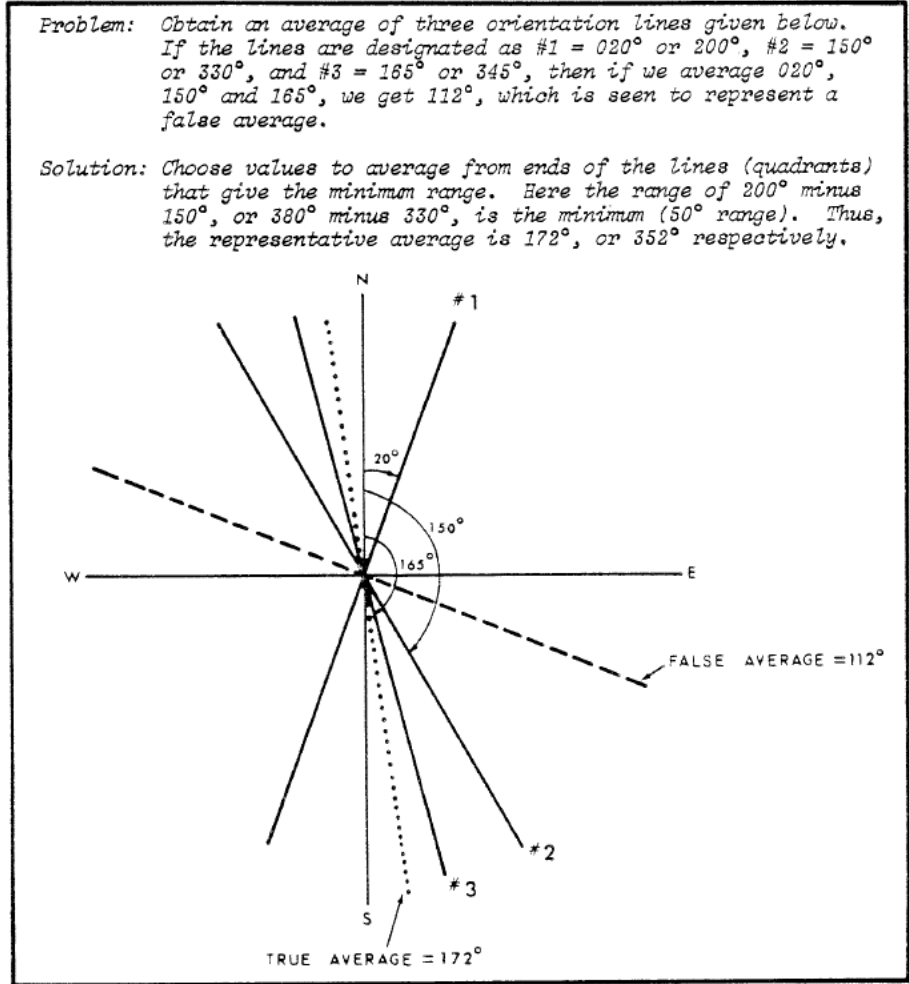


Figure 10.1 Schematic example of problem in averaging isohyetal orientations (reproduced from HMR 52 Figure 6, page 26)

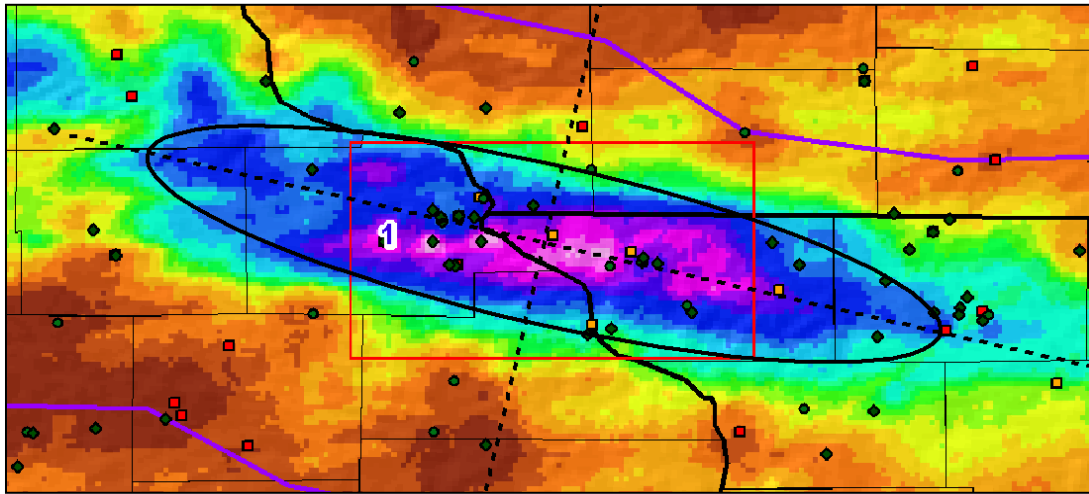


Figure 10.2 Example storm ratio analysis from the Dubuque, OH, July 2011 (AWA Storm Number 127)

Table 10.1 SPAS storms used in the evaluation of storm orientation and ellipse ratios

Station Name	Precipitation Source	AWA Storm Number	St	Lat	Lon	Duration	Year	Month	Day	Max Precip	Storm Orientation	Least Range Orientation	Ratio: Major vs Minor Axis
AURORA COLLEGE	SPAS 1029	112	IL	41.75	-88.3333	24	1996	7	16	18.24	110°/290°	290	1.91
BEAULIEU	UMV 1-11A	14	MN	47.3	-95.9	6	1909	7	18	10.50	110°/290°	290	1.60
BIG FORK	SPAS 1219	94	AR	35.871	-92.121	120	1982	12	1	15.92	50°/230°	230	4.50
BIG RAPIDS	SPAS 1206	100	MI	43.6125	-85.3125	72	1986	9	9	13.42	90°/270°	270	3.65
BONAPARTE	UMV 2-5	10	IA	40.7667	-91.75	6	1905	6	10	12.10	105°/285°	285	2.50
BOYDEN	MR 7-2A	20	IA	43.19	-96.01	24	1926	9	17	24.00	45°/225°	225	2.00
COLE CAMP	MR 7-2A	44	MO	38.460	-93.203	72	1946	8	12	19.40	115°/295°	295	2.00
COLLEGE HILL	SPAS 1226	71	OH	40.0854	-81.6479	48	1963	6	3	19.39	0°/180°	180	1.85
COLLINGSVILLE	MR 7-2B	45	IL	38.6717	-89.98	72	1946	8	12	18.70	115°/295°	295	1.40
COOPER	GL 2-16	18	MI	42.376	-85.610	6	1914	8	31	12.60	115°/295°	295	1.75
COUNCIL GROVE	MR 10-2	58	KS	38.660	-96.490	72	1951	7	9	18.50	105°/285°	285	2.00
DAVID CITY	SPAS 1030	72	NE	41.2132	-97.071	6	1963	6	24	15.98	25°/205°	205	1.07
DOUGLASVILLE	SPAS 1218 ZONE 1	125	GA	33.870	-84.760	72	2009	9	19	25.37	45°/225°	225	3.00
DUBUQUE	SPAS 1220	127	IA	42.44	-90.75	24	2011	7	27	15.14	105°/285°	285	5.00
DUMONT	UMV 3-29	57	IA	42.752	-92.976	15	1951	6	25	12.00	95°/275°	275	2.50
EDGERTON	SPAS 1183	75	MO	40.413	-95.513	72	1965	7	18	20.76	130°/310°	310	1.75
FALL RIVER	SPAS 1228	120	KS	37.63	-96.05	96	2007	6	30	25.50	60°/240°	240	2.50
FOREST CITY	SPAS 1035	96	MN	45.2394	-94.5404	24	1983	6	20	17.00	85°/265°	265	3.00
GRANT TOWNSHIP	MR 4-5	30	NE	42.240	-96.590	6	1940	6	3	13.00	75°/255°	255	2.00
GREELEY	MR 4-3	5	NE	41.55	-98.5333	6	1896	6	4	12.30	40°/220°	220	1.50
HALLETT	SW 2-18	32	OK	36.200	-96.600	12	1940	9	2	24.00	150°/330°	330	2.50
HAYWARD	UMV 1-22	34	WI	46.013007	-91.484621	72	1941	8	28	15.00	95°/275°	275	2.55
HOKAH	SPAS 1048	121	MN	43.813	-91.363	24	2007	8	18	18.32	110°/290°	290	3.75
HOLT	MR 8-20	47	MO	39.45278	-94.342169	6	1947	6	18	17.60	10°/190°	190	1.80
IDA GROVE	FERC MI/WI Storm 19	70	IA	42.3167	-95.4667	24	1962	8	30	12.85	70°/260°	260	3.60
INDEX	LMV 4-25	31	AR	33.547	-94.042	6	1940	6	30	11.50	90°/270°	270	2.00
IRONWOOD	UMV 1-11B	15	MI	46.450	-90.183	72	1909	7	21	13.20	115°/295°	295	2.50
JEFFERSON	OR 9-19	1	OH	40.8017	-82.0223	72	1878	9	10	15.00	95°/275°	275	3.00
LARRABEE	MR 4-2	3	IA	42.8608	-95.5453	24	1891	9	10	13.00	40°/220°	220	2.20
LOUISVILLE	SPAS 1227	88	MS	33.1167	-89.05	96	1979	4	12	22.07	85°/265°	265	3.35
MEEKER	SW 1-11	13	OK	35.503401	-96.902801	126	1908	10	19	16.23	30°/210°	210	2.00
MINNEAPOLIS	SPAS 1210	102	MN	44.889	-93.4021	6	1987	7	23	11.55	95°/275°	275	4.15
MOUNDS	SW 2-21	37	OK	35.877	-96.061	12	1943	5	16	17.00	60°/240°	240	3.30
NEOSHO FALLS	SW 2-1	19	KS	38.082	-95.701	24	1926	9	12	14.00	60°/240°	240	3.55
NEWCOMERTOWN	OR 9-11	29	OH	40.2723	-81.606	12	1935	8	6	12.70	140°/320°	320	2.56
PARIS WATERWORKS	HMB-V18	63	IN	39.05	-87.7	12	1957	6	27	12.40	40°/220°	220	2.00
STANTON	MR 6-15	40	NE	41.867	-97.05	6	1944	6	10	17.30	95°/275°	275	2.67
WARNER	SW 2-20	35	OK	35.49	-95.31	72	1943	5	6	25.00	50°/230°	230	2.35
WARNER PARK	SPAS 1208	126	TN	36.0611	-86.9056	60	2010	4	30	19.71	75°/255°	255	3.75
WOODBURN	MR 1-10	9	IA	41.012	-93.5991	72	1903	8	24	15.50	105°/285°	285	2.60
WOOSTER	SPAS 1209	78	OH	40.9146	-81.9729	24	1969	7	4	14.95	115°/295°	295	3.65
											MAX:	330	
											MIN:	180	
											Range:	150	
											Average	262	2.63

10.2 PMP Design Storm Timing

Fifteen SPAS storms were used for temporal distribution analysis in Ohio: seven MCS storms, four Hybrid (convective and synoptic), and four Synoptic (Table 10.2). The location of the storm center, for each storm analysis, was used for the temporal distribution calculations.

HMR 52 provides guidance on the temporal distribution of PMP in 6-hour increments. In this study, the same procedures outlined in HMR 52 to develop 6-hour incremental precipitation were followed. However, in addition to 6-hour increments, hourly values as a percentage of the maximum x-hour (24-hour or 72-hour) duration precipitation were investigated.

Hourly gridded rainfall data were used for all SPAS analyzed storms (MCS, Hybrid, Synoptic). The maximum rain accumulations per duration were based on rainfall at the storm center. An analysis was completed to determine the maximum precipitation accumulations for the duration of interest (24-hour and 72-hour) using a moving window. In order to determine the proper 24-hour or 72-hour timing, an indexing approach was used because rainfall timing does not occur at the same time and each storm has a different duration. The 6-hr incremental rainfall started at SPAS index hour 1, with the first 6-hour precipitation from index 1:6, the second 6-hour precipitation from index 7:12 and so on. The first 6-hour increments were constrained to contain precipitation, meaning once the largest 24-hour or 72-hour precipitation window was identified a check was made to ensure the first 6-hour period contained precipitation. If the first 6-hour increment did not have precipitation, the window was shifted to make the first 6-hour window contain precipitation (Figure 10.3). Once the proper window was identified for each storm, the accumulations were converted into a ratio of the cumulative rainfall to the total accumulated rainfall for that duration, and a ratio of the cumulative time to the total time. The summation of the ratios always had a value of 1.00. This was done for each of the fifteen storms.

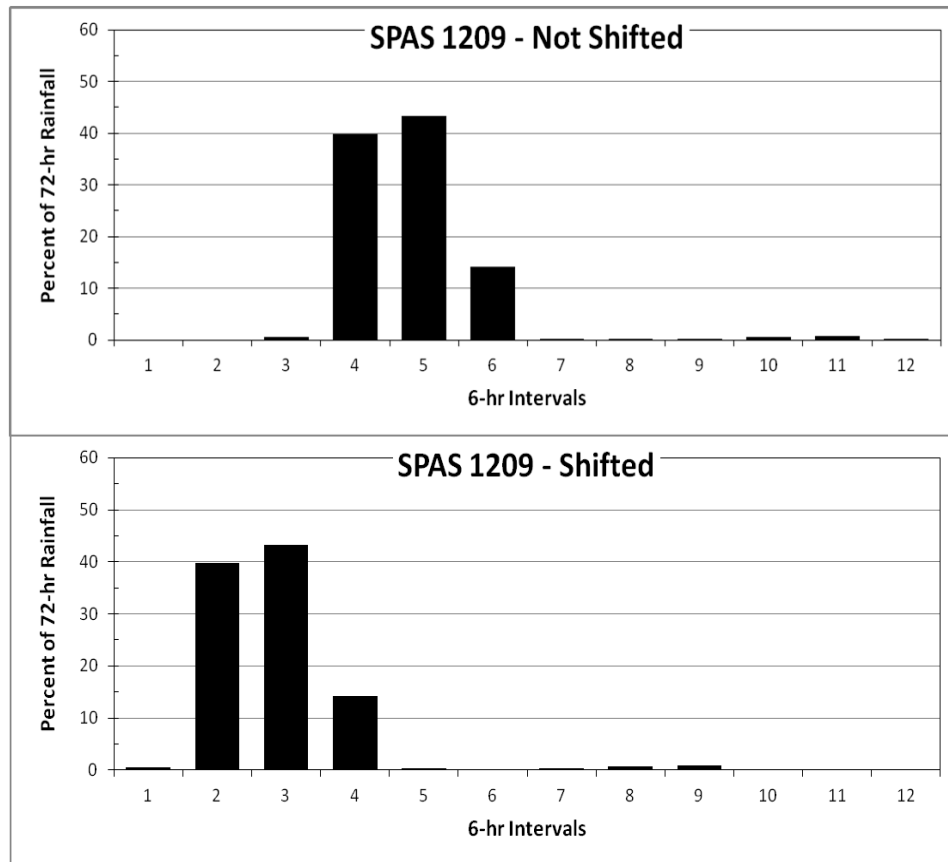


Figure 10.3 Example of 6-hour constrained precipitation, i.e. shift window to include precipitation for first 6-hour increment

Table 10.2 SPAS storm events used in Ohio PMP temporal distribution

SPAS #	Storm Name	State	AWA Storm Number	Lat	Lon	Year	Month	Day	Max Rainfall	Elevation	Storm Duration
Synoptic with Convection											
SPAS 1206	BIG RAPIDS	MI	100	43.6125	-85.3125	1986	9	9	13.42	950	96
SPAS 1208	WARNER PARK	TN	126	36.0611	-86.9056	2010	4	30	19.71	600	60
SPAS 1218	DOUGLASVILLE	GA	125	33.8700	-84.7600	2009	9	19	25.37	950	72
SPAS 1219	BIG FORK	AR	94	35.8708	-92.1208	1982	12	1	15.92	750	96
SPAS 1227	LOUISVILLE	MS	88	33.1167	-89.0500	1979	4	12	22.07	550	96
SPAS 1228	FALL RIVER	KS	120	37.6300	-96.0500	2007	6	30	25.50	900	95
SPAS 1183	EDGERTON	MO	75	40.4125	-95.5125	1965	7	18	20.76	950	61
Hybrid-MCS and Frontal											
SPAS 1029	AURORA COLLEGE	IL	112	41.7500	-88.3333	1996	7	16	18.24	650	39
SPAS 1209	WOOSTER	OH	78	40.9146	-81.9729	1969	7	4	14.95	1150	72
SPAS 1226	COLLEGE HILL	OH	71	40.0854	-81.6479	1963	6	3	19.39	950	49
SPAS 1048	HOKAH	MN	121	43.8125	-91.3625	2007	8	18	18.32	1000	120
Pure MCS											
SPAS 1210	MINNEAPOLIS	MN	102	44.8890	-93.4021	1987	7	23	11.55	900	36
SPAS 1220	DUBUQUE	IA	127	42.4400	90.7500	2011	7	27	15.14	900	24
SPAS 1030	DAVID CITY	NE	72	41.2132	-97.0710	1963	6	24	15.98	1650	72
SPAS 1035	FOREST CITY	MN	96	45.2394	-94.5404	1983	6	20	17.00	1100	96

An example of the 6-hour incremental precipitation for Warner Park, TN, May 2010 (AWA Storm Number 126), is shown in Table 10.3 and Figure 10.4, while Figure 10.4 displays an example of the hourly incremental precipitation for the same storm. In Figure 10.4, the x-axis is the cumulative percentage of the time period and the y-axis is the cumulative percentage of precipitation. For each SPAS storm event, an average temporal distribution was calculated based on all temporal patterns used for each storm type (MCS, Hybrid, and Synoptic). An example of the temporal distribution for the Synoptic storm events and the corresponding average temporal distribution are shown in Figures 10.6 and 10.7.

Table 10.3 Example of 6-hour incremental precipitation timing for Warner Park, TN, May 2010 (AWA Storm Number 126) storm center

	6-hr Increment											
	1	2	3	4	5	6	7	8	9	10	11	12
6hr Ppt (in)	0.07	2.01	4.37	4.46	0.75	0.92	4.45	1.94	0.40	0.34	-	-
Ratio to 72hr Ppt (%)	0.4	10.2	22.1	22.6	3.8	4.7	22.6	9.8	2.0	1.7	-	-
Pct. Accumulation	0.4	10.6	32.7	55.3	59.2	63.8	86.4	96.2	98.3	100.0	100.0	100.0

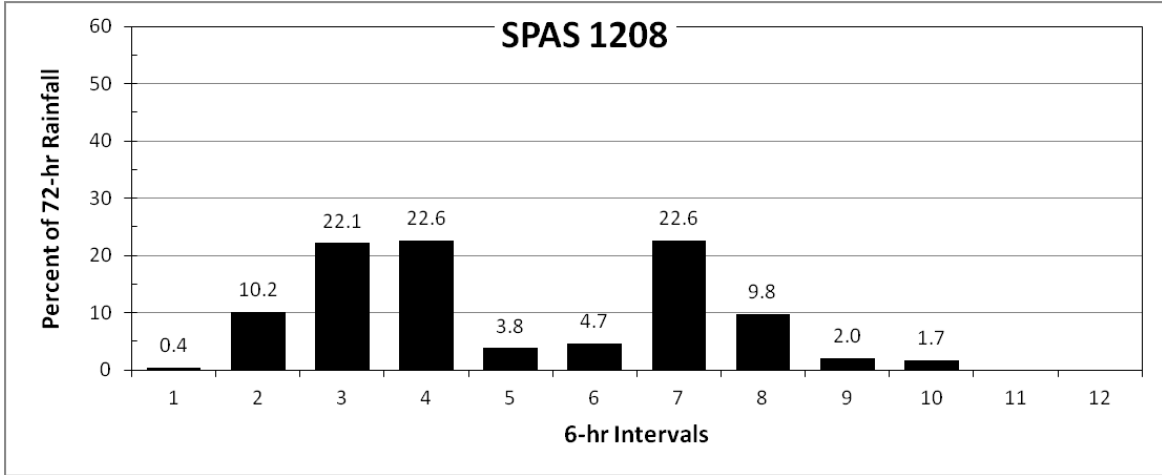


Figure 10.4 Example of 6-hour incremental precipitation timing for AWA Storm Number 2010

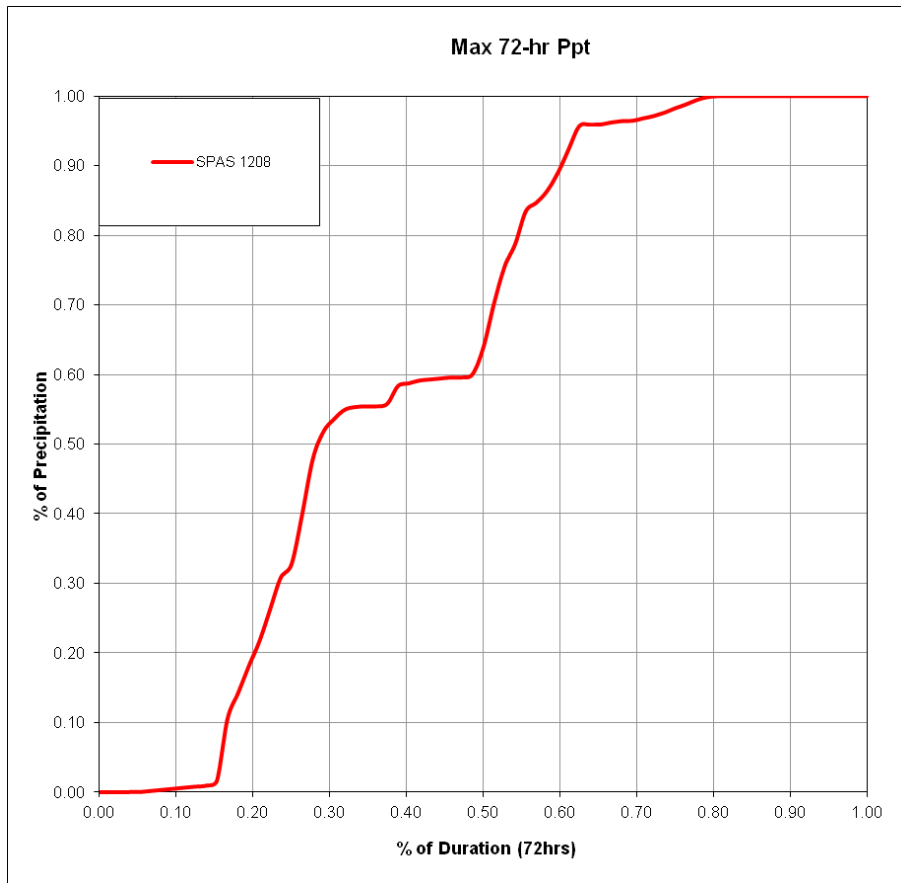


Figure 10.5 Example of hourly incremental precipitation timing for AWA Storm Number 2010

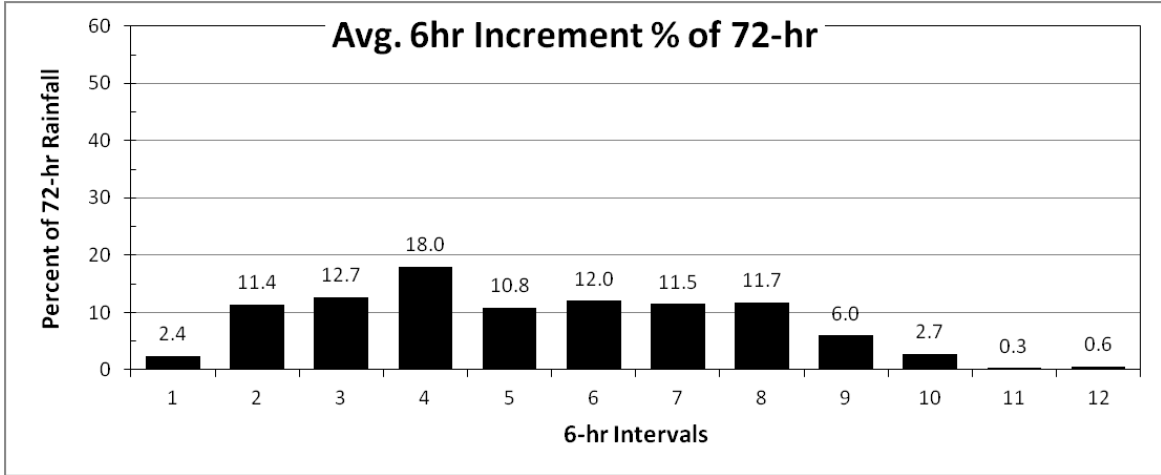


Figure 10.6 Average 6-hour incremental precipitation for Synoptic storm events

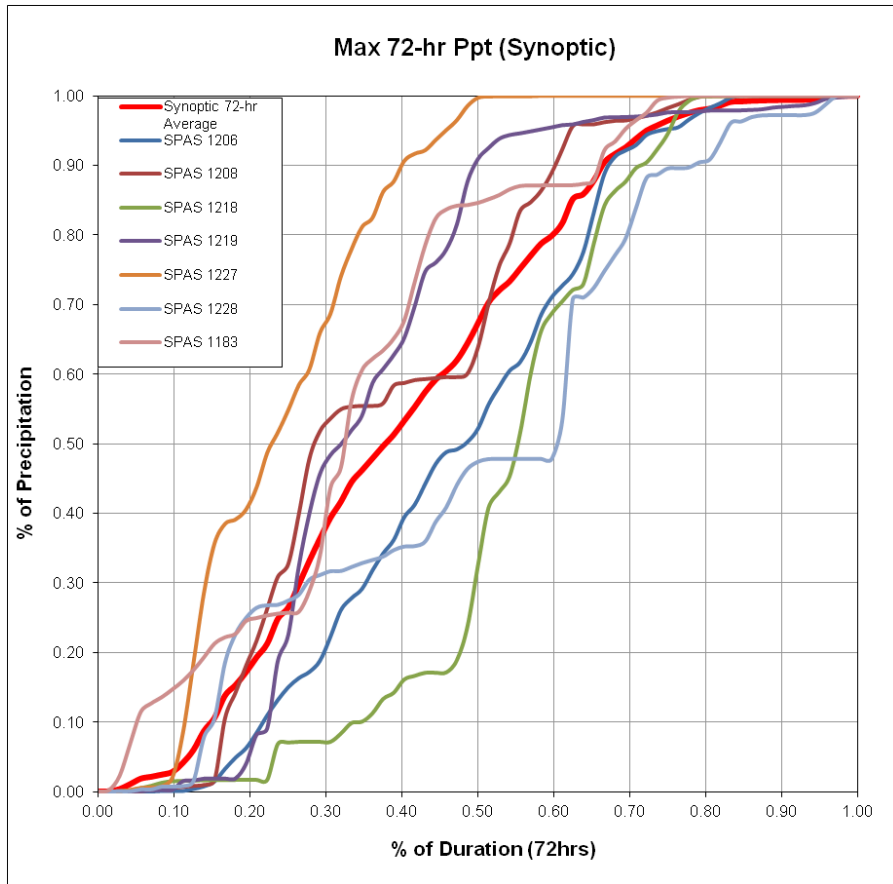


Figure 10.7 Example of average hourly incremental precipitation for Synoptic storm events

Results are presented as 6-hour incremental precipitation plots for MCS, Hybrid, and Synoptic storms. The temporal timing for the MCS and Hybrid storm events are similar in that they have a front-loaded distribution. The temporal timing of the Synoptic events has a 6-hour incremental peak with nearly constant distribution (~10-12%) for the majority of the remaining 6-hour increments. The average incremental 6-hour temporal distribution for MCS, Hybrid, and Synoptic storm events are shown in Figure 10.8. The x-axis is the index of the 6-hour precipitation. The y-axis is the percentage of x-hour precipitation for each 6-hour increment.

These distributions are to be expected when the storm type and storm dynamics of the rainfall are considered. During MCS events, high levels of moisture are fed into a storm environment for a short period of time over a small area size. This leads to high intensity rainfall over a shorter time period. Synoptic events are fed by consistent moisture over a long period of time and affect a large area size, generally as a front stalls or moves slowly over a given location. This leads to steady rainfall, which lasts for several days, with heavier imbedded bursts. However, the peak intensities are much less than MCS events. Hybrid storms have characteristics of both temporal and intensity distributions associated with MCS and synoptic events, except the peak intensities are less than a pure MCS and the duration is less than a pure synoptic event.

These analyses are important when considering how to implement the PMP design storm temporal pattern. Consideration should be given to storm type being evaluated so that MCS temporal distributions are not applied to a synoptic storm type PMP design storm and vice versa.

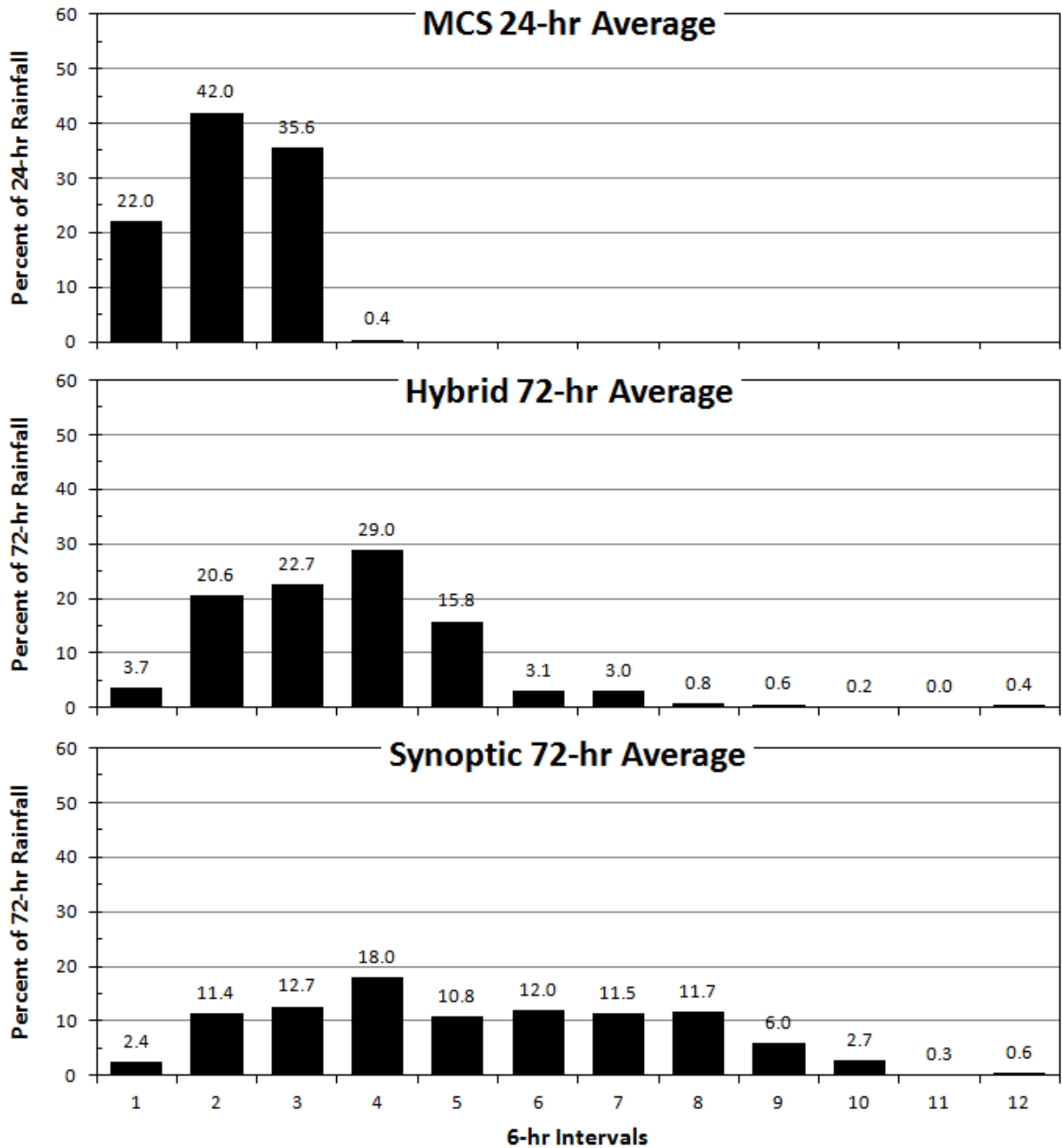


Figure 10.8 Ohio 6-hour incremental temporal distributions based on SPAS storm centers

The temporal distribution results from this analysis are different from the HMR 52 recommendations for the 6-hour sequences for PMP timing. HMR 52 stated that almost any arrangement of 6-hour incremental precipitation was found in their analysis, but has several recommendations:

- 1) 6-hour increments be arranged with single peak.

- 2) Arrange the individual 6-hour increments such that they decrease on either side of the greatest 6-hour increment.
- 3) Place four greatest 6-hour increments at any position in the sequence except within the first 24-hour period.

An example of one potential temporal timing sequence based on HMR 52 recommendations is provided in Figure 10.9.

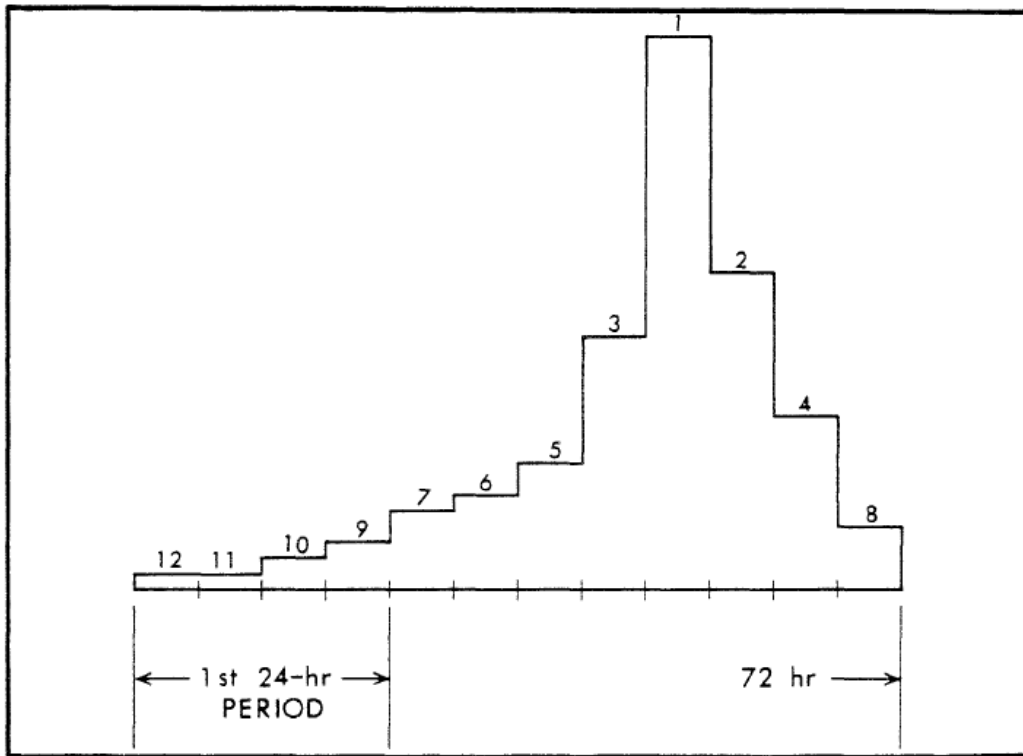


Figure 10.9 Example of one potential temporal timing sequence based on HMR 52 recommendations (image from HMR 52, Figure 3)

Temporal sequences derived from SPAS storms used in this study show a single 6-hour increment peak for the MCS, Hybrid, and Synoptic events, similar to HMR 52 recommendations. The MCS events have 100% of their precipitation occur in the first 24-hour period, the Hybrid storm events have 76% of their precipitation in the first 24-hour period, and the synoptic events have 44.5% of their precipitation in the first 24-hour period. This pattern is different than the HMR 52 recommendation that the top four 6-hour increments cannot be placed in the first 24-hour period. The cause of this difference is not known as reproducing HMR 52 procedures is not possible due to limited information provided in HMR 52. This difference may be due to the constraints that were used in the development of the temporal analysis in this study, i.e. precipitation has to occur in the first 6-hour increment.

10.3 Ohio Standardized Timing Distributions by Storm Type

As described in the previous section, fifteen SPAS storms were used for temporal distribution analysis in Ohio: seven MCS, four Hybrid, and four Synoptic (see Table 10.2). The rainfall mass curve at the storm center was used for the temporal distribution calculations. Rainfall data for the fifteen storm centers were used in this analysis. The Significant Precipitation Period (SPP) for each storm was selected by excluding relatively small rainfall accumulations at the beginning and end of the rainfall duration. Accumulated rainfall (R) amounts during the SPP were used in the analysis for the hourly storm rainfall. The total rainfall during the SSP was used to normalize the hourly rainfall amounts. The time scale (TS) was computed to describe the time duration when half of the accumulated rainfall (R) had fallen. The basic procedure used to calculate these parameters are listed below.

Parameters:

- SPP – Significant Precipitation Period when the majority of the rainfall occurred
- R - Accumulated Rainfall at the storm center during the SSP
- R_n - Normalized R
- T - Time when R occurred
- T_{50} - Time when $R_n = 0.5$
- T_s - Shifted Time

Procedure to calculate parameters

1. Determine the SPP. Inspect each storm's rainfall data for "inconsequential" rainfall at either the beginning and/or the end of the records. Remove these "tails" from calculations. Generally use a criteria of less than 0.1 inches/hour intensity. No internal rainfall data are deleted.
2. Recalculate the accumulated rainfall records for R.
3. Plot the SPAS rainfall and R mass curves and inspect for reasonableness (Figure 10.10).
4. Normalize the R record by dividing all values by the total R to produce R_n for each hour, R_n ranges from 0.0 to 1.0.
5. Determine T_{50} using the time when $R_n = 0.5$.
6. Calculate T_s by subtracting T_{50} from each value of T. Negative time values precede the time to 50% rainfall, and positive values follow.
7. Prepared graphs of a) T vs R, b) T vs R_n , and c) T_s vs R_n for MCS, Hybrid, Synoptic, and all storm events.

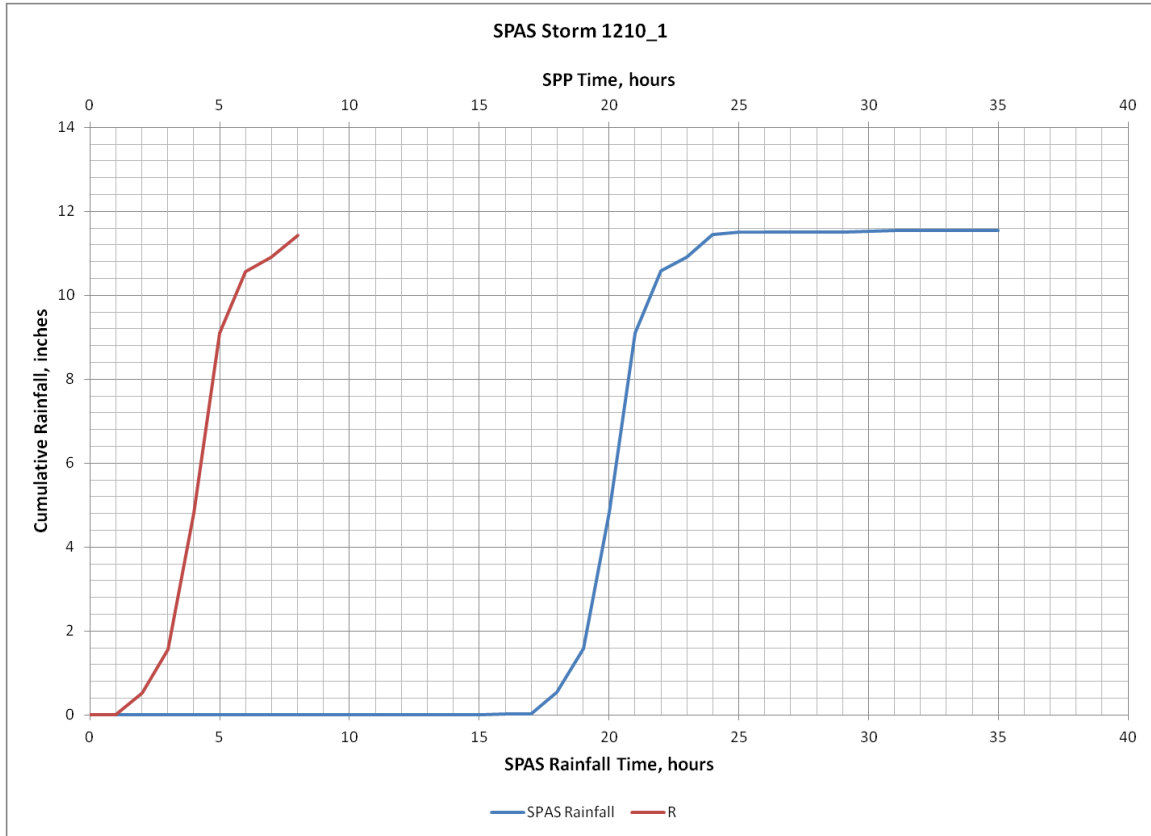


Figure 10.10 R and SPAS rainfall for Minneapolis, MN July 1987, AWA Storm Number 102

10.3.1 Results of the Analysis

Following the procedures and description from the previous section, results are presented as three graphs. The graphs are a) T vs R , b) T vs R_n , and c) T_s vs R_n for MCS, Hybrid, Synoptic, and all storm events. Figures 10.11 - 10.13 show graphs for MCS SPAS storm events comparing T vs R , T vs R_n , and T_s vs R_n . Figures 10.14 - 10.16 show graphs for the Hybrid SPAS storm events comparing T vs R , T vs R_n , and T_s vs R_n . Figures 10.17 - 10.19 show graphs for Synoptic SPAS storm events comparing T vs R , T vs R_n , and T_s vs R_n . Finally, Figures 10.20 - 10.22 show graphs for all three SPAS storm types (MCS, Hybrid, and Synoptic) comparing T vs R , T_s vs R_n , and T_s vs R_n .

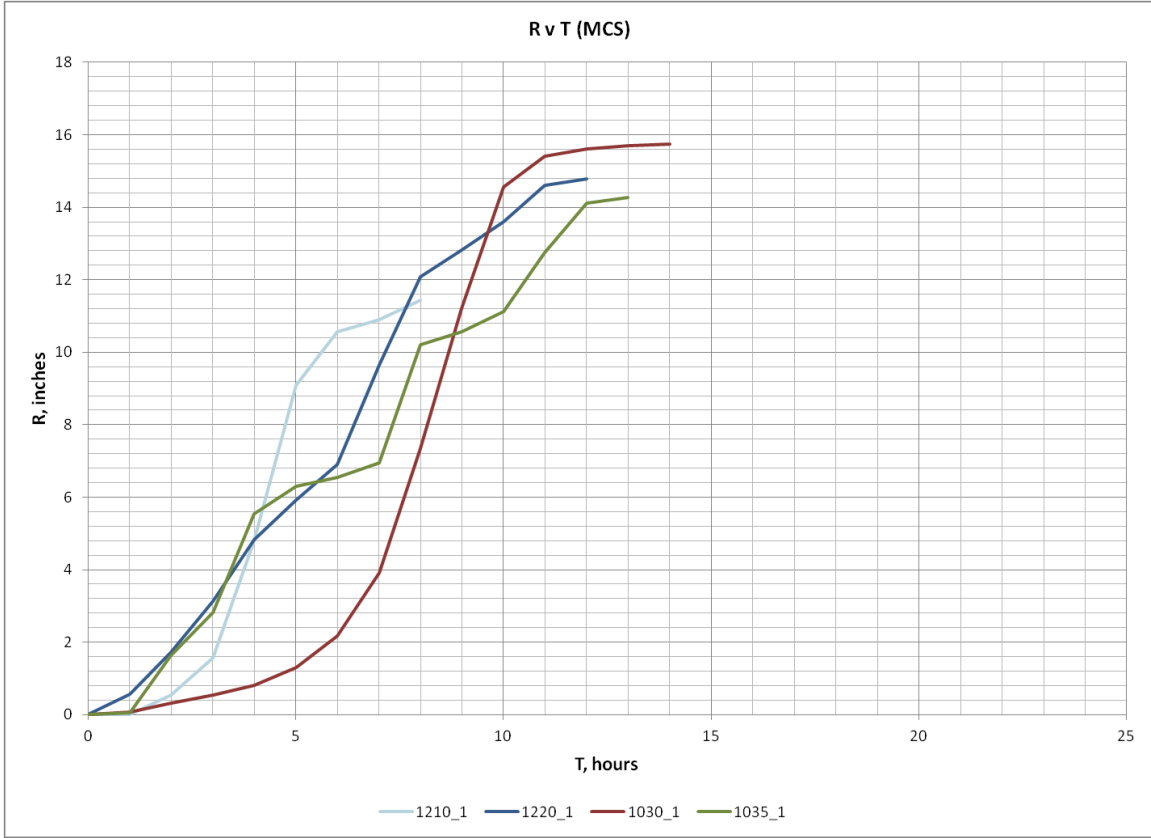


Figure 10.11 Rainfall R versus Time for SPAS MCS storms

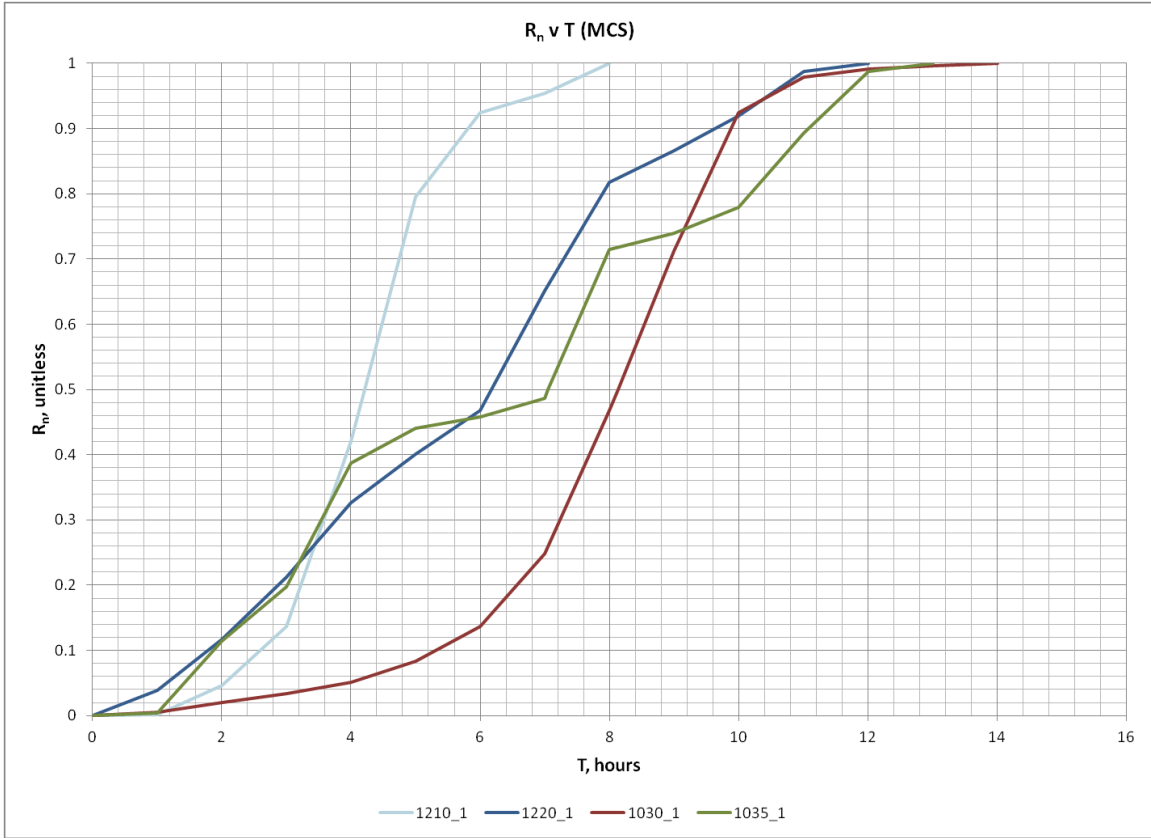


Figure 10.12 Normalized R versus Time for SPAS MCS storms

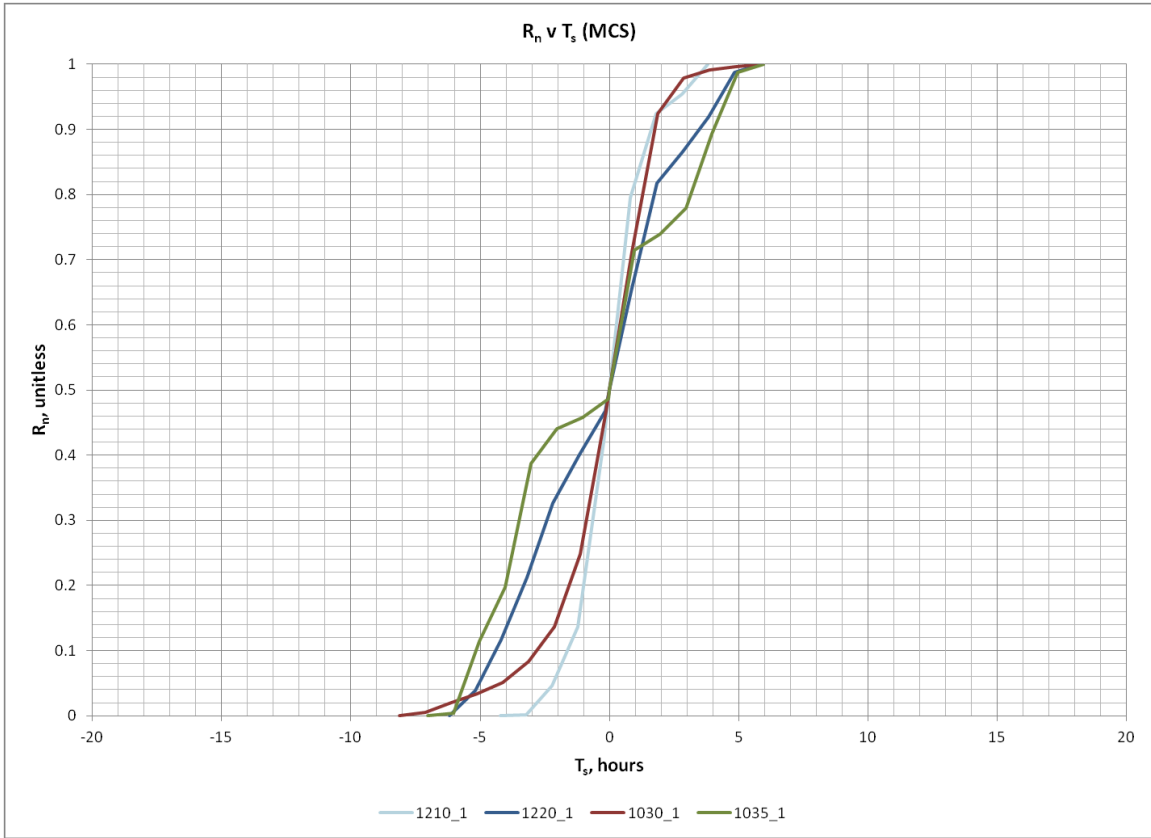


Figure 10.13 Normalized R versus shifted time for SPAS MCS storms

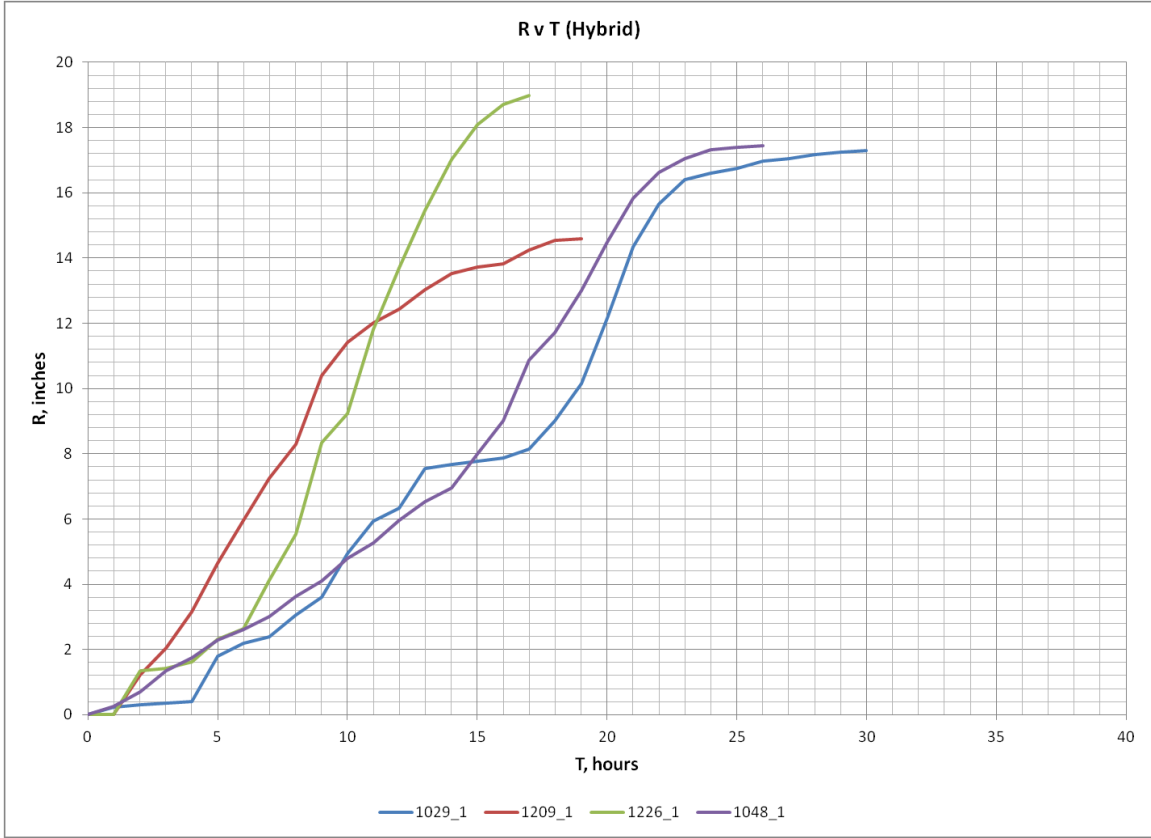


Figure 10.14 Rainfall R versus Time for SPAS Hybrid storms

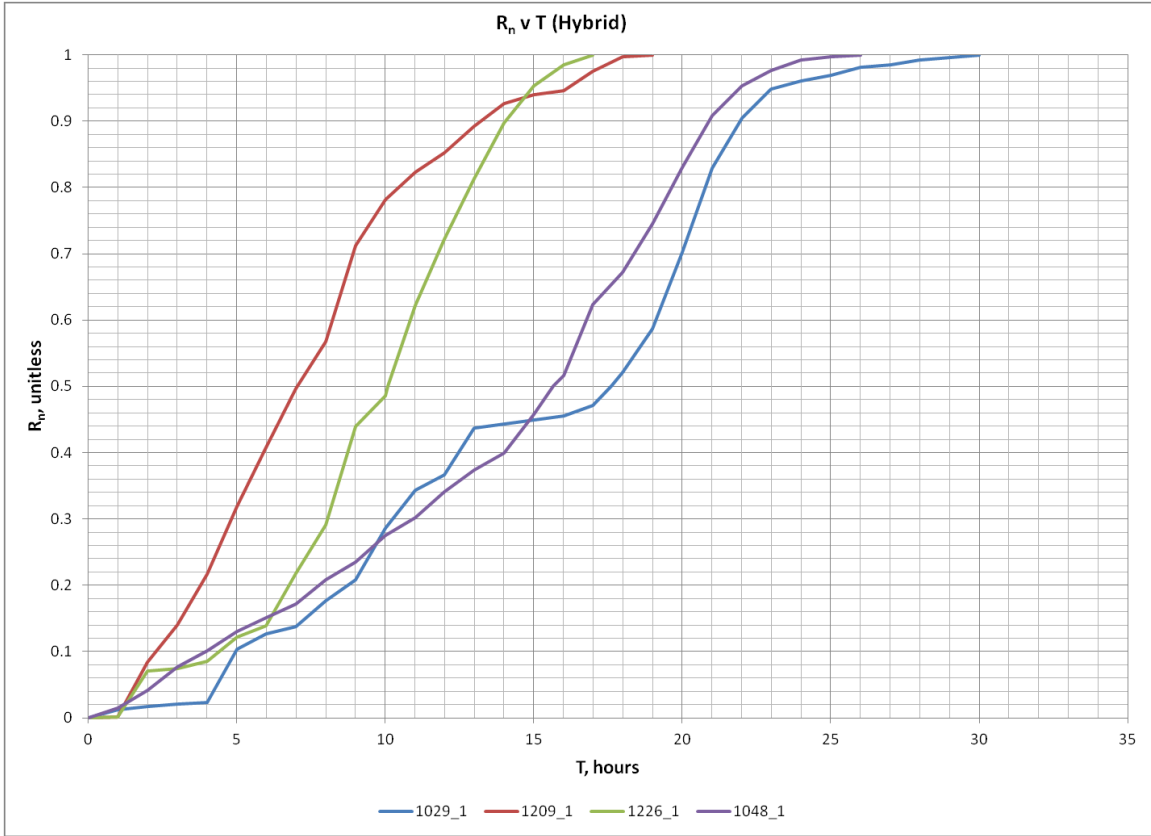


Figure 10.15 Normalized R versus Time for SPAS Hybrid storms

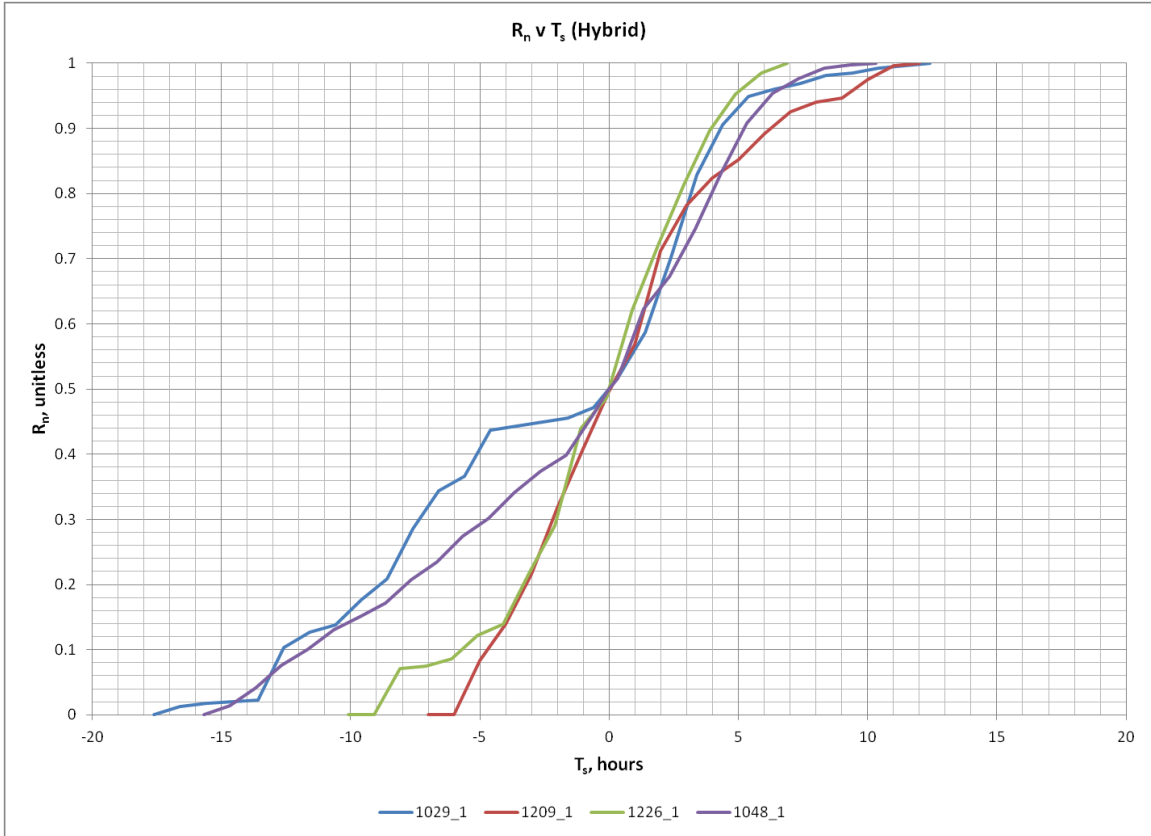


Figure 10.16 Normalized R versus shifted time for SPAS Hybrid storms

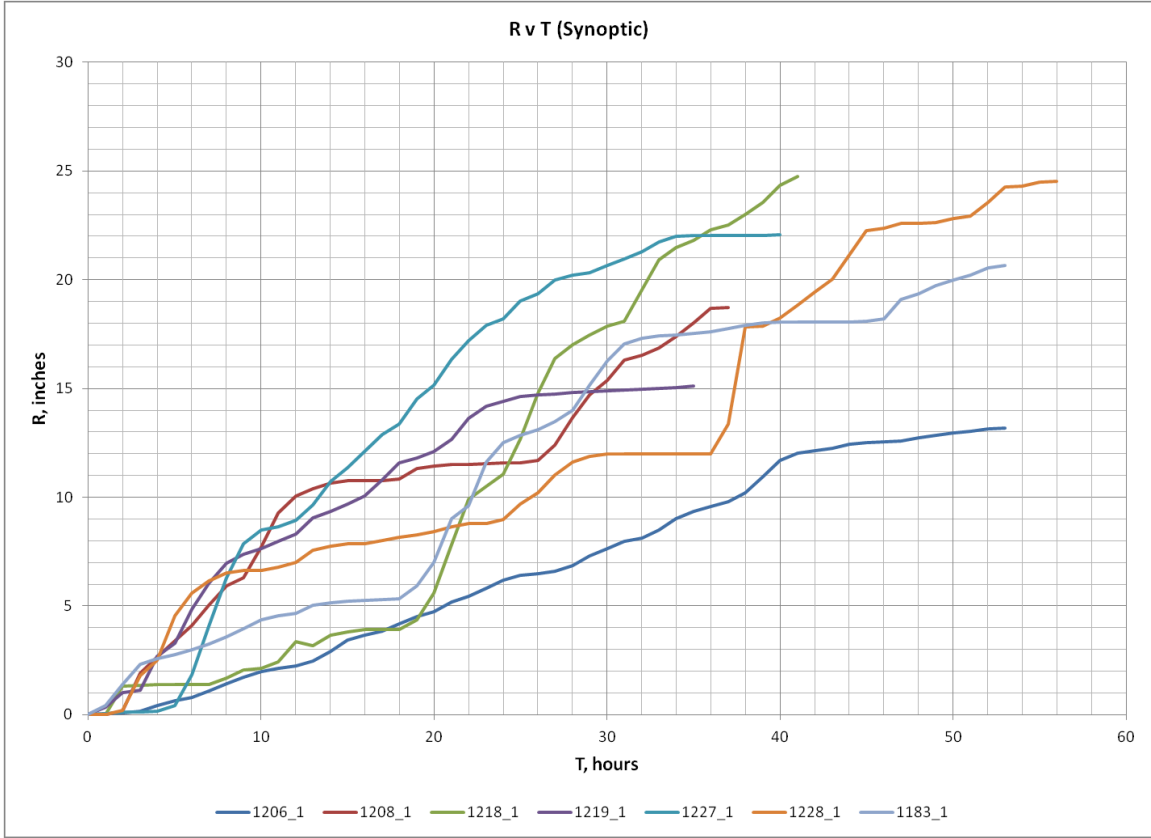


Figure 10.17 Rainfall R versus Time for SPAS Synoptic storms

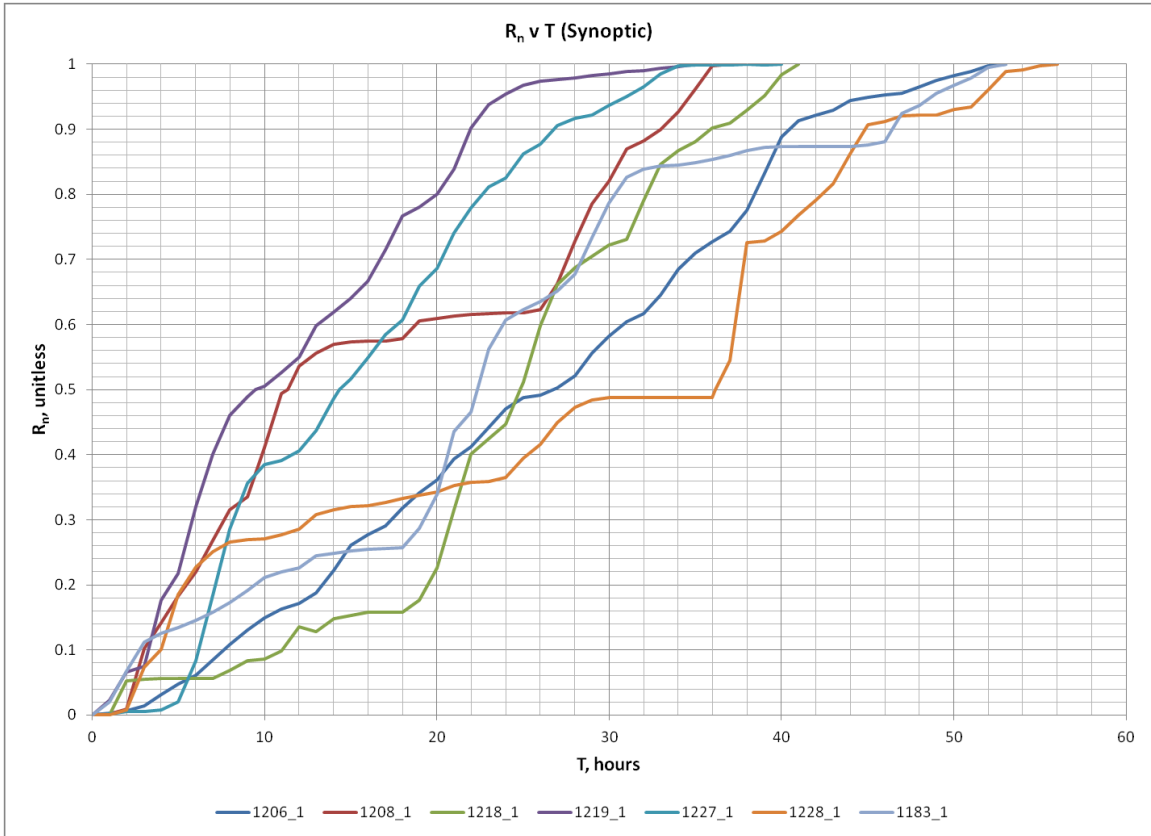


Figure 10.18 Normalized R versus Time for SPAS Synoptic storms

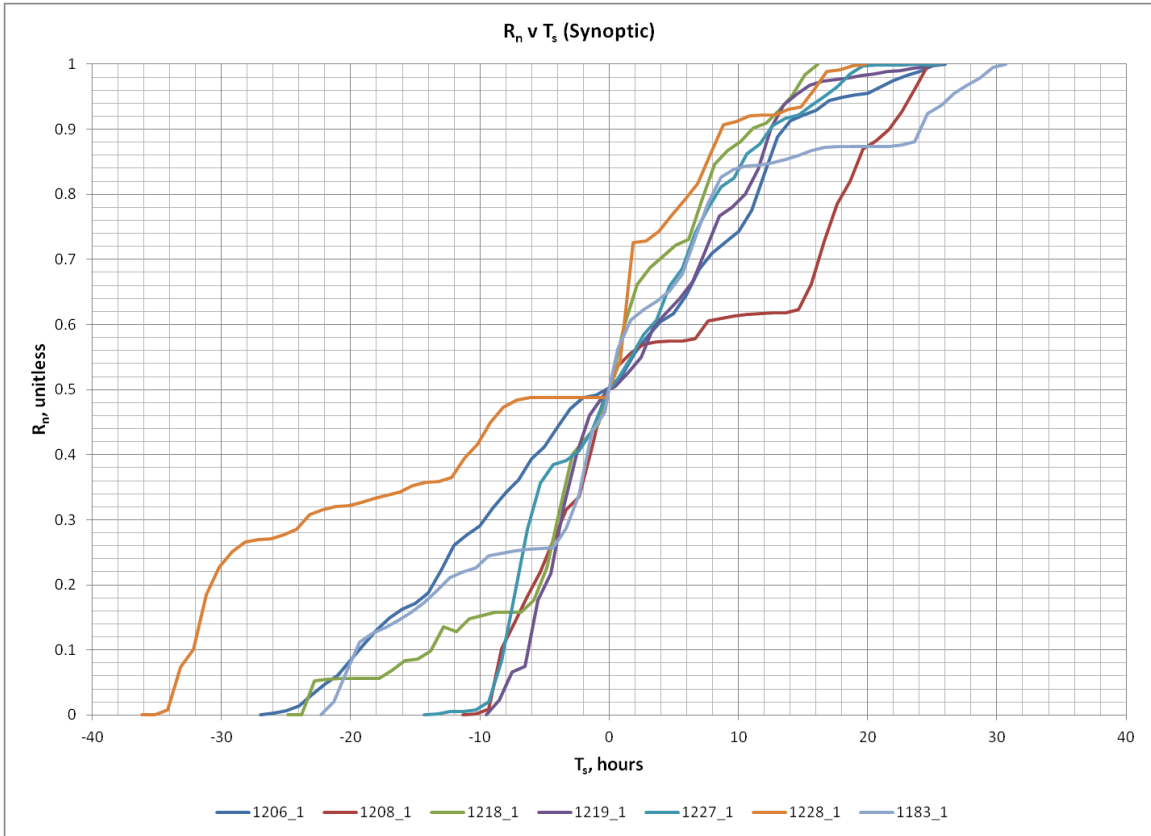


Figure 10.19 Normalized R versus shifted time for SPAS Synoptic storms

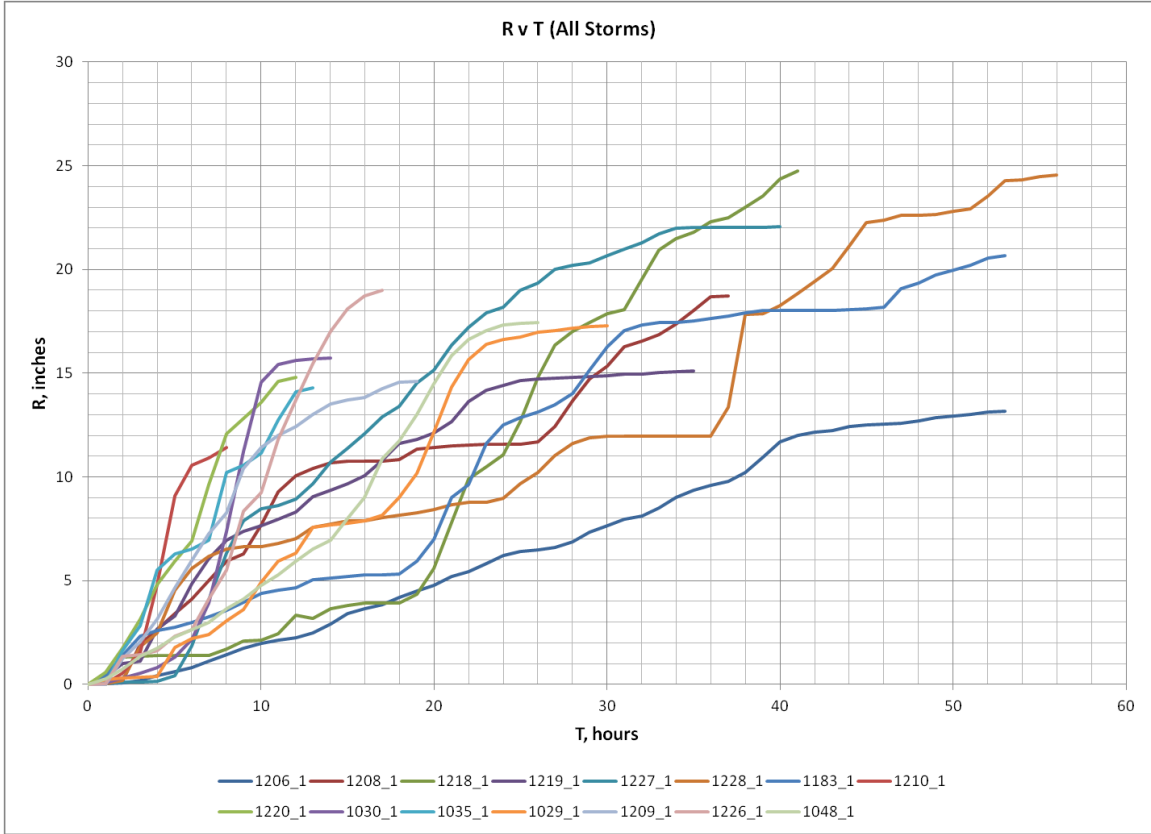


Figure 10.20 Rainfall R versus Time for all SPAS storms

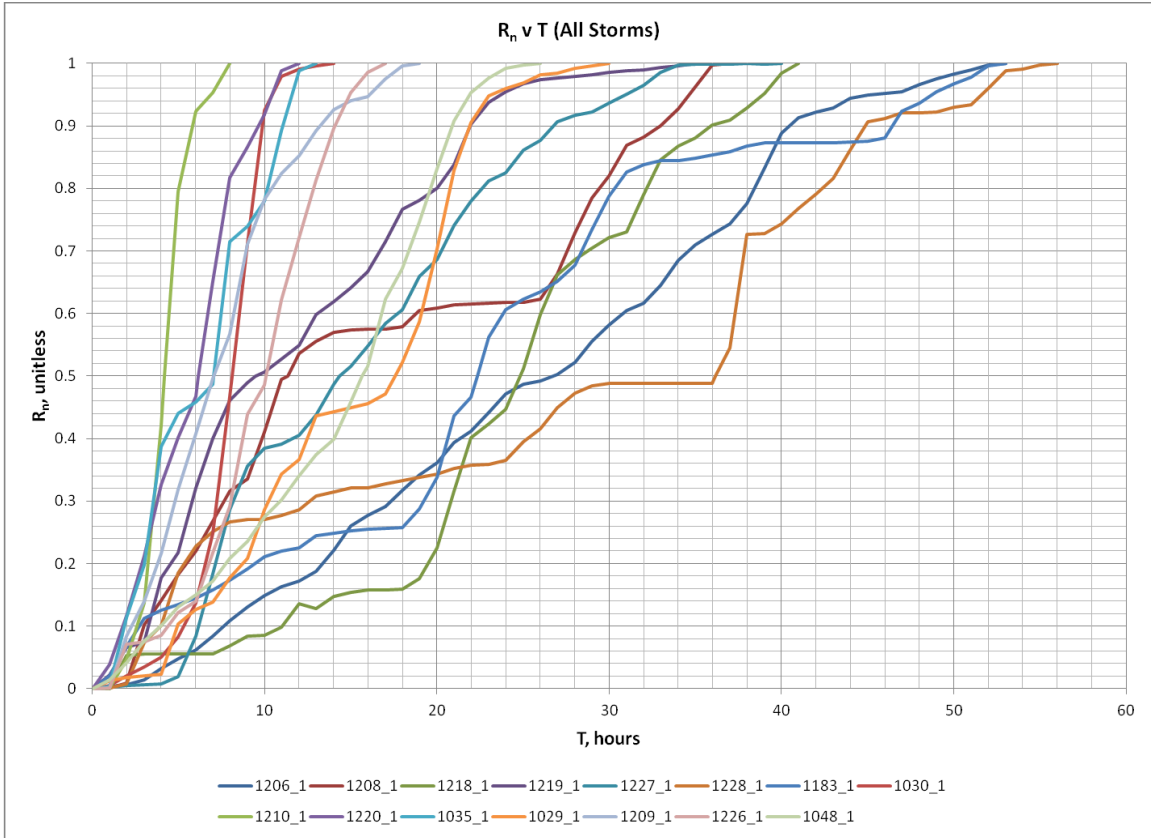


Figure 10.21 Normalized R versus Time for all SPAS storms

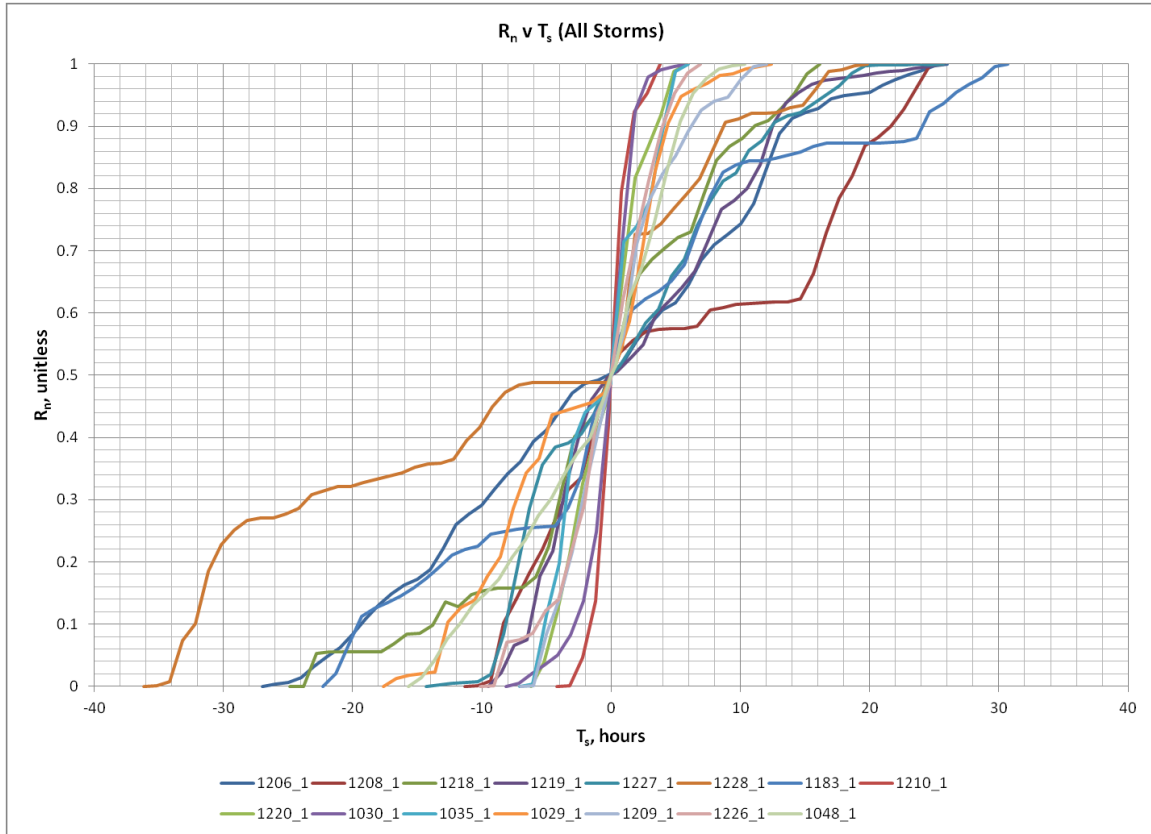


Figure 10.22 Normalized R versus shifted time for all SPAS storms

Results of this investigations show consistent results for each of the three storm types analyzed. The MCS events have 100% of their precipitation occur within durations of 8 and 14 hours, the Hybrid storm events have 100% of their precipitation occur within durations between 17 and 30 hours, and the synoptic events have 100% of their precipitation occur within durations of 36 and 56 hours. The MCS events have 50% of their precipitation occur within durations between 4 and 8.5 hours, the Hybrid storm events have 50% of their precipitation occur within durations between 7 and 18 hours, and the synoptic events have 50% of their precipitation occur within durations between 10 and 36 hours.

The storm temporal pattern evaluations conducted as part of this study resulted in storm temporal patterns that were similar to some of those discussed in Section 2 of HMR 52. Therefore, the PMP-design storm temporal patterns presented in HMR 52 are reasonable for use in PMP/PMF evaluations. In addition, AWA's investigations of the storms used in the this study show that a front loaded temporal scenario is also possible. This is in contrast to HMR 52 where they suggest not allowing the four greatest 6-hour increments to occur in the first 24-hours.

11. Results

The following are the main conclusions from this study:

- HMR 51 PMP values are outdated. This study provided updated PMP values to be used in place of HMR 51 PMP values for Ohio.
- The most recent storm used to derive PMP values in HMR 51 occurred in 1972. This study updated the storm database to include storms thorough 2012, adding 40 years of storm analyses.
- HMRs 51 and 52 did not use computer based technologies in the storm analyses procedures. This study used computer technology and GIS to more accurately analyze storm rainfall patterns and derive the spatially distributed PMP values.
- Storm analyses used in HMRs 51 and 52 did not have NEXRAD weather radar to help spatially distribute rainfall among rain gauge locations. SPAS storm analyses incorporates this information when available to provide the most reliable spatial representation of storm rainfall patterns possible.
- Understanding of meteorological processes, interactions, and storm patterns have advanced greatly since the publication of HMR 51. Satellite and radar technology have greatly added to the understanding of storm patterns over the last 40 years. This study incorporated the state-of-the-science understanding and technology associated with analyzing extreme rainfall events.

11.1 Ohio Statewide PMP Values

This PMP study has produced PMP values for use in computing the PMF using HMR 52 procedures. Values for all durations and area sizes provided in HMR 51, with the addition of the 1-square mile area size, have been computed using the procedures described in this report. In this study, the 1-square mile area size was computed in order to provide data to the users at an area size required for many of the basins in Ohio. AWA has demonstrated that the 10-square mile values in HMR 51 do not represent the 1-square mile value adequately. In HMR 51, the assumption was made that this variation was minimal and more importantly the data used to derive PMP value in HMR 51 did not allow for explicit evaluation of 1-square mile values. Therefore, the explicit analysis of the 1-square mile value was addressed in this study.

Figures 11.1 through 11.50 display the final PMP values for all durations and areas sizes analyzed in this study. PMP values can be most efficiently derived using GIS, but can also be interpolated from the maps included in this report as required.

The PMP values derived in this study can be used in computing the PMF at any location within the state. Although grid points and contours extend beyond the state boundaries, results are only considered applicable within the state boundaries and for watersheds draining into the state. Values at durations of 6-, 12-, 24-, 48-, and 72-hours

and areal sizes from 1-, 10-, 100-, 200-, 500-, 1,000-, 2,000-, 5,000-, 10,000-, and 20,000-square miles have been computed in gridded GIS format.

The study was designed to retain as much continuity as possible with the methodology used in HMR 51 and previous AWA studies, while incorporating improvements based on changes in technology, meteorological understanding, and availability of updated data. In addition, special consideration was given to basin sizes and hydrologic characteristics within Ohio (generally less than 100-square miles).

Full SPAS storm rainfall analyses were completed for 10 storms not analyzed in either HMR 51 or previous AWA studies. The study continued the use of surface dew point data to quantify moisture inflow to storms. However, instead of using the 12-hour persisting value as in HMR 51, an average dew point value for a duration (6-, 12-, or 24-hours) consistent with the storm rainfall was used. This approach provides a more representative parameterization of the moisture available to storms.

Updated maximum dew point climatologies have been developed as part of this study and during previous AWA studies and were used in this study. This allows for use of average maximum dew point values and climatologies at the 100-year return frequency level for 6-hour, 12-hour, and 24-hour durations for use in storm maximization and transposition. Storms were maximized and transpositioned to a set of 23 grid points. This covered the entire state and provided a margin for boundary conditions (see Figure 1.4).

All-Season PMP - 72-hour 1 mi² (inches)
Ohio Statewide PMP Study

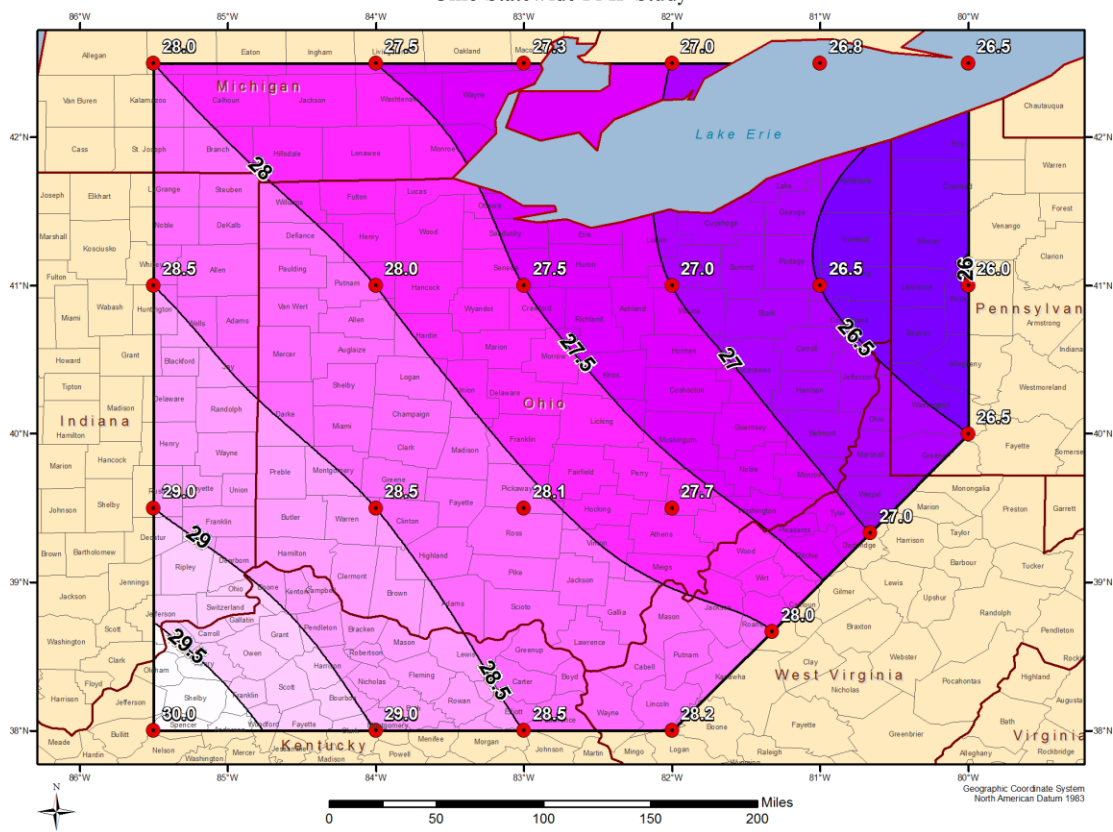


Figure 11.5 All-season PMP (inches) for 72-hour, 1-square mile

All-Season PMP - 6-hour 10 mi² (inches)
Ohio Statewide PMP Study

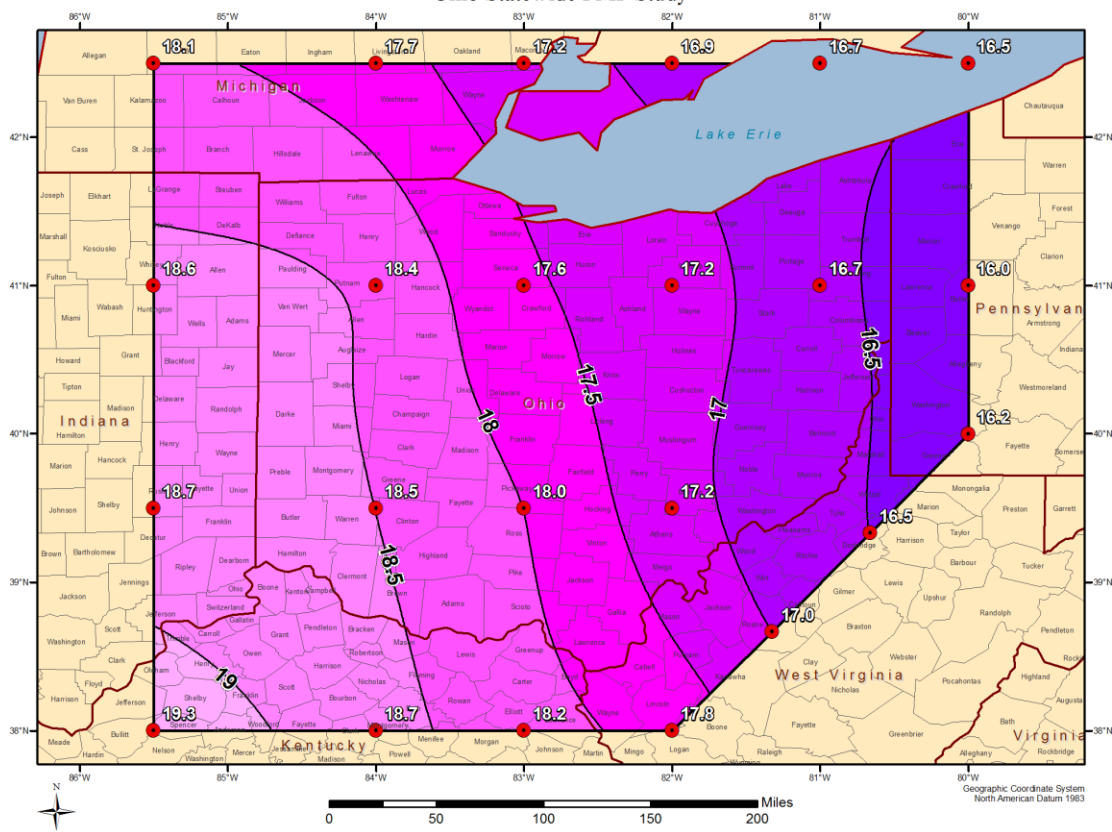


Figure 11.6 All-season PMP (inches) for 6-hour, 10-square mile

All-Season PMP - 48-hour 10 mi² (inches)
Ohio Statewide PMP Study

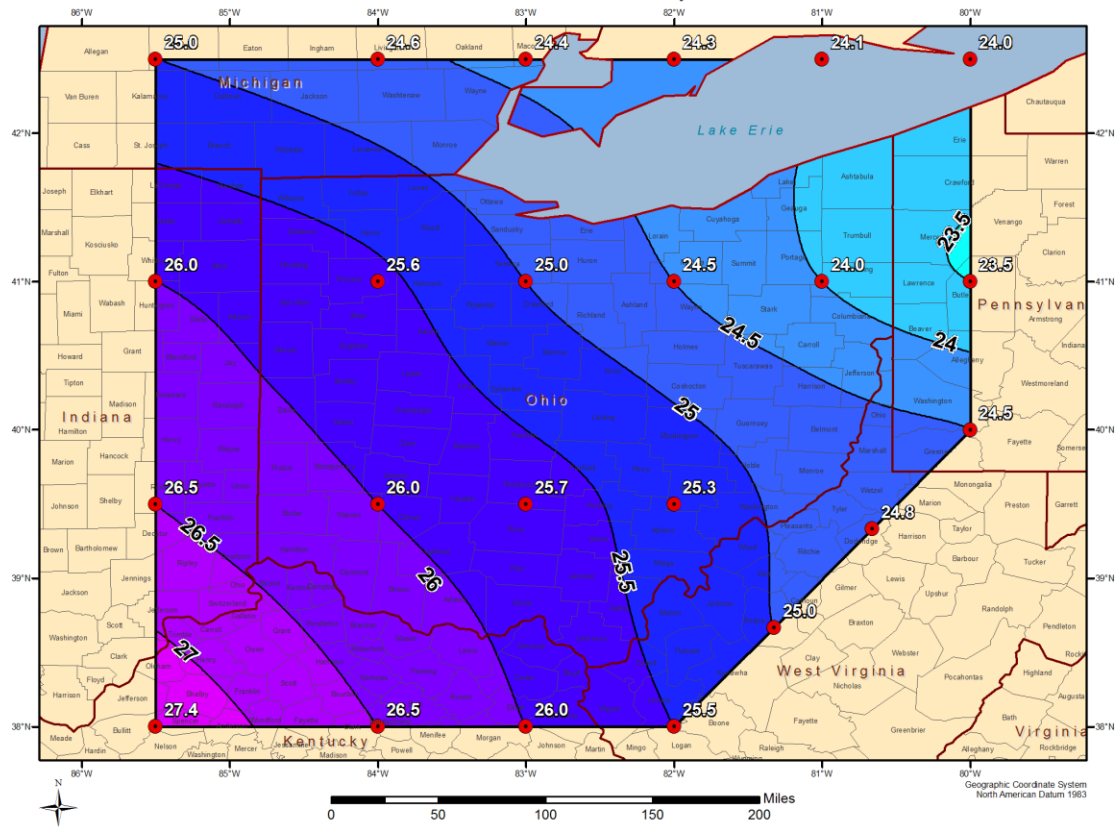


Figure 11.9 All-season PMP (inches) for 48-hour, 10-square mile

All-Season PMP - 6-hour 100 mi² (inches)
Ohio Statewide PMP Study

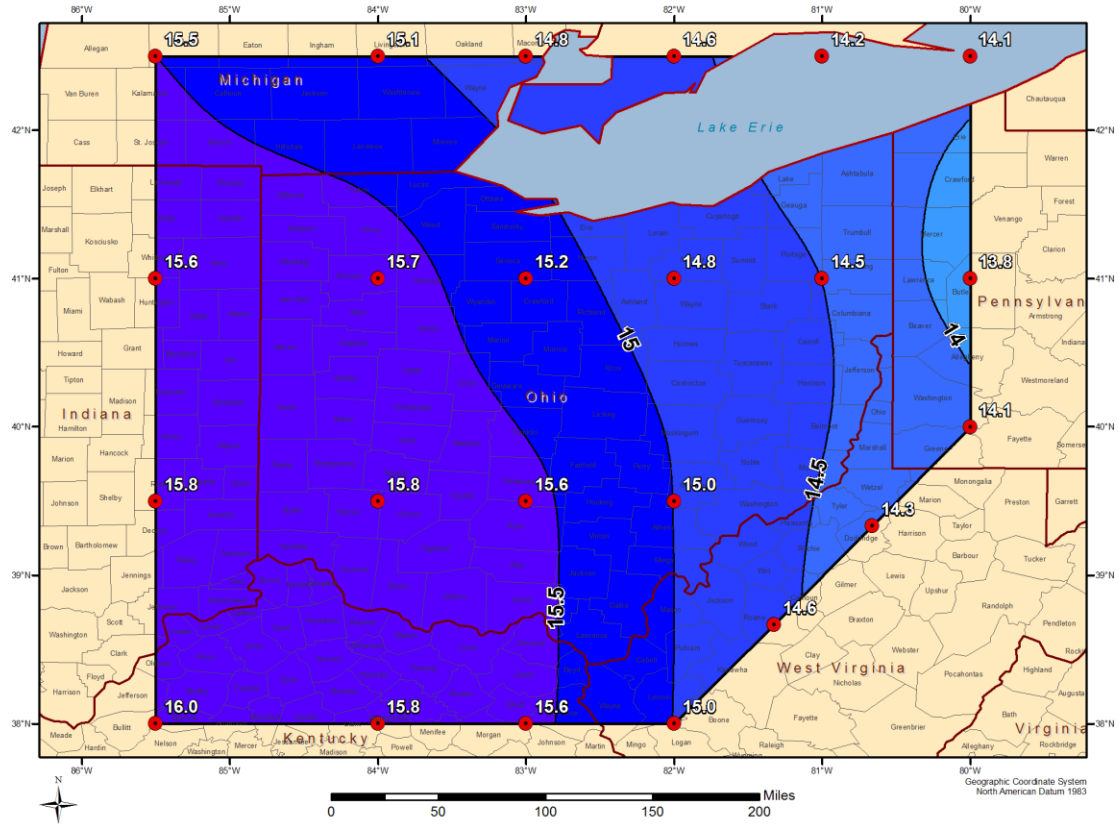


Figure 11.11 All-season PMP (inches) for 6-hour, 100-square mile

All-Season PMP - 48-hour 100 mi² (inches)
Ohio Statewide PMP Study

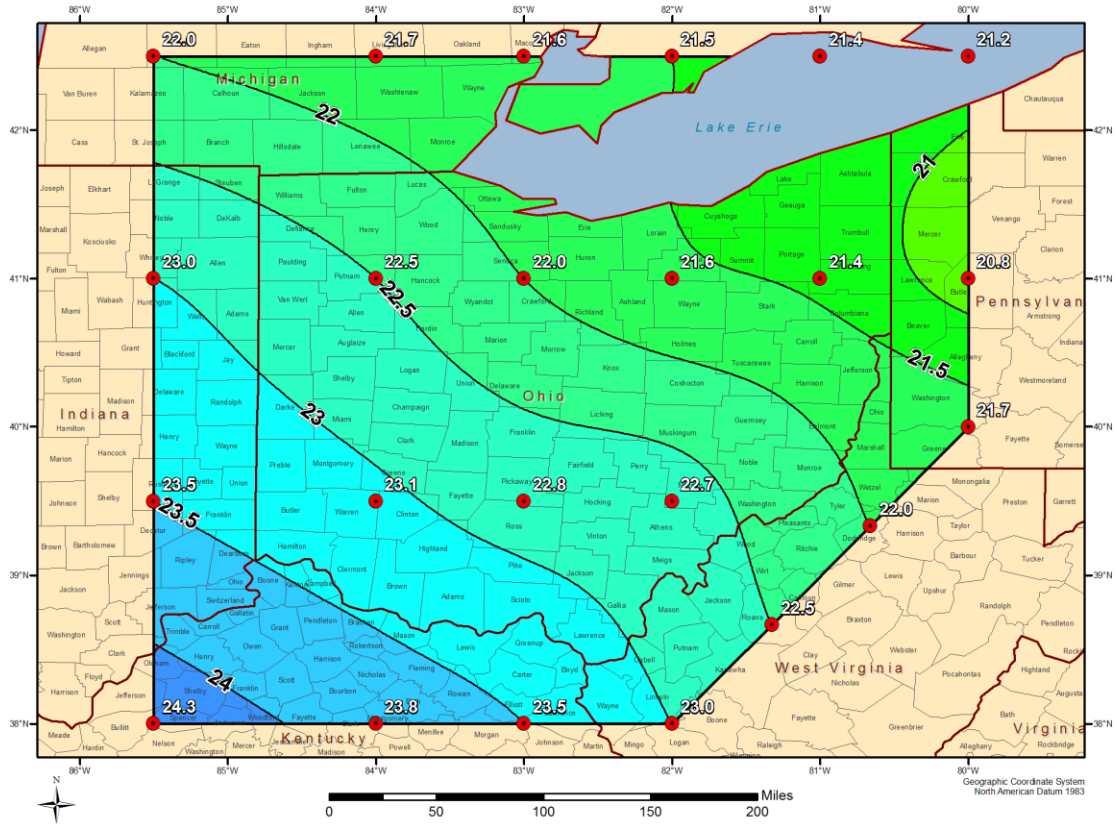


Figure 11.14 All-season PMP (inches) for 48-hour, 100-square mile

All-Season PMP - 72-hour 100 mi² (inches)
Ohio Statewide PMP Study

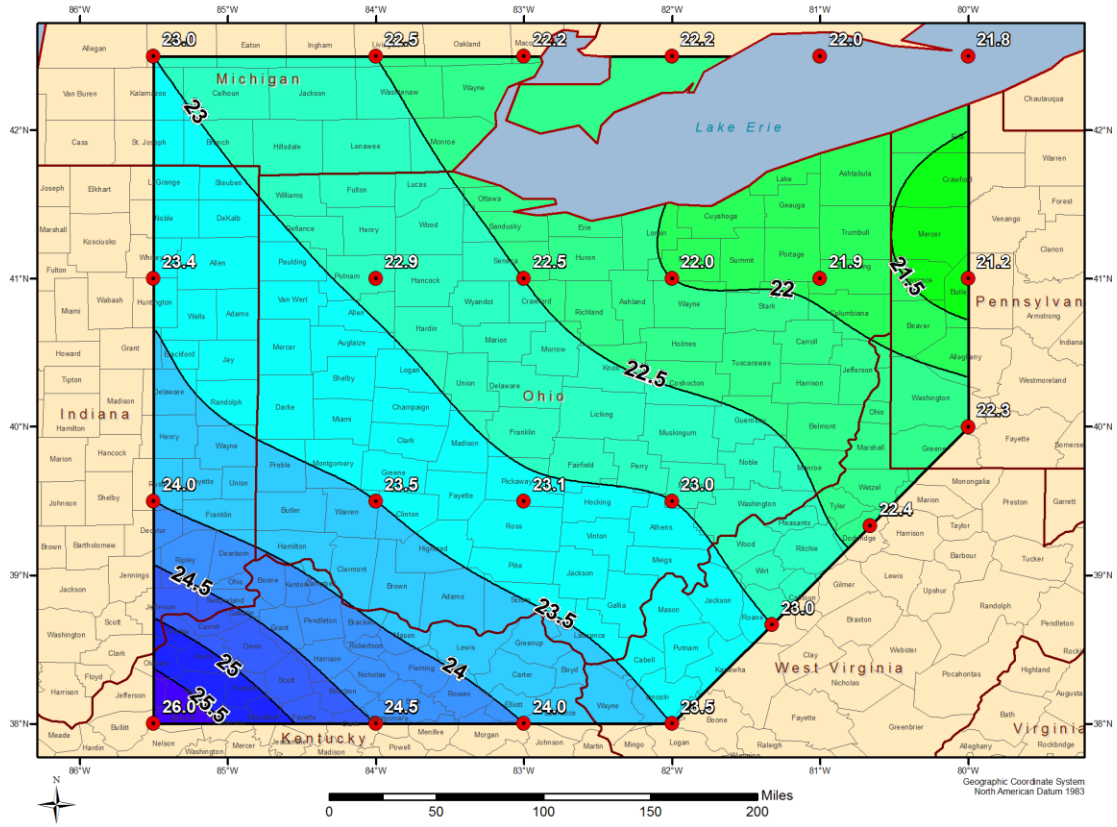


Figure 11.15 All-season PMP (inches) for 72-hour, 100-square mile

All-Season PMP - 6-hour 200 mi² (inches)
Ohio Statewide PMP Study

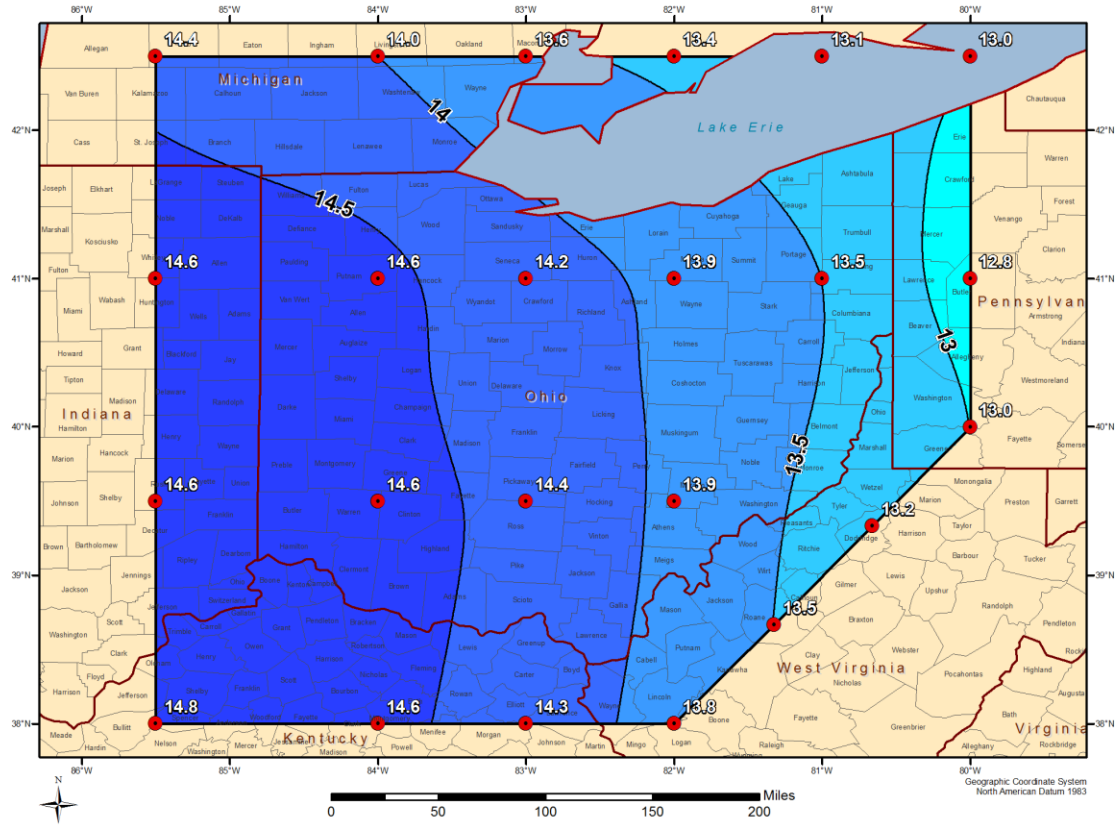


Figure 11.16 All-season PMP (inches) for 6-hour, 200-square mile

All-Season PMP - 12-hour 200 mi² (inches)
Ohio Statewide PMP Study

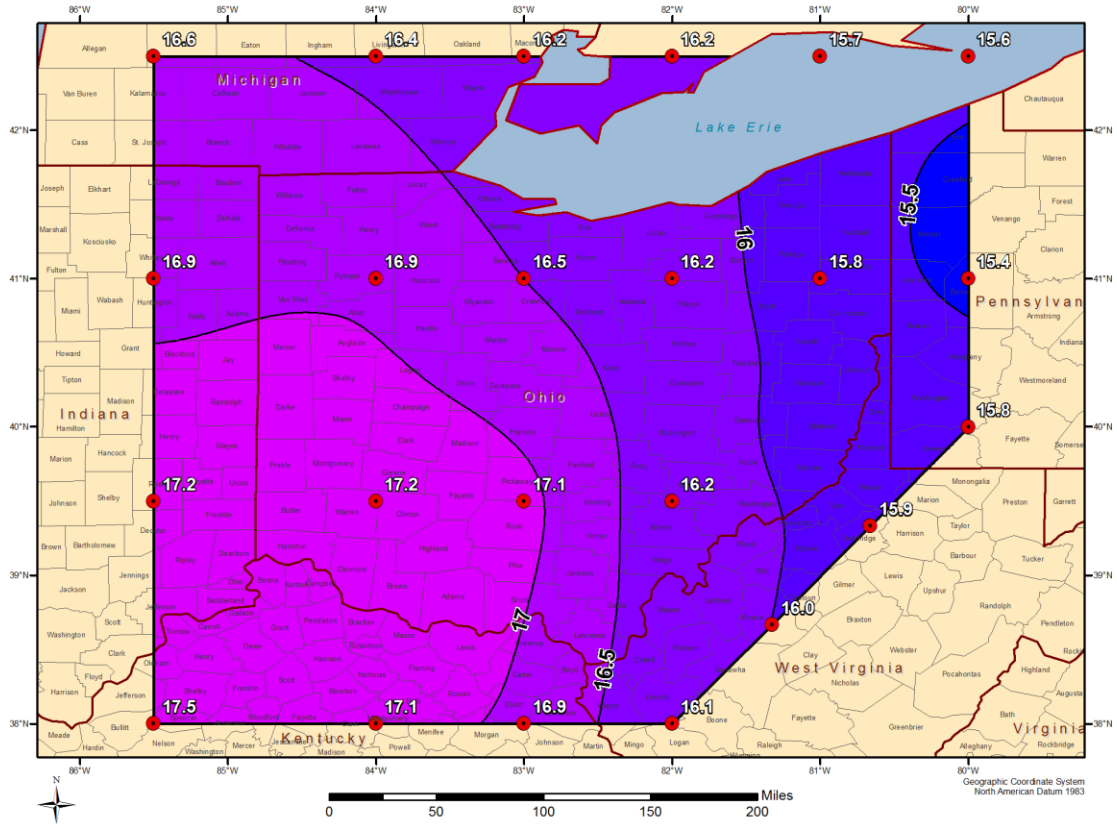


Figure 11.17 All-season PMP (inches) for 12-hour, 200-square mile

All-Season PMP - 48-hour 200 mi² (inches)
Ohio Statewide PMP Study

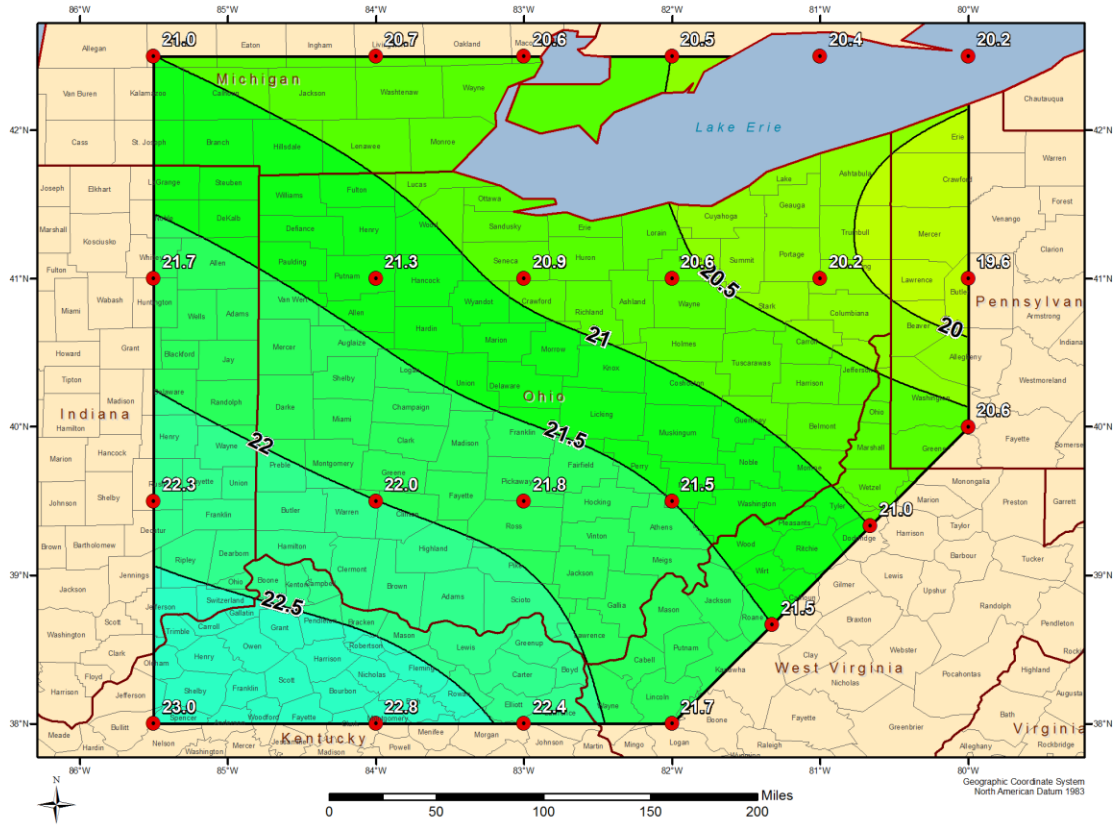


Figure 11.19 All-season PMP (inches) for 48-hour, 200-square mile

All-Season PMP - 72-hour 200 mi² (inches)
Ohio Statewide PMP Study

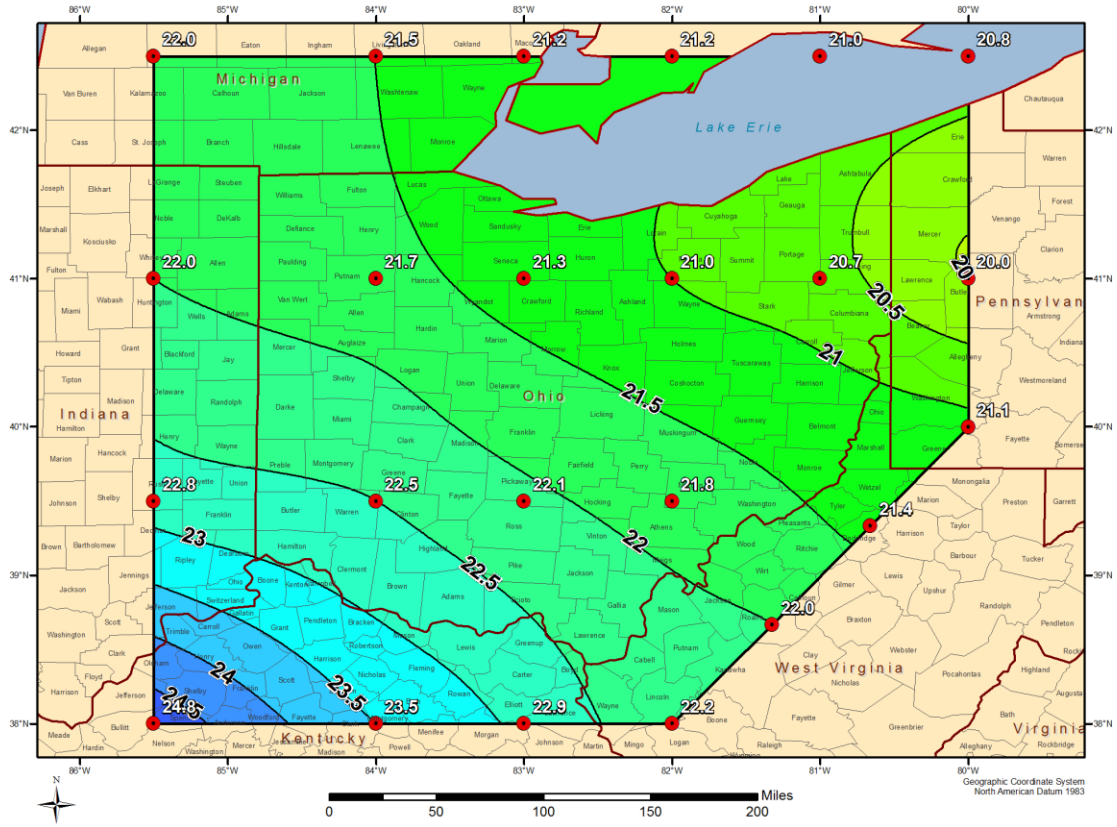


Figure 11.20 All-season PMP (inches) for 72-hour, 200-square mile

All-Season PMP - 6-hour 500 mi² (inches)
Ohio Statewide PMP Study

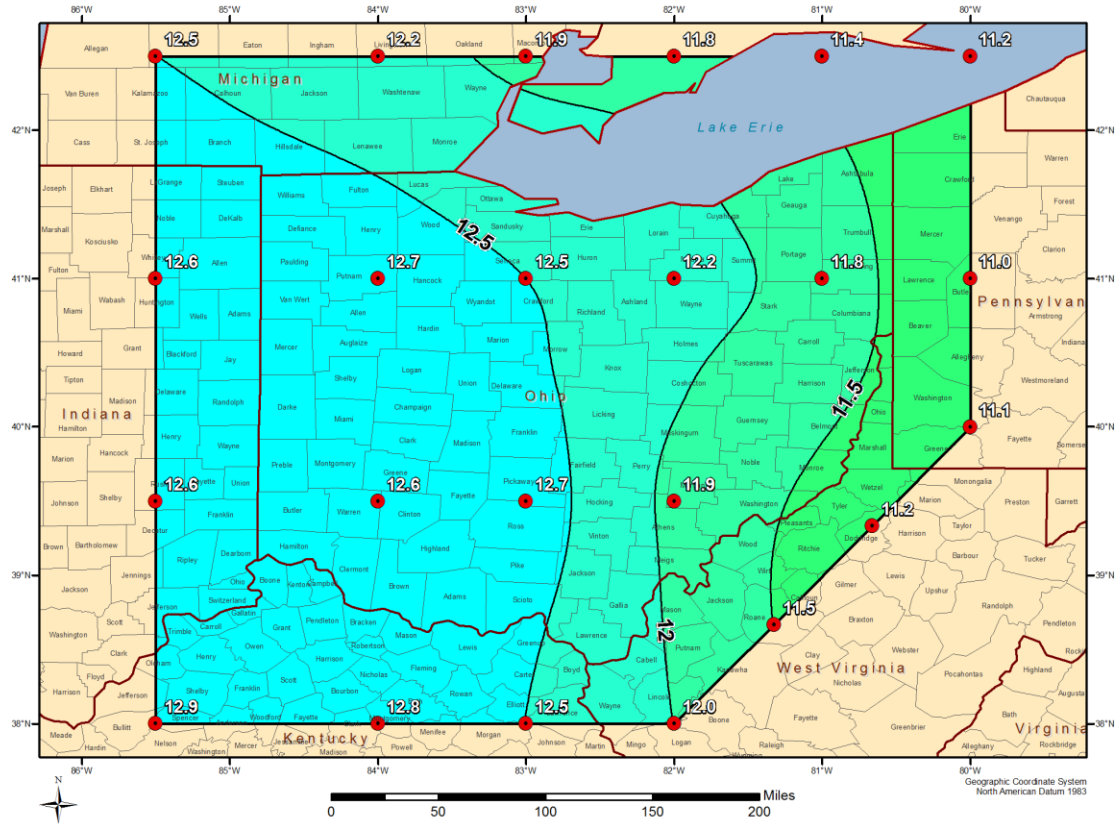


Figure 11.21 All-season PMP (inches) for 6-hour, 500-square mile

All-Season PMP - 72-hour 500 mi² (inches)
Ohio Statewide PMP Study

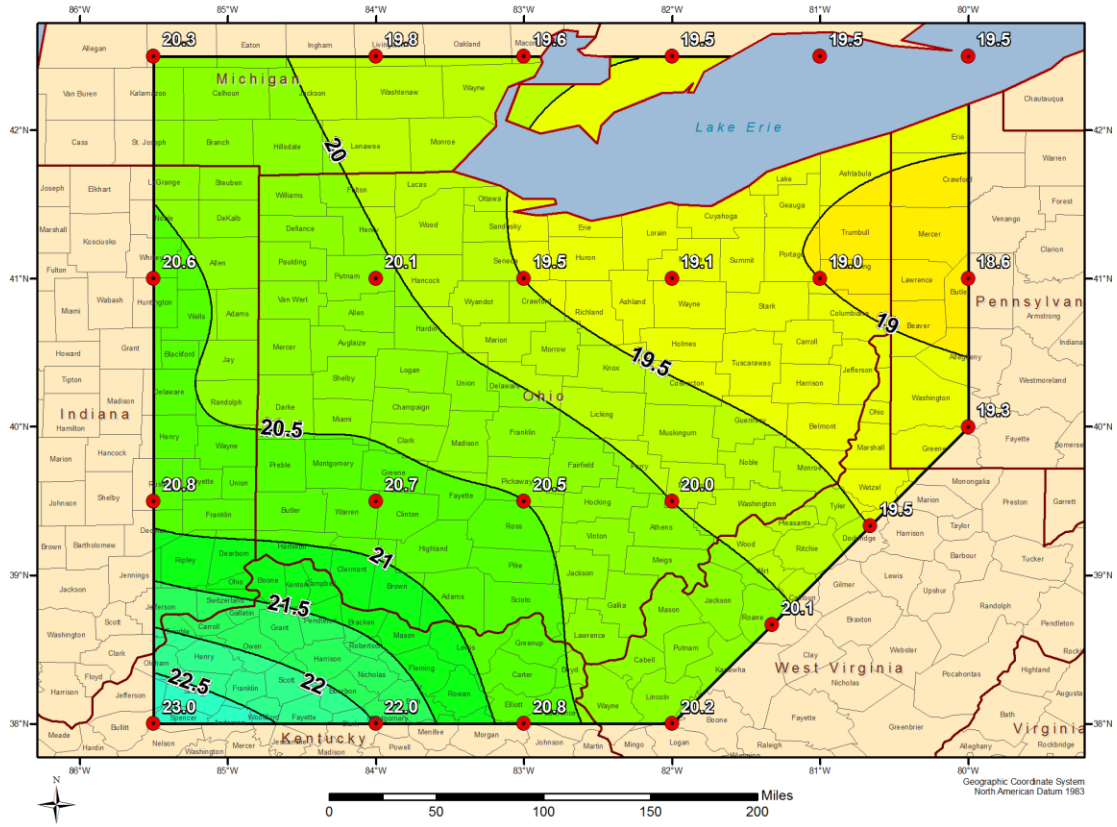


Figure 11.25 All-season PMP (inches) for 72-hour, 500-square mile

All-Season PMP - 6-hour 1,000 mi² (inches)
Ohio Statewide PMP Study

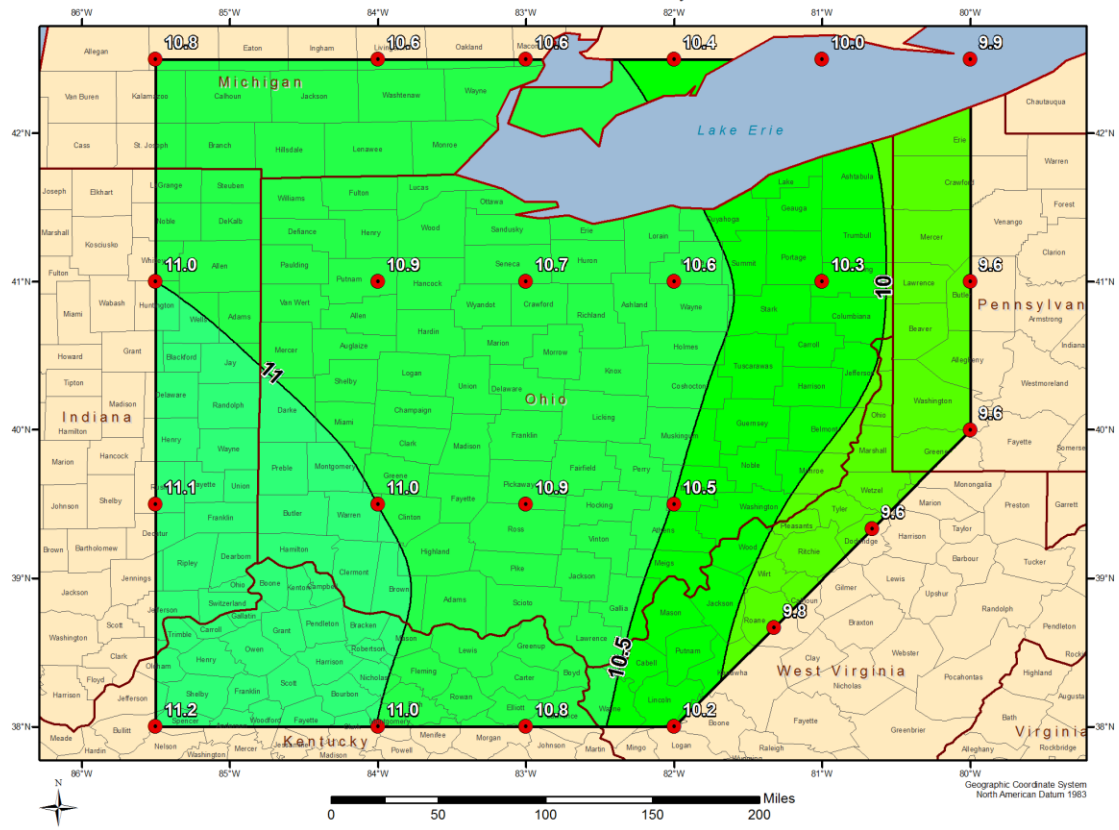


Figure 11.26 All-season PMP (inches) for 6-hour, 1,000-square mile

All-Season PMP - 12-hour 1,000 mi² (inches)
Ohio Statewide PMP Study

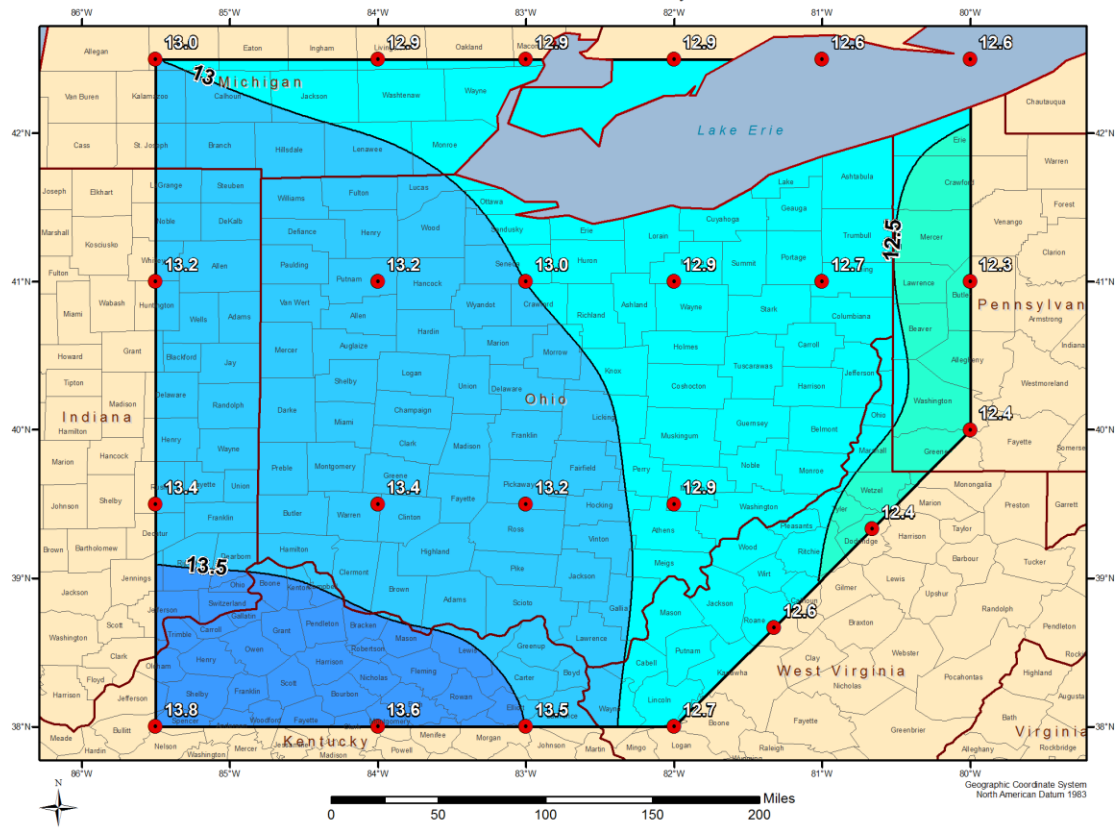


Figure 11.27 All-season PMP (inches) for 12-hour, 1,000-square mile

All-Season PMP - 24-hour 1,000 mi² (inches)
Ohio Statewide PMP Study

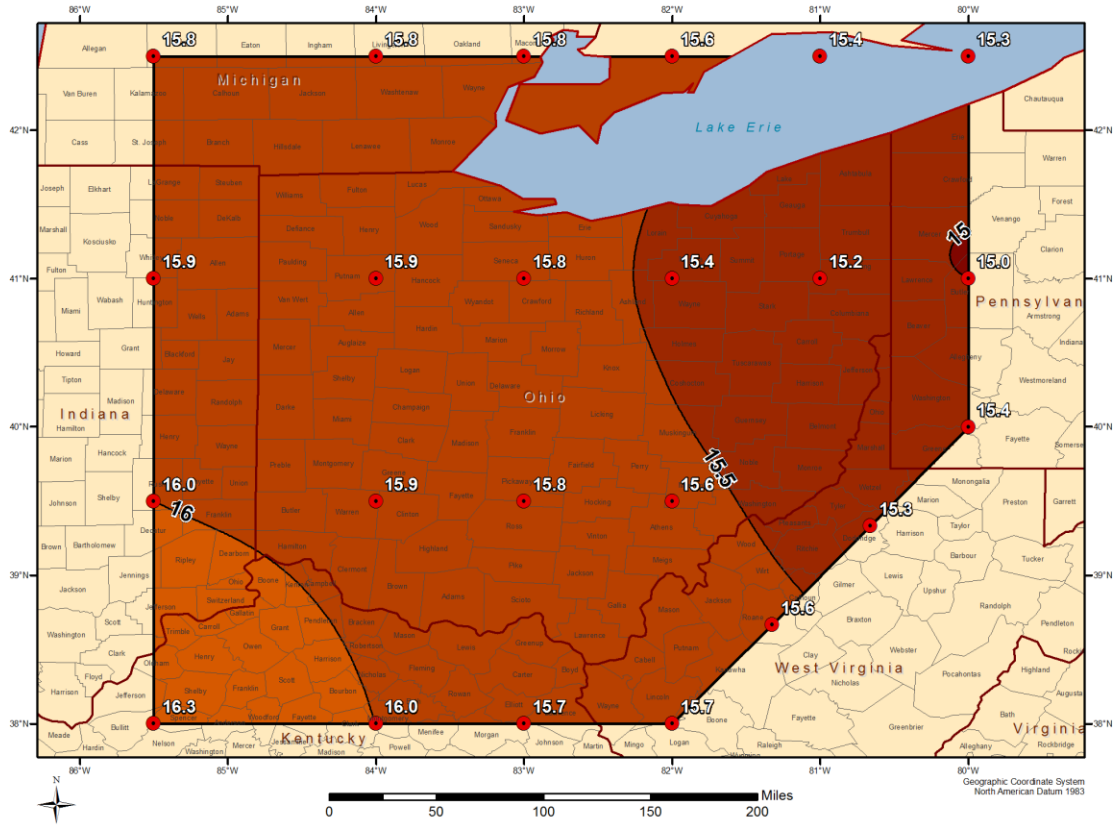


Figure 11.28 All-season PMP (inches) for 24-hour, 1,000-square mile

All-Season PMP - 72-hour 1,000 mi² (inches)
Ohio Statewide PMP Study

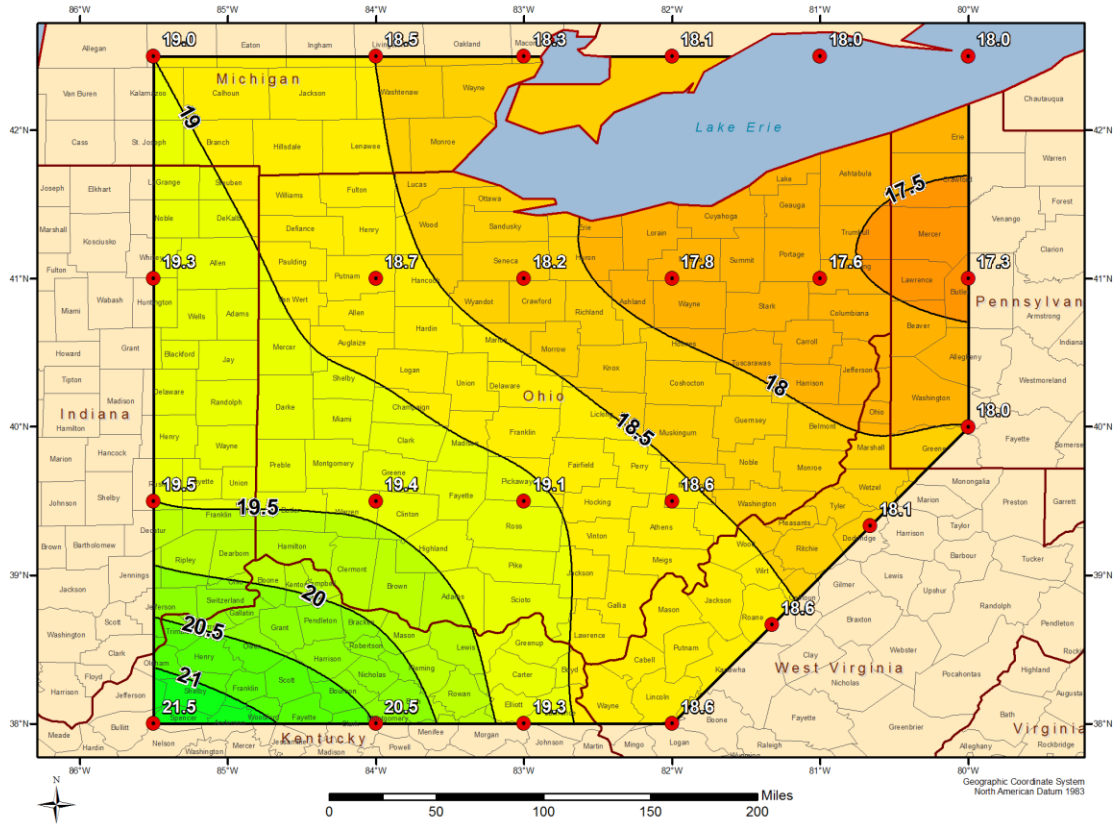


Figure 11.30 All-season PMP (inches) for 72-hour, 1,000-square mile

All-Season PMP - 6-hour 2,000 mi² (inches)
Ohio Statewide PMP Study

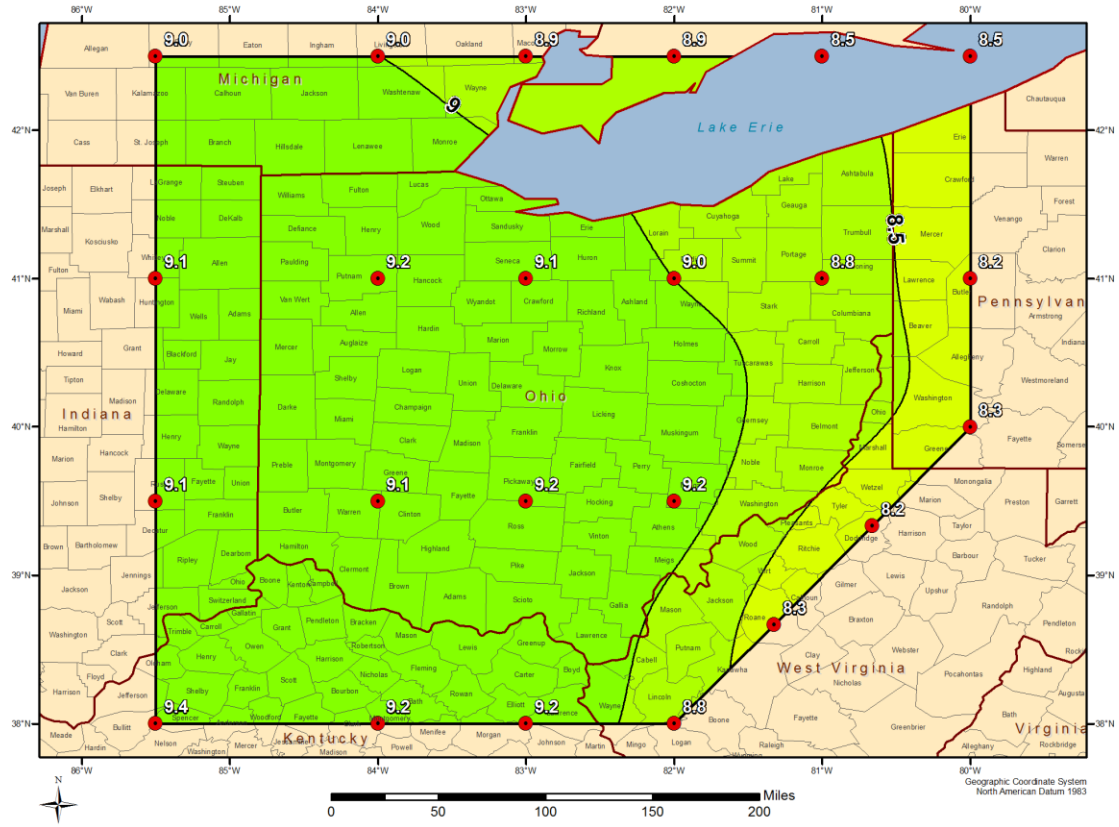


Figure 11.31 All-season PMP (inches) for 6-hour, 2,000-square mile

All-Season PMP - 12-hour 2,000 mi² (inches)
Ohio Statewide PMP Study

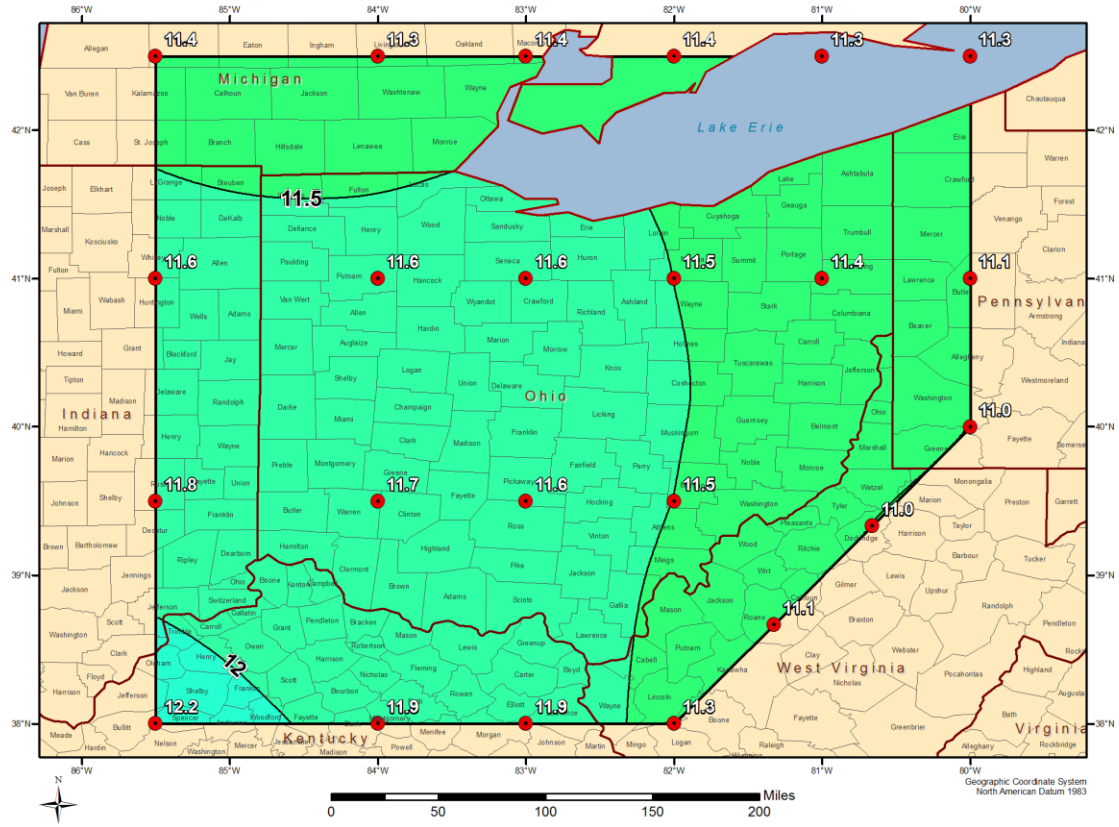


Figure 11.32 All-season PMP (inches) for 12-hour, 2,000-square mile

All-Season PMP - 24-hour 2,000 mi² (inches)
Ohio Statewide PMP Study

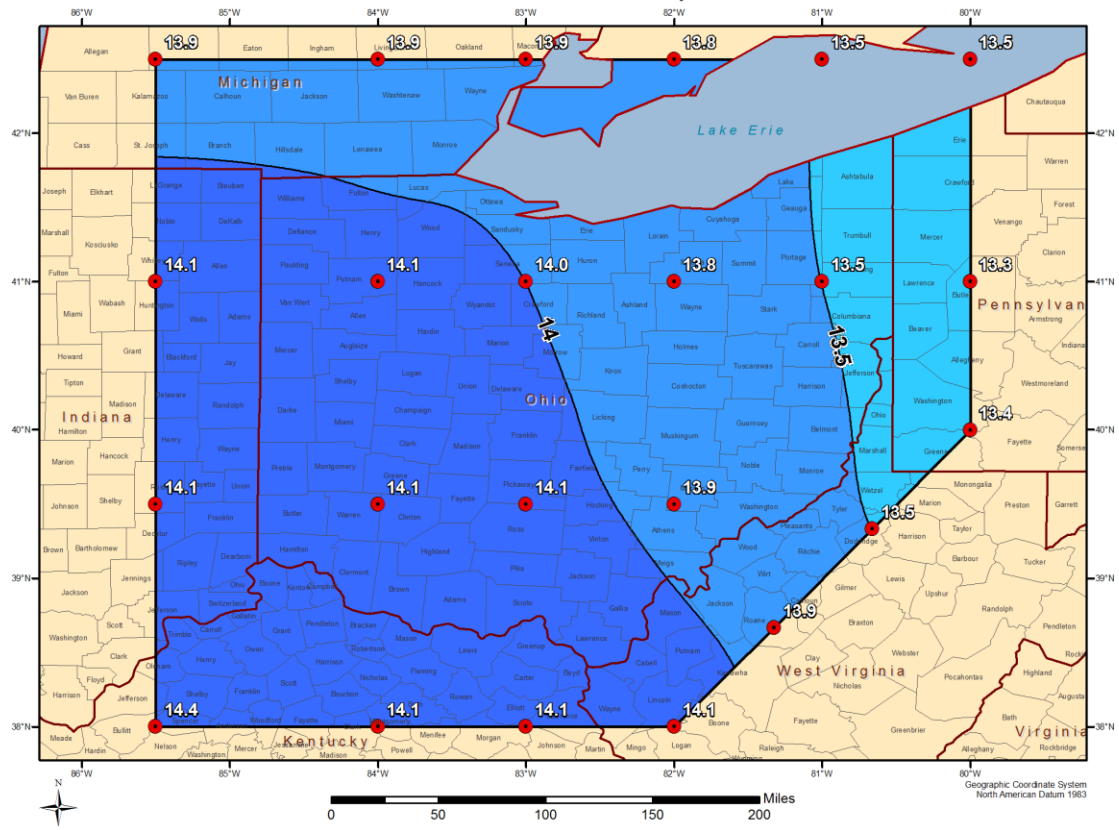


Figure 11.33 All-season PMP (inches) for 24-hour, 2,000-square mile

All-Season PMP - 48-hour 2,000 mi² (inches)
Ohio Statewide PMP Study

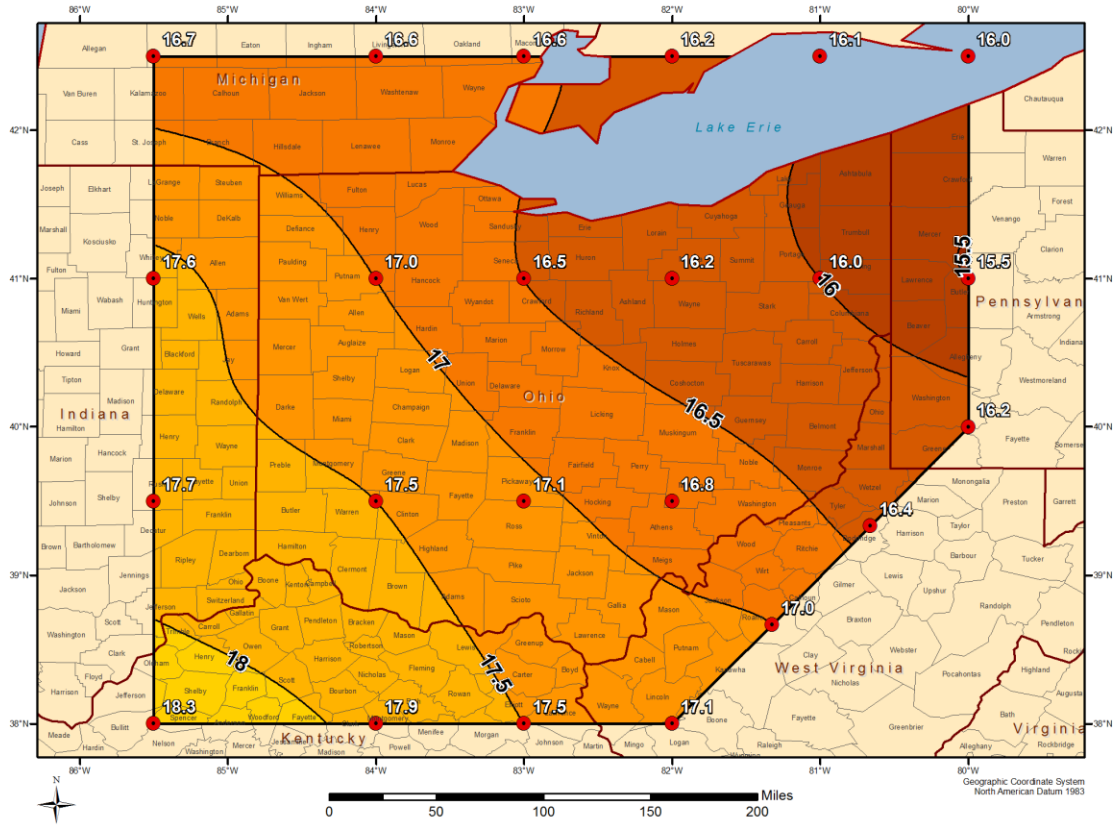


Figure 11.34 All-season PMP (inches) for 48-hour, 2,000-square mile

All-Season PMP - 6-hour 5,000 mi² (inches)
Ohio Statewide PMP Study

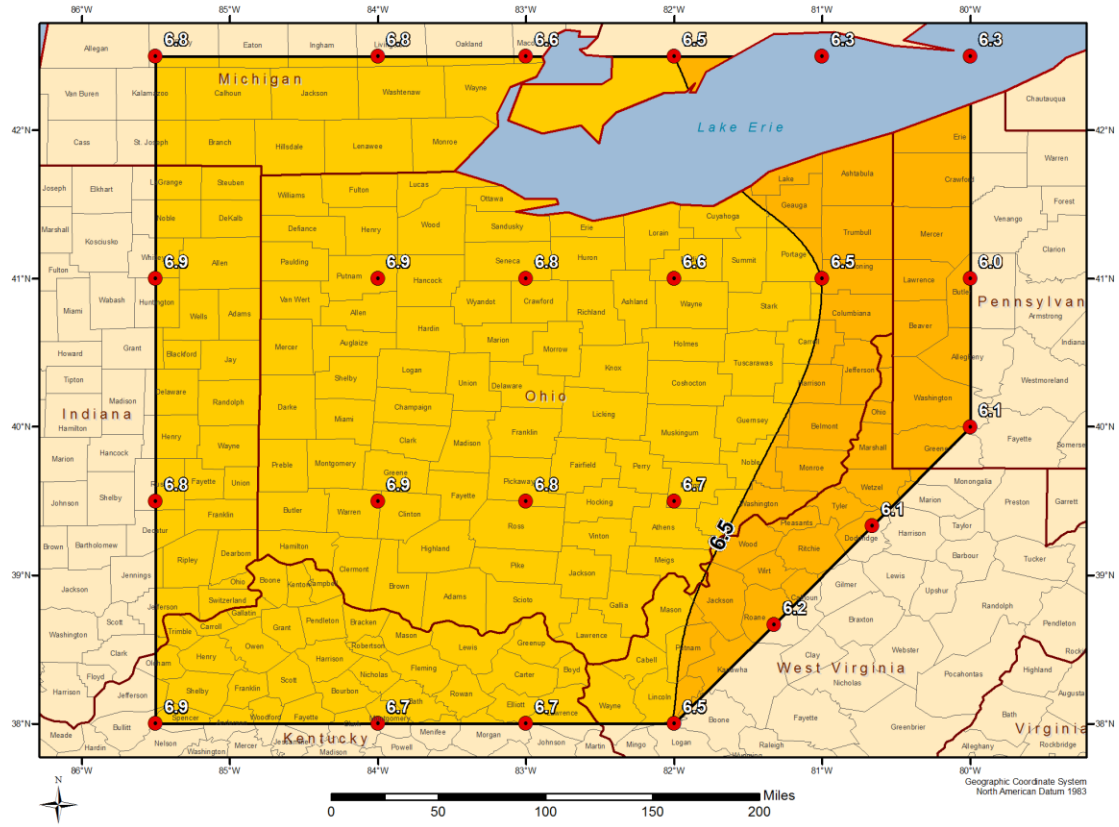


Figure 11.36 All-season PMP (inches) for 6-hour, 5,000-square mile

All-Season PMP - 12-hour 5,000 mi² (inches)
Ohio Statewide PMP Study

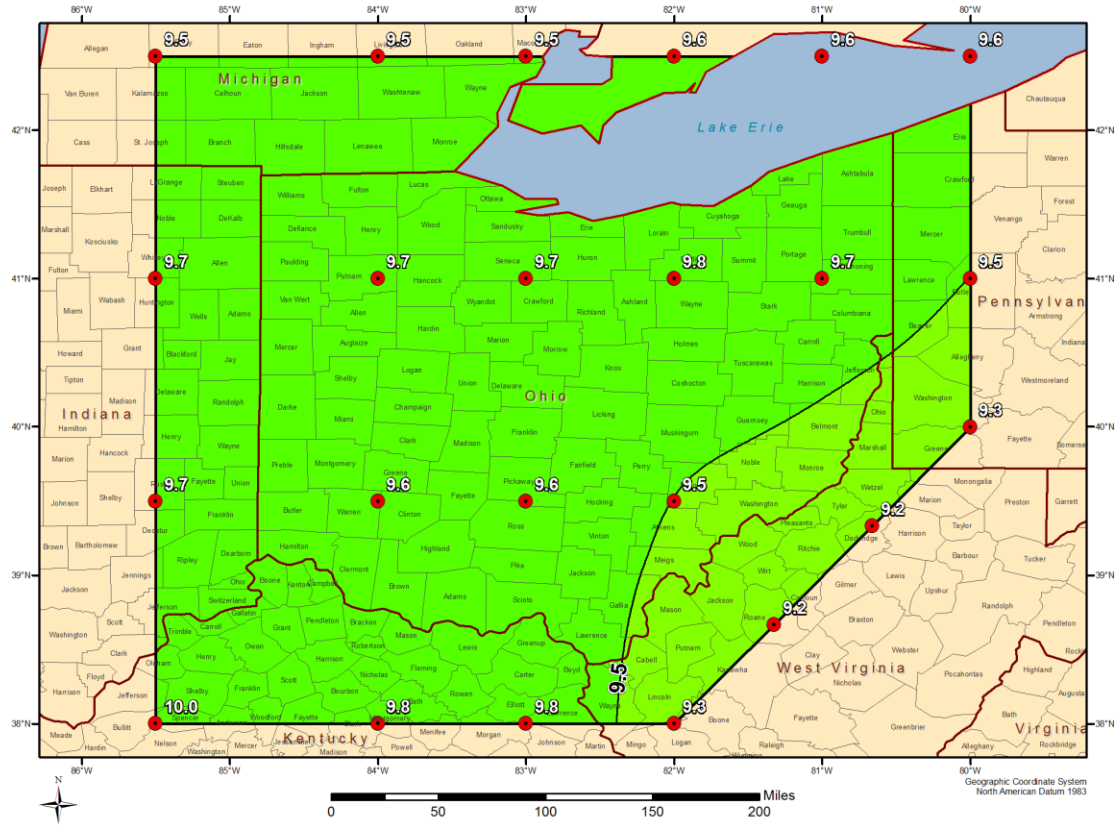


Figure 11.37 All-season PMP (inches) for 12-hour, 5,000-square mile

All-Season PMP - 48-hour 5,000 mi² (inches)
Ohio Statewide PMP Study

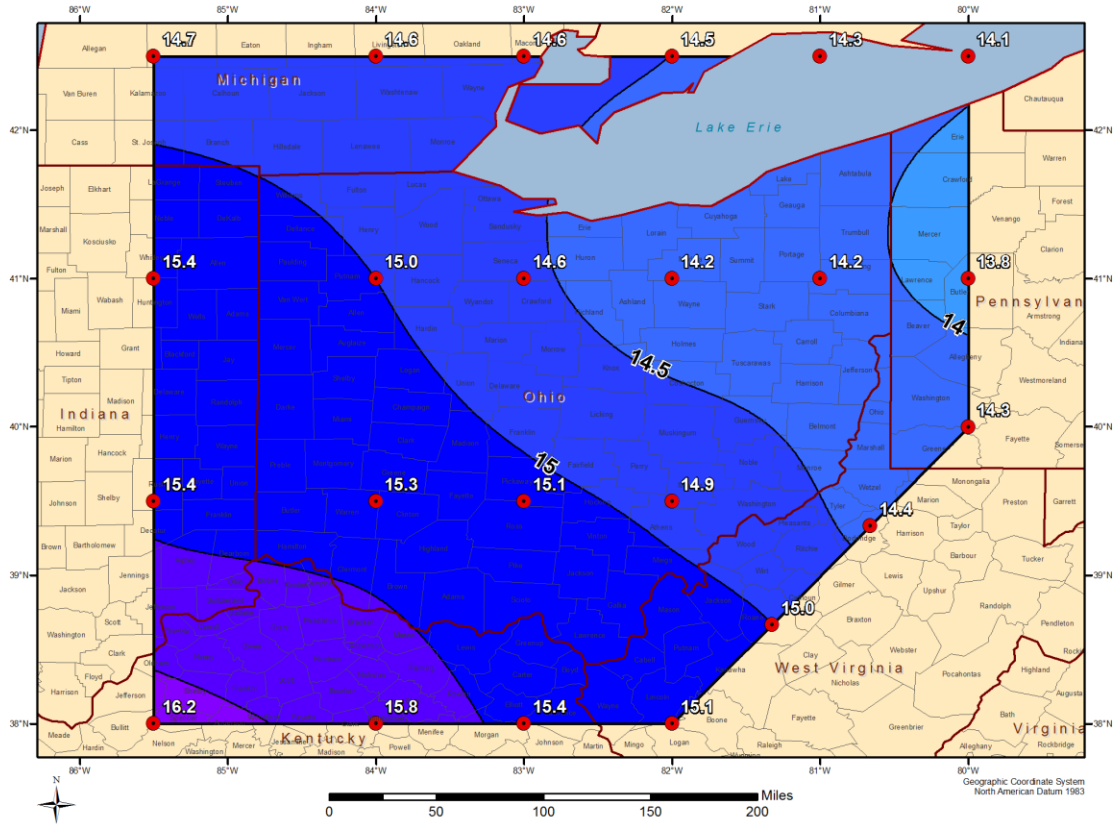


Figure 11.39 All-season PMP (inches) for 48-hour, 5,000-square mile

All-Season PMP - 72-hour 5,000 mi² (inches)
Ohio Statewide PMP Study

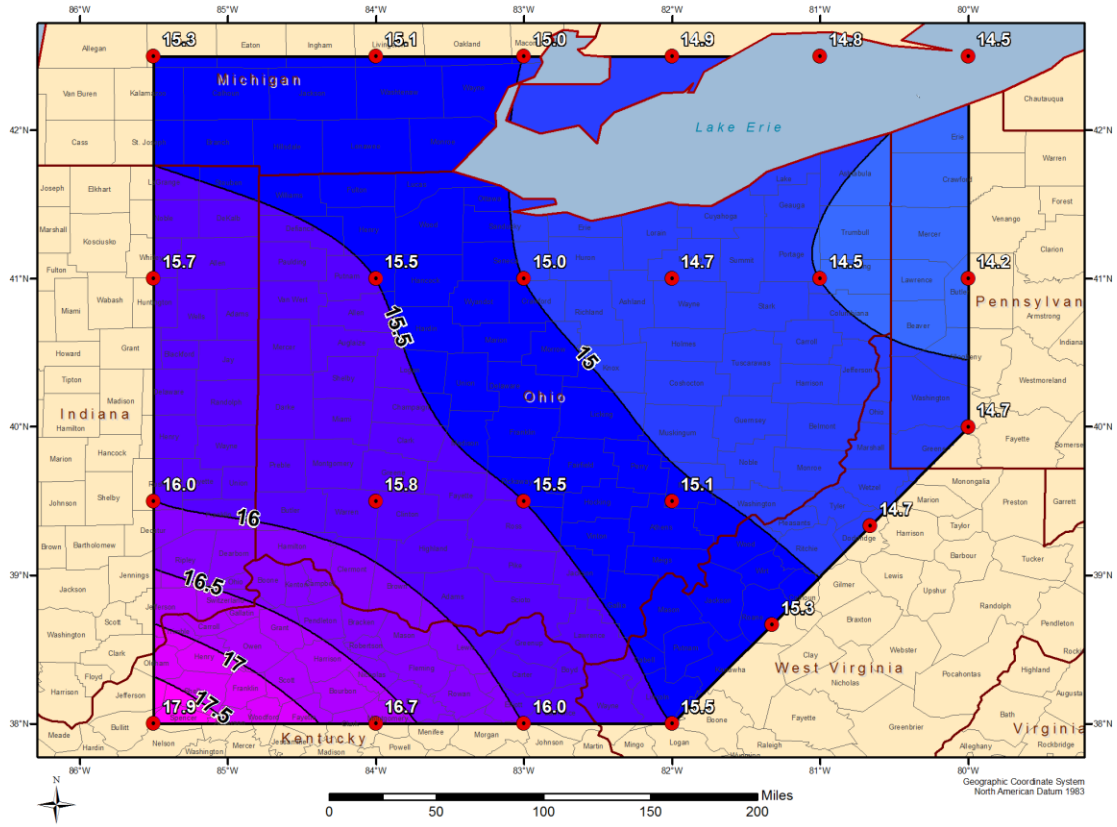


Figure 11.40 All-season PMP (inches) for 72-hour, 5,000-square mile

All-Season PMP - 6-hour 10,000 mi² (inches)
Ohio Statewide PMP Study

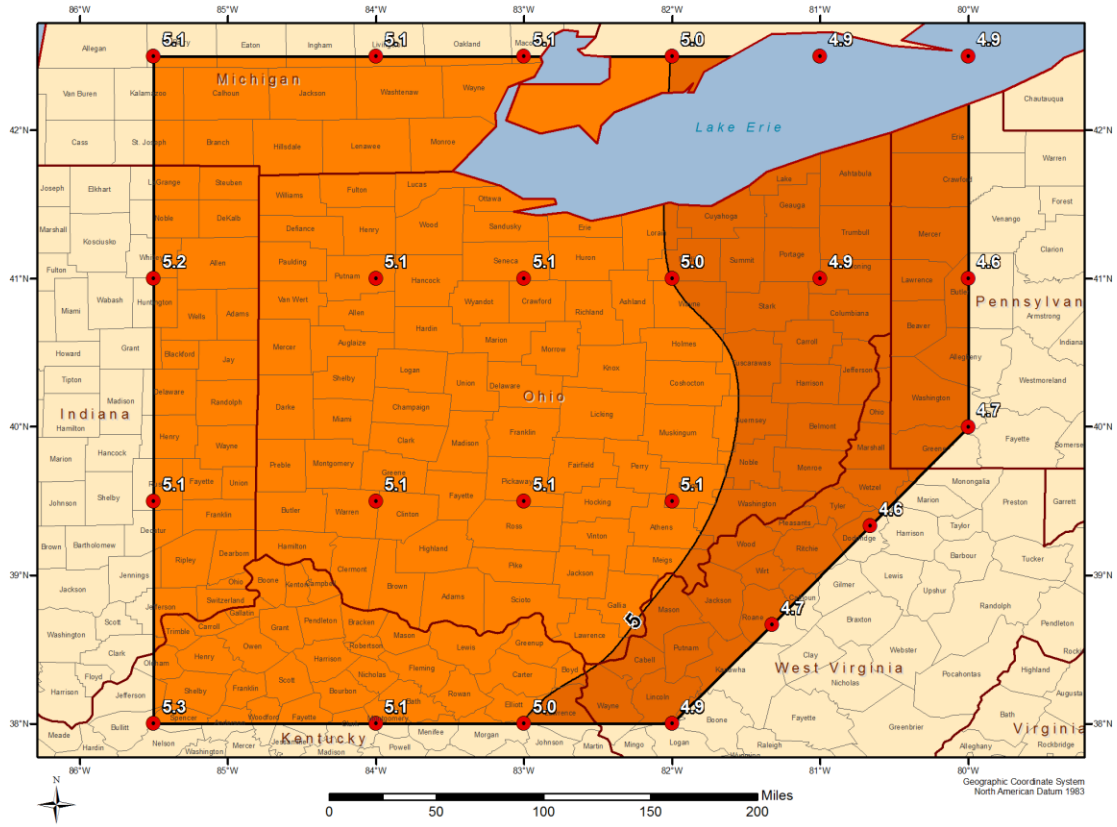


Figure 11.41 All-season PMP (inches) for 6-hour, 10,000-square mile

All-Season PMP - 24-hour 10,000 mi² (inches)
Ohio Statewide PMP Study

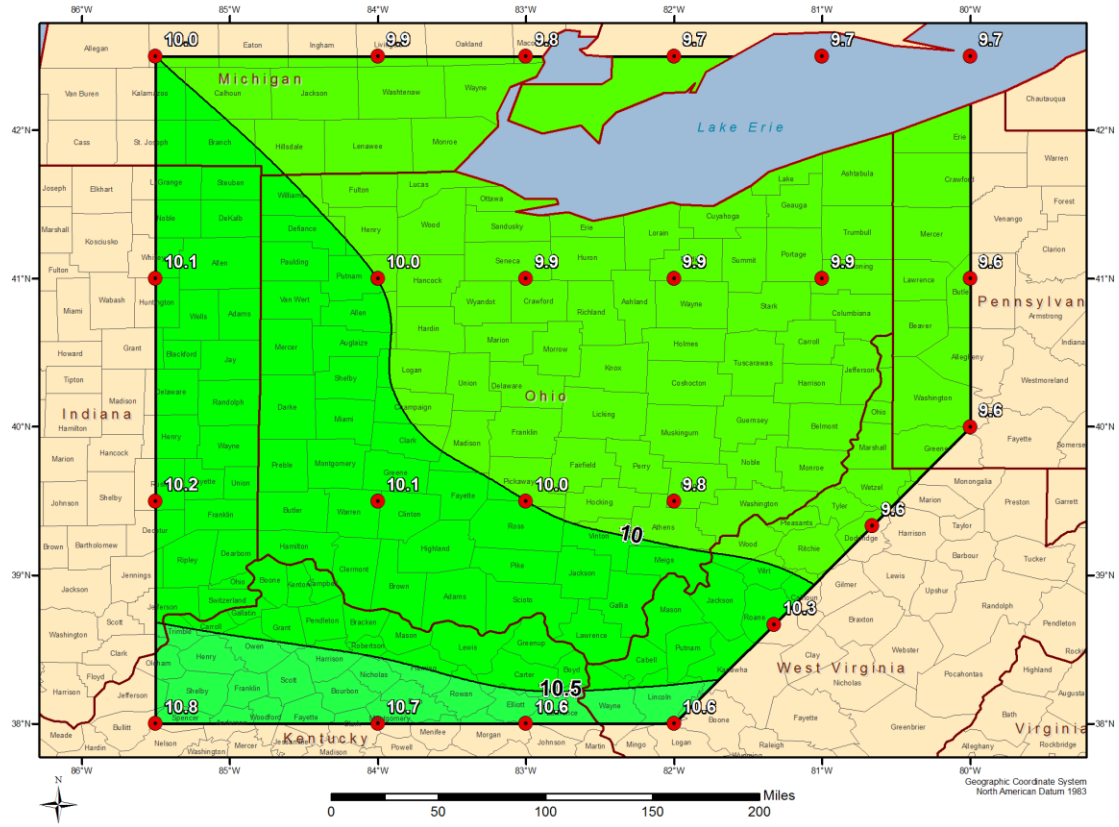


Figure 11.43 All-season PMP (inches) for 24-hour, 10,000-square mile

All-Season PMP - 48-hour 10,000 mi² (inches)
Ohio Statewide PMP Study

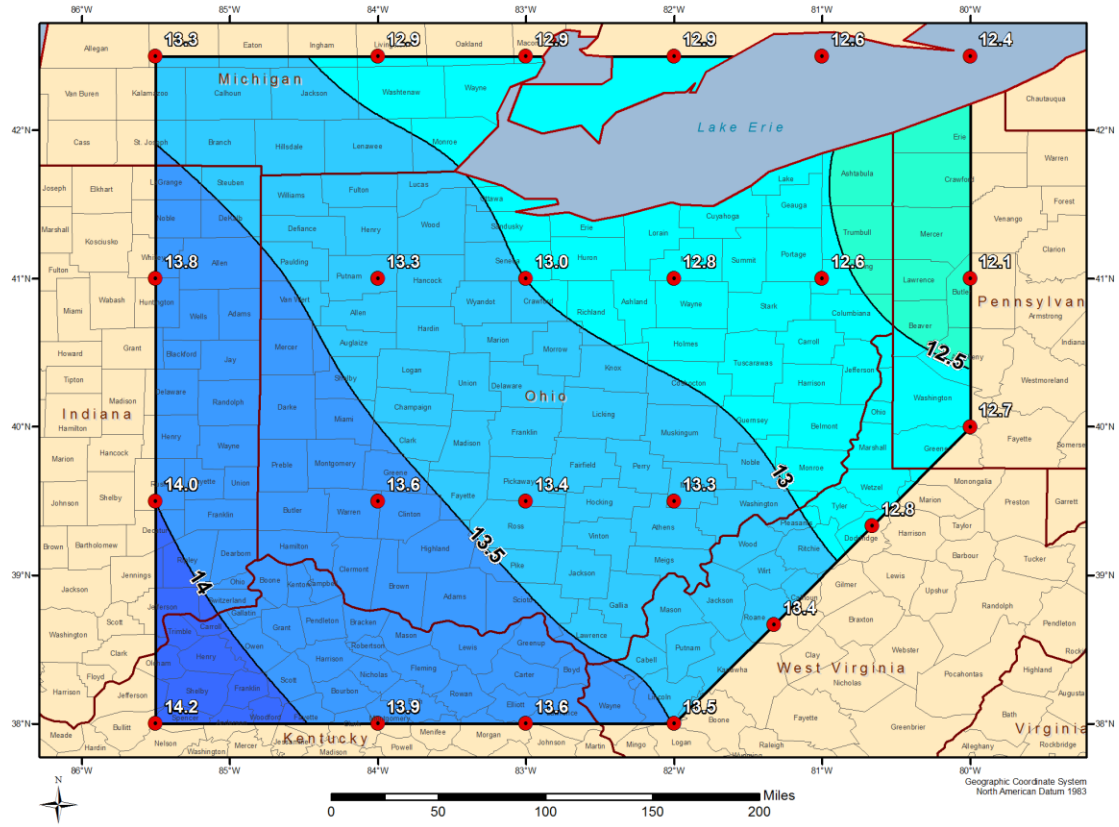


Figure 11.44 All-season PMP (inches) for 48-hour, 10,000-square mile

All-Season PMP - 72-hour 10,000 mi² (inches)
Ohio Statewide PMP Study

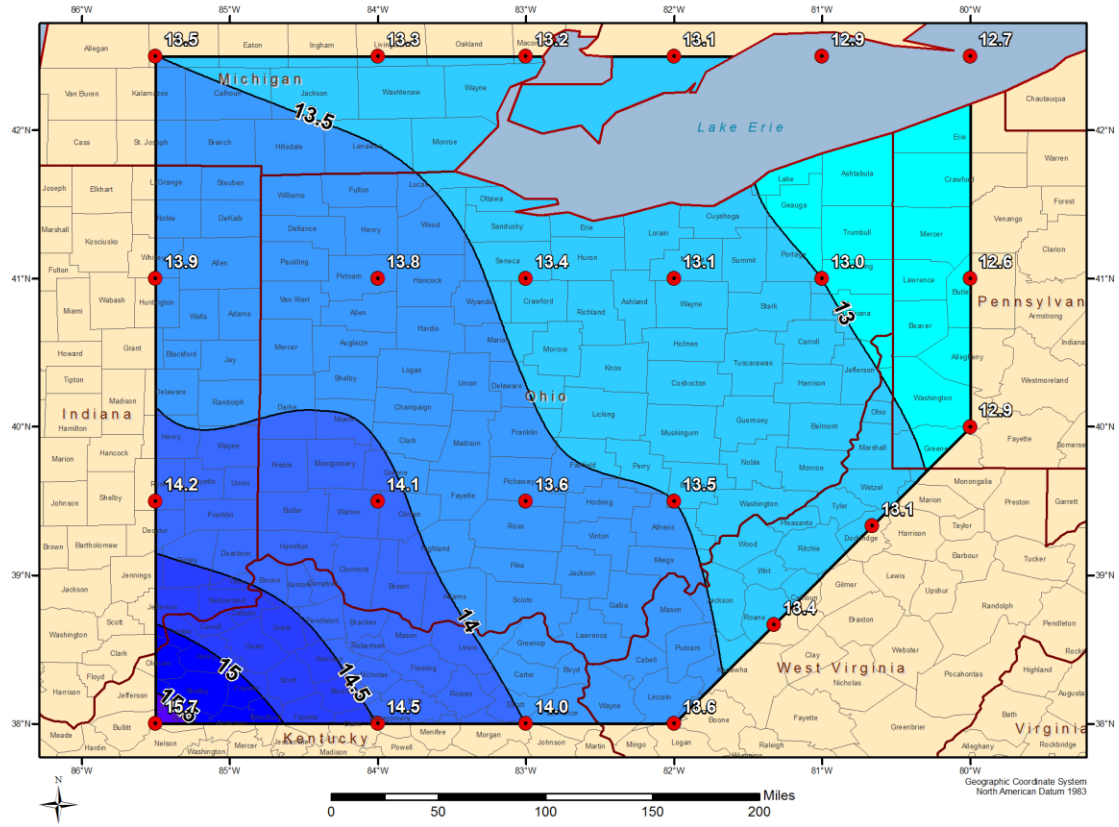


Figure 11.45 All-season PMP (inches) for 72-hour, 10,000-square mile

All-Season PMP - 6-hour 20,000 mi² (inches)
Ohio Statewide PMP Study

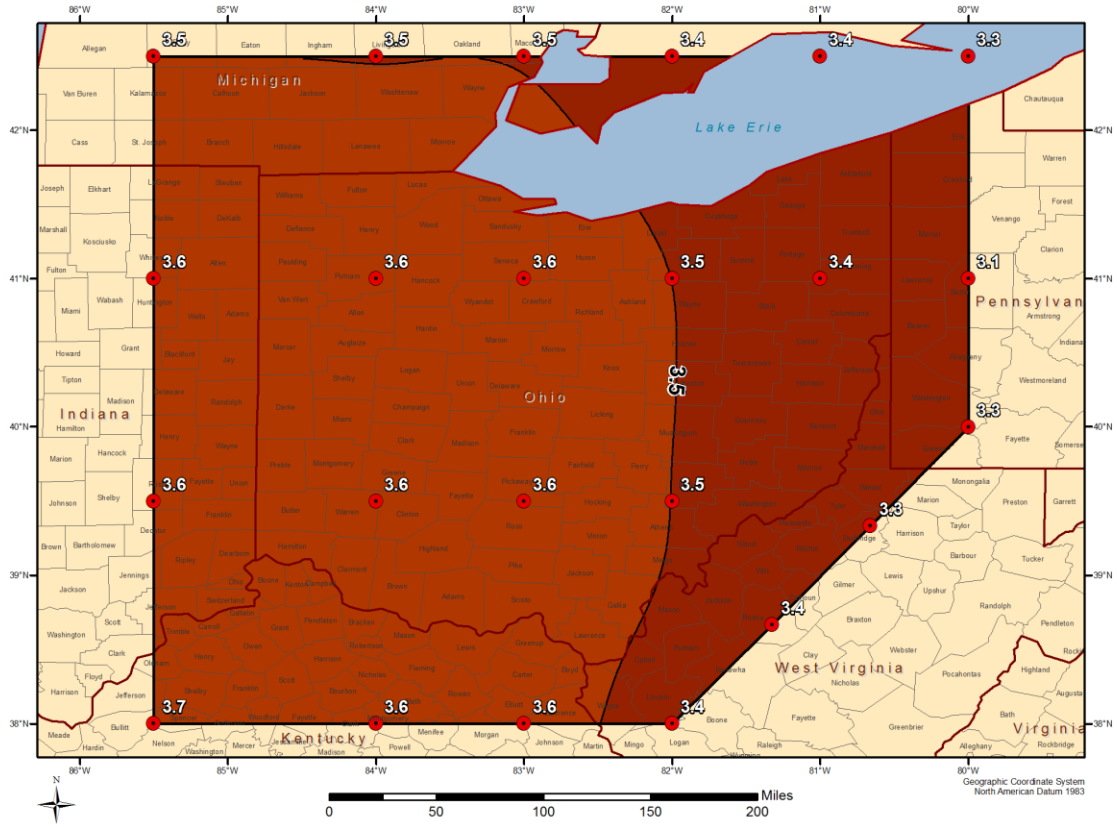


Figure 11.46 All-season PMP (inches) for 6-hour, 20,000-square mile

All-Season PMP - 24-hour 20,000 mi² (inches)
Ohio Statewide PMP Study

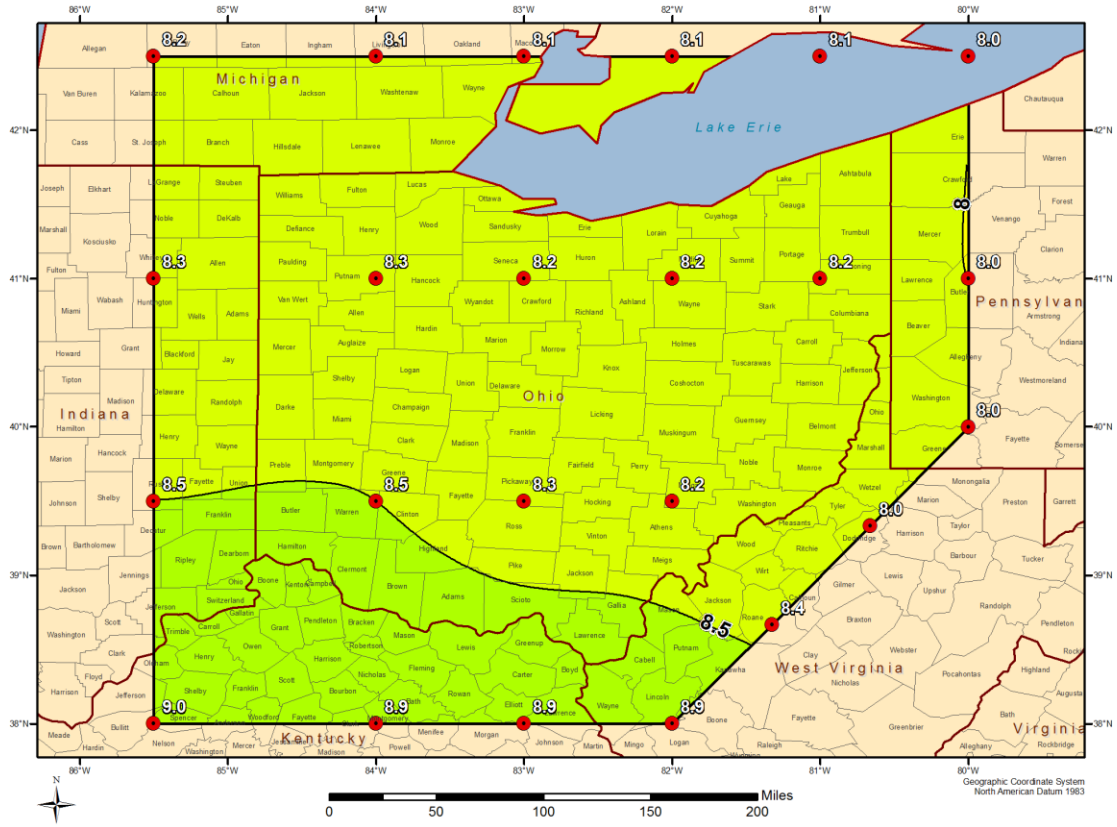


Figure 11.48 All-season PMP (inches) for 24-hour, 20,000-square mile

All-Season PMP - 48-hour 20,000 mi² (inches)
Ohio Statewide PMP Study

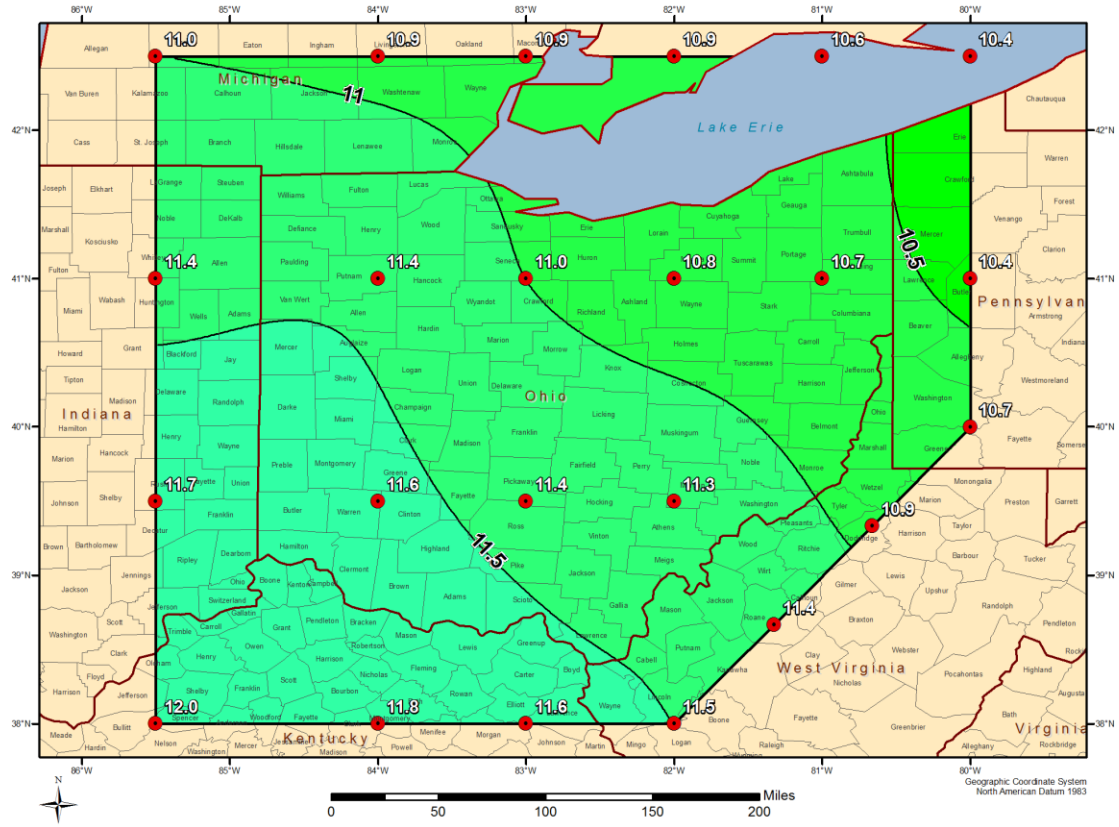


Figure 11.49 All-season PMP (inches) for 48-hour, 20,000-square mile

All-Season PMP - 72-hour 20,000 mi² (inches)
Ohio Statewide PMP Study

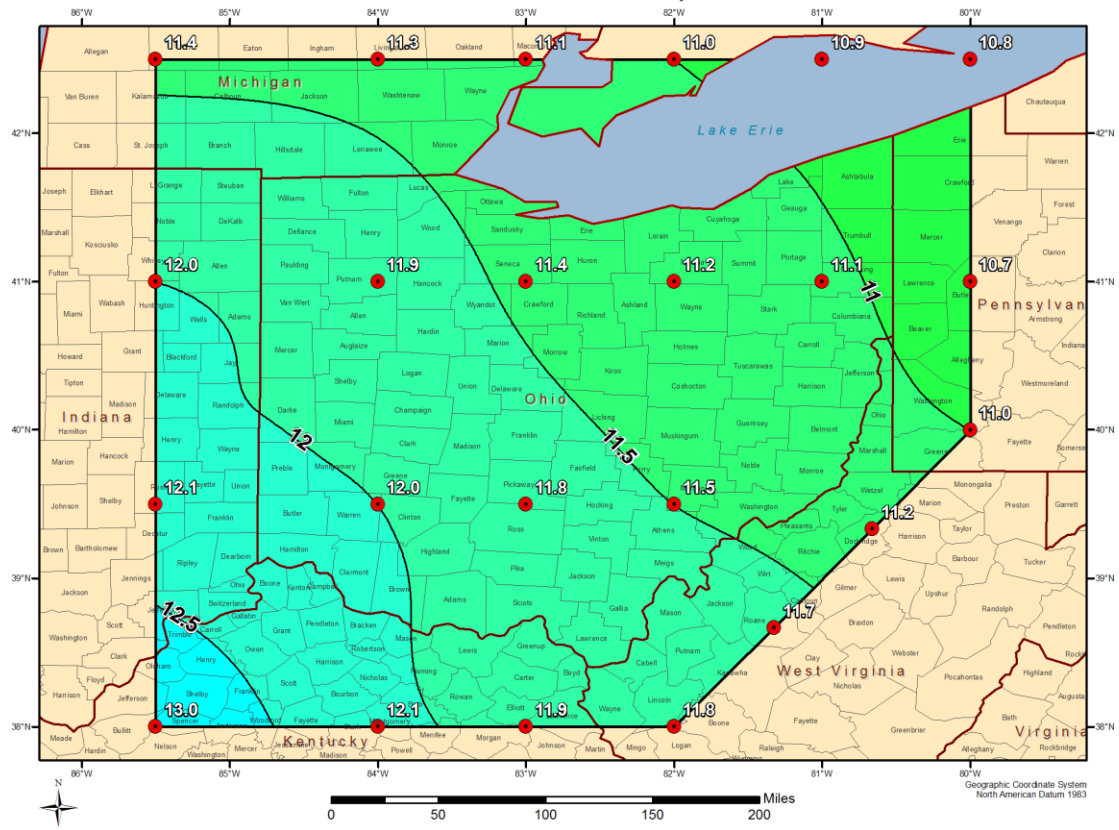


Figure 11.50 All-season PMP (inches) for 72-hour, 20,000-square mile

11.2 Comparison of the All-season PMP Values with HMR 51 PMP

Comparisons were made at standard area sizes and durations with HMR 51 PMP values to determine the difference between results of the PMP values developed during this study and HMR 51. Results of these comparisons at each of the 23 grid points are presented in Appendix E. Table 11.1 provides the percent reductions from HMR 51 PMP values at grid point 15.

Table 11.1 Percent difference between the Ohio statewide PMP values at grid point 15 and the HMR 51 PMP values at that location. Values represent reductions from HMR 51. Rainfall values are in inches.

Grid Point 15 PMP vs HMR 51 PMP						
HMR 51 PMP Values at Grid Point 15 in Inches	Area Size	6-Hour	12-Hour	24-Hour	48-Hour	72-Hour
	10sqmi	26.0	29.6	31.8	34.9	36.7
	200sqmi	18.1	21.5	23.3	26.2	27.8
	1000sqmi	13.1	15.9	18.0	20.5	22.3
	5000sqmi	7.8	10.9	12.8	15.3	17.0
	10000sqmi	6.2	8.9	10.5	13.5	15.0
	20000sqmi	4.3	7.0	8.7	11.3	12.5
Ohio Study PMP Values at Grid Point 15 in Inches	Area Size	6-Hour	12-Hour	24-Hour	48-Hour	72-Hour
	10sqmi	17.2	21.4	23.0	24.5	25.0
	100sqmi	14.8	17.5	20.3	21.6	22.0
	200sqmi	13.9	16.2	19.0	20.6	21.0
	500sqmi	12.2	14.3	17.1	18.7	19.1
	1000sqmi	10.6	12.9	15.4	17.3	17.8
	2000sqmi	9.0	11.5	13.8	16.2	16.6
	5000sqmi	6.6	9.8	11.6	14.2	14.7
	10000sqmi	5.0	8.4	9.9	12.8	13.1
20000sqmi	3.5	6.5	8.2	10.8	11.2	
% Reduction from HMR 51	Area Size	6-Hour	12-Hour	24-Hour	48-Hour	72-Hour
	10sqmi	34%	28%	28%	30%	32%
	200sqmi	23%	25%	18%	21%	24%
	1000sqmi	19%	19%	14%	16%	20%
	5000sqmi	16%	10%	9%	7%	13%
	10000sqmi	19%	5%	6%	5%	13%
	20000sqmi	18%	7%	6%	5%	10%

In addition, the storm(s) which controlled the PMP value at a given area size and duration were identified. This is important to understand which storms are most important across the state and to provide a data set which can be scrutinized further to ensure the final PMP values are appropriate and consistent. Table 11.2 displays the controlling storms data for grid point 15. The number refer to the AWA storm number as listed in Table 4.1 and Appendix F.

Table 11.2 Controlling storms of the PMP values. The number designates the AWA storm numbers assigned to each storm on the short storm list.

Controlling Storms by AWA Storm Number at Grid Point 15					
Area Size	6-Hour	12-Hour	24-Hour	48-Hour	72-Hour
10sqmi	40	20	112	75	75
100sqmi	40, 18	20	112	45	45
200sqmi	40	20	112	45	45
500sqmi	40	40	112	45	45
1000sqmi	14	1	112	45	45
2000sqmi	14	1	112, 1	126	45
5000sqmi	10	1	1	126, 100	100, 126
10000sqmi	10	1	1	100	100, 126
20000sqmi	1, 10	1	1	126, 100	100, 126

Comparisons were also made to the PMP values derived during the FERC Michigan/Wisconsin regional PMP study that overlapped the grid points used in this study. Because most of the processes and storms used in the FERC Michigan/Wisconsin regional PMP study were again employed here, it was informative to see how the results compared. Table 11.3 shows the comparison table of the Ohio statewide PMP values versus the FERC Michigan/Wisconsin PMP values at grid point 15. Comparison tables for the other grid points which overlap the FERC Michigan/Wisconsin PMP study are given in Appendix E.

Table 11.3 Percent difference between Ohio statewide PMP values at grid point 15 and FERC Michigan/Wisconsin regional PMP study values at the same location. Positive values represent reductions from the FERC Michigan/Wisconsin regional PMP study values. Rainfall values are in inches.

Grid Point 15 PMP vs FERC Michigan/Wisconsin PMP						
FERC Michigan Wisconsin Study PMP Values in Inches	Area Size	6-Hour	12-Hour	24-Hour	48-Hour	72-Hour
	100sqmi	15.6	17.5	19.3	21.9	23.7
	200sqmi	14.3	16.5	18.1	21.2	22.0
	500sqmi	12.9	14.5	16.5	19.3	20.3
	1000sqmi	11.6	12.8	15.3	18.1	19.1
	5000sqmi	7.1	9.1	12.0	15.6	16.2
	10000sqmi	5.5	7.3	10.9	14.1	15.0
<hr/>						
Ohio Study PMP Values at Grid Point 15 in Inches	Area Size	6-Hour	12-Hour	24-Hour	48-Hour	72-Hour
	10sqmi	17.2	21.4	23.0	24.5	25.0
	100sqmi	14.8	17.5	20.3	21.6	22.0
	200sqmi	13.9	16.2	19.0	20.6	21.0
	500sqmi	12.2	14.3	17.1	18.7	19.1
	1000sqmi	10.6	12.9	15.4	17.3	17.8
	2000sqmi	9.0	11.5	13.8	16.2	16.6
	5000sqmi	6.6	9.8	11.4	14.2	14.7
	10000sqmi	5.0	8.4	9.9	12.8	13.1
20000sqmi	3.5	6.5	8.2	10.8	11.2	
<hr/>						
% Reduction from FERC Michigan Wisconsin PMP	Area Size	6-Hour	12-Hour	24-Hour	48-Hour	72-Hour
	100sqmi	5%	0%	-5%	1%	7%
	200sqmi	2%	2%	-5%	3%	5%
	500sqmi	5%	1%	-3%	3%	6%
	1000sqmi	8%	-1%	-1%	4%	7%
	5000sqmi	7%	-8%	5%	9%	9%
10000sqmi	9%	-15%	9%	9%	12%	

11.3 Comparison of the Ohio Study PMP Values with 6-, 12-, and 24-Hour 100-Year Return Frequency Rainfall Values

PMP values were compared with 100-year rainfall values as a general check for reasonableness. These 100-year rainfall values are for point locations and are not available for larger area sizes. The ratio of the 10-square mile PMP values derived during this study to the 24-hour 100-year return period rainfall amounts is generally expected to range between two and four, with values as low as 1.7 and as high as 5.5 found in HMRs 57 and 59 (Hansen et al. 1994, Corrigan et al. 1999). In addition, comparisons were also made for the 6-hour, 12-hour, and 72-hour durations as those are readily available in NOAA Atlas 14.

For the majority of the grid points, the 100-year 24-hour return frequency rainfall values were derived from NOAA Atlas 14. However, NOAA Atlas 14 was not available for the state of Michigan and therefore grid points located there were compared against the appropriate precipitation frequency climatology, Technical Paper 40 (TP 40) (US Weather Bureau 1963).

Comparison of the 10-square mile PMP values for grid point 15 against 100-year x-hour rainfall return frequency value are shown in Table 11.4.

Table 11.4 Comparison of the 10-square mile PMP value against the x-hour 100-year precipitation frequency from NOAA Atlas 14 for grid point 15

Ratio of Grid Point 15 PMP Against 100-Year Precipitation Frequency Value			
Rainfall Duration	Grid Point 15 PMP 10sqmi PMP (inches)	100-year value (inches)	Ratio of PMP to Precipitation Frequency Value
6-hour	17.2	4.3	4.1
12-hour	21.4	4.9	4.3
24-hour	23.0	5.6	4.1
72-hour	24.5	6.4	3.9

11.4 Reasons for Reductions of PMP versus HMR 51

This PMP study provided differences in PMP values from those presented in HMR 51. This study explicitly addressed elevation, whereas detailed terrain effects were not evaluated in HMR 51. All HMR 51 storms on the short storm lists were re-evaluated to determine the updated storm representative dew point and maximization using updated maximum dew point climatology.

Since the site-specific study followed the same basic storm rainfall adjustment procedures as HMR 51, it would be useful to understand the cause of the differences in the PMP values. Working papers are not available for HMR 51, so explicit differences in calculations and procedures cannot be evaluated. However, the following issues were treated differently between the studies:

1. HMR 51 provides generalized and smoothed PMP values over a large geographic domain that covers the United States east of the 105th meridian. Specific characteristics unique to Ohio were not addressed. This study considered characteristics specific to the state, and produced PMP values that explicitly considered the meteorology of the PMP storm types which would result in the PMF in the region.
2. The transposition limits of the Smethport, PA July 1942 world record rainfall event were re-evaluated during this study (a detailed discussion of this evaluation is provided in Appendix H). This investigation determined that the storm was not transpositionable to any location within the state of Ohio. The primary reason is the difference in orographic effects between where the storm occurred in north central Pennsylvania and eastern Ohio. The refined transposition limits used in this study differ from HMR 51. Although no explicit delineations of transposition limits are included in HMR 51, documents received from the NWS HDSC office show that this storm was transpositioned to the eastern 1/3rd of Ohio. The refined transposition limits used in this study result in lower PMP values compared to HMR 51 for durations of 6-, 12-, and 24-hours for locations where the Smethport storm apparently influenced PMP values in HMR 51. Smoothing of the PMP isolines in HMR 51 necessarily had to encompass the Smethport maximized in-place rainfall far beyond its explicit transposition limits. Note, Section 3.2.4 of HMR 51 states that they "slightly undercut" the maximized 6-, 12-, and 24-hour values by up to 7% to

avoid "excessive envelopment of all other data in a large region surrounding the Smethport location." This over envelopment effect extended well beyond the transposition limits of the Smethport storm because the PMP isolines required smoothing and fitting over surrounding regions. Therefore, the influence of the Smethport storm on PMP values in HMR 51 implicitly extended well beyond its explicit transposition limits.

3. Each storm's inflow vector was re-evaluated and combined with an updated set of dew point climatologies and when necessary, updated storm representative dew point values were used for the in-place maximization and computation of the total adjustment factors. The HYSPLIT trajectory model was used to evaluate moisture inflow vectors for storms on the short storm list. Trajectory models were not available in previous HMR studies. Use of HYSPLIT allowed for a high degree of confidence when evaluating moisture inflow vectors and storm representative dew points.
4. Several new storms have been analyzed and included in this PMP study that were not included in HMR 51. This provided a higher level of confidence in the final PMP values. Further, this allowed for a refined set of values that better represent the PMP estimates. This expanded the data set used to derive PMP includes a large number of recent storms.
5. The study provided adjustments for storm elevation to the nearest 100 feet of elevation, whereas HMR 51 made no explicit adjustment for elevation. This adjustment depends on the elevation of the historic storm's maximum rainfall location and therefore varies from storm to storm. Further, the average elevation for each grid point was evaluated in this study using GIS, providing more accurate calculations to account for differences in available atmospheric moisture due to that elevation differences.
6. SPAS was used in conjunction with NEXRAD data (when available) to evaluate the spatial and temporal distribution of rainfall. Use of NEXRAD data generally produced higher point rainfall amounts than were observed using only rain gauge observations and provides objective spatial distributions of storm rainfall among rain gauges. SPAS results provided storm DADs, total storm precipitation patterns, and mass curves for the newly analyzed storms. Using these technologies, significant improvements of the storm rainfall analyses were achieved.
7. Previously analyzed storm events that occurred prior to 1948 that used 12-hour persisting dew points were adjusted using storm representative dew point adjustments of 2°F for synoptic type storm events and 7°F for MCS type storm events. This was done to adjust for using average dew point values for varying durations vs. 12-hour persisting dew point values. Recent evaluations of 12-hour persisting storm representative dew points showed those used in HMR 51 underestimated the storm representative values. An updated set of maximum dew point climatology maps were produced. These maps have higher maximum dew point values than those used in HMR studies and therefore compensate to some extent for the higher storm representative dew points.

12. Sensitivity Analysis

In the process of deriving the PMP values, various assumptions were made and explicit procedures were adopted for use. Additionally, various parameters and derived values are used in the calculations. It is of interest to assess the sensitivity of PMP values to assumptions that were made and to the variability of parameter values.

12.1 Assumptions

12.1.1 Saturated Storm Atmospheres

The atmospheric air masses that provide moisture to both the historic storm and the PMP storm are assumed to be saturated through the entire depth of the air column and the atmospheric column is assumed contain the maximum moisture possible based on the surface dew point. This assumes moist pseudo-adiabatic temperature profiles for both the historic storm and the PMP storm. Limited evaluation of this assumption in the FERC Michigan/Wisconsin regional PMP study and the Blenheim Gilboa study indicated that historic storm atmospheric profiles are generally not entirely saturated and contain somewhat less precipitable water than is assumed in the PMP procedure. It follows that the PMP storm (if it were to occur) would also have somewhat less precipitable water available than the assumed saturated PMP atmosphere would contain. What is used in the PMP procedure is the *ratio* of precipitable water associated with each storm. If the precipitable water values for each storm are both slightly overestimated, the ratio of these values will be essentially unchanged. For example, consider the case where instead of a historic storm with a storm representative dew point of 70°F degrees having 2.25 inches of precipitable water assuming a saturated atmosphere, it actually had 90% of that value or about 2.02 inches. The PMP procedure assumes the same type of storm with similar atmospheric characteristics for the maximized storm but with a higher dew point, say 76°F degrees. The maximized storm, having similar atmospheric conditions, would have about 2.69 inches of precipitable water instead of the 2.99 inches associated with a saturated atmosphere with a dew point of 76°F degrees. The maximization factor computed using the assumed saturated atmospheric values would be $2.99/2.25 = 1.33$. If both storms were about 90% saturated instead, the maximization factor would be $2.69/2.02 = 1.33$. Therefore potential inaccuracy of assuming saturated atmospheres (whereas the atmospheres may be somewhat less than saturated) should have a minimal impact on storm maximization and subsequent PMP calculations.

12.1.2 Maximum Storm Efficiency

Maximum storm efficiency allows for the most efficient conversion of atmospheric moisture to rainfall on the ground. By considering a long enough record of storm data and large enough transpositionable region, the assumption is made that at least a few storms would have been observed that attained or came close to attaining the maximum storm efficiency. The further assumption is made that if additional atmospheric moisture had been available, the storm would have maintained the same efficiency for converting atmospheric moisture to rainfall. The ratio of the maximized rainfall amounts to the actual rainfall amounts would be the same as the ratio of the precipitable water in the atmosphere associated with each storm.

There are two issues to be considered. First is the assumption that a storm has occurred that has rainfall efficiency close to the maximum possible. Unfortunately, state-of-the-science in

meteorology does not support a theoretical evaluation to quantify storm efficiency for use in PMP evaluation. This is because there is a lack of direct data from which to derive model parameters that would represent a PMP rainfall event. However, if the period of record is taken into consideration (generally over 100 years), along with an extended geographic region with transpositionable storms, it is accepted that there should have been at least one storm with dynamics that approach the maximum efficiency for rainfall production.

The other issue is the assumption that storm efficiency does not change if additional atmospheric moisture is available. Storm dynamics could potentially become more efficient or possibly less efficient depending on the interaction of cloud microphysical processes with the storm dynamics. Offsetting effects could indeed lead to the storm efficiency remaining essentially unchanged. For the present, the assumption of no change in storm efficiency is accepted, mirroring the HMR and WMO assumptions.

12.2 Parameters

12.2.1 Storm Representative Dew Point and Maximum Dew Point

The in-place maximization factor depends on the determination of storm representative dew points, along with maximum historical dew point values. The magnitude of the maximization factor varies depending on the values used for the storm representative dew point and the maximum dew point. Holding all other variables constant, the maximization factor is smaller for higher storm representative dew points as well as for lower maximum dew point values. Likewise, larger maximization factors result from the use of lower storm representative dew points and/or higher maximum dew points. The magnitude of the change in the maximization factor varies depending on the dew point values. For the range of dew point values used in most PMP studies, the maximization factor for a particular storm will change about 5% for every 1°F difference between the storm representative and maximum dew point values. The same sensitivity applies to the transposition factor, with about a 5% change for every 1°F change in either the in-place maximum dew point or the transposition maximum dew point⁶.

For example, consider the following case:

Storm representative dew point:	75°F	Precipitable water:	2.85"
Maximum dew point:	79°F	Precipitable water:	3.44"
Maximization factor = $3.44"/2.85" = 1.21$			

If the storm representative dew point were 74°F with precipitable water of 2.73",
Maximization Factor = $3.44"/2.73" = 1.26$ (an increase of approximately 4%)

If the maximum dew point were 78°F with precipitable water of 3.29",
Maximization Factor = $3.29"/2.85" = 1.15$ (a decrease of approximately 5%)

⁶ Note that the amount of moisture per degree of dew point temp is not linear, but this 5% formula fits within the range of dew points used in this analysis.

12.2.2 Sensitivity of the Elevation Adjustment Factor

Variations in elevation associated with topographic features remove atmospheric moisture from an air mass as it moves over the terrain. When storms are transpositioned, the elevation of the storm center location is used to compute the amount of atmospheric moisture depleted from the storm atmosphere during the in-place moisture maximization process. The absolute amount of moisture depletion is somewhat dependent on the dew point values, but is primarily dependent on the elevation at the original storm location compared to the elevation of the basin centroid and each grid point. The elevation adjustment is slightly less than 1% for every 100 feet of elevation change between the original storm location and the study basin elevation.

For example, consider the following case:

Maximum dew point:	79°F
Elevation:	1,000'
Precipitable water between 1000mb and the top of the atmosphere:	3.44"
Precipitable water between 1000mb and 1,000':	0.28"
Elevation Adjustment Factor = $(3.44'' - 0.28'') / 3.44''$	= 0.92 (approximately 1% per 100 feet)

If the elevation were 2,000', the precipitable water between 1000mb and 2,000' is 0.55"
Elevation Adjustment Factor = $(3.44'' - 0.55'') / 3.44''$ = 0.84 (approximately 1% per 100 feet)

13. Recommendations for Application

13.1 PMP Application

PMP values have been computed that provide maximum rainfall amounts for use in computing the PMF at any location within the state of Ohio. The study addressed several issues that could potentially affect the magnitude of the PMP storm over the region as compared with HMR 51.

Analysis of moisture availability for previously analyzed storms and analysis of recent extreme storms with up to date state-of-the-science techniques resulted in PMP values which supersede HMR 51 and provide explicit PMP values. These represent the most current PMP values that should be used together with the procedures in HMR 52 and updated PMP design storm parameters to provide PMP rainfall at any location within the state.

13.2 Discussion on the Spatial Limits of the PMP Values

The grid system used in this study was designed such that no regions within the state required extrapolation of storm data, but allowed for interpolation between rainfall values at grid point or the use of the gridded data within GIS. The grid extended beyond the geographic boundaries of the state. The emphasis was to provide the most reliable and consistent analysis within this geographic region. PMP maps are provided to allow for PMP values to be extracted for any location within the state. As an option, a user who has GIS software can use the gridded data to explicitly determine PMP values with no manual interpolation necessary.

For each of the storms analyzed, appropriate transposition grid points were defined (see Appendix F). After all the storms were analyzed, the largest rainfall values were determined for each grid point for each duration and area size. These largest values were enveloped to insure both spatial and temporal continuity.

Once the enveloped values were finalized, lines of constant PMP values were drawn using GIS interpolation software and meteorological judgment for each duration and area size. These PMP contour lines were extended beyond the state boundary such that PMP values could be interpolated at all locations within the state. Hence, the reason that some PMP contour lines extend beyond the state boundary is to allow for gradients to be determined between lines for all locations within Ohio.

For regions outside of the state where extrapolation would be required, the gradient is uncertain. There are probably regions where the extended lines provide reasonable PMP values while for other regions, PMP values are less reliable. This study provides PMP values only for locations within Ohio and watershed draining directly into the state.

13.3 Climate Change Assumptions

Climate change has occurred in the past, is now occurring, and undoubtedly will continue in the future. This is and has always been a natural part of Earth's cycles. Global warming has received much attention recently, with evidence that locations around the globe have experienced

both increasing and decreasing temperatures during the past couple of decades. Much attention has been given to anthropogenic increases in atmospheric greenhouse gases and their potential impact on global temperature and/or accentuating natural climate variability (IPCC 2007). Some researchers have even suggested that global warming may not continue, but that a period of global cooling may have begun around 2000 (Michaels 2004, Manuel 2009). How the climate will change and how this will affect the number and intensity of extreme rainfall events over the basin is unknown as of the date of this report.

With a warming of the atmosphere, there can potentially be an increase in the available atmospheric moisture for storms to convert to rainfall. However, storm dynamics play a significant role in that conversion process and the result of a warming or cooling climate on storm dynamics is not well understood. A warmer or cooler climate may lead to a change in the frequency of storms and/or a change in the intensity of storms, but there is no definitive evidence to indicate the trend or the magnitude of potential changes (Spencer 2008).

AWA recognizes that the climate is in a constant state of change and a warmer future is a distinct possibility. However, the current scientific consensus and understanding cannot agree how climate is changing and more importantly what those changes will be for the region. Whether the region will be wetter or drier, warmer or colder and/or experience more or less extreme rainfall events cannot be determined with any quantitative and statistically significant certainty. Further, most projects of this type have a projected life between 50 to 100 years before they are re-evaluated. In general, most projected changes that *may* occur within the Earth's climate system would be unlikely to significantly affect the project's hydrology beyond the bounds of the PMP values derived as part of this study during its useful life. Based on these discussions, the current practice of PMP determination should not be modified in an attempt to address potential changes associated with climate change. This study has continued the practice of assuming no climate change, as climate trends are not considered when preparing PMP estimates (WMO, Section 1.1.1).

REFERENCES

- Bonnin, G.M., Todd, D., Lin, B., Parzybok, T., Yekta, M., and D. Riley, 2006: Precipitation-Frequency Atlas of the United States, NOAA Atlas 14, Volumes 1 and 2, NOAA, National Weather Service, Silver Spring, Maryland. <http://hdsc.nws.noaa.gov/hdsc/pfds/>
- Corrigan, P., Fenn, D.D., Kluck, D.R., and J.L. Vogel, 1999: Probable Maximum Precipitation Estimates for California. *Hydrometeorological Report No. 59*, U.S. National Weather Service, National Oceanic and Atmospheric Administration, U.S. Department of Commerce, Silver Spring, MD, 392 pp.
- Corps of Engineers, U.S. Army, 1936-1973: Storm Rainfall in the United States, Depth-Area-Duration Data. Office of Chief of Engineers, Washington, D.C.
- Daly, C., R.P. Neilson, and D.L. Phillips, 1994: A Statistical-Topographic Model for Mapping Climatological Precipitation over Mountainous Terrain. *J. Appl. Meteor.*, **33**, 140–158.
- Daly, C., Taylor, G., and W. Gibson, 1997: The PRISM Approach to Mapping Precipitation and Temperature, 10th Conf. on Applied Climatology, Reno, NV, Amer. Meteor. Soc., 10-12.
- Draxler, R.R. and Rolph, G.D., 2003: HYSPLIT (HYbrid Single-Particle Lagrangian Integrated Trajectory) Model access via NOAA ARL READY Website (<http://www.arl.noaa.gov/ready/hysplit4.html>). NOAA Air Resources Laboratory, Silver Spring, MD.
- Draxler, R.R. and Rolph, G.D., 2010. HYSPLIT (HYbrid Single-Particle Lagrangian Integrated Trajectory) Model access via NOAA ARL READY Website (<http://ready.arl.noaa.gov/HYSPLIT.php>). NOAA Air Resources Laboratory, Silver Spring, MD.
- Environmental Data Service, 1968: Maximum Persisting 12-Hour, 1000mb Dew Points (°F) Monthly and of Record. *Climate Atlas of the United States*, Env. Sci. Serv. Adm., U.S. Dept of Commerce, Washington, D.C., pp 59-60.
- GRASS (Geographic Resources Analysis Support System) GIS is an open source, free software GIS with raster, topological vector, image processing, and graphics production functionality that operates on various platforms. <http://grass.itc.it/>.
- Hansen, E.M., and F.K. Schwartz, 1981: Meteorology of Important Rainstorms in the Colorado River and Great Basin Drainages. *Hydrometeorological Report No. 50*, National Weather Service, National Oceanic and Atmospheric Administration, U.S. Department of Commerce, Silver Spring, MD, 167 pp.
- _____, Schreiner, L.C., and J.F., Miller, 1982: Application of Probable Maximum Precipitation Estimates, United States East of the 105th Meridian, *Hydrometeorological Report Number 52*, National weather Service, National Oceanic and Atmospheric Association, U.S. Dept of Commerce, Silver Spring, MD, 179 pp.

- _____, Fenn, D.D., Schreiner, L.C., Stodt, R.W., and J.F., Miller, 1988: Probable Maximum Precipitation Estimates, United States between the Continental Divide and the 103rd Meridian, *Hydrometeorological Report Number 55A*, National Weather Service, National Oceanic and Atmospheric Association, U.S. Dept of Commerce, Silver Spring, MD, 242 pp.
- _____, Schwarz, F.K., and J.T. Riedel, 1994: Probable Maximum Precipitation- Pacific Northwest States, Columbia River (Including portion of Canada), Snake River, and Pacific Drainages. *Hydrometeorological Report No. 57*, National Weather Service, National Oceanic and Atmospheric Administration, U.S. Department of Commerce, Silver Spring, MD, 353 pp.
- Hershfield, D.M., 1961: Rainfall frequency atlas of the United States for durations from 30 minutes to 24 hours and return periods from 1 to 100 years, *Technical Paper No. 40*, U.S. Weather Bureau, Washington, D.C., 61p.
- IPCC, 2007: *Climate Change 2007: The Physical Science Basis. Contribution of Working group I to the Fourth Assessment Report of the Intergovernmental Panel on Climate Change* [Solomon, S., D. Qin, M. Manning, Z. Chen, M. Marquis, K.B. Averyt, M. Tignor, and H.L. Miller (eds)]/ Cambridge University Press, Cambridge, United Kingdom and New York, NY, USA, 996 pp.
- Jennings, A.H., 1952: Maximum 24-hour Precipitation in the United States, *Technical Paper Number 16*, U.S. Weather Bureau, U.S. Department of Commerce, Washington, DC, 284 pp.
- Kalnay, E., M. Kanamitsu, R. Kistler, W. Collins, D. Deaven, L. Gandin, M. Iredell, S. Saha, G. White, J. Woollen, Y. Zhu, A. Leetmaa, R. Reynolds, M. Chelliah, W. Ebisuzaki, W. Higgins, J. Janowiak, K. Mo, C. Ropelewski, J. Wang, R. Jenne, and D. Joseph, 1996: The NCEP/NCAR 40-Year Reanalysis Project. *Bull. Amer. Meteor. Soc.*, **77**, 437–471.
- Kappel, W.D., Tomlinson, E.M., Hultstrand, D.M., and G.A. Muhlestein, August 2012: Site-Specific Probable Maximum Precipitation Study for the Tarrant Regional Water District, Prepared for Tarrant Regional Water District, Fort Worth, Texas.
- _____, Hultstrand, D.M., Tomlinson, E.M., Muhlestein, G.A., and T.P. Parzybok, September 2012: Site-Specific Probable Maximum Precipitation (PMP) Study for the Quad Cities Nuclear Generating Station, Quad Cities, IA.
- Maddox, R.A., 1980: Mesoscale convective complexes. *Bull. Amer. Meteor. Soc.*, **61**, 1374–1387.
- Manuel, O.K., 2009: The Earth's Heat Source – The Sun. *Energy and Environment*. **20**, 131–144.
- Mesinger, F., G. DiMego, E. Kalnay, K. Mitchell, P.C. Shafran, W. Ebisuzaki, D. Jovic, J. Woollen, E. Rogers, E.H. Berbery, M.B. Ek, Y. Fan, R. Grumbine, W. Higgins, H. Li, Y. Lin, G. Manikin, D. Parrish, and W. Shi, 2006: North American Regional Reanalysis. *Bull. Amer. Meteor. Soc.*, **87**, 343–360.

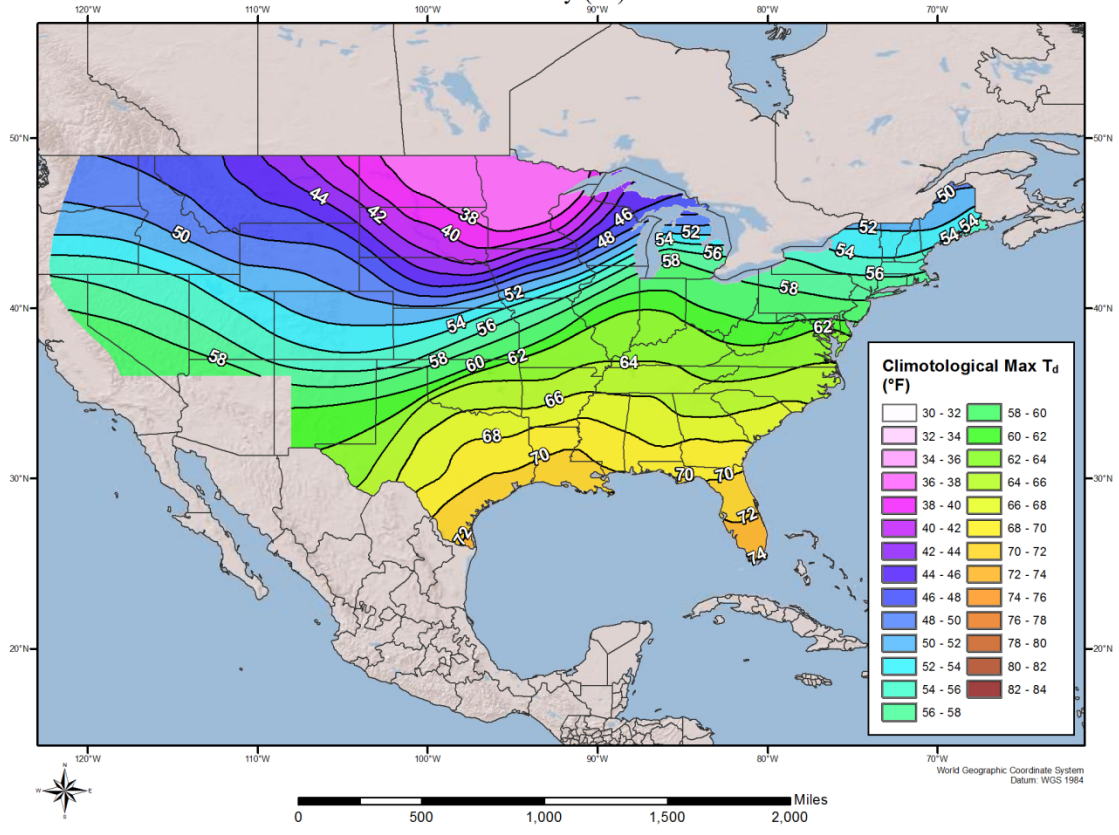
- Michaels, P.J., 2004: Meltdown, The Predictable Distortion of Global Warming by Scientists, Politicians, and Media, the Cato Institute, Washington D.C., 255 pp.
- Miller, J.F., 1964: Two to ten day Precipitation for Return Periods of 2 to 100 Years in the Contiguous United States, Washington, D.C., U.S. Weather Bureau Technical Paper 49, 29p.
- Miller, J.F., Fredrick, R.H., Tracey, R.J., 1973: US Dept of Commerce, NOAA, NWS, Silver Spring, MD., *NOAA Atlas 2, Precipitation Frequency Atlas of the Western United States*.
- National Climatic Data Center (NCDC). NCDC TD-3200 and TD-3206 datasets - Cooperative Summary of the Day.
- National Climatic Data Center (NCDC) Heavy Precipitation Page
<http://www.ncdc.noaa.gov/oa/climate/severeweather/rainfall.html#maps>
- National Oceanic and Atmospheric Administration Central Library Data Imaging Project *Daily weather maps*,
http://docs.lib.noaa.gov/rescue/dwm/data_rescue_daily_weather_maps.html
- Parzybok, T. W., and E. M. Tomlinson, 2006: A New System for Analyzing Precipitation from Storms, *Hydro Review*, Vol. XXV, No. 3, 58-65.
- PRISM Mapping Methodology, <http://www.ocs.oregonstate.edu/prism/index.phtml>
- Remote Automated Weather Stations RAWS, <http://www.raws.dri.edu/index.html>
- Shands, A.L. and G.N. Brancato, March 1946: Applied Meteorology: Mass Curves of Rainfall. Hydrometeorological Section, Office of Hydrologic Director.
- Spencer, R., 2008: Climate Confusion: How Global Warming Hysteria Leads to Bad Science, Pandering Politicians and Misguided Policies that Hurt the Poor, Encounter Books, New York, NY, 184 pp.
- Tomlinson, E.M., 1993: Probable Maximum Precipitation Study for Michigan and Wisconsin, Electric Power Research Institute, Palo Alto, CA, TR-101554, V1.
- _____, G.W. Wilkerson, and Wiscomb T.G., 1994: Probable Maximum Precipitation Study for the Great Miami River Basin, NAWC Report AR 94-3, Salt Lake City, UT, 194pp.
- _____, R.A. Williams, and T.W. Parzybok, September 2002: Site-Specific Probable Maximum Precipitation Study for the Upper and Middle Dams Drainage Basin, Prepared for FPLE, Lewiston, ME.
- _____, R.A. Williams, and T.W. Parzybok, September 2003: Site-Specific Probable Maximum Precipitation (PMP) Study for the Great Sacandaga Lake / Stewarts Bridge Drainage Basin, Prepared for Reliant Energy Corporation, Liverpool, NY.

- _____, R.A. Williams, Kappel, W.D., and T.W. Parzybok, September 2003: Site-Specific Probable Maximum Precipitation (PMP) Study for the Cherry Creek Drainage Basin, Prepared for the Colorado Water Conservation Board, Denver, CO.
- _____, Kappel W.D., Parzybok, T.W., Hultstrand, D.M., Muhlestein, G.A., and B. Rappolt, May 2006: Site-Specific Probable Maximum Precipitation (PMP) Study for the Woodcliff Lake Drainage Basin, Prepared for New Jersey Dept. of Environmental Protection, NJ.
- _____, Kappel W.D., Parzybok, T.W., Hultstrand, D.M., Muhlestein, G.A., and B. Rappolt, May 2008: Site-Specific Probable Maximum Precipitation (PMP) Study for the Wanahoo Drainage Basin, Prepared for Olsson Associates, Omaha, NE.
- _____, Kappel W.D., Parzybok, T.W., Hultstrand, D.M., Muhlestein, G.A., and B. Rappolt, June 2008: Site-Specific Probable Maximum Precipitation (PMP) Study for the Blenheim Gilboa Drainage Basin, Prepared for New York Power Authority, White Plains, NY.
- _____, Kappel W.D., Parzybok, T.W., Hultstrand, D.M., Muhlestein, G.A., and P. Sutter, December 2008: Statewide Probable Maximum Precipitation (PMP) Study for the state of Nebraska, Prepared for Nebraska Dam Safety, Omaha, NE.
- _____, Kappel, W.D., Muhlestein, G.A., and Tye W. Parzybok, February 2009: Site-Specific Probable Maximum Precipitation (PMP) Study for the Tuxedo Lake Drainage Basin, NY.
- _____, Kappel W.D., Parzybok, T.W., Hultstrand, D.M., Muhlestein, G.A., March 2011: Site-Specific Probable Maximum Precipitation Study for the Tarrant Regional Water District, Prepared for Tarrant Regional Water District, Fort Worth, TX.
- _____, Kappel, W.D., Hultstrand, D.M., Muhlestein, G.A., and T. W. Parzybok, December 2011: Site-Specific Probable Maximum Precipitation (PMP) Study for the Brassua Dam basin, Maine.
- _____, and W.D. Kappel, October 2009: Revisiting PMPs, *Hydro Review*, Vol. 28, No. 7, 10-17.
- U.S. Weather Bureau, 1946: Manual for Depth-Area-Duration analysis of storm precipitation. *Cooperative Studies Technical Paper No. 1*, U.S. Department of Commerce, Weather Bureau, Washington, D.C., 73pp.
- U.S. Weather Bureau, 1951: Tables of Precipitable Water and Other Factors for a Saturated Pseudo-adiabatic Atmosphere, *Technical Paper Number 14*, US. Department of Commerce, Washington, DC, 66 pp.
- World Meteorological Organization, 1986: Manual for Estimation of Probable Maximum Precipitation.
- World Meteorological Organization, 2009: Manual for Estimation of Probable Maximum

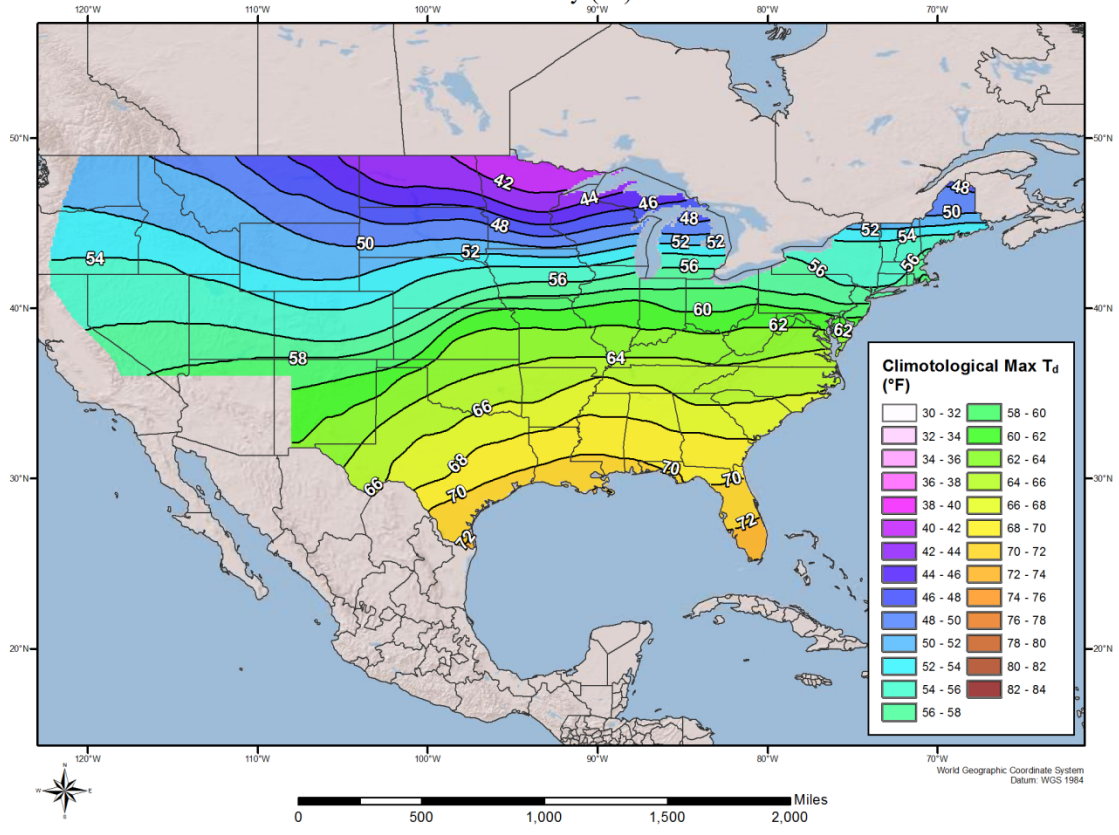
Appendix A

Dew Point Climatology Maps Used in the Storm Maximization and Transposition Processes

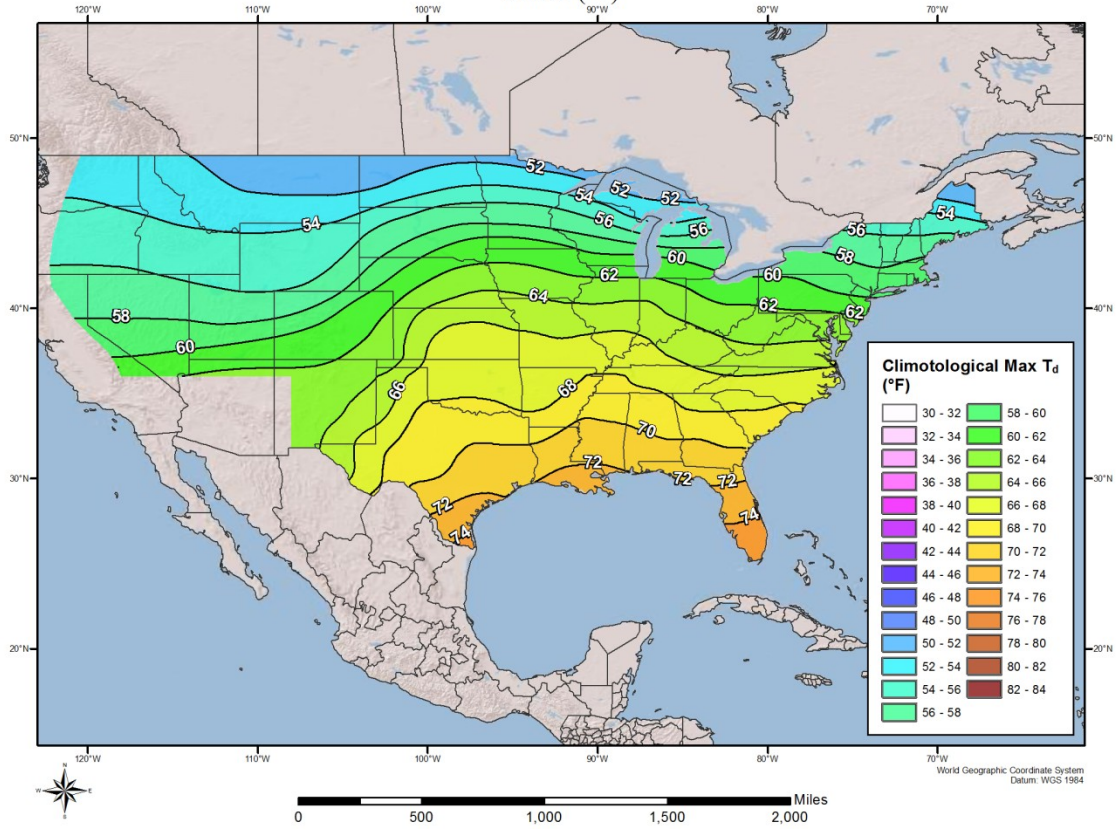
6-hour Monthly Dew Point Climatology January (°F)



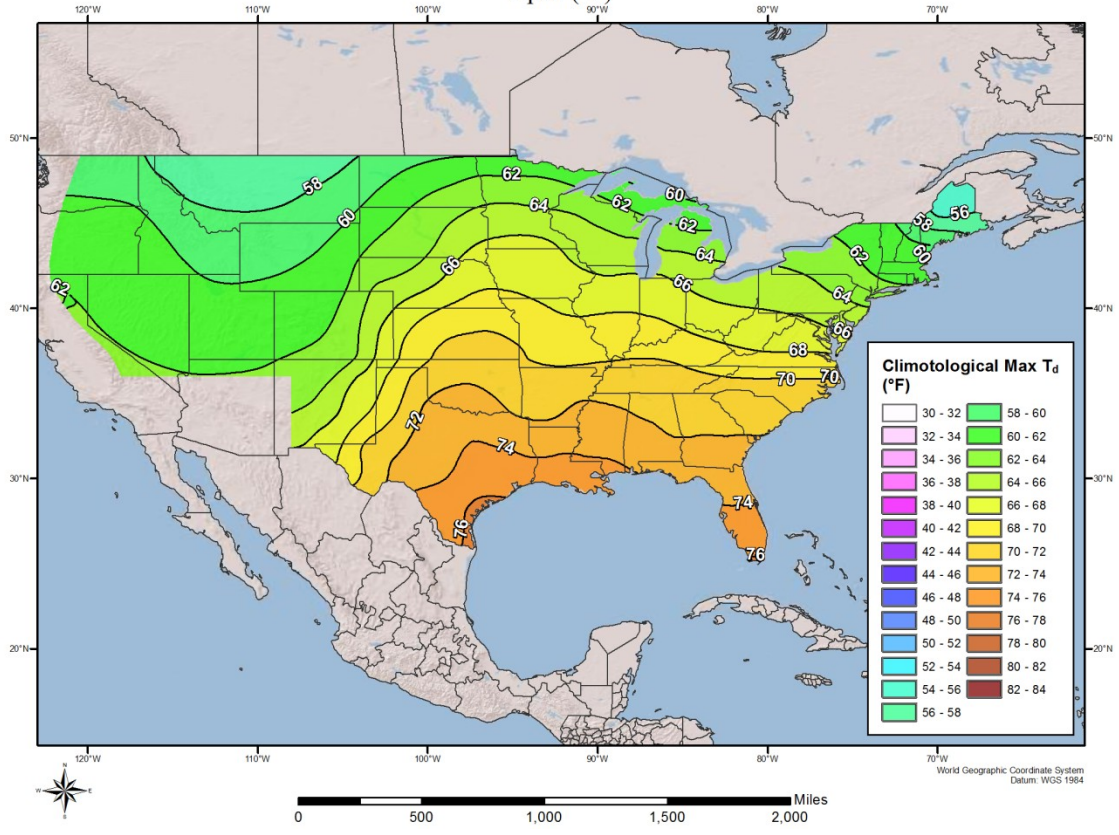
6-hour Monthly Dew Point Climatology February (°F)



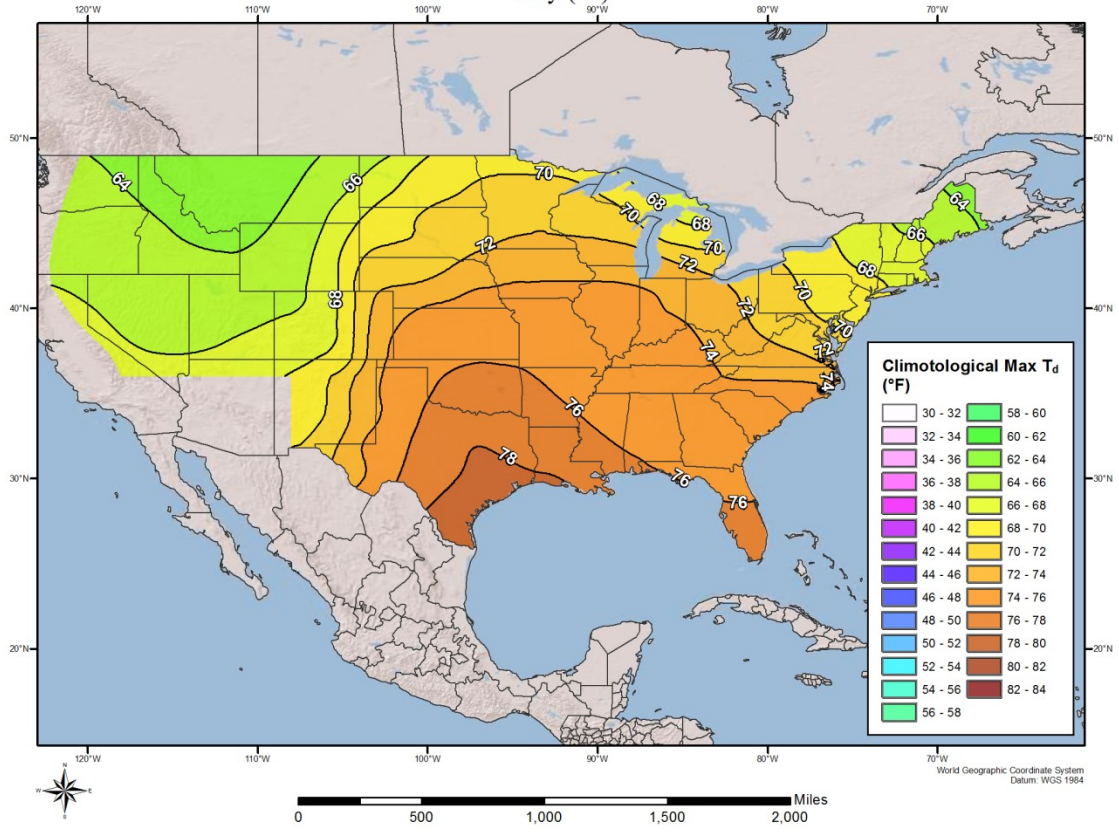
6-hour Monthly Dew Point Climatology March (°F)



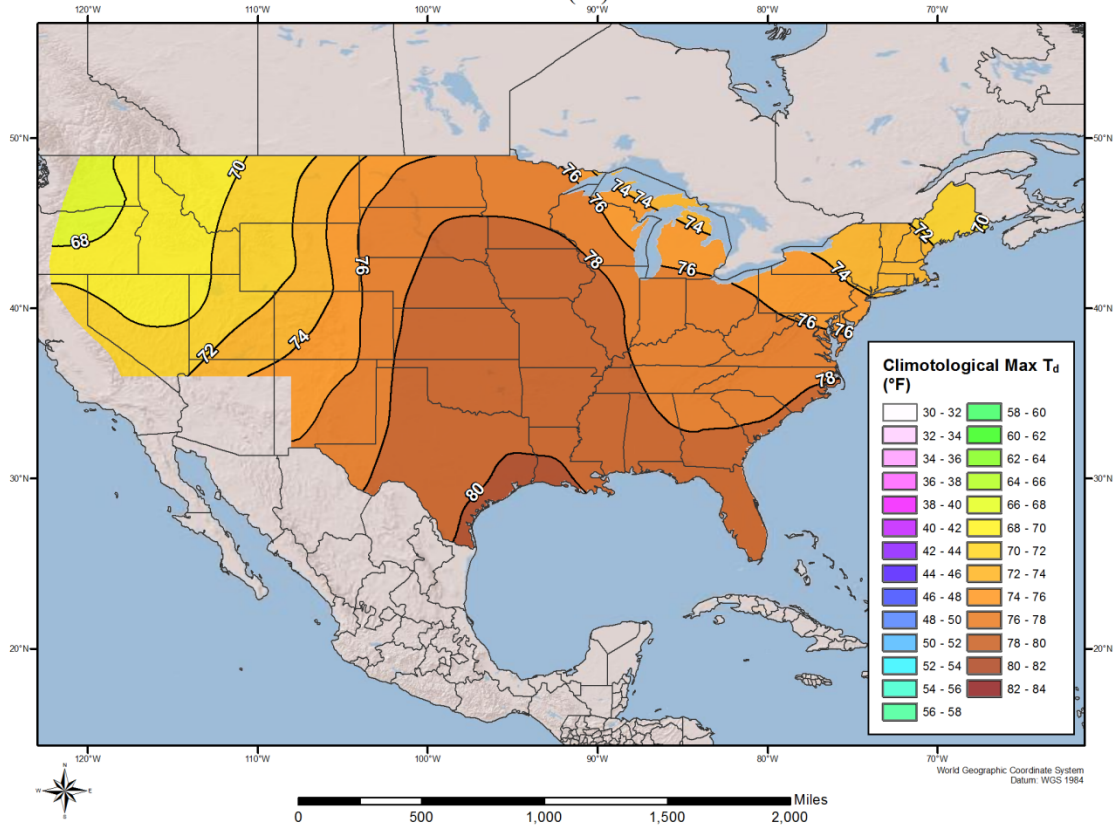
6-hour Monthly Dew Point Climatology April (°F)



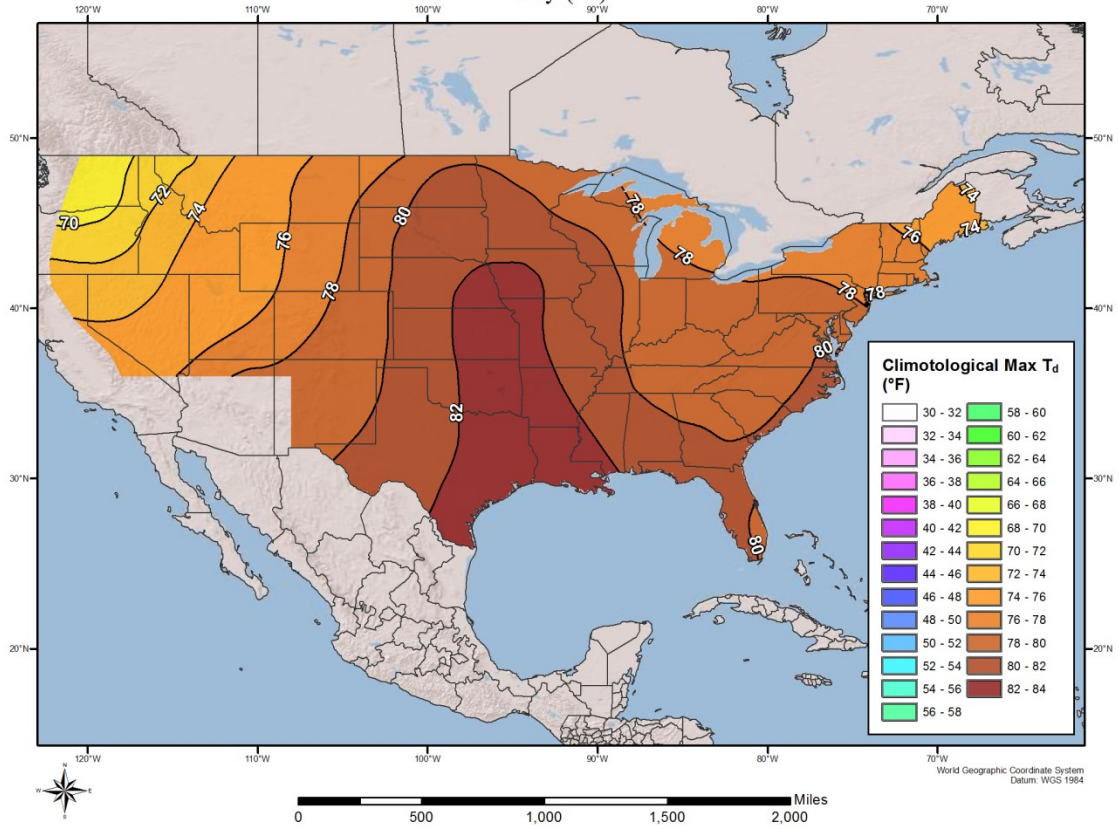
6-hour Monthly Dew Point Climatology May (°F)



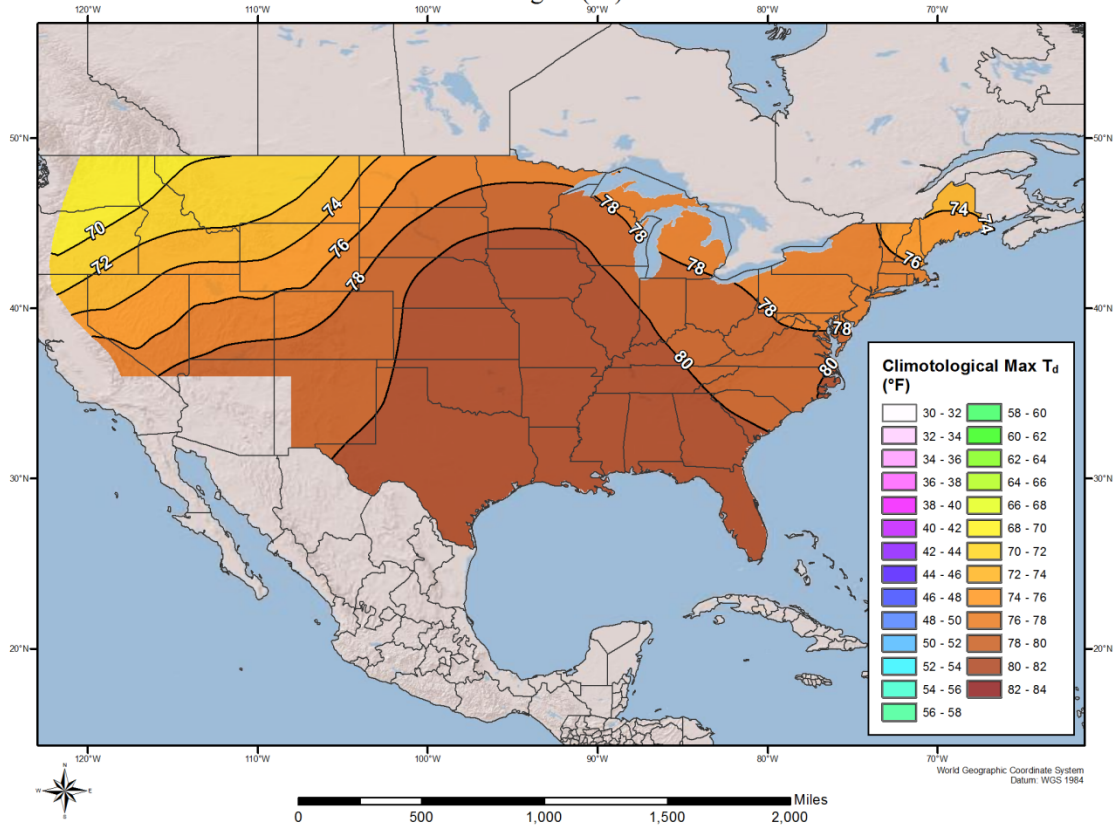
6-hour Monthly Dew Point Climatology June (°F)



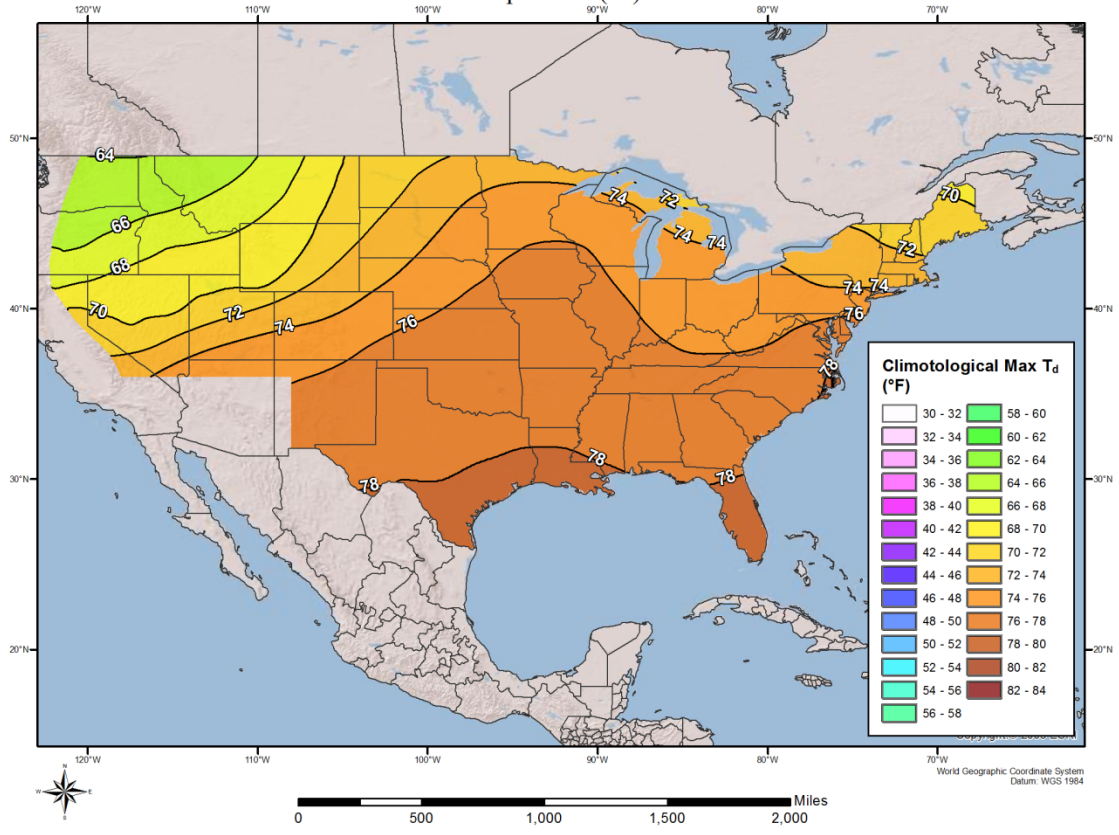
6-hour Monthly Dew Point Climatology July (°F)



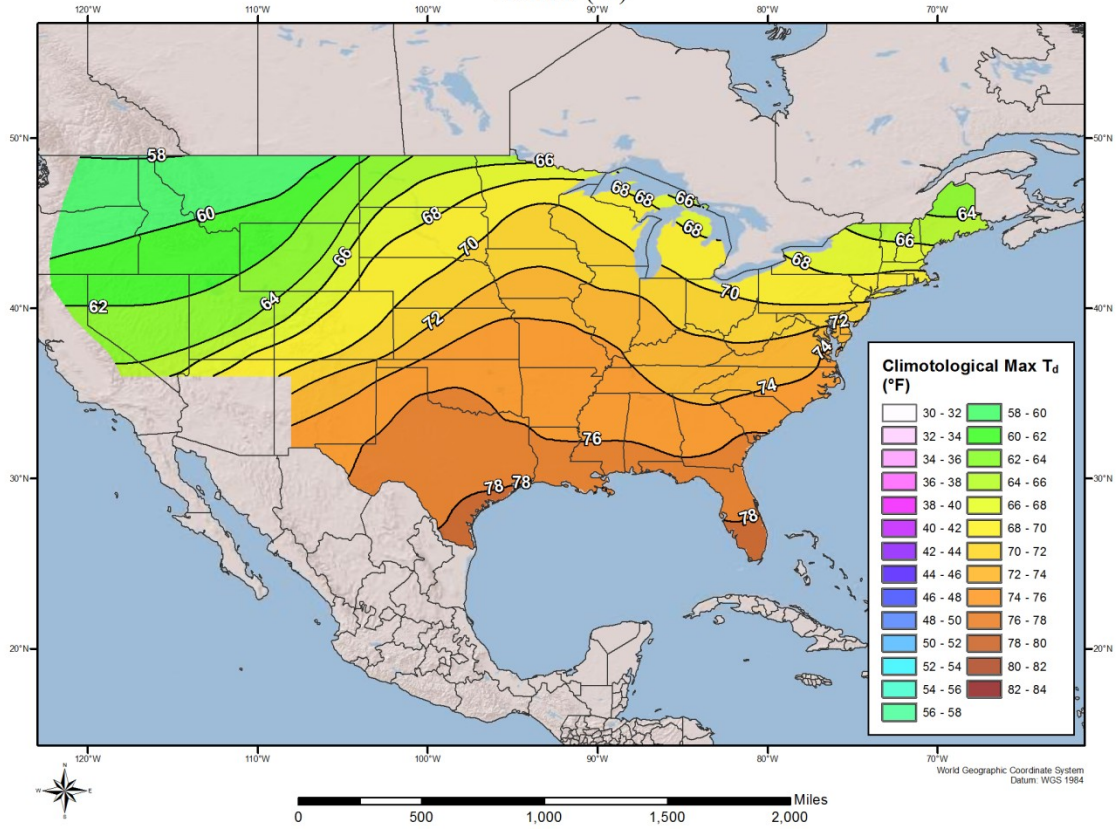
6-hour Monthly Dew Point Climatology August (°F)



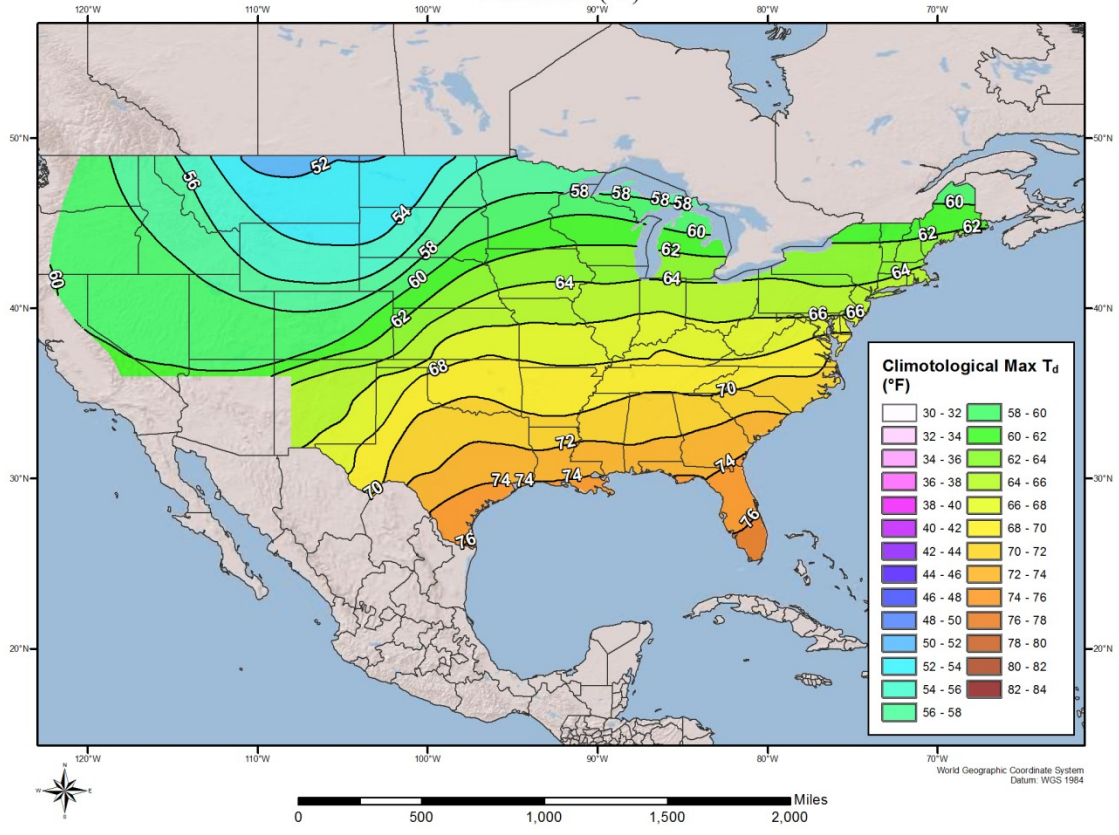
6-hour Monthly Dew Point Climatology September (°F)



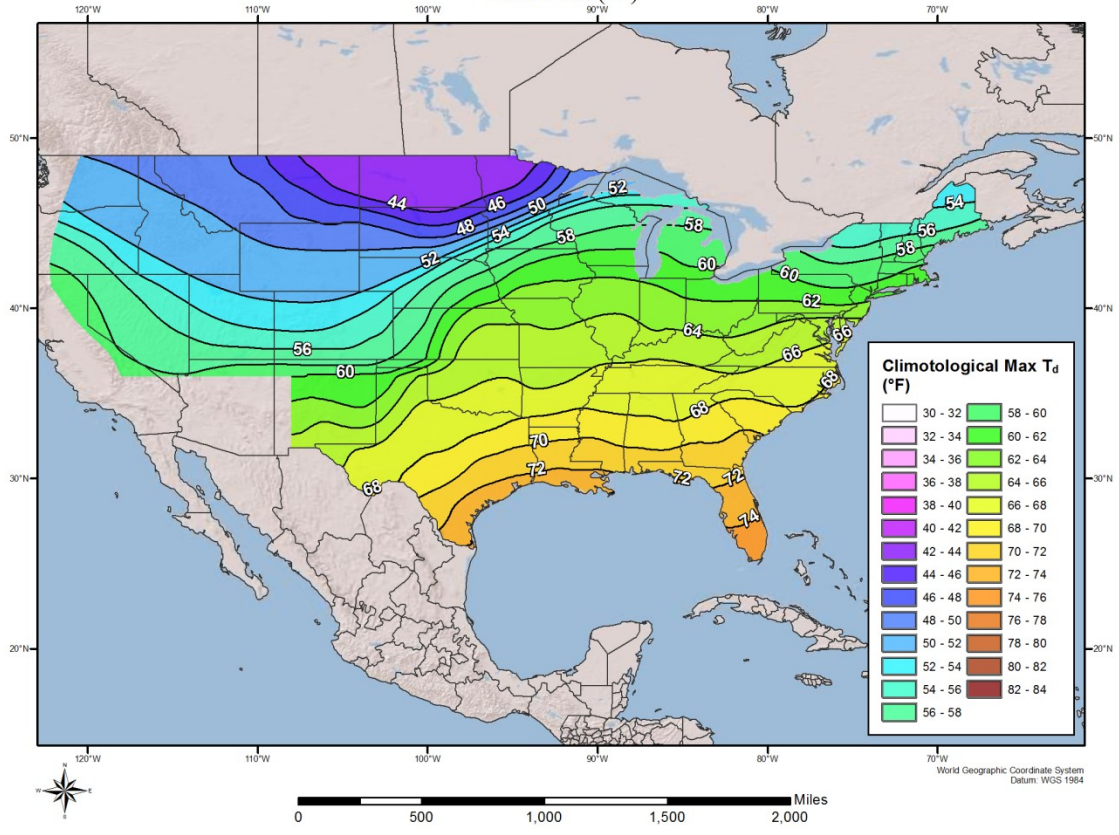
6-hour Monthly Dew Point Climatology October (°F)



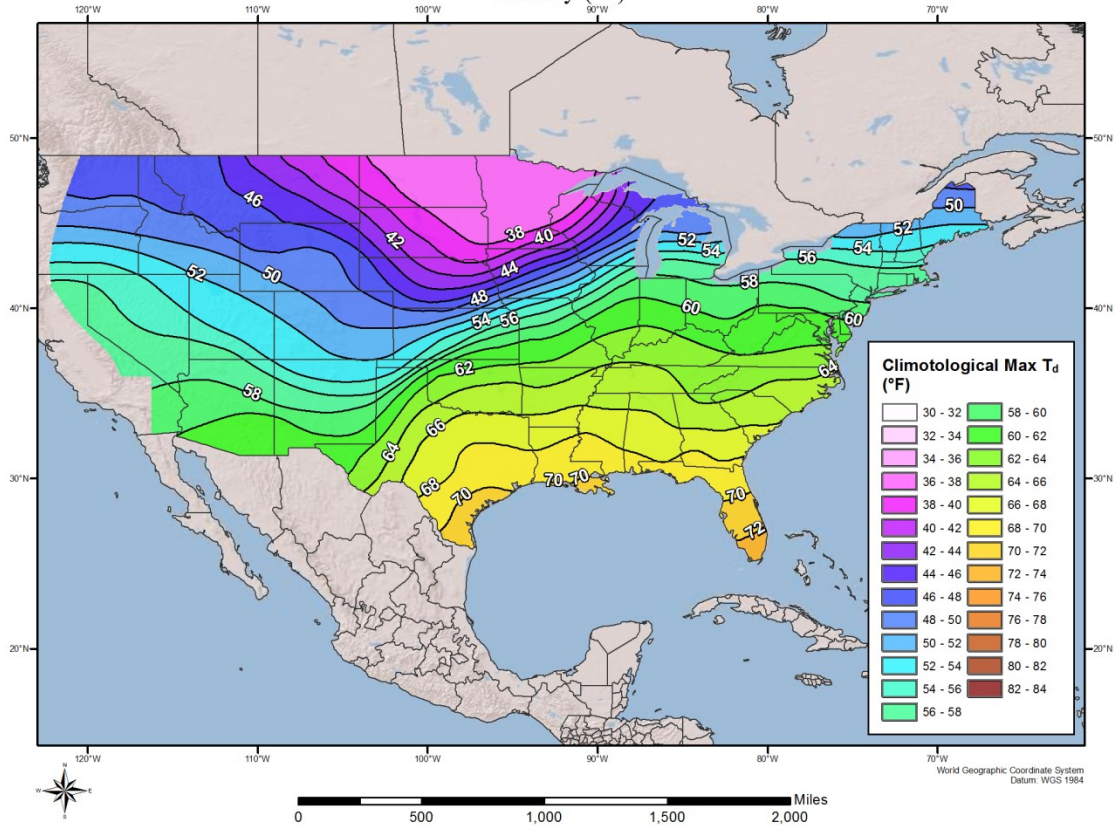
6-hour Monthly Dew Point Climatology November (°F)



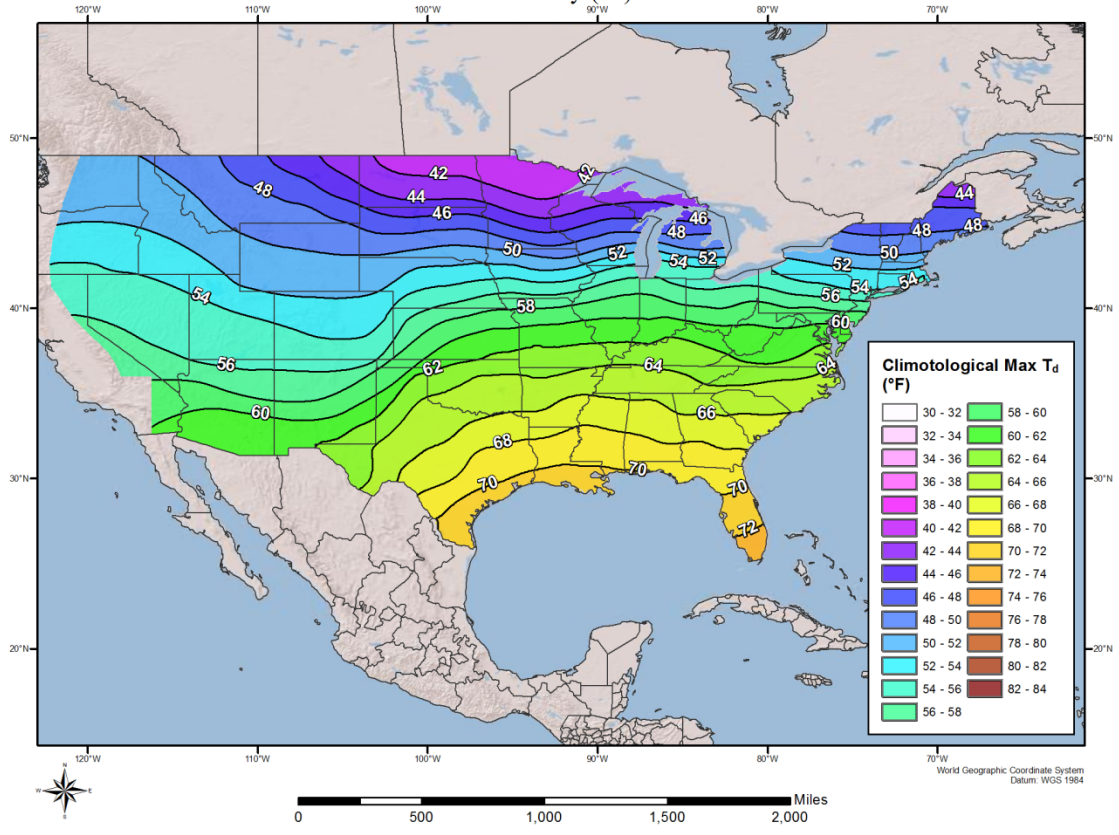
6-hour Monthly Dew Point Climatology December (°F)



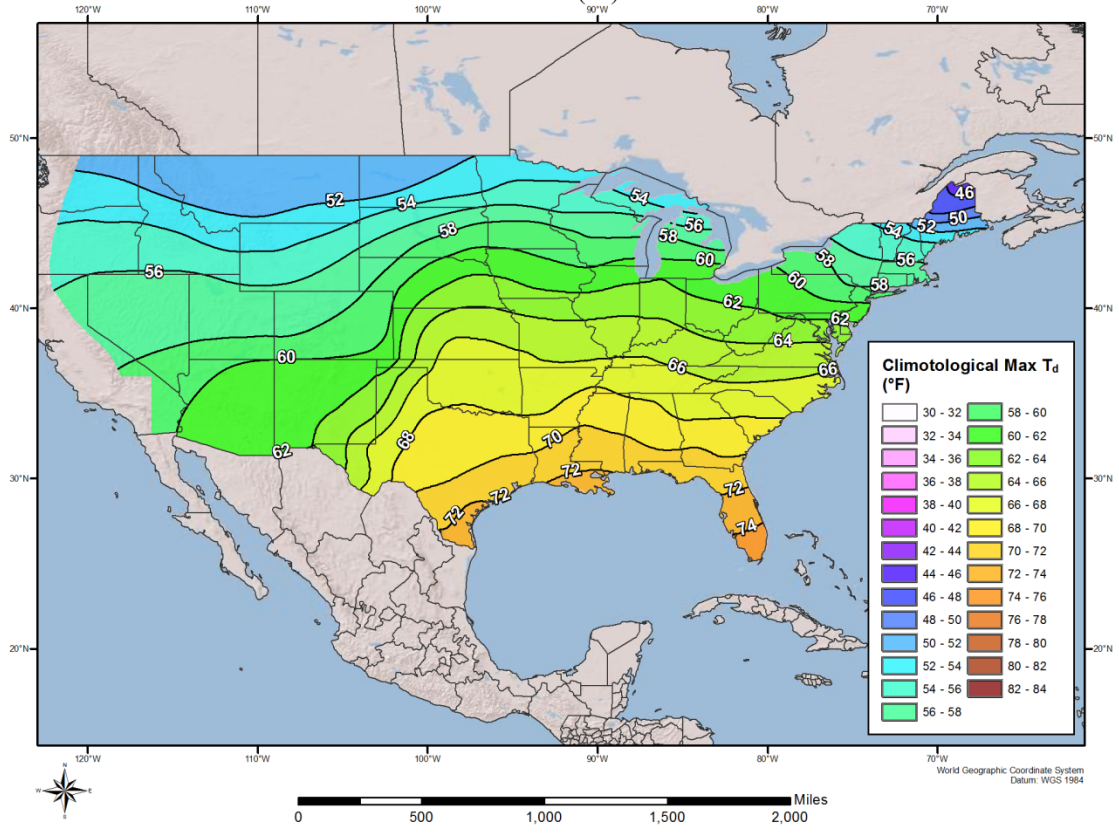
12-hour Monthly Dew Point Climatology January (°F)



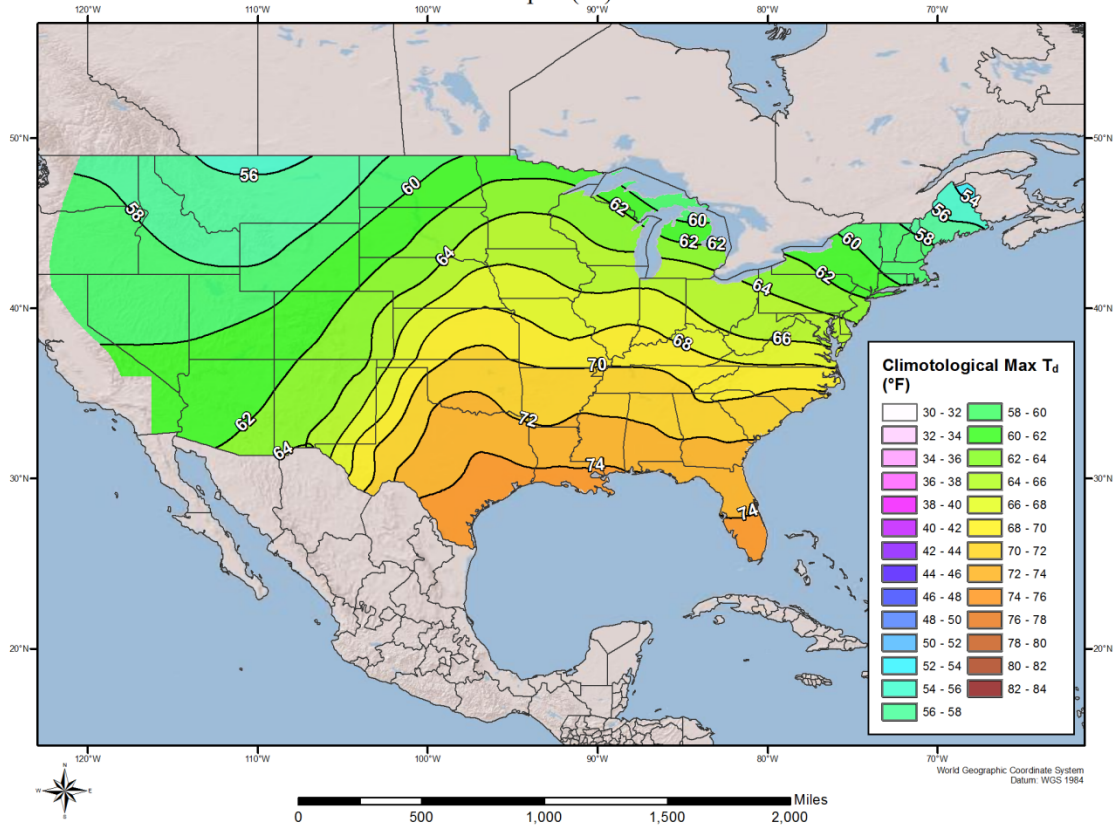
12-hour Monthly Dew Point Climatology February (°F)



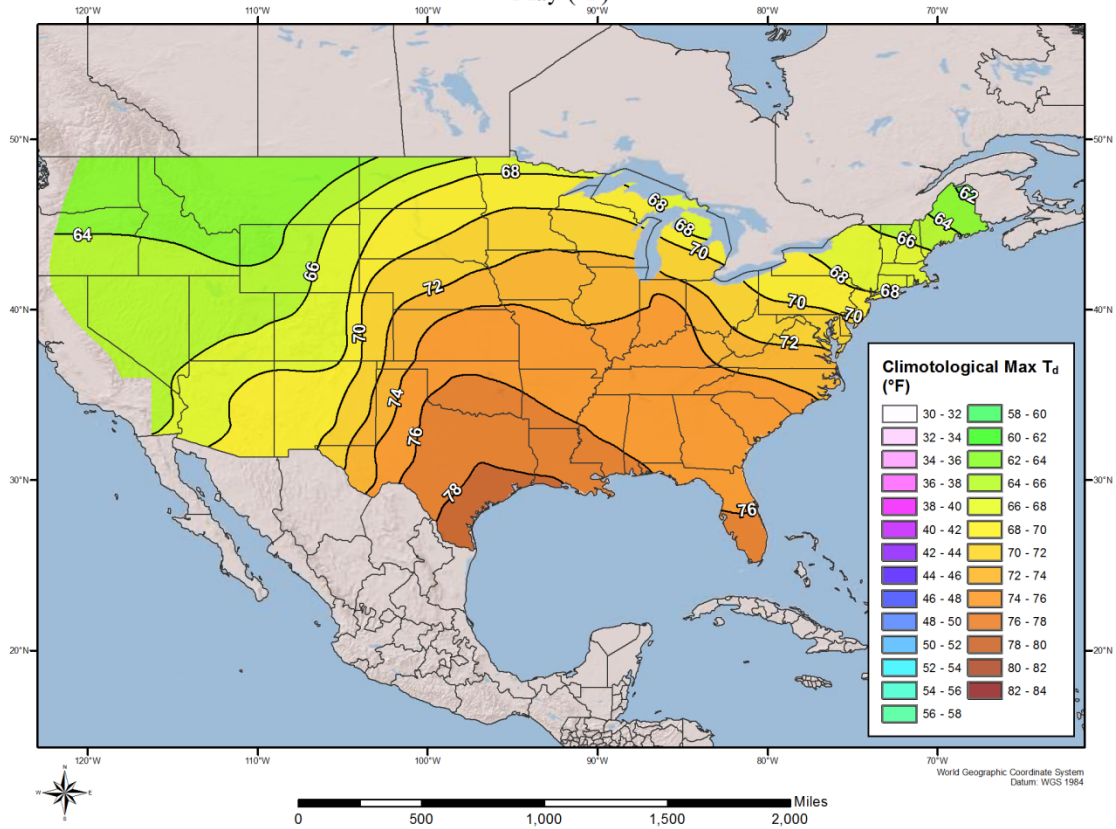
12-hour Monthly Dew Point Climatology March (°F)



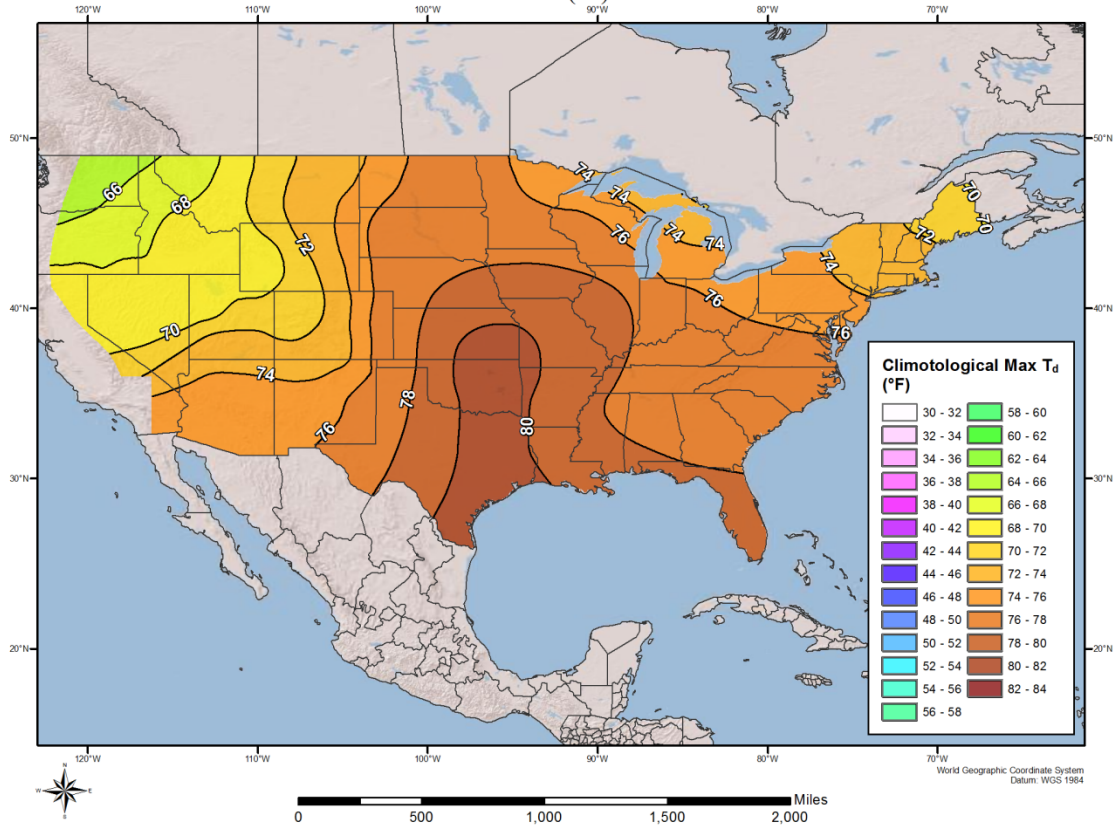
12-hour Monthly Dew Point Climatology April (°F)



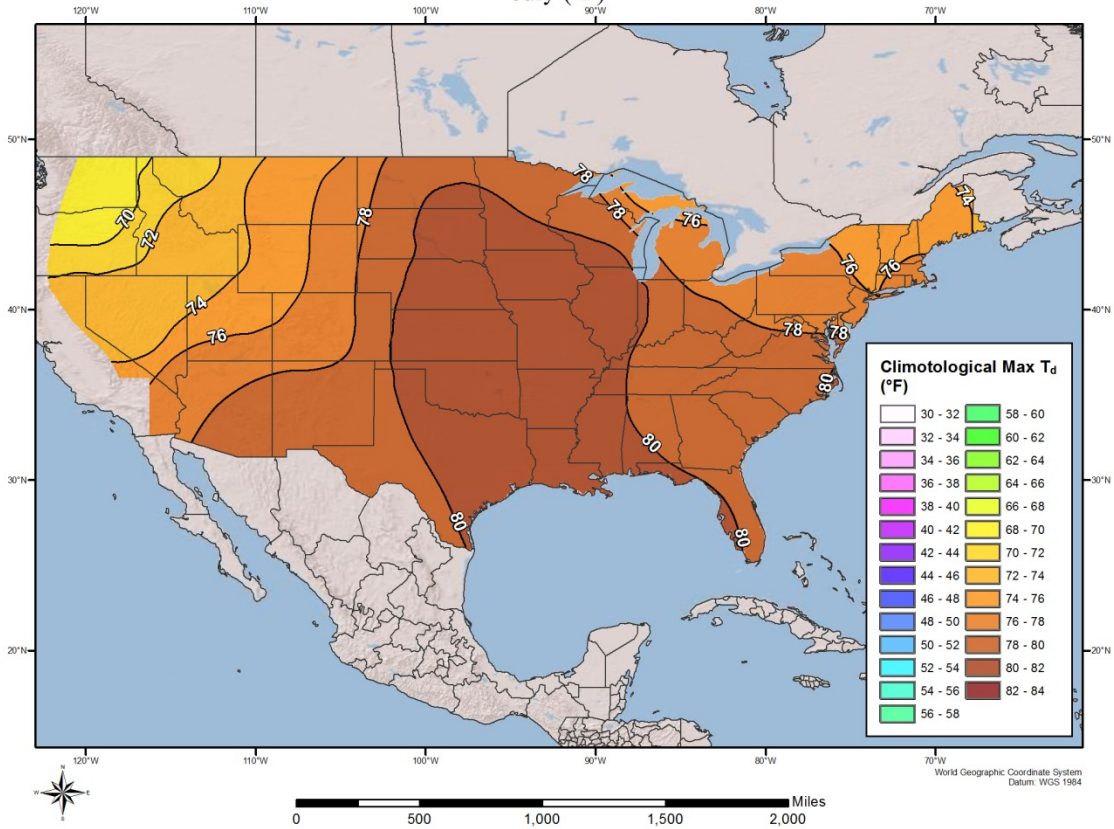
12-hour Monthly Dew Point Climatology May (°F)



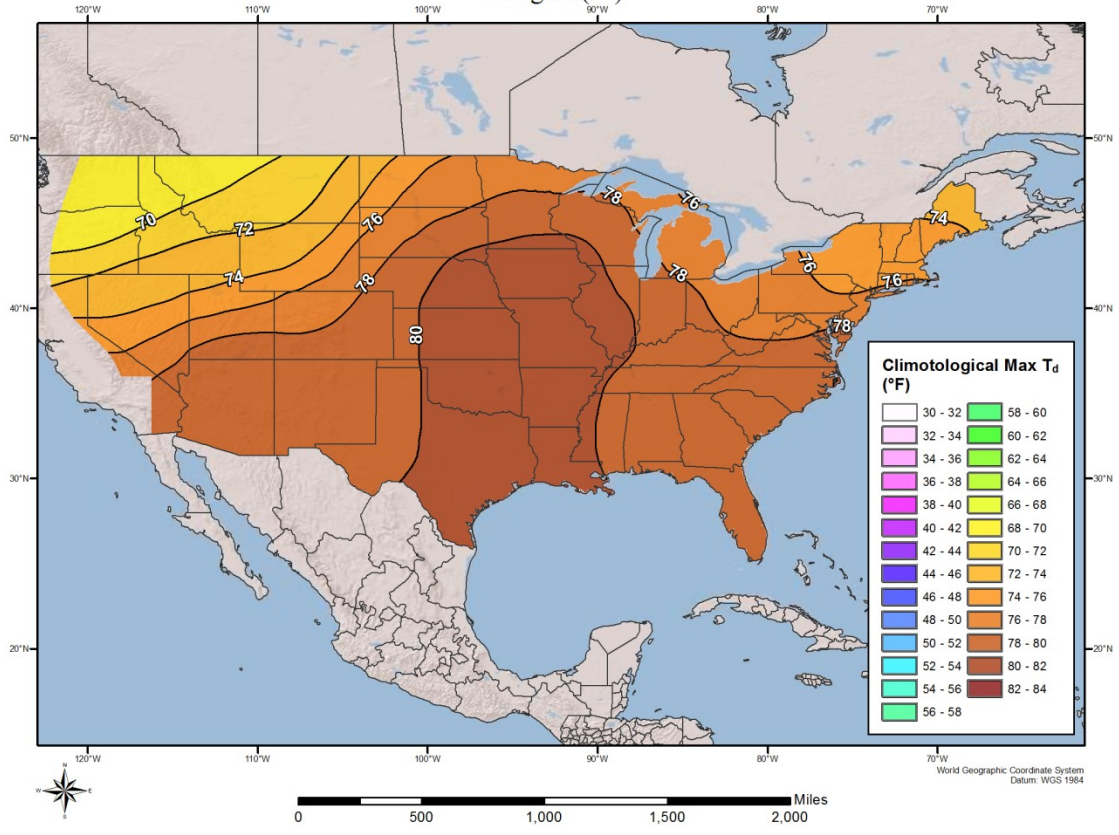
12-hour Monthly Dew Point Climatology June (°F)



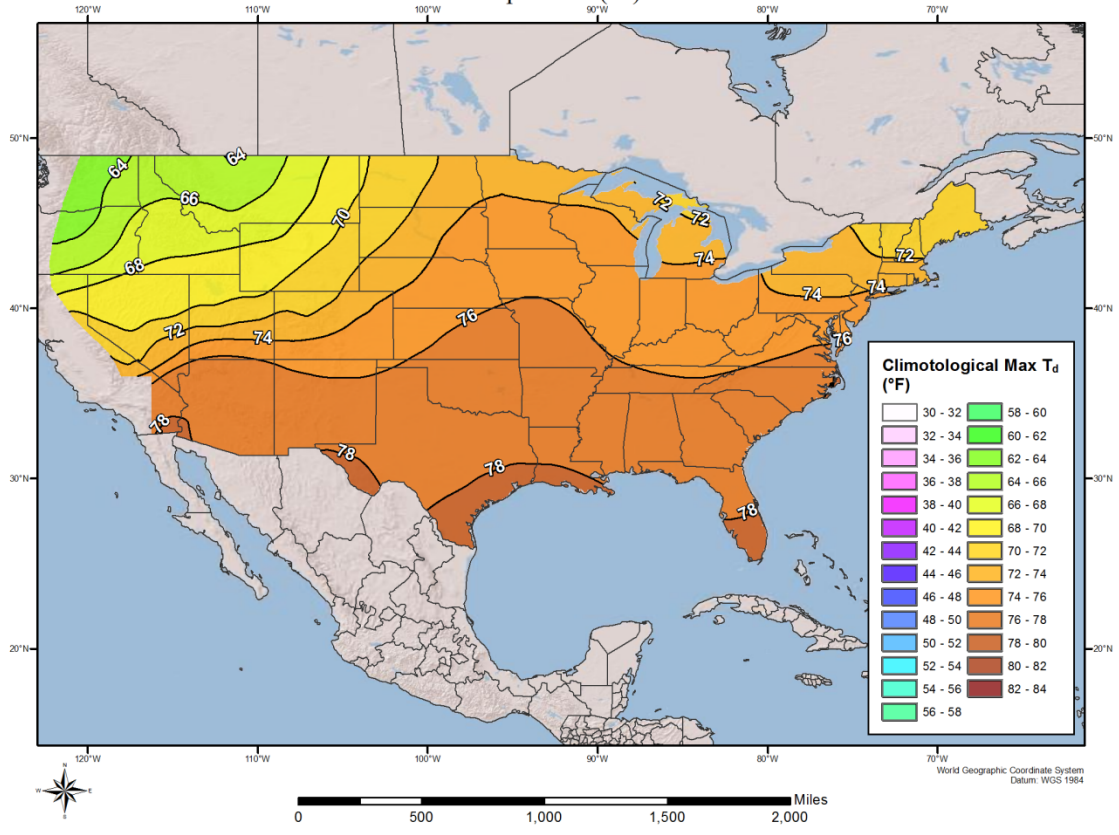
12-hour Monthly Dew Point Climatology July (°F)



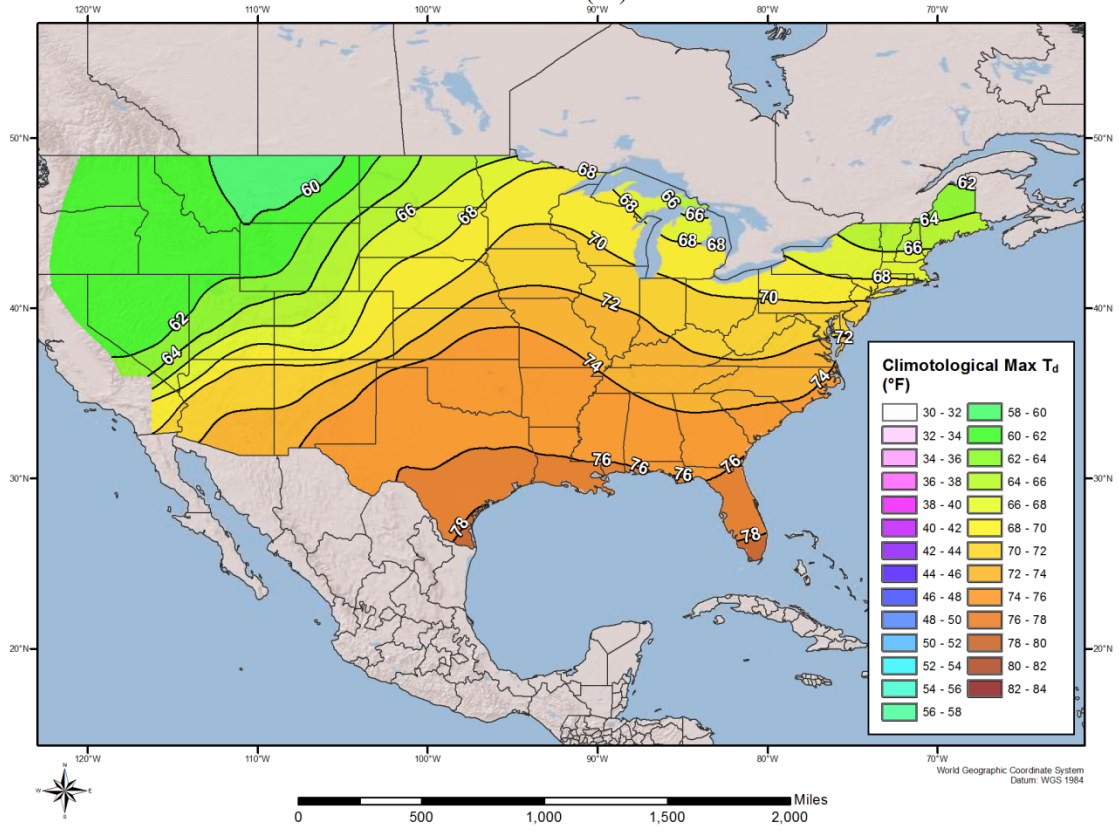
12-hour Monthly Dew Point Climatology August (°F)



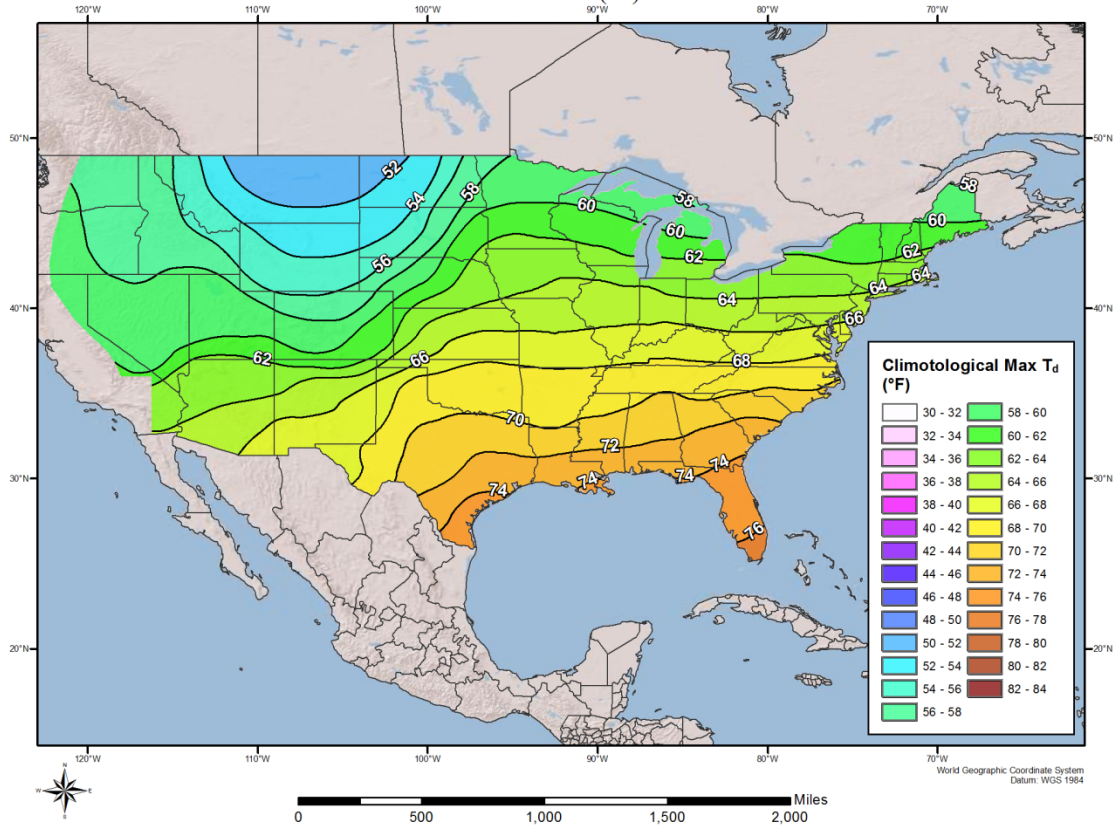
12-hour Monthly Dew Point Climatology September (°F)



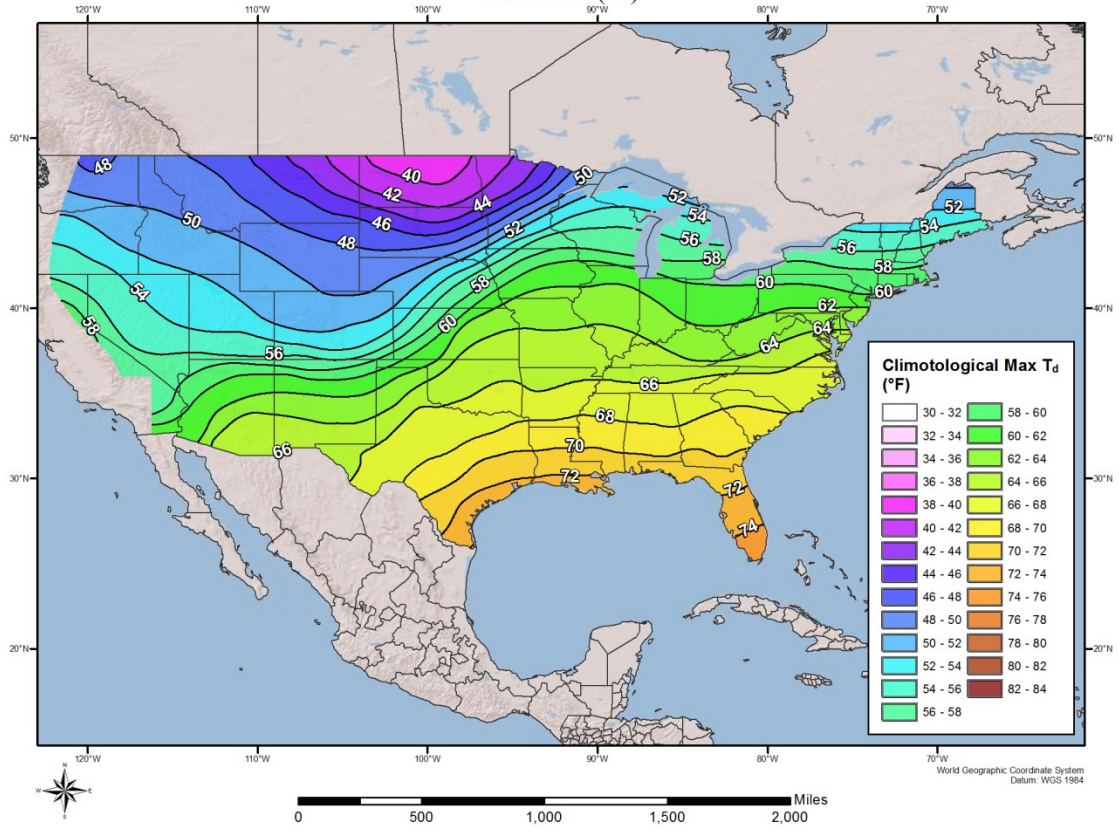
12-hour Monthly Dew Point Climatology October (°F)



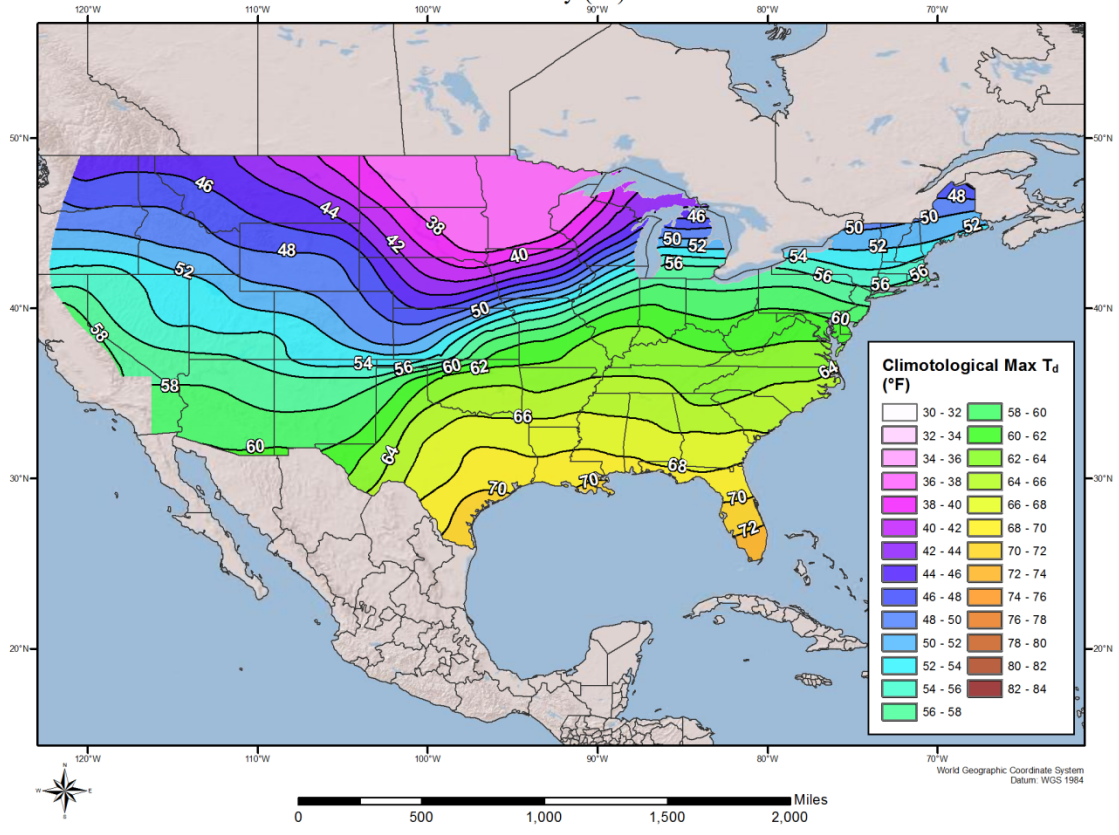
12-hour Monthly Dew Point Climatology November (°F)



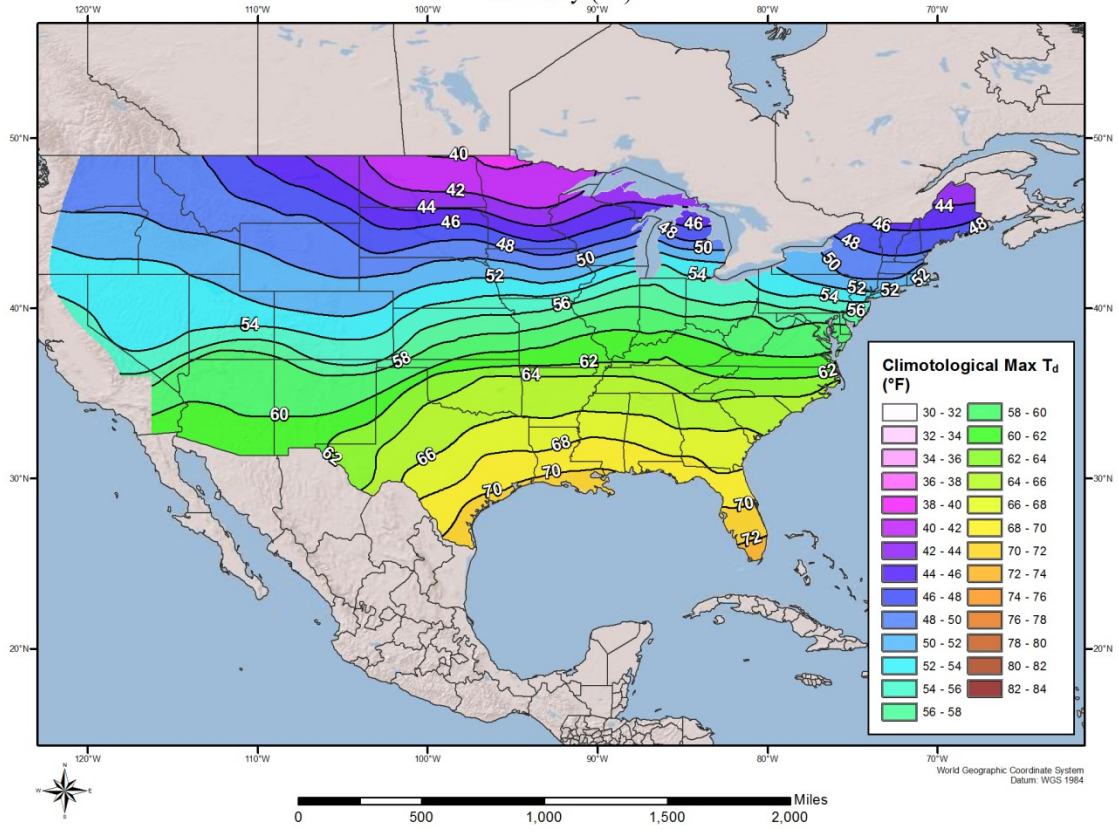
12-hour Monthly Dew Point Climatology December (°F)



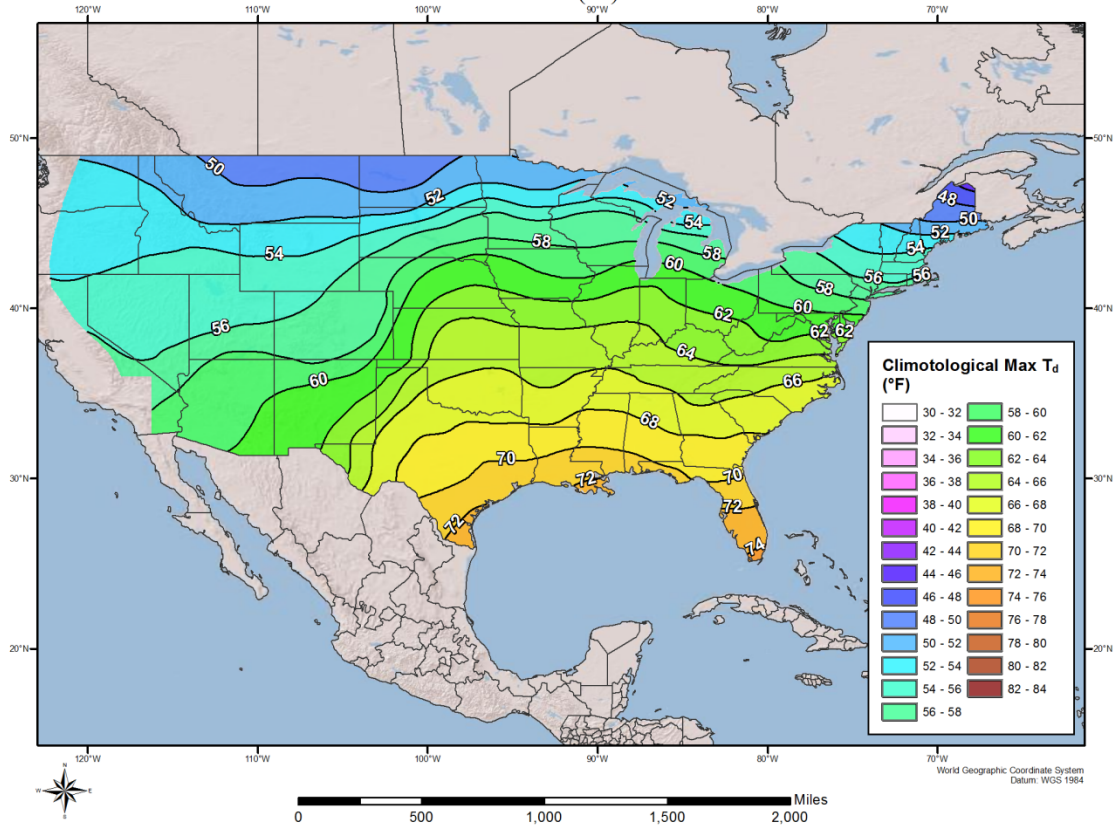
24-hour Monthly Dew Point Climatology January (°F)



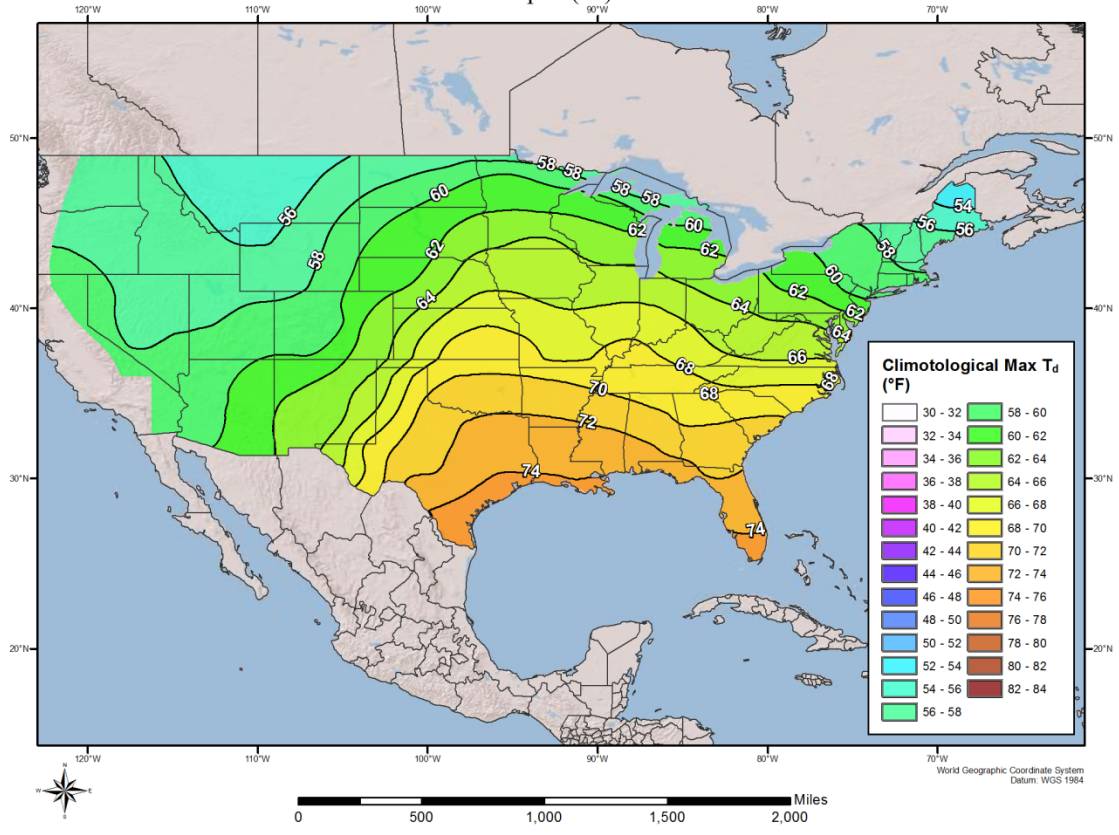
24-hour Monthly Dew Point Climatology February (°F)



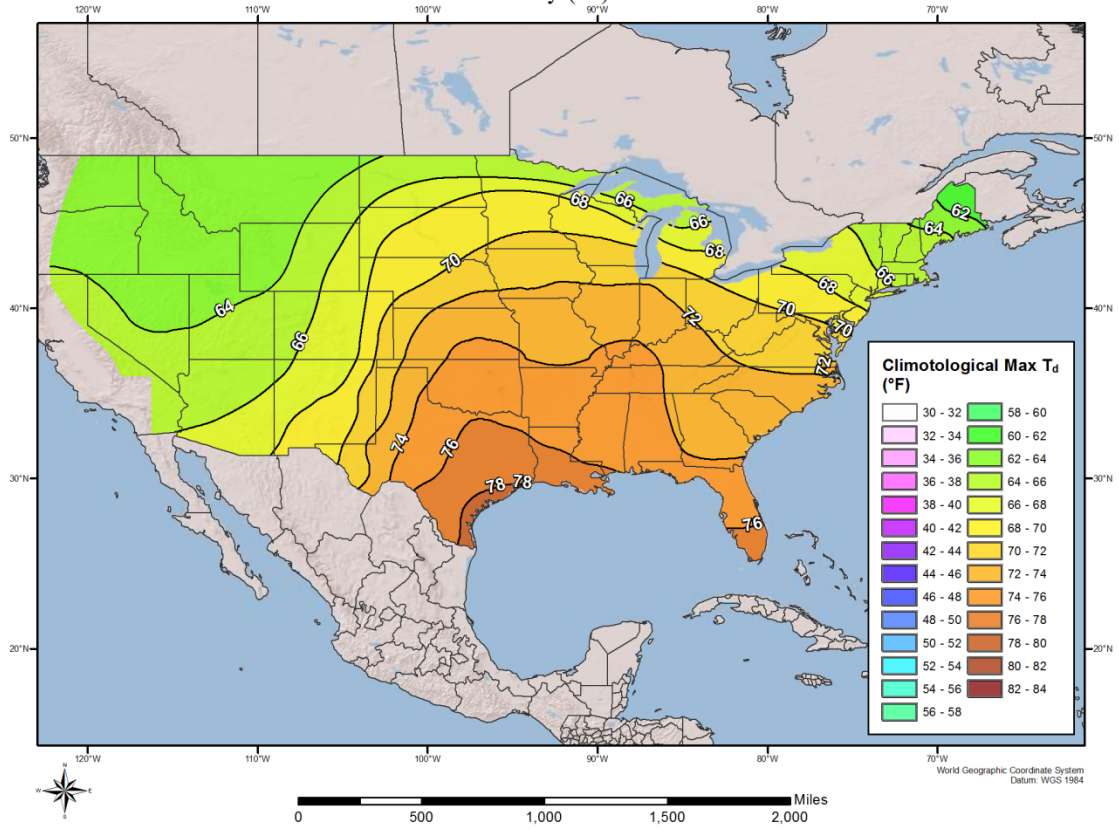
24-hour Monthly Dew Point Climatology March (°F)



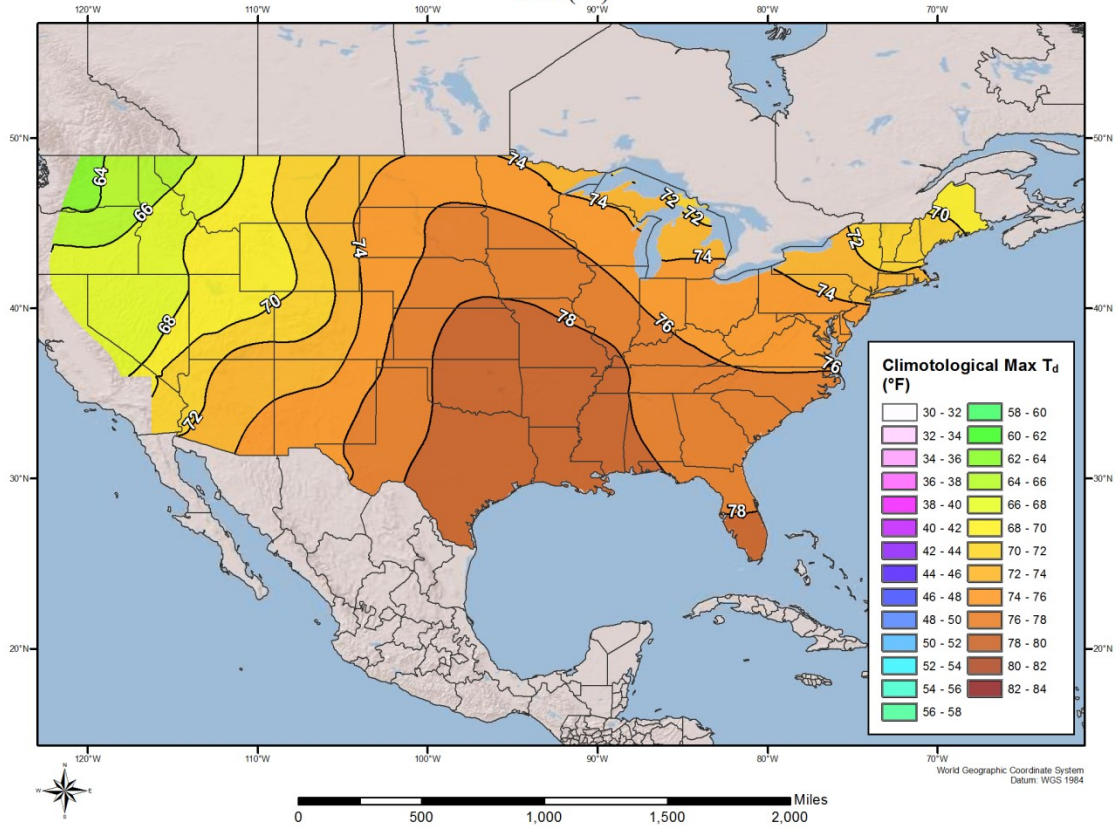
24-hour Monthly Dew Point Climatology April (°F)



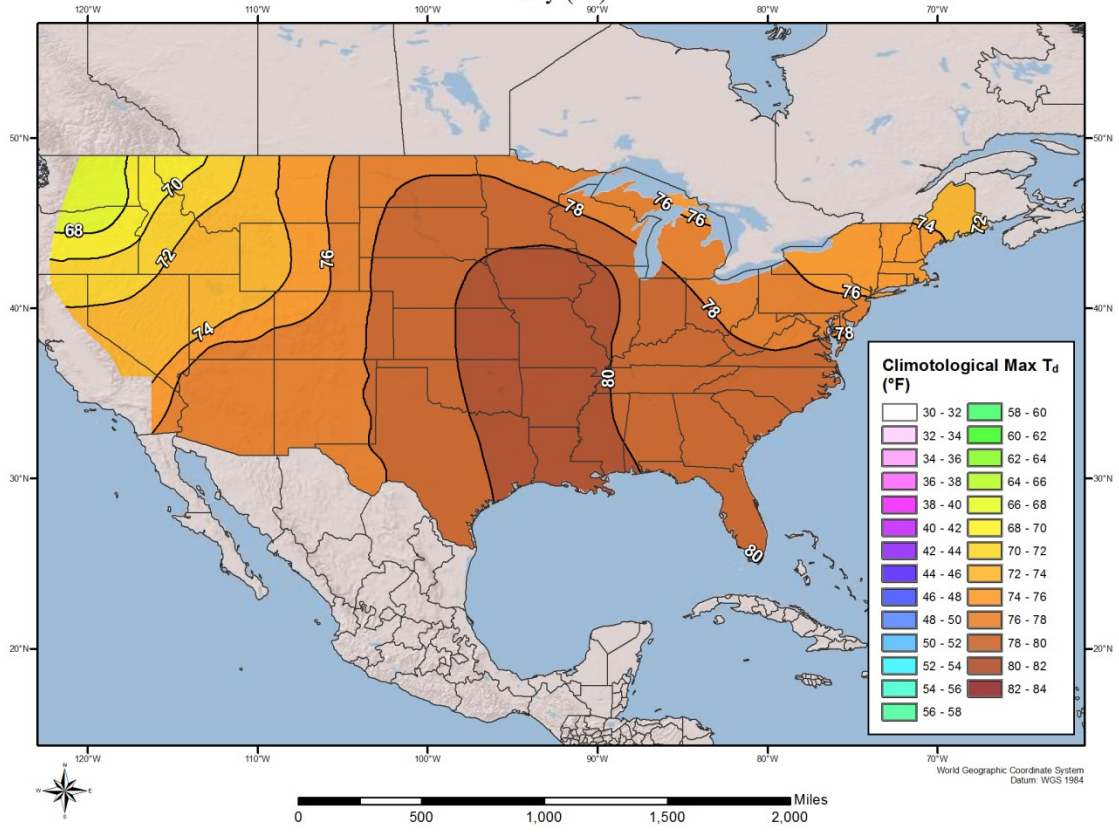
24-hour Monthly Dew Point Climatology May (°F)



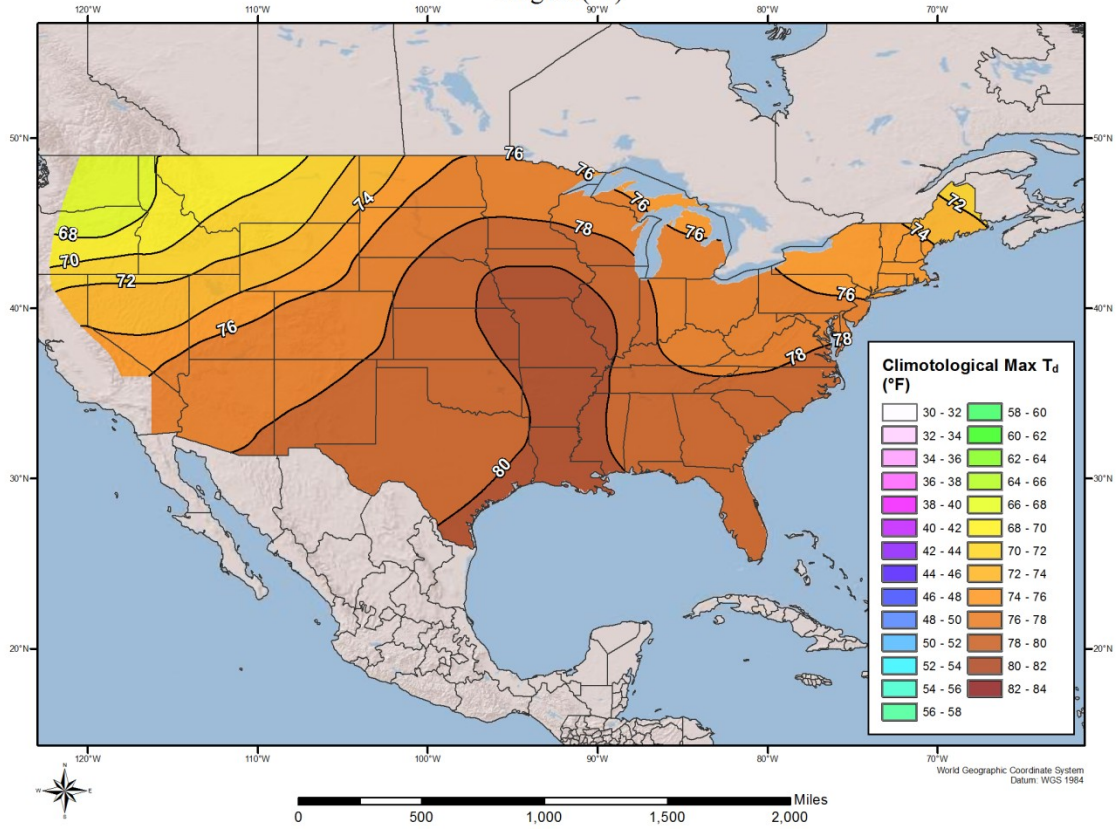
24-hour Monthly Dew Point Climatology June (°F)



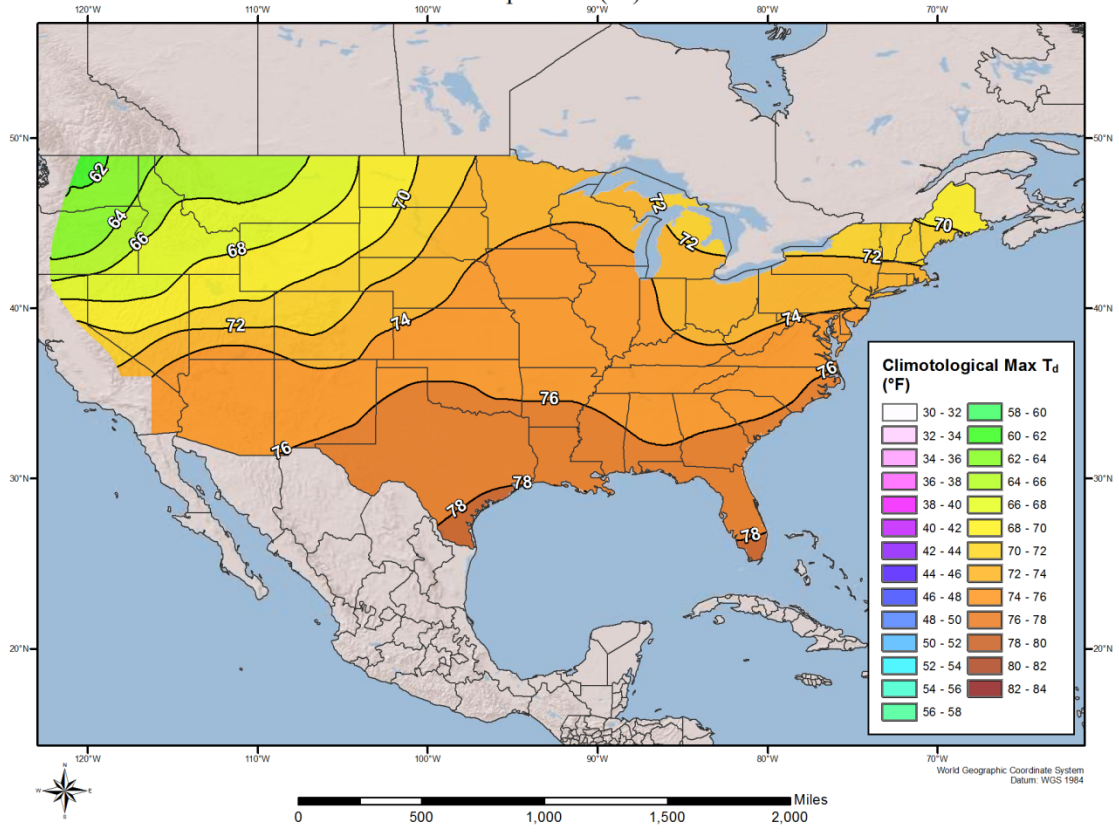
24-hour Monthly Dew Point Climatology July (°F)



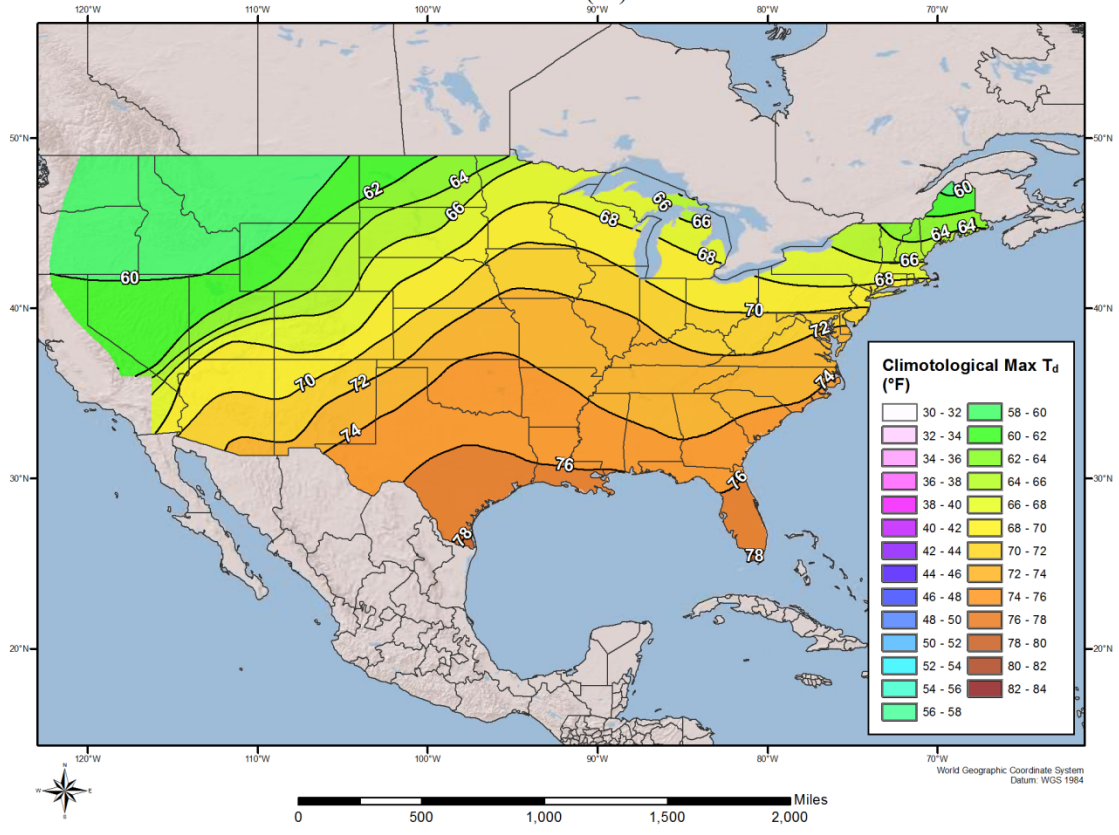
24-hour Monthly Dew Point Climatology August (°F)



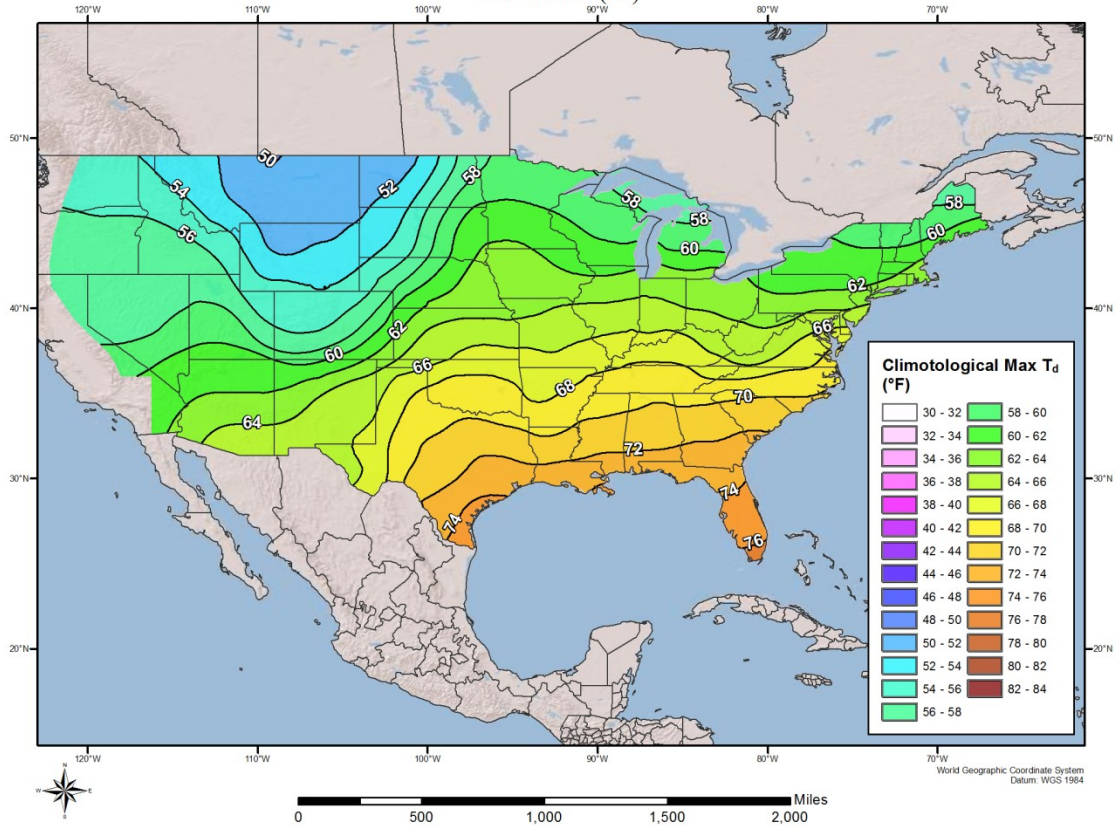
24-hour Monthly Dew Point Climatology September (°F)



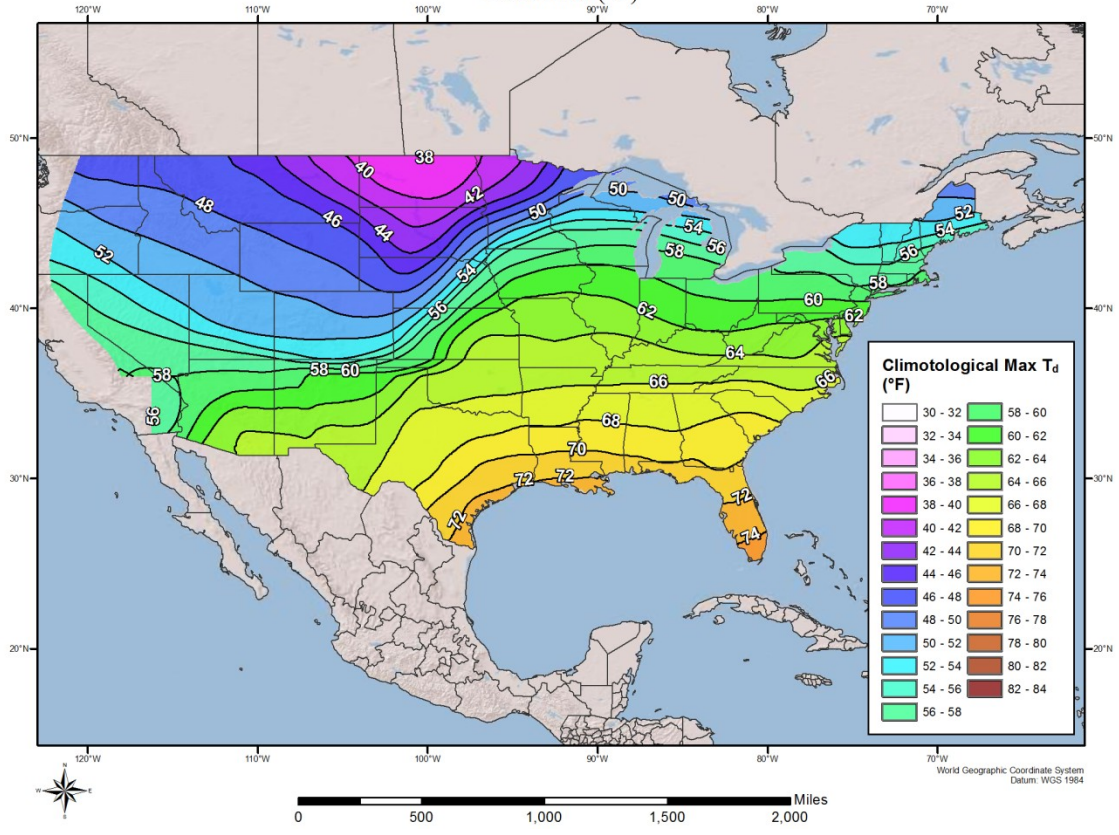
24-hour Monthly Dew Point Climatology October (°F)



24-hour Monthly Dew Point Climatology November (°F)



24-hour Monthly Dew Point Climatology December (°F)



Appendix B

Procedure for using Dew Point Temperatures for Storm Maximization and Transposition

Maximum dew point temperatures (hereafter referred to as dew points) have historically been used for two primary purposes in the PMP computation process:

1. Increase the observed rainfall amounts to a maximum value based on a potential increase in atmospheric moisture available to the storm.
2. Adjust the available atmospheric moisture to account for any increases or decreases associated with the maximized storm potentially occurring at another location within the transposition limits for that storm.

HMR and WMO procedures for storm maximization use a representative storm dew point as the parameter to represent available moisture to a storm. Prior to the mid-1980s, maps of maximum dew point values from the *Climatic Atlas of the United States*, Environmental Data Services, Department of Commerce (1968), were the source for maximum dew point values. HMR 55 published in 1984 updated maximum dew point values for a portion of the United States from the Continental Divide eastward into the central plains. A regional PMP study for Michigan and Wisconsin produced return frequency maps using the L-moments method (Tomlinson 1993). The Review Committee for that study included representatives from NWS, FERC, Bureau of Reclamation, and others. They agreed that the 50-year return frequency values were appropriate for use in PMP calculations. HMR 57 was published in 1994 and HMR 59 in 1999. These latest NWS publications also update the maximum dew point climatology but use maximum observed dew points instead of return frequency values. For this study, the 100-year return frequency dew point climatology maps were appropriate because this added a layer of conservatism and the extra 17 years of data available since the FERC Michigan/Wisconsin regional PMP study and Nebraska studies allow the 100-year return frequency to be more reliable. Storm precipitation amounts are maximized using the ratio of precipitable water for the maximum observed dew point to precipitable water for the storm representative dew point, assuming a vertically saturated atmosphere. This procedure was followed in this study using the updated maximum dew point climatology developed as part of this study.

The procedure for determining a storm representative dew point begins with the determination of the inflow wind vector (direction and magnitude) for the air mass that contains the atmospheric moisture available to the storm. Beginning and ending times of the rainfall event at locations of the most extreme rainfall amounts are determined using rainfall mass curves from those locations.

The storm inflow wind vector is determined using available wind data. The inflow wind vector has historically been determined using winds reported by weather stations, together with upper air winds, when available. Recently, re-analyzed weather and weather model data representing various atmospheric parameters including wind direction and speed in the atmosphere have become available for use from the HYSPLIT trajectory model and the North American Reanalysis Project (Kalnay et al. 1996). These analyses are available back to 1948. Use of these wind fields in the lower portion of the

atmosphere provides much improved reliability in the determination of the storm inflow wind vectors. The program is available through an online interface through the Air Resources Laboratory section of NOAA. Users are able to enter in specific parameters that then produce a trajectory from a starting point going backwards (or forwards) for a specified amount of time. Users can define variables such as the starting point (using latitude and longitude or a map interface), the date and time to start the trajectory, the length of time to run the trajectory, and the pressure level at which to delineate the inflow vector. Figure B.1 shows example inflow vectors generated by HYSPLIT at three levels: 700mb, 850mb, and surface for an example storm event. The data generated from the HYSPLIT runs is then used in conjunction with standard methods to help delineate the source region of the air mass responsible for the storm precipitation. Also, this serves as another tool to determine from which weather stations to derive hourly dew point data for storm representative dew point analysis.

NOAA HYSPLIT MODEL
 Backward trajectories ending at 1200 UTC 28 Jun 07
 CDC1 Meteorological Data

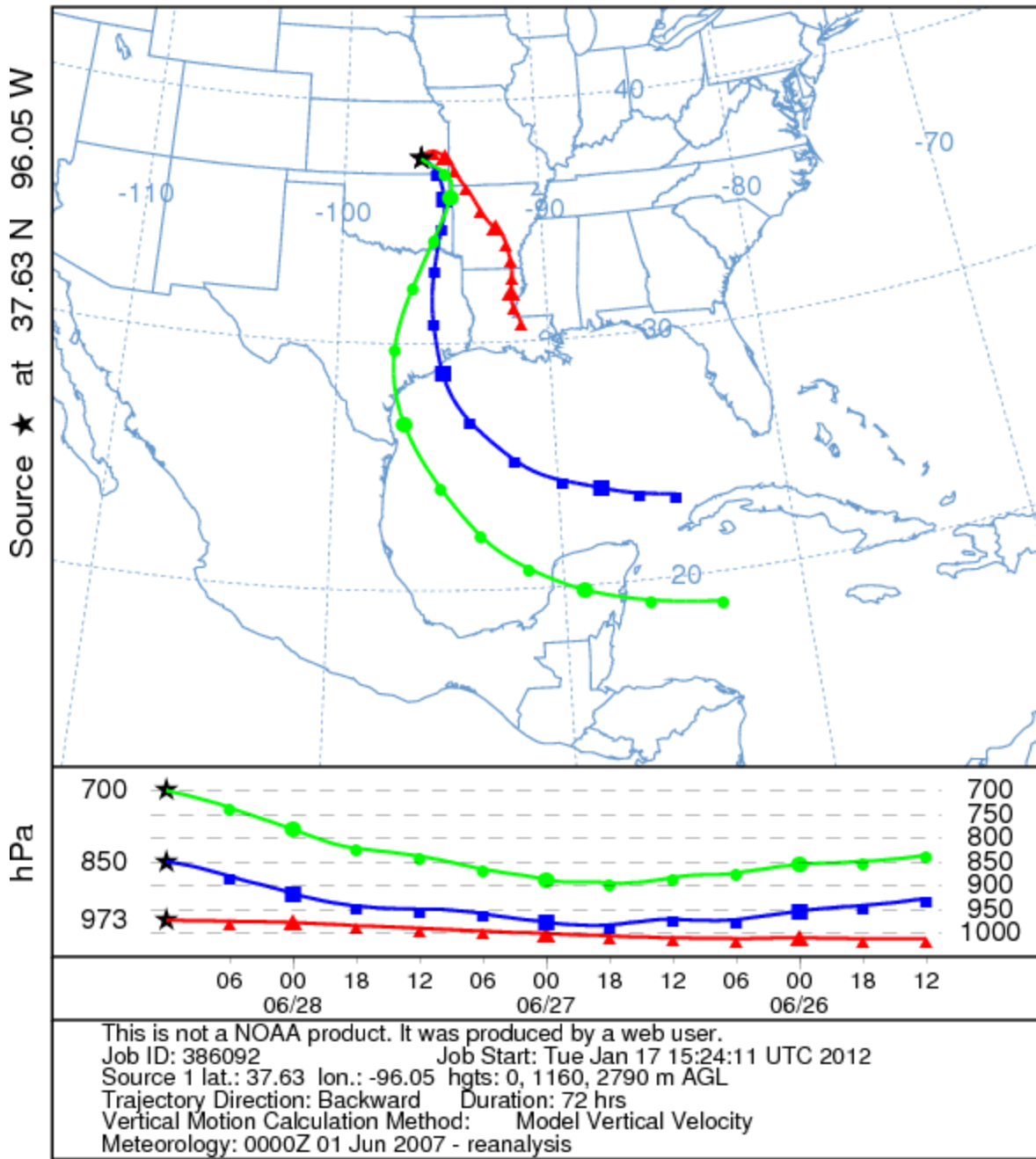


Figure B.1 HYSPLIT trajectory model results for Fall River, KS, June 2007, AWA Storm Number 120

The inflow wind vector is followed upwind until a location is reached that is outside of the storm rainfall. The nearest weather stations that report dew point values are identified. At least two stations are desired but a single station with reliable dew point observations can be used if no other representative or useful data is available. The time period used to identify the appropriate dew point values is determined by computing the time required for the air mass to be transported from the location of the weather station(s) to the location of maximum rainfall. The start time of the extreme rainfall is then adjusted back in time to account for transit time from the dew point observing station(s) to the maximum rainfall location.

For example, consider the following case:

1. Rainfall begins at 11:00am and ends at 6:00pm the following day at the location of maximum rainfall,
2. The storm representative dew point location (the location of the weather stations observing the dew points) is 100 miles from the maximum rainfall location in the direction of the inflow wind vector, and
3. The inflow wind speed is 20 mph.

The transit time for the air mass from the weather stations to the maximum rainfall location is five hours (100 miles divided by 20 mph). The time to begin using the dew point observations is five hours before the rainfall began (11:00am minus 5 hours = 6:00am) and the time to stop using the dew point observations is five hours before the rainfall ended (6:00pm minus 5 hours = 1:00pm the following day). Dew point observations taken between these times are used to determine the storm representative average 24-hour 1000mb dew point value. The storm representative dew point location can come from a single location if only one station is used or from a location between the reporting weather stations if more than one station is used. The vector connecting this location and the location of maximum rainfall becomes the moisture inflow vector for the storm event being analyzed and is used for storm transpositioning.

The storm representative dew point determined from the hourly dew point observations needs to be corrected to the 1,000mb level. The elevation of the storm representative dew point location is used in this correction. The correction factor of 2.7°F per 1,000 feet of elevation is used. This is the same correction factor used in the *Climatic Atlas of the United States* (Environmental Data Services, Department of Commerce, 1968). For example, a storm representative dew point of 72°F at a station location with an elevation of 800 feet above sea level is corrected with a factor of $800 \times 2.7 / 1,000 = 2.2^\circ\text{F}$. The dew point value corrected to 1,000mb (sea level) is $72^\circ\text{F} + 2.2^\circ\text{F} = 74^\circ\text{F}$ after rounding.

The procedure that computes the in-place maximized rainfall for a storm provides an estimate of the maximum amount of rainfall that could have been produced by the same storm at the same location if the maximum amount of atmospheric moisture had been available. This procedure requires that a maximum value for the storm representative dew point be determined. The maximum dew point value is selected at the

same location where the storm dew point was determined using a maximum dew point climatology. The maximum dew point values must be corrected to 1,000mb. The precipitable water in the atmosphere is determined using the storm representative and maximum dew point values. Precipitable water is defined in this study as the total amount of moisture in a column of the atmosphere from sea level to 30,000 feet assuming a vertically saturated atmosphere. Values of atmospheric precipitable water are determined using the moist pseudo-adiabatic assumption, i.e. assume that for the given 1,000mb dew point value, the atmosphere holds the maximum amount of moisture possible. The ratio of the precipitable water associated with the maximum 1,000mb dew point to the precipitable water associated with the 1,000mb storm representative dew point is the maximization factor.

For example, consider the following case:

1,000mb storm representative dew point:	72°F
1,000mb maximum dew point:	76°F
Precipitable water associated with a 1,000mb dew point of 72°F:	2.47"
Precipitable water associated with a 1,000mb dew point of 76°F:	2.99"
Maximization factor: $PW(76°F)/PW(72°F) = 2.99 / 2.47 = 1.21$	

For transpositioning, the storm inflow vector (determined by connecting the storm representative dew point location with the location of maximum rainfall) is moved to the grid point location being studied. The new location of the upwind end of the vector is determined. The maximum dew point associated with that location is then selected using the same maximum dew point climatology map used for in-place maximization. The transpositioning factor is the ratio of the precipitable water associated with the maximum 1,000mb dew point value at the transpositioned location to the precipitable water associated with the maximum 1,000mb dew point for the storm representative dew point location.

An example is provided.

1,000mb maximum dew point at the storm representative dew point location:	76°F
1,000mb maximum dew point at the transpositioned location:	74°F
Precipitable water associated with a 1,000mb dew point of 76°F:	2.99"
Precipitable water associated with a 1,000mb dew point of 74°F:	2.73"
Transposition factor: $PW(74°F)/PW(76°F) = 2.73 / 2.99 = 0.91$	

Appendix C

Procedure for Deriving PMP Values from Storm Depth-Area-Duration (DAD) Analyses

Although PMP rainfall amounts are theoretical values, there currently is no theoretical method for determining the values. The accepted procedure for determining PMP values begins with the identification of the largest identified historic observed rainfall amounts in the region and applies the following procedures:

1. Increase the rainfall amounts to some maximized value (in-place maximization),
2. Adjust the "maximized" rainfall amounts to the potential situation where the historic storm occurs over the location being studied (transposition),
3. Adjust the "maximized transpositioned" rainfall amounts for elevation changes, intervening topographic barriers, and/or orographic affects which could potentially affect the storm moisture and subsequently the rainfall amounts for the "maximized transpositioned" storm (barrier adjustment or orographic transposition factor).

The procedure begins with the Depth-Area-Duration (DAD) analysis from the largest of the identified storms that have occurred over regions that are climatologically and topographically similar to the area being studied. Identification of the largest rainfall events is accomplished by identifying the largest station rainfall amounts, correlating the dates among adjacent stations to identify the areal extent of the heavy rainfall and the storm period, and then applying a multi-step process to determine which storms should be used for final PMP calculations. The DAD for each storm is computed using the SPAS program which includes an isohyetal analysis for each hour during the storm and determining the largest rainfall totals for each duration of interest over each area size of interest. HMR 51 uses temporal periods of 6-, 12-, 24-, 48- and 72- hours. Standard area sizes of 10-, 200-, 1,000-, 5,000-, 10,000- and 20,000-square miles are used. Other durations and area sizes can also be used in the DAD analysis as desired.

The US Army Corps of Engineers, the Bureau of Reclamation and the National Weather Service have performed storm studies and produced DADs for many storms. This study reviewed additional weather station data to identify extreme rainfall storms that had not been identified and studied previously. The new storms identified primarily occurred since the publication of HMR 51, but additional storms that occurred prior to HMR 51 publication were also identified. DADs that had been previously developed are used in this report. Newly identified storms are analyzed in this study, and DADs are developed for these storms. These DADs quantify the rainfall associated with each storm event, providing the largest rainfall amounts for each of the durations and area sizes used in this study.

Identification of storms that can be transpositioned to any of the 23 grid points used in this analysis is largely based on subjective judgments. For a storm to be transpositionable, it should have occurred over a region that is climatologically and topographically similar to the basin being studied. Storms generally should not be transpositioned across significant topographic features or into different climate regions. The largest rainfall events identified in the storm search generally occurred over locations

closer to the Gulf of Mexico with moisture moving in from the south and north. These storms occurred in similar meteorological, climatological, and topographical settings. Therefore, it is assumed that the same moisture sources and dynamics that produced these events could have produced a similar storm over one or more of the grid points.

Maximization of the storm DADs involves deriving the in-place and transposition factors to adjust the observed rainfall to look like it would have occurred had the storm been located over the grid point its transpositioned to. This accounts for the three factors which could affect a particular storm as it's moved from its original location to Ohio; the storm could have been some amount bigger in-place had more moisture been available, the storm would have had more or less moisture available to it versus where it originally occurred based on it being moved toward or away from its moisture source, and the storm would have occurred at a lower or higher elevation than its original location. This follows the procedures and calculations described in Appendix B.

For this study, all computations associated with historic storms are computed at the 1,000mb level (approximately sea level). The elevation of the location where the largest rainfall was observed is used as the storm elevation. An adjustment is applied to the storm moisture to account for the elevation of the storm above sea level. For example, if the maximum rainfall occurred at an elevation of 500 feet, the total atmospheric moisture (500 to 30,000 feet) is decreased by the amount of moisture associated with the storm representative dew point between sea level and 500 feet. The adjustment factor uses precipitable water contained in the moisture maximized atmosphere above the storm elevation, i.e., the moisture contained in the entire depth of the moisture maximized atmosphere, minus the moisture contained in the moisture maximized atmosphere below the storm elevation. An adjustment was made to account for the storm's elevation (either higher or lower than the particular grid point elevation) and the amount of precipitable water that would be available, more if the elevation was lower and less if the elevation was higher. This elevation adjustment factor is determined by computing the ratio of precipitable water in the moisture maximized atmosphere above the elevation to the precipitable water in the entire depth of the moisture maximized atmosphere.

The equations for the computation of the in-place maximization factor, transposition and elevation adjustment factors are as follows:

In-place maximization factor =
(storm representative maximum dew point PW – in-place storm elevation maximum dew point PW) / (storm representative dew point PW – in-place storm elevation representative dew point PW)

Transpositioned/elevation to basin factor =
(transpositioned maximum dew point PW – average basin elevation maximum dew point PW)/(storm representative maximum dew point PW – in-place storm elevation representative dew point PW)

Multiplication of these terms leads to a simplified computation where all the required adjustments are combined in a single equation.

Total adjustment factor =
 (in-place max factor) * (transpositioned/elevation to basin factor) * (barrier/elevation adjustment factor)

The total adjustment factor modifies the storm DAD by a factor using two computed values:

- 1) The maximum atmospheric moisture available to a historic storm if it were to occur over the study basin. This air mass is assumed to contain the maximum amount of atmospheric moisture for the basin location and is adjusted for elevation upwind of the basin and within the basin.
- 2) The atmospheric moisture available for the historic storm at the location and elevation where it occurred.

The total adjustment factor is applied as a linear multiplier for all rainfall amounts in the storm DAD.

As an example, the DAD from the Warner Park, TN AWA Storm Number 126 storm center is maximized, transpositioned, and elevation/barrier adjusted. The following are values for the parameters used in computing the adjustments:

Storm representative Td:	75.0° F
In-place maximum Td:	76.5° F
Transpositioned maximum Td:	74.0° F
Storm elevation:	600'
Grid point elevation:	1,150'
Total atmospheric precipitable water for 75.0° F:	2.85"
Total atmospheric precipitable water for 76.5° F:	3.07"
Total atmospheric precipitable water for 74.0° F:	2.73"
Adjustment for storm elevation, 1,000mb to 600' at 75.0°F:	0.15"
Adjustment for storm elevation, 1,000mb to 600' at 76.5°F:	0.16"
Adjustment for ave basin elevation, 1,000mb to 1,150' at 74.0°F:	0.28"
Adjustment for inflow barrier elevation, 1,000mb to 1150' at 74.0°F:	0.28"

Total adjustment factor =
 (in-place max factor) * (transpositioned to basin factor) * (elevation/barrier adjustment factor)

$$= ((3.07" - 0.16") / (2.85" - 0.15")) * ((2.73" - 0.28") / (3.07" - 0.16")) * ((2.73" - 0.28") / (2.73" - 0.28")) = (1.08) * (0.84) * (1.00) = 0.91$$

To explicitly show how each adjustment factor (in-place maximization, transposition and elevation/barrier adjustment) affects the total adjustment, separate computation are provided.

In-place maximization factor

Storm representative dew point:	75.0° F
In-place maximum dew point:	76.5° F
Storm atmospheric precipitable water for 75.0° F:	2.85"
Maximum atmospheric precipitable water for 76.5° F:	3.07"
Adjustment for storm elevation, 1,000mb to 600' at 75.0°F:	0.15"
Adjustment for storm elevation, 1,000mb to 600' at 76.5°F:	0.16"

In-place maximization factor =
 (storm representative maximum dew point PW – in place storm elevation maximum PW)/(storm representative dew point PW – in place storm elevation maximum dew point PW)

$$= (3.07" - 0.16) / (2.85" - 0.15")$$

$$= 2.91" / 2.70"$$

$$= 1.08$$

Transposition factor

In-place maximum dew point	76.5° F
Transpositioned maximum dew point	74.0° F
Maximum atmospheric precipitable water for 82.0° F:	3.07"
Maximum atmospheric precipitable water for 80.5° F:	2.73"
Adjustment for storm elevation, 1,000mb to 600' at 76.0°F:	0.16"
Adjustment for storm elevation, 1,000mb to 1,150' at 74.0°F:	0.28"

Transposition factor =
 (transpositioned maximum dew point PW – basin elevation maximum dew point PW)/(storm representative maximum dew point PW – in place storm elevation maximum dew point PW)

$$= (2.73" - 0.28") / (3.07" - 0.16")$$

$$= 2.45" / 2.91"$$

$$= 0.84$$

Moisture inflow barrier adjustment factor

For this study there were no intervening barriers that would deplete moisture before reaching any of the grid points where a storm was transpositioned. Therefore, in all cases this factor was equal to 1.00.

Total adjustment factor = (In-Place maximization) X (Transposition) X (Barrier Adjustment/Storm elevation)

$$\begin{aligned} &= 1.08 * 0.84 * 1.00 \\ &= 0.91 \end{aligned}$$

This is the same total adjustment computed earlier (within round-off error) using the single equation to compute the total adjustment factor.

Since these procedures involve linear multiplication, Excel spreadsheets can be used to incorporate the storm DAD and apply the factors to compute the total adjusted DAD. Each storm spreadsheet and all the data used for the calculations are presented for each short list storm in Appendix F.

Once the total adjustment factors are applied to all of the storms being considered, rainfall amounts from largest storms are plotted on a log-linear plot with rainfall depth plotted on the linear scale and area size plotted on the log scale. A separate graph is constructed for each duration period, e.g., 6-hour, 12-hour, etc. The graphs provide curves of the transpositioned maximized adjusted storm rainfall amounts for all area sizes. These DA curves represent the maximum rainfall potential based on standard procedure modifications of the largest observed historic storms in the region surrounding the basins. An enveloping curve is drawn using the largest rainfall values. All of the plotted rainfall amounts either lie on the enveloping curve or below it. The exception is in the case where there is reason to suspect that a value is larger than is reasonable and that rainfall value may be undercut, i.e. the envelop curve should be drawn beneath the value. Undercutting should rarely be done and each case needs to be justified. No undercutting was done in this study. In general, the enveloping curve should provide a smooth transition among the maximum rainfall values for various area sizes. This process of enveloping DA plots provides continuity in space for the rainfall amounts among various area sizes.

After enveloping curves are completed for each of the duration periods, DD curves are plotted on a linear-linear graph, with duration on one axis and depth on the other. Since there is only a single curve for each area size from the enveloped DA plots, all of DA curves can be plotted as a family of curves on a single graph. Enveloping of curves is completed for each area size. The enveloping curve should provide a smooth transition among the maximum rainfall values for various durations. This procedure of enveloping DD plots provides continuity in time for the rainfall amounts among various durations.

The final envelopment curves provide the maximum rainfall amounts that represent PMP values for each particular grid point. Rainfall amounts for each area size and each duration are taken from the curves and used to construct the PMP DAD table.

Appendix D
Depth-Area-Duration Comparison Tables
Ohio Statewide PMP vs. HMR 51 PMP

Grid Point 1 PMP vs HMR 51 PMP						
HMR 51 PMP Values at Grid Point 1 in Inches	Area Size	6-Hour	12-Hour	24-Hour	48-Hour	72-Hour
	10sqmi	28.1	33.1	35.2	38.8	40.4
	200sqmi	20.0	24.1	26.2	29.8	31.5
	1000sqmi	14.7	18.3	20.5	23.6	25.4
	5000sqmi	9.0	12.3	14.3	17.5	19.0
	10000sqmi	6.9	9.9	12.0	15.2	16.6
	20000sqmi	4.9	7.8	9.8	12.9	14.2
Grid Point 1 PMP Values in Inches	Area Size	6-Hour	12-Hour	24-Hour	48-Hour	72-Hour
	10sqmi	19.3	22.8	24.5	27.4	29.5
	100sqmi	16.0	18.9	21.7	24.3	26.0
	200sqmi	14.8	17.5	20.4	23.0	24.8
	500sqmi	12.9	15.3	18.1	21.3	23.0
	1000sqmi	11.2	13.8	16.3	19.8	21.5
	2000sqmi	9.4	12.2	14.4	18.3	20.1
	5000sqmi	6.9	10.0	12.3	16.2	17.9
	10000sqmi	5.3	8.4	10.8	14.2	15.7
	20000sqmi	3.7	6.5	9.0	12.0	13.0
% Reduction from HMR 51	Area Size	6-Hour	12-Hour	24-Hour	48-Hour	72-Hour
	10sqmi	31%	31%	30%	29%	27%
	200sqmi	26%	27%	22%	23%	21%
	1000sqmi	24%	24%	20%	16%	15%
	5000sqmi	23%	19%	14%	7%	6%
	10000sqmi	23%	15%	10%	7%	5%
	20000sqmi	24%	17%	9%	7%	8%

Grid Point 2 PMP vs HMR 51 PMP						
HMR 51 PMP Values at Grid Point 2 in Inches	Area Size	6-Hour	12-Hour	24-Hour	48-Hour	72-Hour
	10sqmi	28.1	33.0	35.4	39.0	40.4
	200sqmi	19.9	23.9	26.2	29.9	31.5
	1000sqmi	14.6	18.2	20.6	23.5	25.3
	5000sqmi	8.8	12.1	14.3	17.6	19.0
	10000sqmi	6.8	9.8	12.0	15.3	16.6
	20000sqmi	4.8	7.8	9.9	12.9	14.2
Grid Point 2 PMP Values in Inches	Area Size	6-Hour	12-Hour	24-Hour	48-Hour	72-Hour
	10sqmi	18.7	22.2	24.0	26.5	27.5
	100sqmi	15.8	18.6	21.0	23.8	24.5
	200sqmi	14.6	17.1	20.0	22.8	23.5
	500sqmi	12.8	15.1	17.7	21.0	22.0
	1000sqmi	11.0	13.6	16.0	19.5	20.5
	2000sqmi	9.2	11.9	14.1	17.9	18.9
	5000sqmi	6.7	9.8	12.2	15.8	16.7
	10000sqmi	5.0	8.4	10.7	13.9	14.5
	20000sqmi	3.6	6.5	8.9	11.8	12.1
% Reduction from HMR 51	Area Size	6-Hour	12-Hour	24-Hour	48-Hour	72-Hour
	10sqmi	33%	33%	32%	32%	32%
	200sqmi	27%	28%	24%	24%	25%
	1000sqmi	25%	25%	22%	17%	19%
	5000sqmi	24%	19%	15%	10%	12%
	10000sqmi	26%	14%	11%	9%	12%
	20000sqmi	24%	16%	10%	8%	15%

Grid Point 3 PMP vs HMR 51 PMP						
HMR 51 PMP Values at Grid Point 3 in Inches	Area Size	6-Hour	12-Hour	24-Hour	48-Hour	72-Hour
	10sqmi	28.1	33.0	35.6	39.1	40.6
	200sqmi	19.9	23.8	26.3	30.0	31.6
	1000sqmi	14.5	18.2	20.9	23.5	25.3
	5000sqmi	8.8	12.1	14.3	17.7	19.1
	10000sqmi	6.8	9.7	12.0	15.3	16.6
	20000sqmi	4.7	7.8	9.9	12.9	14.2
Grid Point 3 PMP Values in Inches	Area Size	6-Hour	12-Hour	24-Hour	48-Hour	72-Hour
	10sqmi	18.2	22.1	23.7	26.0	26.5
	100sqmi	15.6	18.5	20.6	23.5	24.0
	200sqmi	14.3	16.9	19.5	22.4	22.9
	500sqmi	12.5	15.0	17.6	20.4	20.8
	1000sqmi	10.8	13.5	15.7	19.0	19.3
	2000sqmi	9.2	11.9	14.1	17.5	18.0
	5000sqmi	6.7	9.8	12.2	15.4	16.0
	10000sqmi	5.0	8.2	10.6	13.6	14.0
	20000sqmi	3.6	6.5	8.9	11.6	12.0
% Reduction from HMR 51	Area Size	6-Hour	12-Hour	24-Hour	48-Hour	72-Hour
	10sqmi	35%	33%	33%	33%	35%
	200sqmi	28%	29%	26%	25%	28%
	1000sqmi	26%	26%	25%	19%	24%
	5000sqmi	24%	19%	15%	13%	16%
	10000sqmi	26%	15%	12%	11%	16%
	20000sqmi	23%	16%	10%	10%	15%

Grid Point 4 PMP vs HMR 51 PMP						
HMR 51 PMP Values at Grid Point 4 in Inches	Area Size	6-Hour	12-Hour	24-Hour	48-Hour	72-Hour
	10sqmi	28.1	33.0	35.8	39.3	41.0
	200sqmi	19.8	23.7	26.5	30.2	31.8
	1000sqmi	14.5	18.2	21.1	23.7	25.4
	5000sqmi	8.8	12.0	14.4	17.8	19.2
	10000sqmi	6.7	9.7	12.1	15.3	16.7
	20000sqmi	4.7	7.8	10.0	13.0	14.2
Grid Point 4 PMP Values in Inches	Area Size	6-Hour	12-Hour	24-Hour	48-Hour	72-Hour
	10sqmi	17.8	21.5	23.7	25.5	26.0
	100sqmi	15.0	18.1	20.7	23.0	23.5
	200sqmi	13.8	16.1	19.5	21.7	22.2
	500sqmi	12.0	14.3	17.5	19.9	20.2
	1000sqmi	10.2	12.7	15.7	18.6	18.6
	2000sqmi	8.8	11.3	14.1	17.1	17.5
	5000sqmi	6.5	9.3	12.2	15.1	15.5
	10000sqmi	4.9	8.0	10.6	13.5	13.6
	20000sqmi	3.4	6.4	8.9	11.5	11.8
% Reduction from HMR 51	Area Size	6-Hour	12-Hour	24-Hour	48-Hour	72-Hour
	10sqmi	37%	35%	34%	35%	37%
	200sqmi	30%	32%	26%	28%	30%
	1000sqmi	30%	30%	26%	21%	27%
	5000sqmi	26%	22%	15%	15%	19%
	10000sqmi	27%	17%	12%	12%	18%
	20000sqmi	28%	18%	11%	11%	17%

Grid Point 5 PMP vs HMR 51 PMP						
HMR 51 PMP Values at Grid Point 5 in Inches	Area Size	6-Hour	12-Hour	24-Hour	48-Hour	72-Hour
	10sqmi	27.7	32.3	35.0	38.5	41.0
	200sqmi	19.4	23.2	25.9	29.5	31.8
	1000sqmi	14.1	17.6	20.4	22.9	25.4
	5000sqmi	8.5	11.7	14.0	17.3	19.2
	10000sqmi	6.6	9.5	11.8	14.9	16.7
	20000sqmi	4.6	7.6	9.8	12.7	14.2
Grid Point 5 PMP Values in Inches	Area Size	6-Hour	12-Hour	24-Hour	48-Hour	72-Hour
	10sqmi	17.0	21.2	23.5	25.0	25.5
	100sqmi	14.6	17.8	20.6	22.5	23.0
	200sqmi	13.5	16.0	19.4	21.5	22.0
	500sqmi	11.5	14.0	17.3	19.7	20.1
	1000sqmi	9.8	12.6	15.6	18.4	18.6
	2000sqmi	8.3	11.1	13.9	17.0	17.4
	5000sqmi	6.2	9.2	11.8	15.0	15.3
	10000sqmi	4.7	7.8	10.3	13.1	13.4
	20000sqmi	3.4	6.3	8.4	11.4	11.7
% Reduction from HMR 51	Area Size	6-Hour	12-Hour	24-Hour	48-Hour	72-Hour
	10sqmi	39%	34%	33%	35%	38%
	200sqmi	30%	31%	25%	27%	31%
	1000sqmi	30%	29%	24%	20%	27%
	5000sqmi	27%	21%	16%	13%	20%
	10000sqmi	28%	18%	13%	12%	20%
	20000sqmi	26%	17%	14%	10%	18%

Grid Point 6 PMP vs HMR 51 PMP						
HMR 51 PMP Values at Grid Point 6 in Inches	Area Size	6-Hour	12-Hour	24-Hour	48-Hour	72-Hour
	10sqmi	27.2	31.6	33.4	37.1	38.6
	200sqmi	19.2	23.0	24.9	28.2	29.9
	1000sqmi	14.0	17.2	19.3	22.1	24.0
	5000sqmi	8.6	11.8	13.6	16.4	18.0
	10000sqmi	6.7	9.4	11.3	14.4	15.9
	20000sqmi	4.7	7.4	9.3	12.2	13.5
Grid Point 6 PMP Values in Inches	Area Size	6-Hour	12-Hour	24-Hour	48-Hour	72-Hour
	10sqmi	18.7	22.2	24.3	26.5	27.0
	100sqmi	15.8	18.6	21.3	23.5	24.0
	200sqmi	14.6	17.2	20.0	22.3	22.8
	500sqmi	12.6	15.2	17.9	20.3	20.8
	1000sqmi	11.0	13.4	16.0	19.0	19.5
	2000sqmi	9.1	11.8	14.1	17.7	18.0
	5000sqmi	6.8	9.7	11.8	15.4	16.0
	10000sqmi	5.1	8.4	10.2	14.0	14.2
	20000sqmi	3.6	6.5	8.5	11.7	12.1
% Reduction from HMR 51	Area Size	6-Hour	12-Hour	24-Hour	48-Hour	72-Hour
	10sqmi	31%	30%	27%	29%	30%
	200sqmi	24%	25%	20%	21%	24%
	1000sqmi	21%	22%	17%	14%	19%
	5000sqmi	21%	18%	13%	6%	11%
	10000sqmi	23%	11%	10%	3%	10%
	20000sqmi	24%	12%	8%	4%	10%

Grid Point 7 PMP vs HMR 51 PMP						
HMR 51 PMP Values at Grid Point 7 in Inches	Area Size	6-Hour	12-Hour	24-Hour	48-Hour	72-Hour
	10sqmi	27.1	31.4	33.5	37.0	38.5
	200sqmi	19.1	22.8	24.8	28.1	29.7
	1000sqmi	13.9	17.1	19.2	21.9	23.7
	5000sqmi	8.5	11.6	13.5	16.4	18.0
	10000sqmi	6.6	9.3	11.3	14.3	15.8
	20000sqmi	4.6	7.4	9.3	12.2	13.4
Grid Point 7 PMP Values in Inches	Area Size	6-Hour	12-Hour	24-Hour	48-Hour	72-Hour
	10sqmi	18.4	22.3	24.2	26.0	26.6
	100sqmi	15.8	18.5	21.2	23.1	23.5
	200sqmi	14.6	17.2	19.9	22.0	22.5
	500sqmi	12.6	15.1	17.6	20.2	20.7
	1000sqmi	11.0	13.4	15.9	18.8	19.1
	2000sqmi	9.1	11.7	14.0	17.5	17.8
	5000sqmi	6.9	9.6	11.7	15.3	15.8
	10000sqmi	5.1	8.4	10.1	13.6	14.1
	20000sqmi	3.6	6.5	8.5	11.6	12.0
% Reduction from HMR 51	Area Size	6-Hour	12-Hour	24-Hour	48-Hour	72-Hour
	10sqmi	32%	29%	28%	30%	31%
	200sqmi	24%	25%	20%	22%	24%
	1000sqmi	21%	22%	17%	14%	20%
	5000sqmi	18%	17%	14%	7%	12%
	10000sqmi	22%	10%	10%	5%	11%
	20000sqmi	22%	12%	8%	5%	10%

Grid Point 8 PMP vs HMR 51 PMP						
HMR 51 PMP Values at Grid Point 8 in Inches	Area Size	6-Hour	12-Hour	24-Hour	48-Hour	72-Hour
	10sqmi	27.1	30.1	33.6	36.9	38.5
	200sqmi	19.1	22.1	24.9	28.1	29.7
	1000sqmi	13.8	16.3	19.3	21.9	23.6
	5000sqmi	8.4	11.2	13.5	16.3	18.0
	10000sqmi	6.5	9.0	11.3	14.3	15.7
	20000sqmi	4.5	7.0	9.3	12.2	13.3
Grid Point 8 PMP Values in Inches	Area Size	6-Hour	12-Hour	24-Hour	48-Hour	72-Hour
	10sqmi	18.0	22.4	24.0	25.7	26.5
	100sqmi	15.6	18.5	21.0	23.0	23.1
	200sqmi	14.4	17.1	19.8	21.8	22.1
	500sqmi	12.7	15.1	17.6	20.0	20.5
	1000sqmi	11.1	13.2	15.8	18.5	19.1
	2000sqmi	9.2	11.6	14.0	17.1	17.5
	5000sqmi	6.8	9.6	11.6	15.1	15.5
	10000sqmi	5.1	8.4	10.0	13.4	13.7
	20000sqmi	3.6	6.5	8.3	11.4	11.7
% Reduction from HMR 51	Area Size	6-Hour	12-Hour	24-Hour	48-Hour	72-Hour
	10sqmi	34%	26%	29%	30%	31%
	200sqmi	24%	22%	20%	22%	25%
	1000sqmi	19%	19%	18%	15%	19%
	5000sqmi	19%	14%	14%	8%	14%
	10000sqmi	21%	6%	11%	6%	13%
	20000sqmi	20%	7%	11%	6%	12%

Grid Point 9 PMP vs HMR 51 PMP						
HMR 51 PMP Values at Grid Point 9 in Inches	Area Size	6-Hour	12-Hour	24-Hour	48-Hour	72-Hour
	10sqmi	27.1	31.3	33.8	37.0	38.6
	200sqmi	19.0	22.6	25.0	28.2	29.7
	1000sqmi	13.7	17.0	19.4	21.9	23.5
	5000sqmi	8.3	11.4	13.5	16.4	18.0
	10000sqmi	6.4	9.3	11.3	14.3	15.7
	20000sqmi	4.5	7.4	9.4	12.2	13.3
Grid Point 9 PMP Values in Inches	Area Size	6-Hour	12-Hour	24-Hour	48-Hour	72-Hour
	10sqmi	17.2	21.3	23.3	25.3	25.7
	100sqmi	15.0	17.8	20.6	22.7	23.0
	200sqmi	13.9	16.2	19.4	21.5	21.8
	500sqmi	11.9	14.5	17.4	19.7	20.0
	1000sqmi	10.5	12.9	15.6	18.3	18.6
	2000sqmi	9.2	11.5	13.8	16.8	17.2
	5000sqmi	6.7	9.5	11.5	14.9	15.1
	10000sqmi	5.1	8.2	9.8	13.3	13.5
	20000sqmi	3.5	6.5	8.2	11.3	11.5
% Reduction from HMR 51	Area Size	6-Hour	12-Hour	24-Hour	48-Hour	72-Hour
	10sqmi	36%	32%	31%	32%	33%
	200sqmi	27%	28%	22%	24%	27%
	1000sqmi	23%	24%	19%	17%	21%
	5000sqmi	19%	17%	15%	9%	16%
	10000sqmi	21%	11%	13%	7%	14%
	20000sqmi	21%	12%	12%	7%	13%

Grid Point 10 PMP vs HMR 51 PMP						
HMR 51 PMP Values at Grid Point 10 in Inches	Area Size	6-Hour	12-Hour	24-Hour	48-Hour	72-Hour
	10sqmi	27.2	31.5	34.3	37.5	39.2
	200sqmi	19.0	22.6	25.4	28.7	30.1
	1000sqmi	13.7	17.1	19.8	22.4	23.8
	5000sqmi	8.3	11.5	13.7	16.8	18.3
	10000sqmi	6.4	9.3	11.5	14.5	15.8
	20000sqmi	4.5	7.5	9.5	12.4	13.4
Grid Point 10 PMP Values in Inches	Area Size	6-Hour	12-Hour	24-Hour	48-Hour	72-Hour
	10sqmi	16.5	21.0	23.0	24.8	25.2
	100sqmi	14.3	17.4	20.1	22.0	22.4
	200sqmi	13.2	15.9	19.0	21.0	21.4
	500sqmi	11.2	13.8	17.1	19.2	19.5
	1000sqmi	9.6	12.4	15.3	17.8	18.1
	2000sqmi	8.2	11.0	13.5	16.4	16.7
	5000sqmi	6.1	9.2	11.2	14.4	14.7
	10000sqmi	4.6	7.8	9.6	12.8	13.1
	20000sqmi	3.3	6.3	8.0	10.9	11.2
% Reduction from HMR 51	Area Size	6-Hour	12-Hour	24-Hour	48-Hour	72-Hour
	10sqmi	39%	33%	33%	34%	36%
	200sqmi	30%	30%	25%	27%	29%
	1000sqmi	30%	27%	23%	20%	24%
	5000sqmi	27%	20%	18%	14%	20%
	10000sqmi	28%	16%	16%	12%	17%
	20000sqmi	26%	15%	16%	12%	17%

Grid Point 11 PMP vs HMR 51 PMP						
HMR 51 PMP Values at Grid Point 11 in Inches	Area Size	6-Hour	12-Hour	24-Hour	48-Hour	72-Hour
	10sqmi	26.8	30.8	33.5	36.6	38.2
	200sqmi	18.4	22.0	24.7	27.9	29.2
	1000sqmi	13.3	16.6	19.2	21.8	23.2
	5000sqmi	8.1	11.2	13.4	16.3	17.7
	10000sqmi	6.3	9.2	11.2	14.0	15.4
	20000sqmi	4.4	7.3	9.2	12.0	13.0
Grid Point 11 PMP Values in Inches	Area Size	6-Hour	12-Hour	24-Hour	48-Hour	72-Hour
	10sqmi	16.2	20.8	22.8	24.5	25.0
	100sqmi	14.1	17.0	20.0	21.7	22.3
	200sqmi	13.0	15.8	18.8	20.6	21.1
	500sqmi	11.1	13.8	17.0	18.8	19.5
	1000sqmi	9.6	12.4	15.4	17.5	18.0
	2000sqmi	8.3	11.0	13.4	16.2	16.7
	5000sqmi	6.1	9.3	11.1	14.3	14.7
	10000sqmi	4.7	8.0	9.6	12.7	12.9
	20000sqmi	3.3	6.4	7.8	10.7	11.0
% Reduction from HMR 51	Area Size	6-Hour	12-Hour	24-Hour	48-Hour	72-Hour
	10sqmi	39%	32%	32%	33%	35%
	200sqmi	30%	28%	24%	26%	28%
	1000sqmi	28%	25%	20%	20%	22%
	5000sqmi	25%	17%	17%	12%	17%
	10000sqmi	25%	13%	14%	10%	16%
	20000sqmi	24%	12%	16%	11%	16%

Grid Point 12 PMP vs HMR 51 PMP						
HMR 51 PMP Values at Grid Point 12in Inches	Area Size	6-Hour	12-Hour	24-Hour	48-Hour	72-Hour
	10sqmi	26.2	30.1	31.9	35.2	37.1
	200sqmi	18.6	22.1	23.8	26.7	28.4
	1000sqmi	13.5	16.3	18.3	21.0	22.9
	5000sqmi	8.2	11.2	13.0	15.5	17.3
	10000sqmi	6.4	9.0	10.6	13.7	15.2
	20000sqmi	4.6	7.0	8.7	11.5	12.9
Grid Point 12 PMP Values in Inches	Area Size	6-Hour	12-Hour	24-Hour	48-Hour	72-Hour
	10sqmi	18.5	22.0	24.0	26.0	26.5
	100sqmi	15.6	18.3	21.0	23.0	23.4
	200sqmi	14.6	16.9	19.9	21.7	22.0
	500sqmi	12.6	14.9	17.8	20.0	20.5
	1000sqmi	11.0	13.2	15.9	18.9	19.3
	2000sqmi	9.1	11.6	14.1	17.6	17.9
	5000sqmi	6.9	9.7	11.7	15.4	15.7
	10000sqmi	5.2	8.4	10.1	13.8	14.1
	20000sqmi	3.6	6.5	8.3	11.4	12.0
% Reduction from HMR 51	Area Size	6-Hour	12-Hour	24-Hour	48-Hour	72-Hour
	10sqmi	29%	27%	25%	26%	29%
	200sqmi	22%	23%	16%	19%	23%
	1000sqmi	18%	19%	13%	10%	16%
	5000sqmi	16%	13%	10%	1%	9%
	10000sqmi	19%	6%	5%	-1%	7%
	20000sqmi	22%	7%	5%	0%	7%

Grid Point 13 PMP vs HMR 51 PMP						
HMR 51 PMP Values at Grid Point 13 in Inches	Area Size	6-Hour	12-Hour	24-Hour	48-Hour	72-Hour
	10sqmi	26.1	29.8	31.8	35.0	36.9
	200sqmi	18.4	21.9	23.5	26.4	28.1
	1000sqmi	13.3	16.1	18.1	20.7	22.5
	5000sqmi	8.1	11.1	12.9	15.4	17.1
	10000sqmi	6.3	8.9	10.5	13.5	15.1
	20000sqmi	4.5	6.9	8.7	11.4	12.8
Grid Point 13 PMP Values in Inches	Area Size	6-Hour	12-Hour	24-Hour	48-Hour	72-Hour
	10sqmi	18.4	21.8	24.0	25.6	26.0
	100sqmi	15.7	18.2	21.0	22.5	22.9
	200sqmi	14.6	16.9	19.9	21.3	21.7
	500sqmi	12.7	14.9	17.9	19.5	20.0
	1000sqmi	10.9	13.2	15.9	18.3	18.7
	2000sqmi	9.2	11.6	14.0	17.0	17.3
	5000sqmi	6.9	9.7	11.8	15.0	15.5
	10000sqmi	5.1	8.4	10.0	13.3	14.0
	20000sqmi	3.5	6.5	8.3	11.4	11.9
% Reduction from HMR 51	Area Size	6-Hour	12-Hour	24-Hour	48-Hour	72-Hour
	10sqmi	29%	27%	25%	27%	30%
	200sqmi	21%	23%	15%	19%	23%
	1000sqmi	18%	18%	12%	12%	17%
	5000sqmi	14%	12%	8%	3%	9%
	10000sqmi	19%	6%	5%	2%	7%
	20000sqmi	22%	6%	5%	0%	7%

Grid Point 14 PMP vs HMR 51 PMP						
HMR 51 PMP Values at Grid Point 14 in Inches	Area Size	6-Hour	12-Hour	24-Hour	48-Hour	72-Hour
	10sqmi	26.0	29.7	31.8	34.9	36.8
	200sqmi	18.2	21.7	23.4	26.3	28.0
	1000sqmi	13.2	16.0	18.0	20.6	22.4
	5000sqmi	8.0	11.0	12.8	15.3	17.0
	10000sqmi	6.2	8.9	10.5	13.5	15.1
	20000sqmi	4.4	7.0	8.7	11.4	12.6
Grid Point 14 PMP Values in Inches	Area Size	6-Hour	12-Hour	24-Hour	48-Hour	72-Hour
	10sqmi	17.6	21.5	23.5	25.0	25.5
	100sqmi	15.2	17.7	20.5	22.0	22.5
	200sqmi	14.2	16.5	19.4	20.9	21.3
	500sqmi	12.5	14.7	17.5	19.1	19.5
	1000sqmi	10.7	13.0	15.6	17.7	18.2
	2000sqmi	9.1	11.6	14.0	16.5	16.8
	5000sqmi	6.8	9.7	11.6	14.6	15.0
	10000sqmi	5.1	8.4	9.9	13.0	13.4
	20000sqmi	3.5	6.5	8.2	11.0	11.4
% Reduction from HMR 51	Area Size	6-Hour	12-Hour	24-Hour	48-Hour	72-Hour
	10sqmi	32%	28%	26%	28%	31%
	200sqmi	22%	24%	17%	20%	24%
	1000sqmi	19%	19%	14%	14%	19%
	5000sqmi	14%	11%	9%	5%	12%
	10000sqmi	18%	5%	5%	4%	11%
	20000sqmi	20%	6%	6%	3%	10%

Grid Point 15 PMP vs HMR 51 PMP						
HMR 51 PMP Values at Grid Point 15 in Inches	Area Size	6-Hour	12-Hour	24-Hour	48-Hour	72-Hour
	10sqmi	26.0	29.6	31.8	34.9	36.7
	200sqmi	18.1	21.5	23.3	26.2	27.8
	1000sqmi	13.1	15.9	18.0	20.5	22.3
	5000sqmi	7.8	10.9	12.8	15.3	17.0
	10000sqmi	6.2	8.9	10.5	13.5	15.0
	20000sqmi	4.3	7.0	8.7	11.3	12.5
Grid Point 15 PMP Values in Inches	Area Size	6-Hour	12-Hour	24-Hour	48-Hour	72-Hour
	10sqmi	17.2	21.4	23.0	24.5	25.0
	100sqmi	14.8	17.5	20.3	21.6	22.0
	200sqmi	13.9	16.2	19.0	20.6	21.0
	500sqmi	12.2	14.3	17.1	18.7	19.1
	1000sqmi	10.6	12.9	15.4	17.3	17.8
	2000sqmi	9.0	11.5	13.8	16.2	16.6
	5000sqmi	6.6	9.8	11.6	14.2	14.7
	10000sqmi	5.0	8.4	9.9	12.8	13.1
20000sqmi	3.5	6.5	8.2	10.8	11.2	
% Reduction from HMR 51	Area Size	6-Hour	12-Hour	24-Hour	48-Hour	72-Hour
	10sqmi	34%	28%	28%	30%	32%
	200sqmi	23%	25%	18%	21%	24%
	1000sqmi	19%	19%	14%	16%	20%
	5000sqmi	16%	10%	9%	7%	13%
	10000sqmi	19%	5%	6%	5%	13%
	20000sqmi	18%	7%	6%	5%	10%

Grid Point 16 PMP vs HMR 51 PMP						
HMR 51 PMP Values at Grid Point 16 in Inches	Area Size	6-Hour	12-Hour	24-Hour	48-Hour	72-Hour
	10sqmi	26.0	29.6	31.8	34.9	36.7
	200sqmi	17.9	21.3	23.3	26.2	27.7
	1000sqmi	13.0	15.9	18.0	20.5	22.2
	5000sqmi	7.8	10.8	12.8	15.3	16.9
	10000sqmi	6.1	8.9	10.6	13.4	14.9
	20000sqmi	4.2	7.0	8.8	11.3	12.5
Grid Point 16 PMP Values in Inches	Area Size	6-Hour	12-Hour	24-Hour	48-Hour	72-Hour
	10sqmi	16.7	21.1	22.5	24.0	24.5
	100sqmi	14.5	17.0	20.0	21.4	21.9
	200sqmi	13.5	15.8	18.8	20.2	20.7
	500sqmi	11.8	14.0	17.0	18.5	19.0
	1000sqmi	10.3	12.7	15.2	17.2	17.6
	2000sqmi	8.8	11.4	13.5	16.0	16.5
	5000sqmi	6.5	9.7	11.4	14.2	14.5
	10000sqmi	4.9	8.3	9.9	12.6	13.0
	20000sqmi	3.4	6.6	8.2	10.7	11.1
% Reduction from HMR 51	Area Size	6-Hour	12-Hour	24-Hour	48-Hour	72-Hour
	10sqmi	36%	29%	29%	31%	33%
	200sqmi	25%	26%	19%	23%	25%
	1000sqmi	21%	20%	16%	16%	21%
	5000sqmi	16%	10%	11%	7%	14%
	10000sqmi	20%	7%	6%	6%	13%
	20000sqmi	19%	6%	6%	6%	11%

Grid Point 17 PMP vs HMR 51 PMP						
HMR 51 PMP Values at Grid Point 17 in Inches	Area Size	6-Hour	12-Hour	24-Hour	48-Hour	72-Hour
	10sqmi	26.0	29.6	31.9	35.0	36.7
	200sqmi	17.8	21.2	23.4	26.3	27.6
	1000sqmi	12.9	15.9	18.1	20.5	22.2
	5000sqmi	7.8	10.8	12.9	15.4	16.9
	10000sqmi	6.1	8.9	10.7	13.3	14.9
	20000sqmi	4.2	7.0	8.8	11.4	12.5
Grid Point 17 PMP Values in Inches	Area Size	6-Hour	12-Hour	24-Hour	48-Hour	72-Hour
	10sqmi	16.0	20.0	22.0	23.5	24.0
	100sqmi	13.8	16.5	19.5	20.8	21.2
	200sqmi	12.8	15.4	18.3	19.6	20.0
	500sqmi	11.0	13.6	16.5	18.0	18.5
	1000sqmi	9.6	12.3	15.0	16.7	17.3
	2000sqmi	8.2	11.1	13.3	15.5	16.1
	5000sqmi	6.0	9.5	11.1	13.8	14.2
	10000sqmi	4.6	8.1	9.6	12.1	12.6
	20000sqmi	3.1	6.4	8.0	10.4	10.7
% Reduction from HMR 51	Area Size	6-Hour	12-Hour	24-Hour	48-Hour	72-Hour
	10sqmi	38%	32%	31%	33%	35%
	200sqmi	28%	27%	22%	25%	28%
	1000sqmi	26%	22%	17%	19%	22%
	5000sqmi	23%	12%	14%	10%	16%
	10000sqmi	24%	9%	10%	9%	15%
	20000sqmi	26%	9%	9%	9%	14%

Grid Point 18 PMP vs HMR 51 PMP						
HMR 51 PMP Values at Grid Point 18 in Inches	Area Size	6-Hour	12-Hour	24-Hour	48-Hour	72-Hour
	10sqmi	25.2	28.6	30.5	33.4	35.4
	200sqmi	18.0	21.3	22.7	25.5	27.5
	1000sqmi	13.0	15.5	17.3	20.1	22.0
	5000sqmi	8.0	10.7	12.3	14.8	16.7
	10000sqmi	6.2	8.5	10.0	13.0	14.7
	20000sqmi	4.4	6.6	8.1	10.8	12.4
Grid Point 18 PMP Values in Inches	Area Size	6-Hour	12-Hour	24-Hour	48-Hour	72-Hour
	10sqmi	18.1	21.2	23.6	25.0	26.0
	100sqmi	15.5	18.0	20.7	22.0	23.0
	200sqmi	14.4	16.6	19.7	21.0	22.0
	500sqmi	12.5	14.6	17.7	19.3	20.3
	1000sqmi	10.8	13.0	15.8	18.0	19.0
	2000sqmi	9.0	11.4	13.9	16.7	17.5
	5000sqmi	6.8	9.5	11.6	14.7	15.3
	10000sqmi	5.1	8.2	10.0	13.3	13.8
	20000sqmi	3.5	6.5	8.2	11.0	11.5
% Reduction from HMR 51	Area Size	6-Hour	12-Hour	24-Hour	48-Hour	72-Hour
	10sqmi	28%	26%	23%	25%	27%
	200sqmi	20%	22%	13%	18%	20%
	1000sqmi	17%	16%	9%	10%	14%
	5000sqmi	15%	11%	6%	1%	8%
	10000sqmi	18%	4%	0%	-3%	6%
	20000sqmi	21%	1%	-1%	-2%	7%

Grid Point 19 PMP vs HMR 51 PMP						
HMR 51 PMP Values at Grid Point 19 in Inches	Area Size	6-Hour	12-Hour	24-Hour	48-Hour	72-Hour
	10sqmi	25.1	28.3	30.4	33.2	35.1
	200sqmi	17.7	21.0	22.5	25.2	27.1
	1000sqmi	12.9	15.3	17.1	19.8	21.8
	5000sqmi	7.8	10.5	12.2	14.6	16.4
	10000sqmi	6.1	8.4	9.9	12.8	14.5
	20000sqmi	4.3	6.5	8.1	10.6	12.3
Grid Point 19 PMP Values in Inches	Area Size	6-Hour	12-Hour	24-Hour	48-Hour	72-Hour
	10sqmi	17.7	21.2	23.3	24.6	25.5
	100sqmi	15.1	17.7	20.6	21.7	22.5
	200sqmi	14.0	16.4	19.5	20.7	21.5
	500sqmi	12.2	14.4	17.6	19.1	19.8
	1000sqmi	10.6	12.9	15.8	17.8	18.5
	2000sqmi	9.0	11.3	13.9	16.6	17.0
	5000sqmi	6.8	9.5	11.6	14.6	15.1
	10000sqmi	5.1	8.2	9.9	12.9	13.4
	20000sqmi	3.5	6.5	8.1	10.9	11.4
% Reduction from HMR 51	Area Size	6-Hour	12-Hour	24-Hour	48-Hour	72-Hour
	10sqmi	29%	25%	23%	26%	27%
	200sqmi	21%	22%	13%	18%	21%
	1000sqmi	18%	16%	8%	10%	15%
	5000sqmi	13%	9%	5%	0%	8%
	10000sqmi	16%	3%	0%	-1%	8%
	20000sqmi	19%	0%	-1%	-3%	7%

Grid Point 20 PMP vs HMR 51 PMP						
HMR 51 PMP Values at Grid Point 20 in Inches	Area Size	6-Hour	12-Hour	24-Hour	48-Hour	72-Hour
	10sqmi	24.9	28.2	30.3	33.1	35.0
	200sqmi	17.5	20.8	22.3	25.0	26.8
	1000sqmi	12.8	15.2	17.0	19.6	21.5
	5000sqmi	7.7	10.3	12.1	14.5	16.3
	10000sqmi	6.0	8.4	9.9	12.7	14.4
	20000sqmi	4.2	6.5	8.0	10.5	12.2
Grid Point 20 PMP Values in Inches	Area Size	6-Hour	12-Hour	24-Hour	48-Hour	72-Hour
	10sqmi	17.2	21.2	23.3	24.4	25.2
	100sqmi	14.8	17.5	20.6	21.6	22.2
	200sqmi	13.6	16.2	19.5	20.6	21.2
	500sqmi	11.9	14.3	17.6	19.0	19.6
	1000sqmi	10.6	12.9	15.8	17.7	18.3
	2000sqmi	8.9	11.4	13.9	16.6	16.9
	5000sqmi	6.6	9.5	11.5	14.5	15.0
	10000sqmi	5.1	8.1	9.8	12.9	13.3
	20000sqmi	3.5	6.5	8.1	10.9	11.3
% Reduction from HMR 51	Area Size	6-Hour	12-Hour	24-Hour	48-Hour	72-Hour
	10sqmi	31%	25%	23%	26%	28%
	200sqmi	22%	22%	13%	18%	21%
	1000sqmi	17%	15%	7%	10%	15%
	5000sqmi	14%	8%	5%	0%	8%
	10000sqmi	15%	3%	1%	-2%	8%
	20000sqmi	17%	0%	-1%	-3%	7%

Grid Point 21 PMP vs HMR 51 PMP						
HMR 51 PMP Values at Grid Point 21 in Inches	Area Size	6-Hour	12-Hour	24-Hour	48-Hour	72-Hour
	10sqmi	24.7	28.1	30.2	33.0	34.8
	200sqmi	17.3	20.6	22.1	24.8	26.6
	1000sqmi	12.6	15.1	16.9	19.5	21.3
	5000sqmi	7.4	10.2	12.0	14.4	16.2
	10000sqmi	5.9	8.3	9.9	12.6	14.3
	20000sqmi	4.1	6.6	8.1	10.5	12.0
Grid Point 21 PMP Values in Inches	Area Size	6-Hour	12-Hour	24-Hour	48-Hour	72-Hour
	10sqmi	16.9	21.2	23.2	24.3	25.0
	100sqmi	14.6	17.5	20.4	21.5	22.2
	200sqmi	13.4	16.2	19.3	20.5	21.2
	500sqmi	11.8	14.3	17.4	18.9	19.5
	1000sqmi	10.4	12.9	15.6	17.5	18.1
	2000sqmi	8.9	11.4	13.8	16.2	16.8
	5000sqmi	6.5	9.6	11.4	14.5	14.9
	10000sqmi	5.0	8.1	9.7	12.9	13.3
	20000sqmi	3.4	6.5	8.1	10.9	11.3
% Reduction from HMR 51	Area Size	6-Hour	12-Hour	24-Hour	48-Hour	72-Hour
	10sqmi	32%	25%	23%	26%	28%
	200sqmi	22%	21%	13%	17%	20%
	1000sqmi	18%	15%	8%	10%	15%
	5000sqmi	13%	6%	5%	-1%	8%
	10000sqmi	15%	3%	2%	-2%	7%
	20000sqmi	18%	1%	0%	-4%	6%

Grid Point 22 PMP vs HMR 51 PMP						
HMR 51 PMP Values at Grid Point 22 in Inches	Area Size	6-Hour	12-Hour	24-Hour	48-Hour	72-Hour
	10sqmi	24.7	28.0	30.1	33.0	34.7
	200sqmi	17.0	20.3	22.0	24.6	26.3
	1000sqmi	12.5	14.9	16.9	19.3	21.2
	5000sqmi	7.1	10.2	12.0	14.4	16.0
	10000sqmi	5.7	8.3	9.9	12.5	14.2
	20000sqmi	4.0	6.6	8.1	10.6	11.7
Grid Point 22 PMP Values in Inches	Area Size	6-Hour	12-Hour	24-Hour	48-Hour	72-Hour
	10sqmi	16.7	20.9	23.0	24.3	24.8
	100sqmi	14.2	16.9	20.0	21.4	22.0
	200sqmi	13.1	15.7	19.0	20.4	21.0
	500sqmi	11.4	14.0	17.2	18.8	19.5
	1000sqmi	10.0	12.6	15.4	17.5	18.0
	2000sqmi	8.5	11.3	13.5	16.1	16.7
	5000sqmi	6.3	9.6	11.4	14.3	14.8
	10000sqmi	4.9	8.1	9.7	12.6	13.2
	20000sqmi	3.4	6.5	8.1	10.6	11.2
% Reduction from HMR 51	Area Size	6-Hour	12-Hour	24-Hour	48-Hour	72-Hour
	10sqmi	32%	25%	24%	26%	28%
	200sqmi	23%	23%	14%	17%	20%
	1000sqmi	20%	16%	9%	9%	15%
	5000sqmi	12%	5%	5%	0%	8%
	10000sqmi	15%	3%	2%	-1%	7%
	20000sqmi	16%	1%	0%	0%	4%

Grid Point 23 PMP vs HMR 51 PMP						
HMR 51 PMP Values at Grid Point 23 in Inches	Area Size	6-Hour	12-Hour	24-Hour	48-Hour	72-Hour
	10sqmi	24.7	28.0	30.0	33.0	34.7
	200sqmi	16.8	20.1	22.0	24.5	26.0
	1000sqmi	12.4	14.9	16.9	19.2	20.9
	5000sqmi	7.2	10.1	12.1	14.3	15.9
	10000sqmi	5.7	8.3	9.9	12.4	14.0
	20000sqmi	4.0	6.6	8.1	10.5	11.7
Grid Point 23 PMP Values in Inches	Area Size	6-Hour	12-Hour	24-Hour	48-Hour	72-Hour
	10sqmi	16.5	20.8	23.0	24.0	24.6
	100sqmi	14.1	16.8	20.0	21.2	21.8
	200sqmi	13.0	15.6	18.9	20.2	20.8
	500sqmi	11.2	13.9	17.0	18.7	19.5
	1000sqmi	9.9	12.6	15.3	17.4	18.0
	2000sqmi	8.5	11.3	13.5	16.0	16.5
	5000sqmi	6.3	9.6	11.3	14.0	14.5
	10000sqmi	4.9	8.1	9.7	12.4	12.7
	20000sqmi	3.3	6.5	8.0	10.4	10.8
% Reduction from HMR 51	Area Size	6-Hour	12-Hour	24-Hour	48-Hour	72-Hour
	10sqmi	33%	26%	23%	27%	29%
	200sqmi	23%	22%	14%	17%	20%
	1000sqmi	20%	16%	9%	10%	14%
	5000sqmi	12%	5%	6%	2%	9%
	10000sqmi	14%	3%	2%	0%	9%
	20000sqmi	17%	2%	2%	1%	8%

Appendix E
Depth-Area-Duration Comparison Tables
Ohio Statewide PMP vs. FERC
Michigan/Wisconsin PMP

Grid Point 12 PMP vs FERC Michigan/Wisconsin PMP						
FERC Michigan Wisconsin Study PMP Values in Inches	Area Size	6-Hour	12-Hour	24-Hour	48-Hour	72-Hour
	100sqmi	16.2	18.5	20.1	23.0	24.4
	200sqmi	14.8	17.4	18.8	21.9	22.6
	500sqmi	13.4	15.4	16.9	20.0	20.8
	1000sqmi	11.9	13.4	15.8	18.7	19.7
	5000sqmi	7.4	9.6	12.3	15.8	16.6
	10000sqmi	5.6	7.4	11.1	14.3	15.2
<hr/>						
Ohio Study PMP Values at Grid Point 12 in Inches	Area Size	6-Hour	12-Hour	24-Hour	48-Hour	72-Hour
	10sqmi	18.5	22.0	24.0	26.0	26.5
	100sqmi	15.6	18.3	21.0	23.0	23.4
	200sqmi	14.6	16.9	19.9	21.7	22.0
	500sqmi	12.6	14.9	17.8	20.0	20.5
	1000sqmi	11.0	13.2	15.9	18.9	19.3
	2000sqmi	9.1	11.6	14.1	17.6	17.9
	5000sqmi	6.9	9.7	11.7	15.4	15.7
	10000sqmi	5.2	8.4	10.1	13.8	14.1
	20000sqmi	3.6	6.5	8.3	11.4	12.0
<hr/>						
% Reduction from FERC Michigan Wisconsin PMP	Area Size	6-Hour	12-Hour	24-Hour	48-Hour	72-Hour
	100sqmi	4%	1%	-5%	0%	4%
	200sqmi	2%	3%	-6%	1%	3%
	500sqmi	6%	3%	-5%	0%	1%
	1000sqmi	7%	1%	-1%	-1%	2%
	5000sqmi	6%	-1%	5%	3%	5%
	10000sqmi	8%	-13%	9%	3%	7%

Grid Point 13 PMP vs FERC Michigan/Wisconsin PMP						
FERC Michigan Wisconsin Study PMP Values in Inches	Area Size	6-Hour	12-Hour	24-Hour	48-Hour	72-Hour
	100sqmi	15.9	18.2	19.8	22.5	24.1
	200sqmi	14.6	17.0	18.5	21.6	22.3
	500sqmi	13.2	15.0	16.8	19.7	20.6
	1000sqmi	11.8	13.1	15.6	18.5	19.5
	5000sqmi	7.3	9.4	12.2	15.8	16.4
	10000sqmi	5.6	7.4	11.0	14.2	15.1
<hr/>						
Ohio Study PMP Values at Grid Point 13 in Inches	Area Size	6-Hour	12-Hour	24-Hour	48-Hour	72-Hour
	10sqmi	18.4	21.8	24.0	25.6	26.0
	100sqmi	15.7	18.2	21.0	22.5	22.9
	200sqmi	14.6	16.9	19.9	21.3	21.7
	500sqmi	12.7	14.9	17.9	19.5	20.0
	1000sqmi	10.9	13.2	15.9	18.3	18.7
	2000sqmi	9.2	11.6	14.0	17.0	17.3
	5000sqmi	6.9	9.7	11.8	15.0	15.5
	10000sqmi	5.1	8.4	10.0	13.3	14.0
	20000sqmi	3.5	6.5	8.3	11.4	11.9
<hr/>						
% Reduction from FERC Michigan Wisconsin PMP	Area Size	6-Hour	12-Hour	24-Hour	48-Hour	72-Hour
	100sqmi	1%	0%	-6%	0%	5%
	200sqmi	0%	1%	-7%	1%	3%
	500sqmi	4%	1%	-7%	1%	3%
	1000sqmi	7%	-1%	-2%	1%	4%
	5000sqmi	5%	-3%	3%	5%	6%
	10000sqmi	9%	-14%	9%	6%	7%

Grid Point 14 PMP vs FERC Michigan/Wisconsin PMP						
FERC Michigan Wisconsin Study PMP Values in Inches	Area Size	6-Hour	12-Hour	24-Hour	48-Hour	72-Hour
	100sqmi	15.7	17.8	19.5	22.2	23.9
	200sqmi	14.5	16.8	18.3	21.4	22.1
	500sqmi	13.1	14.8	16.7	19.5	20.4
	1000sqmi	11.7	13.0	15.4	18.3	19.3
	5000sqmi	7.2	9.3	12.1	15.7	16.3
	10000sqmi	5.6	7.3	10.9	14.1	15.0
<hr/>						
Ohio Study PMP Values at Grid Point 14 in Inches	Area Size	6-Hour	12-Hour	24-Hour	48-Hour	72-Hour
	10sqmi	17.6	21.5	23.5	25.0	25.5
	100sqmi	15.2	17.7	20.5	22.0	22.5
	200sqmi	14.2	16.5	19.4	20.9	21.3
	500sqmi	12.5	14.7	17.5	19.1	19.5
	1000sqmi	10.7	13.0	15.8	17.7	18.2
	2000sqmi	9.1	11.6	14.0	16.5	16.8
	5000sqmi	6.8	9.7	11.6	14.6	15.0
	10000sqmi	5.1	8.4	9.9	13.0	13.4
20000sqmi	3.5	6.5	8.2	11.0	11.4	
<hr/>						
% Reduction from FERC Michigan Wisconsin PMP	Area Size	6-Hour	12-Hour	24-Hour	48-Hour	72-Hour
	100sqmi	3%	1%	-5%	1%	6%
	200sqmi	2%	2%	-6%	2%	4%
	500sqmi	4%	1%	-5%	2%	4%
	1000sqmi	8%	0%	-2%	3%	6%
	5000sqmi	5%	-5%	4%	7%	8%
10000sqmi	8%	-15%	9%	8%	11%	

Grid Point 15 PMP vs FERC Michigan/Wisconsin PMP						
FERC Michigan Wisconsin Study PMP Values in Inches	Area Size	6-Hour	12-Hour	24-Hour	48-Hour	72-Hour
	100sqmi	15.6	17.5	19.3	21.9	23.7
	200sqmi	14.3	16.5	18.1	21.2	22.0
	500sqmi	12.9	14.5	16.5	19.3	20.3
	1000sqmi	11.6	12.8	15.3	18.1	19.1
	5000sqmi	7.1	9.1	12.0	15.6	16.2
	10000sqmi	5.5	7.3	10.9	14.1	15.0
<hr/>						
Ohio Study PMP Values at Grid Point 15 in Inches	Area Size	6-Hour	12-Hour	24-Hour	48-Hour	72-Hour
	10sqmi	17.2	21.4	23.0	24.5	25.0
	100sqmi	14.8	17.5	20.3	21.6	22.0
	200sqmi	13.9	16.2	19.0	20.6	21.0
	500sqmi	12.2	14.3	17.1	18.7	19.1
	1000sqmi	10.6	12.9	15.4	17.3	17.8
	2000sqmi	9.0	11.5	13.8	16.2	16.6
	5000sqmi	6.6	9.8	11.4	14.2	14.7
	10000sqmi	5.0	8.4	9.9	12.8	13.1
	20000sqmi	3.5	6.5	8.2	10.8	11.2
<hr/>						
% Reduction from FERC Michigan Wisconsin PMP	Area Size	6-Hour	12-Hour	24-Hour	48-Hour	72-Hour
	100sqmi	5%	0%	-5%	1%	7%
	200sqmi	2%	2%	-5%	3%	5%
	500sqmi	5%	1%	-3%	3%	6%
	1000sqmi	8%	-1%	-1%	4%	7%
	5000sqmi	7%	-8%	5%	9%	9%
	10000sqmi	9%	-15%	9%	9%	12%

Grid Point 18 PMP vs FERC Michigan/Wisconsin PMP						
FERC Michigan Wisconsin Study PMP Values in Inches	Area Size	6-Hour	12-Hour	24-Hour	48-Hour	72-Hour
	100sqmi	15.8	17.9	19.4	22.1	23.6
	200sqmi	14.5	16.8	18.3	21.1	21.8
	500sqmi	13.1	14.8	16.4	19.3	20.2
	1000sqmi	11.7	13.0	15.1	18.0	19.1
	5000sqmi	7.2	9.2	11.9	15.4	16.1
10000sqmi	5.5	7.3	10.7	13.9	14.8	
Ohio Study PMP Values at Grid Point 15 in Inches	Area Size	6-Hour	12-Hour	24-Hour	48-Hour	72-Hour
	10sqmi	18.1	21.2	23.6	25.0	26.0
	100sqmi	15.5	18.0	20.7	22.0	23.0
	200sqmi	14.4	16.6	19.7	21.0	22.0
	500sqmi	12.5	14.6	17.7	19.3	20.3
	1000sqmi	10.8	13.0	15.8	18.0	19.0
	2000sqmi	9.0	11.4	13.9	16.7	17.5
	5000sqmi	6.8	9.5	11.6	14.7	15.3
	10000sqmi	5.1	8.2	10.0	13.3	13.8
	20000sqmi	3.5	6.5	8.2	11.0	11.5
% Reduction from FERC Michigan Wisconsin PMP	Area Size	6-Hour	12-Hour	24-Hour	48-Hour	72-Hour
	100sqmi	2%	0%	-6%	0%	3%
	200sqmi	1%	1%	-8%	1%	-1%
	500sqmi	5%	2%	-8%	0%	-1%
	1000sqmi	8%	0%	-4%	0%	0%
	5000sqmi	6%	-3%	3%	4%	5%
10000sqmi	7%	-13%	6%	4%	7%	

Grid Point 19 PMP vs FERC Michigan/Wisconsin PMP						
FERC Michigan Wisconsin Study PMP Values in Inches	Area Size	6-Hour	12-Hour	24-Hour	48-Hour	72-Hour
	100sqmi	15.6	17.4	19.1	21.5	23.3
	200sqmi	14.3	16.4	17.9	20.8	21.5
	500sqmi	12.9	14.4	16.2	19.0	19.9
	1000sqmi	11.6	12.7	14.9	17.7	18.8
	5000sqmi	7.1	9.0	11.7	15.2	16.0
	10000sqmi	5.4	7.2	10.6	13.8	14.7
<hr/>						
Ohio Study PMP Values at Grid Point 15 in Inches	Area Size	6-Hour	12-Hour	24-Hour	48-Hour	72-Hour
	10sqmi	17.7	21.2	23.3	24.6	25.5
	100sqmi	15.1	17.7	20.6	21.7	22.5
	200sqmi	14.0	16.4	19.5	20.7	21.5
	500sqmi	12.2	14.4	17.6	19.1	19.8
	1000sqmi	10.6	12.9	15.8	17.8	18.5
	2000sqmi	9.0	11.3	13.9	16.6	17.0
	5000sqmi	6.8	9.5	11.6	14.6	15.1
	10000sqmi	5.1	8.2	9.9	12.9	13.4
	20000sqmi	3.5	6.5	8.1	10.9	11.4
<hr/>						
% Reduction from FERC Michigan Wisconsin PMP	Area Size	6-Hour	12-Hour	24-Hour	48-Hour	72-Hour
	100sqmi	3%	-1%	-8%	-1%	3%
	200sqmi	2%	0%	-9%	0%	0%
	500sqmi	5%	0%	-9%	-1%	1%
	1000sqmi	8%	-1%	-6%	-1%	2%
	5000sqmi	4%	-6%	1%	4%	5%
	10000sqmi	6%	-14%	6%	6%	9%

Grid Point 20 PMP vs FERC Michigan/Wisconsin PMP						
FERC Michigan Wisconsin Study PMP Values in Inches	Area Size	6-Hour	12-Hour	24-Hour	48-Hour	72-Hour
	100sqmi	15.4	17.0	18.8	21.1	23.1
	200sqmi	14.1	16.1	17.6	20.5	21.4
	500sqmi	12.7	14.1	16.0	18.8	19.8
	1000sqmi	11.5	12.6	14.8	17.5	18.7
	5000sqmi	7.0	8.8	11.6	15.1	15.9
10000sqmi	5.4	7.1	10.5	13.7	14.6	
<hr/>						
Ohio Study PMP Values at Grid Point 15 in Inches	Area Size	6-Hour	12-Hour	24-Hour	48-Hour	72-Hour
	10sqmi	17.2	21.2	23.3	24.4	25.2
	100sqmi	14.8	17.5	20.6	21.6	22.2
	200sqmi	13.6	16.2	19.5	20.6	21.2
	500sqmi	11.9	14.3	17.6	19.0	19.6
	1000sqmi	10.6	12.9	15.8	17.7	18.3
	2000sqmi	8.9	11.4	13.9	16.6	16.9
	5000sqmi	6.6	9.5	11.5	14.5	15.0
	10000sqmi	5.1	8.1	9.8	12.9	13.3
20000sqmi	3.5	6.5	8.1	10.9	11.3	
<hr/>						
% Reduction from FERC Michigan Wisconsin PMP	Area Size	6-Hour	12-Hour	24-Hour	48-Hour	72-Hour
	100sqmi	4%	-3%	-10%	-2%	4%
	200sqmi	3%	-1%	-11%	0%	1%
	500sqmi	6%	-1%	-10%	-1%	1%
	1000sqmi	7%	-3%	-7%	-1%	2%
	5000sqmi	6%	-7%	1%	4%	5%
10000sqmi	5%	-14%	7%	6%	9%	

Grid Point 21 PMP vs FERC Michigan/Wisconsin PMP						
FERC Michigan Wisconsin Study PMP Values in Inches	Area Size	6-Hour	12-Hour	24-Hour	48-Hour	72-Hour
	100sqmi	15.2	16.6	18.5	20.8	22.7
	200sqmi	13.8	15.7	17.4	20.2	21.1
	500sqmi	12.4	13.8	15.8	18.5	19.6
	1000sqmi	11.4	12.4	14.5	17.2	18.5
	5000sqmi	6.9	8.7	11.5	14.9	15.8
	10000sqmi	5.3	7.1	10.4	13.6	14.5
<hr/>						
Ohio Study PMP Values at Grid Point 15 in Inches	Area Size	6-Hour	12-Hour	24-Hour	48-Hour	72-Hour
	10sqmi	16.9	21.2	23.2	24.3	25.0
	100sqmi	14.6	17.5	20.4	21.5	22.2
	200sqmi	13.4	16.2	19.3	20.5	21.2
	500sqmi	11.8	14.3	17.4	18.9	19.5
	1000sqmi	10.4	12.9	15.6	17.5	18.1
	2000sqmi	8.9	11.4	13.8	16.2	16.8
	5000sqmi	6.5	9.6	11.4	14.5	14.9
	10000sqmi	5.0	8.1	9.7	12.9	13.3
	20000sqmi	3.4	6.5	8.1	10.9	11.3
<hr/>						
% Reduction from FERC Michigan Wisconsin PMP	Area Size	6-Hour	12-Hour	24-Hour	48-Hour	72-Hour
	100sqmi	4%	-5%	-11%	-3%	2%
	200sqmi	3%	-3%	-11%	-1%	0%
	500sqmi	5%	-4%	-10%	-2%	0%
	1000sqmi	8%	-4%	-7%	-2%	2%
	5000sqmi	6%	-10%	1%	3%	5%
	10000sqmi	6%	-15%	7%	5%	8%

Appendix F
Short Storm List Storm Analysis
Separate Binding

Appendix G
Storm Precipitation Analysis System (SPAS)
Description

INTRODUCTION

The Storm Precipitation Analysis System (SPAS) is grounded on years of scientific research with a demonstrated reliability in hundreds of post-storm precipitation analyses. It has evolved into a trusted hydrometeorological tool that provides accurate precipitation data at a high spatial and temporal resolution for use in a variety of sensitive hydrologic applications (Faulkner et al. 2004, Tomlinson et al. 2003-2012). Applied Weather Associates, LLC and METSTAT, Inc. initially developed SPAS in 2002 for use in producing Depth-Area-Duration values for Probable Maximum Precipitator (PMP) analyses. SPAS utilizes precipitation gauge data, “basemaps” and radar data (when available) to produce gridded precipitation at time intervals as short as 5-minutes, at spatial scales as fine as 1 km² and in a variety of customizable formats. To date (April 2012) SPAS has been used to analyze over 230 storm centers across all types of terrain, among highly varied meteorological settings and some occurring over 100-years ago.

SPAS output has many applications including, but not limited to: hydrologic model calibration/validation, flood event reconstruction, storm water runoff analysis, forensic cases and PMP studies. Detailed SPAS-computed precipitation data allow hydrologists to accurately model runoff from basins, particularly when the precipitation is unevenly distributed over the drainage basin or when rain gauge data is limited or not available. The increased spatial and temporal accuracy of precipitation estimates has eliminated the need for commonly made assumptions about precipitation characteristics (such as uniform precipitation over a watershed), thereby greatly improving the precision and reliability of hydrologic analyses.

In order to instill consistency in SPAS analyses, many of the core methods have remained consistent from beginning. However, SPAS is constantly evolving and improving through new scientific advancements and as new data and improvements are incorporated. This write-up describes the current inter-workings of SPAS, but the reader should realize SPAS can be customized on a case-by-case basis to account for special circumstances; these adaptations are documented and included in the deliverables. The over arching goal of SPAS is to combine the strengths of rain gauge data and radar data (when available) to provide sound, reliable and accurate spatial precipitation data.

Hourly precipitation observations are generally limited to a small number of locations, with many basins lacking observational precipitation data entirely. Meanwhile Next Generation Radar (NEXRAD) data provides valuable spatial and temporal information over data-sparse basins; it has historically lacked reliability for determining precipitation rates and reliable quantitative precipitation estimates (QPE). The improved reliability in SPAS is made possible by hourly calibration of the NEXRAD radar-precipitation relationship using data from locations with hourly rainfall observations within the overall SPAS analysis domain, combined with local hourly bias adjustments to force consistency between the final result and “ground truth” precipitation measurements. If NEXRAD radar data is available (generally for storm events since the mid-1990's), precipitation at temporal scales as frequent as 5-minutes is available, otherwise the

precipitation data is available hourly. A summary of the general SPAS processes are shown in flow chart in Figure G.1.

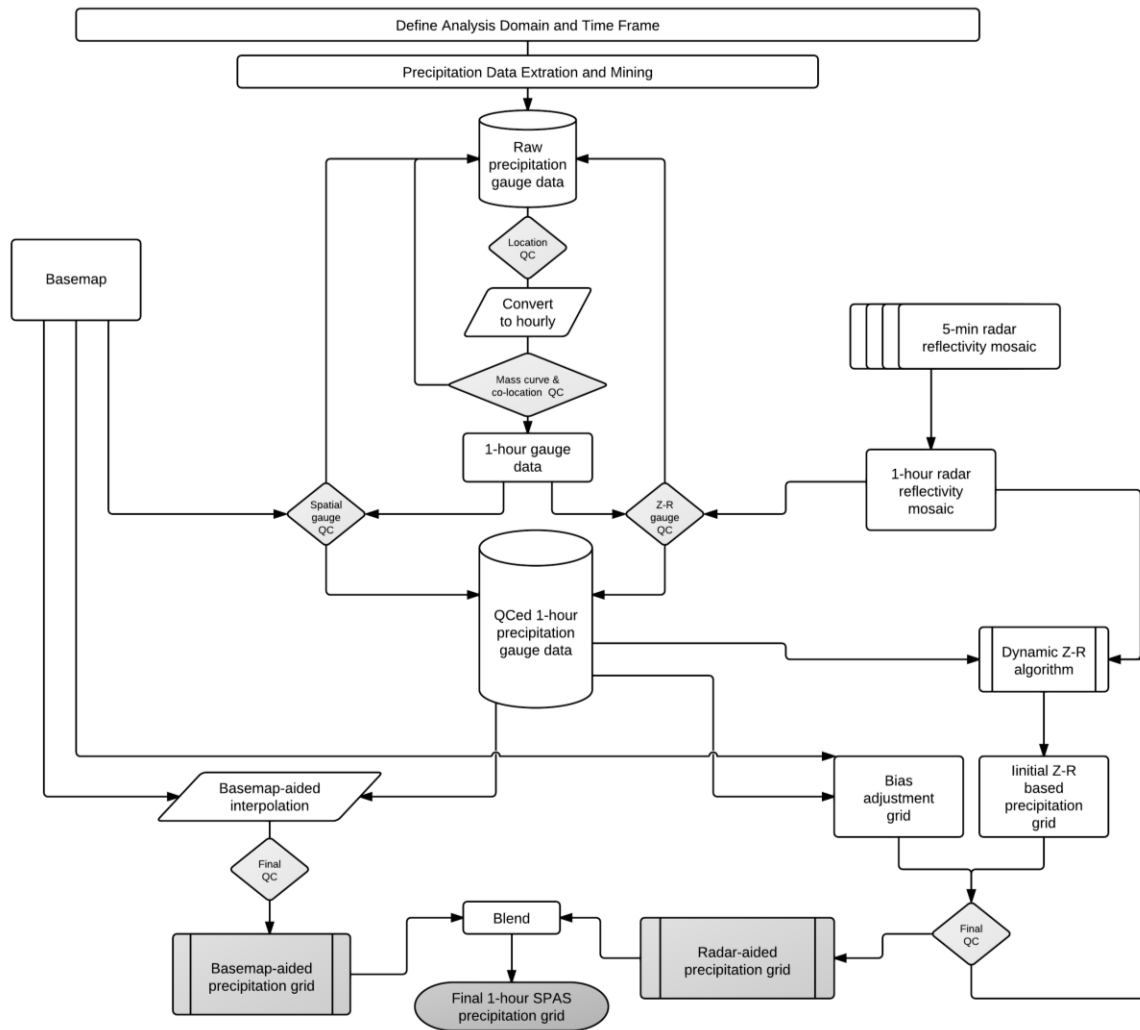


Figure G.1 SPAS flow chart

SETUP

Prior to a SPAS analysis careful definition of the storm analysis domain and time frame to be analyzed is established. Several considerations are made to ensure the domain (longitude-latitude box) and time frame are sufficient for the given application.

SPAS Analysis Domain

For PMP applications it is important to establish an analysis domain that completely encompasses a storm center, meanwhile hydrologic modeling applications are more concerned about a specific basin, watershed or catchment. If radar data is available, then it is also important to establish an area large enough to encompass enough stations

(minimum of ~30) to adequately derive reliable radar-precipitation intensity relationships (discussed later). The domain is defined by evaluating existing documentation on the storm as well as plotting and evaluating initial precipitation gauge data on a map. The analysis domain is defined to include as many hourly recording gauges as possible given their importance in timing. The domain must include enough of a buffer to accurately model the nested domain of interest. The domain is defined as a longitude-latitude (upper left and lower right corner) rectangular region.

SPAS Analysis Time Frame

Ideally, the analysis time frame, also referred to as the Storm Precipitation Period (SPP), will extend from a dry period through the target wet period then back into another dry period. This is to ensure that total storm precipitation amounts can be confidently associated with the storm in question and not contaminated by adjacent wet periods. If this is not possible, a reasonable time period is selected that is bounded by relatively lighter precipitation. The time frame of the hourly data must be sufficient to capture the full range of daily gauge observational periods in order for the daily observations to be disaggregated into estimated incremental hourly values (discussed later). For example, if a daily gauge takes observations at 8:00 AM, then the hourly data must be available from 8:00 AM the day prior. Given the configuration of SPAS, the minimum SPP is 72 hours and aligns midnight to midnight.

The core precipitation period (CPP) is a sub-set of the SPP and represents the time period with the most precipitation and the greatest number of reporting gauges. The CPP represents the time period of interest and where our confidence in the results is highest.

DATA

The foundation of a SPAS analysis is the “ground truth” precipitation measurements. In fact, the level of effort involved in “data mining” and quality control represent over half of the total level of effort needed to conduct a complete storm analysis. SPAS operates with three primary data sets: precipitation gauge data, a “basemap” and, if available, radar data. Table G.1 conveys the variety of precipitation gauges usable by SPAS. For each gauge, the following elements are gathered, entered and archived into to SPAS database:

- Station ID
- Station name
- Station type (H=hourly, D=Daily, S=Supplemental, etc.)
- Longitude in decimal degrees
- Latitude in decimal degrees
- Elevation in feet above MSL
- Observed precipitation
- Observation times
- Source
- If unofficial, the measurement equipment and/or method is also noted.

Based on the SPP and analysis domain, hourly and daily precipitation gauge data are extracted from our in-house database as well as the Meteorological Assimilation Data Ingest System (MADIS). Our in-house database contains data dating back to the late 1800s, while the MADIS system (described below) contains archived data back to 2002.

Hourly Precipitation Data

Our hourly precipitation database is largely comprised of data from NCDC TD-3240, but also precipitation data from other mesonets and meteorological networks (e.g., ALERT, Flood Control Districts, etc.) that we have collected and archived as part of previous studies. Meanwhile, MADIS provides data from a large number of networks across the U.S., including NOAA’s HADS (Hydrometeorological Automated Data System), numerous mesonets, the Citizen Weather Observers Program (CWOP), departments of transportation, etc. (see http://madis.noaa.gov/mesonet_providers.html for a list of providers). Although our automatic data extraction is fast, cost-effective and efficient, it never captures all of the available precipitation data for a storm event. For this reason, a thorough “data mining” effort is undertaken to acquire all available data from sources such as U.S. Geological Survey (USGS), Remote Automated Weather Stations (RAWS), Community Collaborative Rain, Hail & Snow Network (CoCoRaHS), National Atmospheric Deposition Program (NADP), Clean Air Status and Trends Network (CASTNET), local observer networks, Climate Reference Network (CRN), Global Summary of the Day (GSD) and Soil Climate Analysis Network (SCAN). Unofficial hourly precipitation are gathered to give guidance on either timing or magnitude in areas otherwise void of precipitation data. The WeatherUnderground and MesoWest, two of the largest weather databases on the Internet, contain a good deal of official data, but also unofficial gauges.

Table G.1 Different precipitation gauge types used by SPAS

Precipitation Gauge Type	Description
Hourly	Hourly gauges with complete, or nearly complete, incremental hourly precipitation data.
Hourly estimated	Hourly gauges with some estimated hourly values, but otherwise reliable.
Hourly pseudo	Hourly gauges with reliable temporal precipitation data, but the magnitude is questionable in relation to co-located daily or supplemental gauge.
Daily	Daily gauge with complete data and known observation times.
Daily estimated	Daily gauges with some or all estimated

	data.
Supplemental	Gauges with unknown or irregular observation times, but reliable total storm precipitation data. (e.g., public reports, storms reports, “Bucket surveys”, etc.)
Supplemental estimated	Gauges with estimated total storm precipitation values based on other information (e.g., newspaper articles, stream flow discharge, inferences from nearby gauges, pre-existing total storm isohyetal maps, etc.)

Daily Precipitation Data

Our daily database is largely based on NCDC’s TD-3206 (pre-1948) and TD-3200 (1948 through present) as well as SNOTEL data from NRCS. Since the late 1990s, the CoCoRaHS network of more than 15,000 observes in the U.S. has become a very important daily precipitation source. Other daily data is gathered from similar, but smaller gauge networks, for instance the High Spatial Density Precipitation Network in Minnesota.

As part of the daily data extraction process, the time of observation, as indicted in database (if available), accompanies each measured precipitation value. Accurate observation times are necessary for SPAS to disaggregate the daily precipitation into estimated incremental values (discussed later). Knowing the observation time also allows SPAS to maintain precipitation amounts within given time bounds, thereby retaining known precipitation intensities. Given the importance of observation times, efforts are taken to insure the observation times are accurate. Hardcopy reports of “Climatological Data,” scanned observational forms (available on-line) and/or gauge metadata forms have proven to be valuable and accurate resources for validating observation times. Furthermore, erroneous observation times are identified in the mass-curve quality-control procedure (discussed later) and can be corrected at that point in the process.

Supplemental Precipitation Gauge Data

For gauges with unknown or irregular observation times, the gauge is considered a “supplemental” gauge. A supplemental gauge can either be added to the storm database with a storm total and the associated SPP as the temporal bounds or as a gauge with the known, but irregular observation times and associated precipitation amounts. For instance, if all that is known is 3” fell between 0800-0900, then that information can be entered. Gauges or reports with nothing more than a storm total are often abundant, but in order to use them, it is important the precipitation is only from the storm period in question. Therefore, it is ideal to have the analysis time frame bounded by dry periods.

Perhaps the most important source of data, if available, is from “bucket surveys,” which provide comprehensive lists of precipitation measurements collected during a post-storm field exercise. Although some bucket survey amounts are not from conventional precipitation gauges, they provide important information, especially in areas lacking data. Particularly for PMP-storm analysis applications, it is customary to accept extreme, but valid non-measured precipitation values in order to capture the highest precipitation values.

Basemap

“Basemaps” are independent grids of spatially distributed weather or climate variables that are used to govern the spatial patterns of the hourly precipitation. The basemap also governs the spatial resolution of the final SPAS grids, unless radar data is available/used to govern the spatial resolution. Note that a base map is not required as the hourly precipitation patterns can be based on a station characteristics and an inverse distance weighting technique (discussed later). Basemaps in complex terrain are often based on the PRISM mean monthly precipitation (Figure G.2a) or Hydrometeorological Design Studies Center precipitation frequency grids (Figure G.2b) given they resolve orographic enhancement areas and micro-climates at a spatial resolution of 30-seconds (about 800 m). Basemaps of this nature in flat terrain are not as effective given the small terrain forced precipitation gradients. Therefore, basemaps for SPAS analyses in flat terrain are often developed from pre-existing (hand-drawn) isohyetal patterns (Figure G.2c), composite radar imagery or a blend of both.

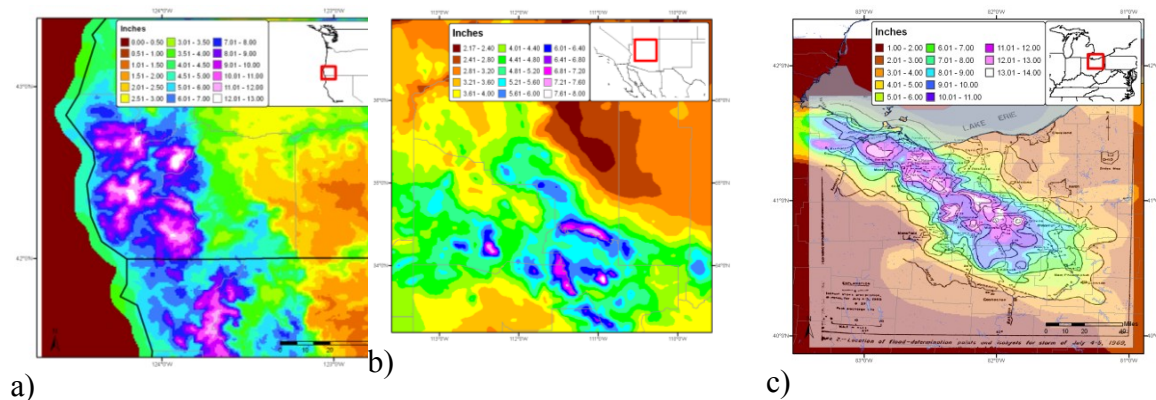


Figure G.2 Sample SPAS “basemaps” (a) A pre-existing (USGS) isohyetal pattern across flat terrain (SPAS 1209), (b) PRISM mean monthly (October) precipitation (SPAS 1192) and (c) A 100-year 24-hour precipitation grid from NOAA Atlas 14 (SPAS 1138)

Radar Data

For storms occurring since approximately the mid-1990's, weather radar data is available to supplement the SPAS analysis. A fundamental requirement for high quality radar-estimated precipitation is a high quality radar mosaic, which is a seamless collection of concurrent weather radar data from individual radar sites, however in some cases a single radar is sufficient (i.e. for a small area size storm event such as a thunderstorm). Weather

radar data has been in use by meteorologists since the 1960's to estimate precipitation depths, but it was not until the early 1990's that new, more accurate NEXRAD Doppler radar (WSR88D) was placed into service across the United States. Currently efforts are underway to convert the WSR88D radars to dual polarization (DualPol) radar. Today, NEXRAD radar coverage of the contiguous United States is comprised of 159 operational sites and 30 in Canada. Each U.S. radar covers an approximate 285 mile (460 km) radial extent while Canadian radars have approximately 256 km (138 nautical miles) radial extent over which the radar can detect precipitation. (see Figure G.3) The primary vendor of NEXRAD weather radar data for SPAS is Weather Decision Technologies, Inc. (WDT), who accesses, mosaics, archives and quality-controls NEXRAD radar data from NOAA and Environment Canada. SPAS utilizes Level II NEXRAD radar reflectivity data in units of dBZ, available every 5-minutes in the U.S. and 10-minutes in Canada.

NEXRAD Coverage Below 10,000 Feet AGL

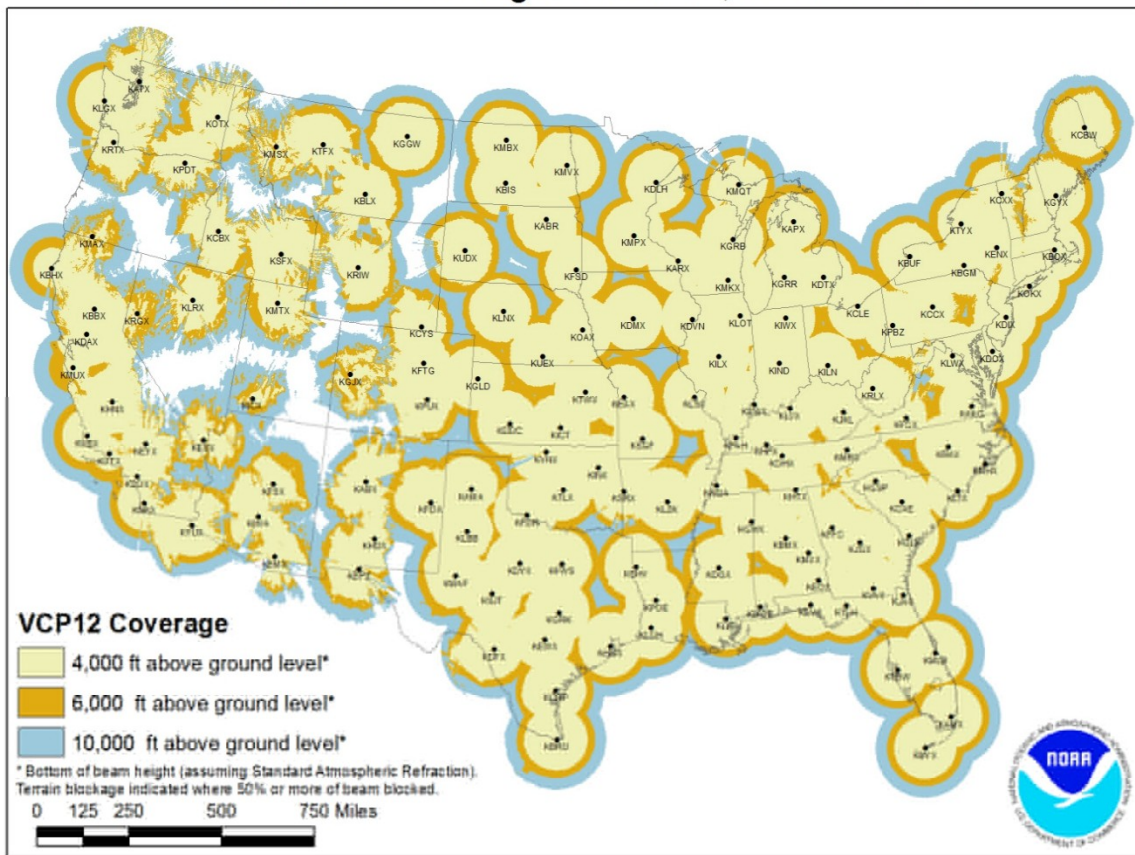
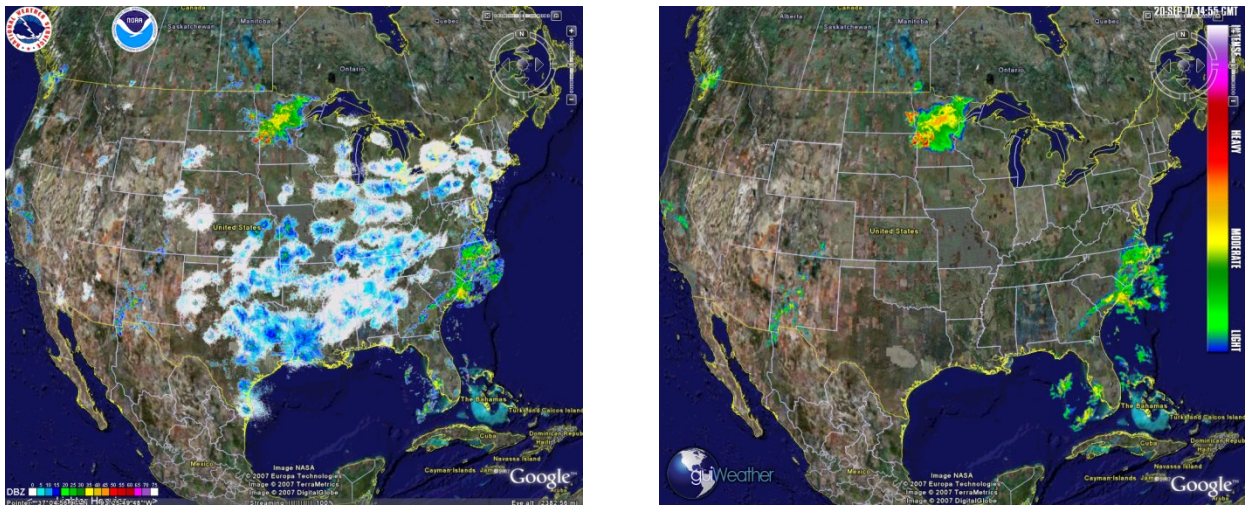


Figure G.3 U.S. radar locations and their radial extents of coverage below 10,000 feet above ground level (AGL). Each U.S. radar covers an approximate 285 mile radial extent over which the radar can detect precipitation.

The WDT and National Severe Storms Lab (NSSL) Radar Data Quality Control Algorithm (RDQC) removes non-precipitation artifacts from base Level-II radar data and remaps the data from polar coordinates to a Cartesian (latitude/longitude) grid. Non-precipitation artifacts include ground clutter, bright banding, sea clutter, anomalous

propagation, sun strobes, clear air returns, chaff, biological targets, electronic interference and hardware test patterns. The RDQC algorithm uses sophisticated data processing and a Quality Control Neural Network (QCNN) to delineate the precipitation echoes caused by radar artifacts (Lakshmanan and Valente 2004). Beam blockages due to terrain are mitigated by using 30 meter DEM data to compute and then discard data from a radar beam that clears the ground by less than 50 meters and incurs more than 50% power blockage. A clear-air echo removal scheme is applied to radars in clear-air mode when there is no precipitation reported from observation gauges within the vicinity of the radar. In areas of radar coverage overlap, a distance weighting scheme is applied to assign reflectivity to each grid cell, for multiple vertical levels. This scheme is applied to data from the nearest radar that is unblocked by terrain.

Once the data from individual radars have passed through the RDQC, they are merged to create a seamless mosaic for the United States and southern Canada as shown in Figure G.4. A multi-sensor quality control can be applied by post-processing the mosaic to remove any remaining “false echoes”. This technique uses observations of infra-red cloud top temperatures by GOES satellite and surface temperature to create a precipitation/no-precipitation mask. Figure 4 shows the impact of WDT’s quality control measures. Upon completing all QC, WDT converts the radar data from its native polar coordinate projection (1 degree x 1.0 km) into a longitude-latitude Cartesian grid (based on the WGS84 datum), at a spatial resolution of $\sim 1/3^{\text{rd}}$ -square mile for processing in SPAS.



a)

b)

Figure G.4 (a) Level-II radar mosaic of CONUS radar with no quality control, (b) WDT quality controlled Level-II radar mosaic

SPAS conducts further QC on the radar mosaic by infilling areas contaminated by beam blockages. Beam blocked areas are objectively determined by evaluating total storm reflectivity grid which naturally amplifies areas of the SPAS analysis domain suffering from beam blockage as shown in Figure G.5.

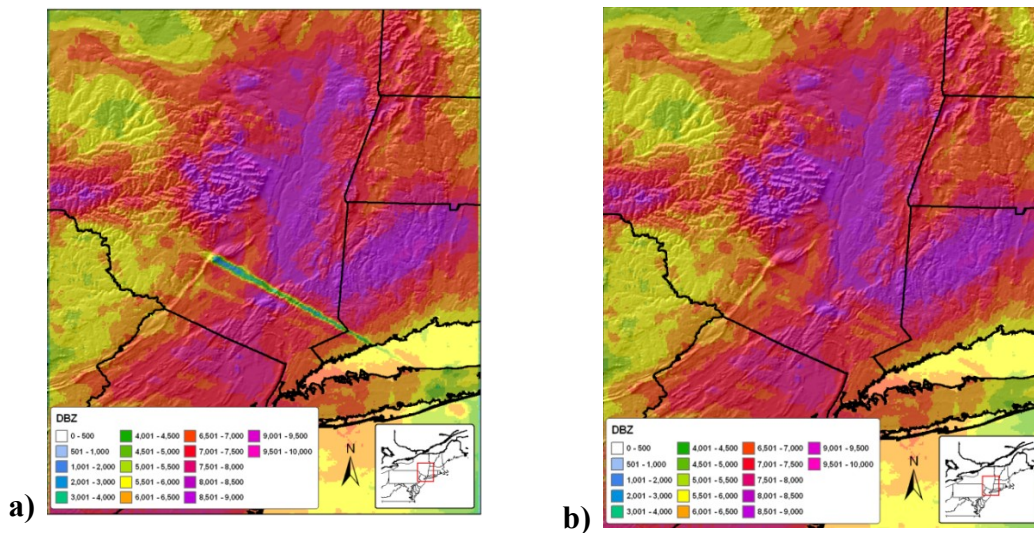


Figure G.5 Illustration of SPAS-beam blockage infilling where (a) is raw, blocked radar and (b) is filled for a 42-hour storm event

METHODOLOGY

Daily and Supplemental Precipitation to Hourly

To obtain one hour temporal resolutions and utilize all gauge data, it is necessary to disaggregate the daily and supplemental precipitation observations into estimated hourly amounts. This process has traditionally been accomplished by distributing (temporally) the precipitation at each daily/supplemental gauge in accordance to a single nearby hourly gauge (Thiessen polygon approach). However, this may introduce biases and not correctly represent hourly precipitation at daily/supplemental gauges situated in-between hourly gauges. Instead, SPAS uses a spatial approach by which the estimated hourly precipitation at each daily and supplemental gauge is governed by a distance weighted algorithm of all nearby true hourly gauges.

In order to disaggregate (i.e. distribute) daily/supplemental gauge data into estimate hourly values, the true hourly gauge data is first evaluated and quality controlled using synoptic maps, nearby gauges, orographic effects, gauge history and other documentation on the storm. Any problems with the hourly data are resolved, and when possible/necessary accumulated hourly values are distributed. If an hourly value is missing, the analyst can choose to either estimate it or leave it missing for SPAS to estimate later based on nearby hourly gauges. At this point in the process, pseudo (hourly) gauges can be added to represent precipitation timing in topographically complex locations, areas with limited/no hourly data or to capture localized convection. In order to adequately capture the temporal variations of the precipitation a pseudo hourly gauge is sometimes necessary. A pseudo gauge is created by distributing the precipitation at a co-located daily gauge or by creating a completely new pseudo gauge from other information such as inferences from COOP observation forms, METAR

visibility data (if hourly precipitation isn't already available), lightning data, satellite data, or radar data. Often radar data is the best/only choice for creating pseudo hourly gauges, but this is done cautiously given the potential differences (over-shooting of the radar beam equating to erroneous precipitation) between radar data and precipitation. In any case, the pseudo hourly gauge is flagged so SPAS only uses it for timing and not magnitude. Care is taken to ensure hourly pseudo gauges represent justifiably important physical and meteorological characteristics before being incorporated into the SPAS database. Although pseudo gauges provide a very important role, their use is kept to a minimum. The importance of insuring the reliability of every hourly gauge cannot be over emphasized. All of the final hourly gauge data, including pseudos, are included in the hourly SPAS precipitation database.

Using the hourly SPAS precipitation database, each hourly precipitation value is converted into a percentage that represents the incremental hourly precipitation divided by the total SPP precipitation. The GIS-ready x-y-z file is constructed for each hour that contains the latitude (x), longitude(y) and percent of precipitation (z) for a particular hour. Using the GRASS GIS, an inverse-distance-weighting squared (IDW) interpolation technique is applied to each of the hourly files. The result is a continuous grid with percentage values for the entire analysis domain, keeping the grid cells on which the hourly gauge resides faithful to the observed/actual percentage. Since the percentages typically have a high degree of spatial autocorrelation, the spatial interpolation has skill in determining the percentages between gauges, especially since the percentages are somewhat independent of the precipitation magnitude. The end result is a GIS grid for each hour that represents the percentage of the SPP precipitation that fell during that hour.

After the hourly percentage grids are generated and QC'ed for the entire SPP, a program is executed that converts the daily/supplemental gauge data into incremental hourly data. The timing at each of the daily/supplemental gauges is based on (1) the daily/supplemental gauge observation time, (2) daily/supplemental precipitation amount and (3) the series of interpolated hourly percentages extracted from grids (described above).

This procedure is detailed in Figure G.6 below. In this example, a supplemental gauge reported 1.40" of precipitation during the storm event and is located equal distance from the three surrounding hourly recording gauges. The procedure steps are:

- Step 1. For each hour, extract the percent of SPP from the hourly gauge-based percentage at the location of the daily/supplemental gauge. In this example, assume these values are the average of all the hourly gauges.
- Step 2. Multiply the individual hourly percentages by the total storm precipitation at the daily/supplemental gauge to arrive at estimated hourly precipitation at the daily/supplemental gauge. To make the daily/supplemental accumulated precipitation data faithful to the daily/supplemental observations, it is sometimes necessary to adjust the hourly percentages so they add up to 100% and account for 100% of the daily observed precipitation.

	Hour						
Precipitation	1	2	3	4	5	6	Total
Hourly station 1	0.02	0.12	0.42	0.50	0.10	0.00	1.16
Hourly station 2	0.01	0.15	0.48	0.62	0.05	0.01	1.32
Hourly station 3	0.00	0.18	0.38	0.55	0.20	0.05	1.36
	Hour						
Percent of total storm precip.	1	2	3	4	5	6	Total
Hourly station 1	2%	10%	36%	43%	9%	0%	100%
Hourly station 2	1%	11%	36%	47%	4%	1%	100%
Hourly station 3	0%	13%	28%	40%	15%	4%	100%
<i>Average</i>	1%	12%	34%	44%	9%	1%	100%
Storm total precipitation at daily gauge				1.40			
	Hour						
Precipitation (estimated)	1	2	3	4	5	6	Total
Daily station	0.01	0.16	0.47	0.61	0.13	0.02	1.40

Figure G.6 Example of disaggregation of daily precipitation into estimated hourly precipitation based on three (3) surrounding hourly recording gauges

In cases where the hourly grids do not indicate any precipitation falling during the daily/supplemental gauge observational period, yet the daily/supplemental gauge reported precipitation, the daily/supplemental total precipitation is evenly distributed throughout the hours that make up the observational period; although this does not happen very often, this solution is consistent with NWS procedures. However, the SPAS analyst is notified of these cases in a comprehensive log file, and in most cases they are resolvable, sometimes with a pseudo hourly gauge.

GAUGE QUALITY CONTROL

Exhaustive quality control measures are taken throughout the SPAS analysis. Below are a few of the most significant QC measures taken.

Mass Curve Check

A mass curve-based QC-methodology is used to ensure the timing of precipitation at all gauges is consistent with nearby gauges. SPAS groups each gauge with the nearest four gauges (regardless of type) into a single file. These files are subsequently used in software for graphing and evaluation. Unusual characteristics in the mass curve are investigated and the gauge data corrected, if possible and warranted. See Figure G.7 for an example.

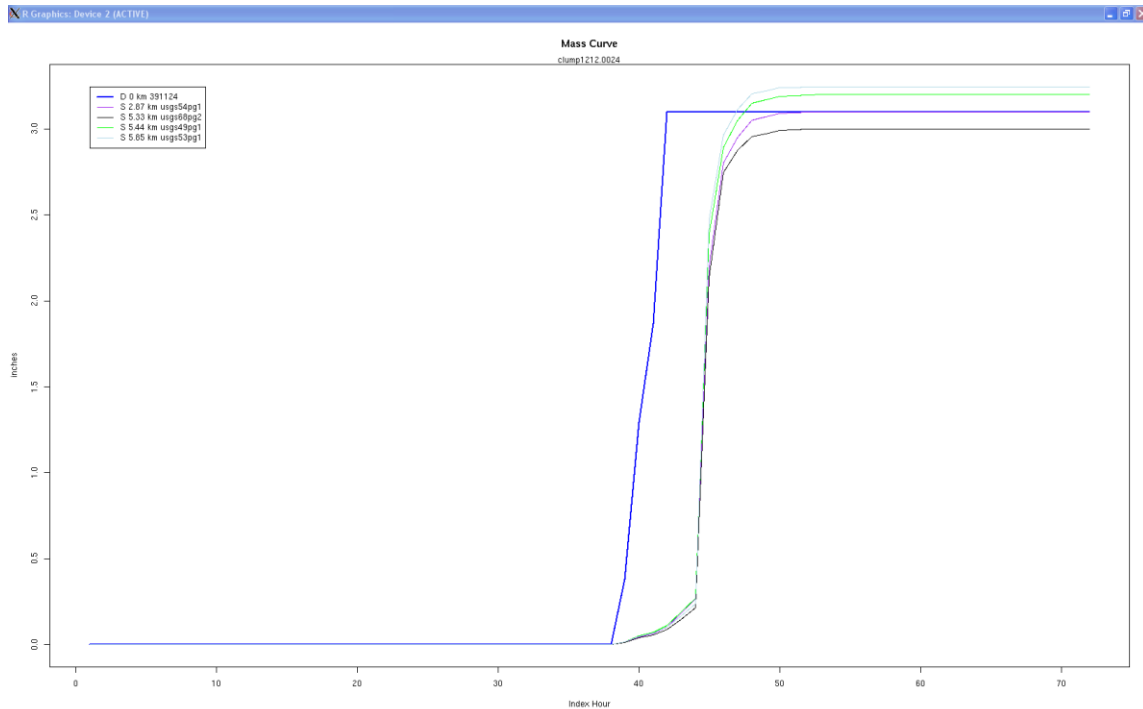


Figure G.7 Sample mass curve plot depicting a precipitation gauge with an erroneous observation time (blue line). X-axis is the SPAS index hour and the y-axis is inches. The statistics in the upper left denote gauge type, distance from target gauge (in km), and gauge ID. In this example, the center gauge (blue line) was found to have an observation error/shift of 1 day.

Gauge Mis-location Check

Although the gauge elevation is not explicitly used in SPAS, it is however used as a means of QC'ing gauge location. Gauge elevations are compared to a high-resolution 15-second DEM to identify gauges with large differences, which may indicate erroneous longitude and/or latitude values.

Co-located Gauge QC

Care is also taken to establish the most accurate precipitation depths at all co-located gauges. In general, where a co-located gauge pair exists, the highest precipitation is accepted (if accurate). If the hourly gauge reports higher precipitation, then the co-located daily (or supplemental) is removed from the analysis since it would not add anything to the analysis. Often daily (or supplemental) gauges report greater precipitation than a co-located hourly station since hourly tipping bucket gauges tend to suffer from gauge under-catch, particularly during extreme events, due to loss of precipitation during tips. In these cases the daily/supplemental is retained for the magnitude and the hourly used as a pseudo hourly gauge for timing. Large discrepancies between any co-located gauges are investigated and resolved since SPAS can only utilize a single gauge magnitude at each co-located site.

SPATIAL INTERPOLATION

At this point the QC'ed observed hourly and disaggregated daily/supplemental hourly precipitation data are spatially interpolated into hourly precipitation grids. SPAS has three options for conducting the hourly precipitation interpolation, depending on the terrain and availability of radar data, thereby allowing SPAS to be optimized for any particular storm type or location. Figure G.8 depicts the results of each spatial interpolation methodology based on the same precipitation gauge data.

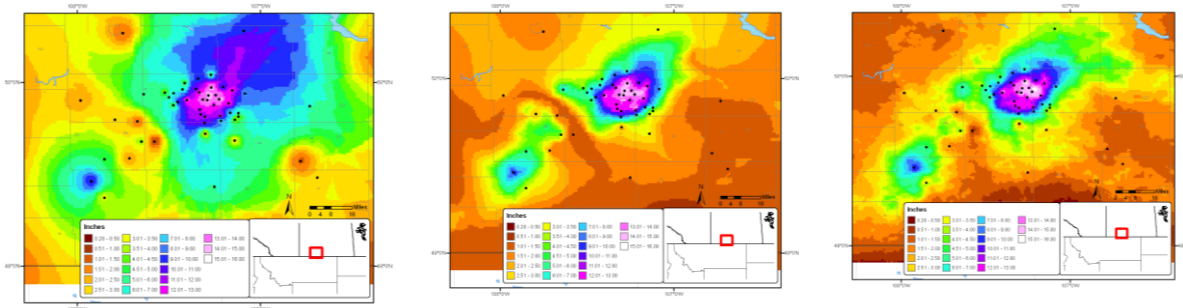


Figure G.8 Depictions of total storm precipitation based on the three SPAS interpolation methodologies for a storm (SPAS #1177, Vanguard, Canada) across flat terrain: (a) no basemap, (b) basemap-aided and (c) radar

Basic Approach

The basic approach interpolates the hourly precipitation point values to a grid using an inverse distance weighting squared GIS algorithm. This is sometimes the best choice for convective storms over flat terrain when radar data is not available, yet high gauge density instills reliable precipitation patterns. This approach is rarely used.

Basemap Approach

Another option includes the use of a “basemap”, also known as a climatologically-aided interpolation (Hunter 2005). As noted before, the spatial patterns of the basemap govern the interpolation between points of hourly precipitation estimates, while the actual hourly precipitation values govern the magnitude. This approach to interpolating point data across complex terrain is widely used. In fact, it was used extensively by the NWS during their storm analysis era from the 1940s through the 1970s.

In application, the hourly precipitation gauge values are first normalized by the corresponding grid cell value of the basemap before being interpolated. The normalization allows information and knowledge from the basemap to be transferred to the spatial distribution of the hourly precipitation. Using an IDW squared algorithm, the normalized hourly precipitation values are interpolated to a grid. The resulting grid is then multiplied by the basemap grid to produce the hourly precipitation grid. This is repeated each hour of the storm.

Radar Approach

The coupling of SPAS with NEXRAD provides the most accurate method of spatially and temporally distributing precipitation. To increase the accuracy of the results however, quality-controlled precipitation observations are used for calibrating the radar reflectivity to rain rate relationship (Z-R relationship) each hour instead of assuming a default Z-R relationship. Also, spatial variability in the Z-R relationship is accounted for through local bias corrections (described later). The radar approach involves several steps, each briefly described below. The radar approach cannot operate alone – either the basic or basemap approach must be completed before radar data can be incorporated.

Z-R Relationship

SPAS derives high quality precipitation estimates by relating quality controlled level-II NEXRAD radar reflectivity radar data with quality-controlled precipitation gauge data in order to calibrate the Z-R (radar reflectivity, Z, and precipitation, R) relationship. Optimizing the Z-R relationship is essential for capturing temporal changes in the Z-R. Most current radar-derived precipitation techniques rely on a constant relationship between radar reflectivity and precipitation rate for a given storm type (e.g., tropical, convective), vertical structure of reflectivity and/or reflectivity magnitudes. This non-linear relationship is described by the Z-R equation below:

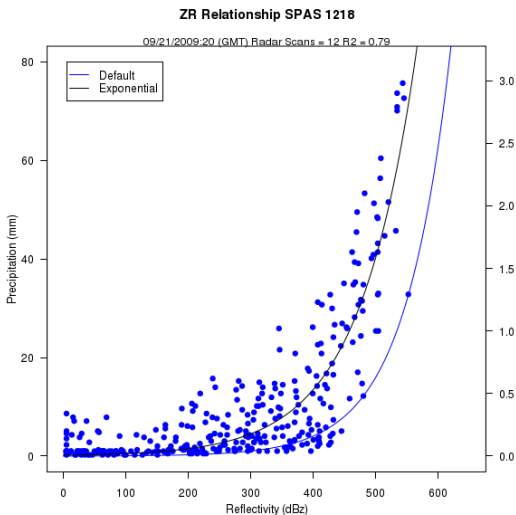


Figure G.9 Example SPAS (denoted as “Exponential”) vs. default Z-R relationship (SPAS #1218, Georgia September 2009)

SPAS calculates an optimized Z-R relationship across the analysis domain each hour based on observed precipitation rates and radar reflectivity (see Figure G.9).

The National Weather Service (NWS) utilizes different default Z-R algorithms, depending on the precipitation-causing event, to estimate precipitation through the use of NEXRAD radar reflectivity data across the United States (see Figure G.10) (Baeck and

$$Z = A R^b \quad (1)$$

Where Z is the radar reflectivity (measured in units of dBZ), R is the precipitation (precipitation) rate (millimeters per hour), A is the “multiplicative coefficient” and b is the “power coefficient”. Both A and b are directly related to the rain drop size distribution (DSD) and rain drop number distribution (DND) within a cloud (Martner and Dubovskiy 2005). The variability in the results of Z versus R is a direct result of differing DSD, DND and air mass

characteristics (Dickens 2003). The DSD and DND are determined by complex interactions of microphysical processes that fluctuate regionally, seasonally, daily, hourly, and even within the same cloud. For these reasons,

Smith 1998 and Hunter 1999). A default Z-R relationship of $Z = 300R^{1.4}$ is the primary algorithm used throughout the continental U.S. However, it is widely known that this, compared to unadjusted radar-aided estimates of precipitation, suffers from deficiencies that may lead to significant over or under-estimation of precipitation.

RELATIONSHIP	Optimum for:	Also recommended for:
Marshall-Palmer ($z=200R^{1.6}$)	General stratiform precipitation	
East-Cool Stratiform ($z=130R^{2.0}$)	Winter stratiform precipitation - east of continental divide	Orographic rain - East
West-Cool Stratiform ($z=75R^{2.0}$)	Winter stratiform precipitation - west of continental divide	Orographic rain - West
WSR-88D Convective ($z=300R^{1.4}$)	Summer deep convection	Other non-tropical convection
Rosenfeld Tropical ($z=250R^{1.2}$)	Tropical convective systems	

Figure G.10 Commonly used Z-R algorithms used by the NWS

Instead of adopting a standard Z-R, SPAS utilizes a least squares fit procedure for optimizing the Z-R relationship each hour of the SPP. The process begins by determining if sufficient (minimum 12) observed hourly precipitation and radar data pairs are available to compute a reliable Z-R. If insufficient (<12) gauge pairs are available, then SPAS adopts the previous hour Z-R relationship, if available, or applies a user-defined default Z-R algorithm from Figure 9. If sufficient data are available, the one hour sum of NEXRAD reflectivity (Z) is related to the 1-hour precipitation at each gauge. A least-squares-fit exponential function using the data points is computed. The resulting best-fit, one hour-based Z-R is subjected to several tests to determine if the Z-R relationship and its resulting precipitation rates are within a certain tolerance based on the R-squared fit measure and difference between the derived and default Z-R precipitation results. Experience has shown the actual Z-R versus the default Z-R can be significantly different (Figure G.11).

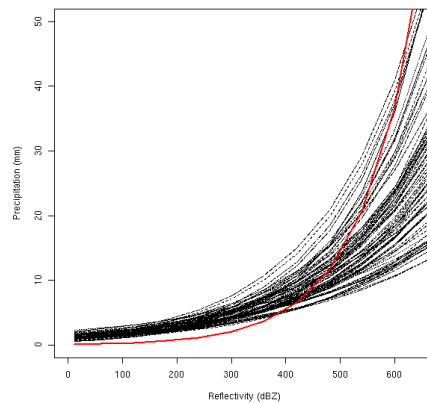


Figure G.11 Comparison of the SPAS optimized hourly Z-R relationships (black lines) versus a default $Z=75R^{2.0}$ Z-R relationship (red line) for a period of 99 hours for a storm over southern California

Radar-aided Hourly Precipitation Grids

Once a mathematically optimized hourly Z-R relationship is determined, it is applied to the total hourly Z grid to compute an initial precipitation rate (inches/hour) at each grid cell. To account for spatial differences in the Z-R relationship, SPAS computes residuals, the difference between the initial precipitation analysis (via the Z-R equation) and the actual “ground truth” precipitation (observed – initial analysis), at each gauge. The point residuals, also referred to as local biases, are normalized and interpolated to a residual grid using an inverse distance squared weighting algorithm. A radar-based hourly precipitation grid is created by adding the residual grid to the initial grid; this allows the precipitation at the grid cells for which gauges are “on” to be true and faithful to the gauge measurement. The pre-final radar-aided precipitation grid is subject to some final, visual QC checks to ensure the precipitation patterns are consistent with the terrain; these checks are particularly important in areas of complex terrain where even QC'ed radar data can be unreliable. The next incremental improvement with SPAS program will come as the NEXRAD radar sites are upgraded to dual-polarimetric capability.

Radar- and Basemap-Aided Hourly Precipitation Grids

At this stage of the radar approach, a radar- and basemap-aided hourly precipitation grid exists for each hour. At locations with precipitation gauges, the grids are equal, however elsewhere the grids can vary for a number of reasons. For instance, the basemap-aided hourly precipitation grid may depict heavy precipitation in an area of complex terrain, blocked by the radar, whereas the radar-aided hourly precipitation grid may suggest little, if any, precipitation fell in the same area. Similarly, the radar-aided hourly precipitation grid may depict an area of heavy precipitation in flat terrain that the basemap-approach missed since the area of heavy precipitation occurred in an area without gauges. SPAS uses an algorithm to compute the hourly precipitation at each pixel given the two results. Areas that are completely blocked from a radar signal are accounted for with the basemap-aided results (discussed earlier). The precipitation in areas with orographically effective terrain and reliable radar data are governed by a blend of the basemap- and radar-aided precipitation. Elsewhere, the radar-aided precipitation is used exclusively. This blended approach has proven effective for resolving precipitation in complex terrain, yet retaining accurate radar-aided precipitation across areas where radar data is reliable. Figure G.12 illustrates the evolution of final precipitation from radar reflectivity in an area of complex terrain in southern California.

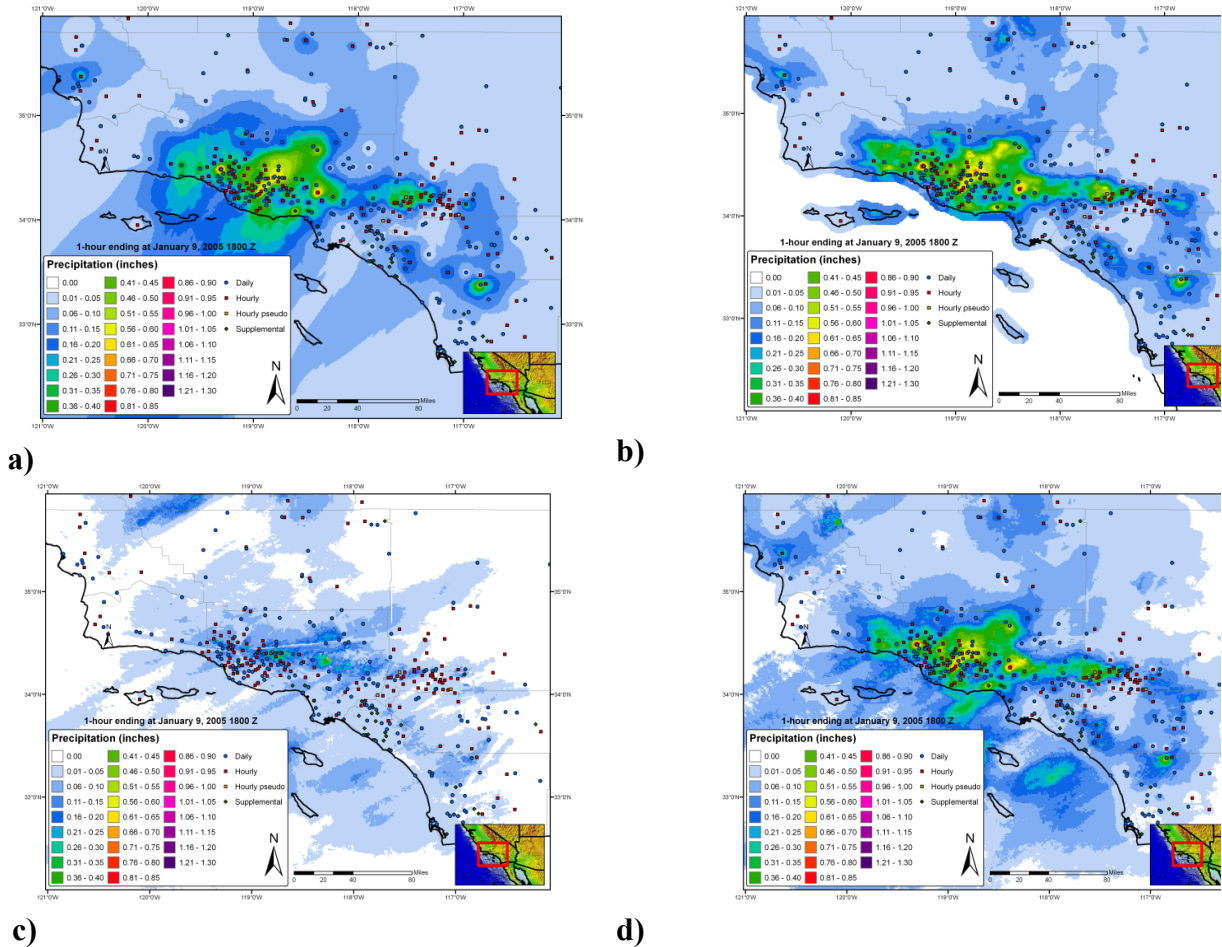


Figure G.12 A series of maps depicting 1-hour of precipitation utilizing (a) inverse distance weighting of gauge precipitation, (b) gauge data together with a climatologically-aided interpolation scheme, (c) default Z-R radar-estimated interpolation (no gauge correction) and (d) SPAS precipitation for a January 2005 storm in southern California

SPAS versus Gauge Precipitation

Performance measures are computed and evaluated each hour to detect errors and inconsistencies in the analysis. The measures include: hourly Z-R coefficients, observed hourly maximum precipitation, maximum gridded precipitation, hourly bias, hourly mean absolute error (MAE), root mean square error (RMSE), and hourly coefficient of determination (r^2).

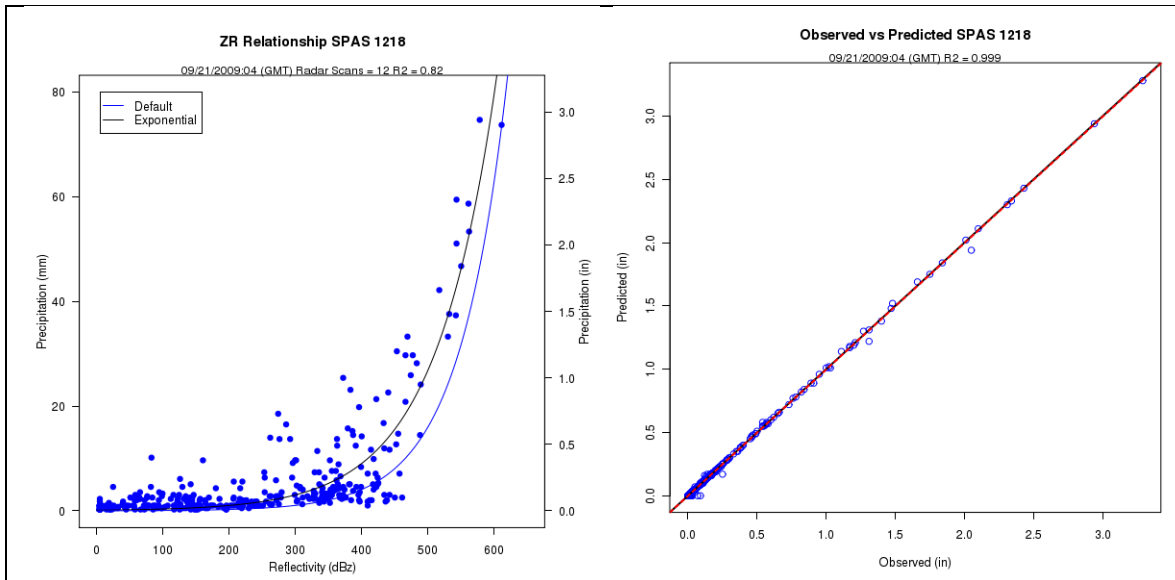


Figure G.13 Z-R plot (a), where the blue line is the SPAS derived Z-R and the black line is the default Z-R, and the (b) associated observed versus SPAS scatter plot at gauge locations

Comparing SPAS-calculated precipitation (R_{spas}) to observed point precipitation depths at the gauge locations provides an objective measure of the consistency, accuracy and bias. Generally speaking SPAS is usually within 5% of the observed precipitation (see Figure G.13). Less-than-perfect correlations between SPAS precipitation depths and observed precipitation at gauged locations could be the result of any number of issues, including:

- Point versus area:** A rain gauge observation represents a much smaller area than the area sampled by the radar. The area that the radar is sampling is approximately 1 km^2 , whereas a rain gauge only samples approximately $8.0 \times 10^{-9} \text{ km}^2$. Furthermore, the radar data represents an average reflectivity (Z) over the grid cell, when in fact the reflectivity can vary across the 1 km^2 grid cell. Therefore, comparing a grid cell radar derived precipitation value to a gauge (point) precipitation depth measured may vary.
- Precipitation gauge under-catch:** Although we consider gauge data “ground truth,” we recognize gauges themselves suffer from inaccuracies. Precipitation gauges, shielded and unshielded, inherently underestimate total precipitation due to local airflow, wind under-catch, wetting, and evaporation. The wind under-catch errors are usually around 5% but can be as large as 40% in high winds (Guo et al. 2001, Duchon and Essenberg 2001, Ciach 2003, Tokay et al. 2010). Tipping buckets miss a small amount of precipitation during each tip of the bucket due to the bucket travel and tip time. As precipitation intensities increase, the volumetric loss of precipitation due to tipping tends to increase. Smaller tipping buckets can have higher volumetric losses due to higher tip frequencies, but on the other hand capture higher precision timing.

- Radar Calibration:** NEXRAD radars calibrate reflectivity every volume scan, using an internally generated test. The test determines changes in internal variables such as beam power and path loss of the receiver signal processor since the last off-line calibration. If this value becomes large, it is likely that there is a radar calibration error that will translate into less reliable precipitation estimates. The calibration test is supposed to maintain a reflectivity precision of 1 dBZ. A 1 dBZ error can result in an error of up to 17% in R_{spas} using the default Z-R relationship $Z=300R^{1.4}$. Higher calibration errors will result in higher R_{spas} errors. However, by performing correlations each hour, the calibration issue is minimized in SPAS.
- Attenuation:** Attenuation is the reduction in power of the radar beams' energy as it travels from the antenna to the target and back. It is caused by the absorption and the scattering of power from the beam by precipitation. Attenuation can result in errors in Z as large as 1 dBZ especially when the radar beam is sampling a large area of heavy precipitation. In some cases, storm precipitation is so intense (>12 inches/hour) that individual storm cells become "opaque" and the radar beam is totally attenuated. Armed with sufficient gauge data however, SPAS will overcome attenuation issues.
- Range effects:** The curvature of the Earth and radar beam refraction result in the radar beam becoming more elevated above the surface with increasing range. With the increased elevation of the radar beam comes a decrease in Z values due to the radar beam not sampling the main precipitation portion of the cloud (i.e. "over topping" the precipitation and/or cloud altogether). Additionally, as the radar beam gets further from the radar, it naturally samples a larger and larger area, therefore amplifying point versus area differences (described above).
- Radar Beam Occultation/Ground Clutter:** Radar occultation (beam blockage) results when the radar beam's energy intersects terrain features as depicted in Figure G.14. The result is an increase in radar reflectivity values that can result in higher than normal precipitation estimates. The WDT processing algorithms account for these issues, but SPAS uses GIS spatial interpolation functions to infill areas suffering from poor or no radar coverage.
- Anomalous Propagation (AP) - AP** is false reflectivity echoes produced by unusual rates of refraction in the atmosphere. WDT algorithms remove most of the AP and false echoes, however in extreme cases the air near the ground may be so cold and dense that a radar beam that starts out moving upward is bent all the way down to the ground. This produces erroneously strong echoes at large distances from the radar. Again, equipped with sufficient gauge data, the SPAS bias corrections will overcome AP issues.

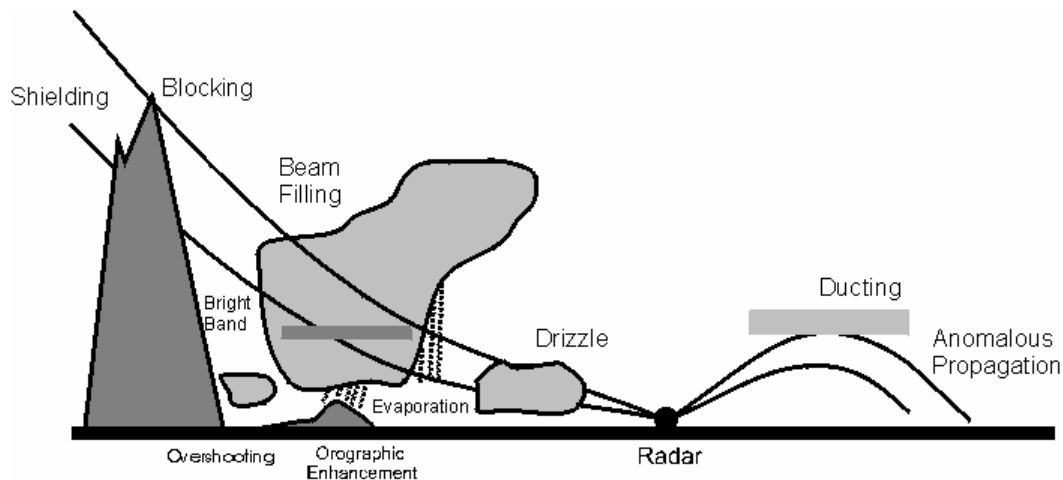


Figure G.14 Depiction of radar artifacts (Source: Wikipedia)

SPAS is designed to overcome many of these short-comings by carefully using radar data for defining the spatial patterns and relative magnitudes of precipitation, but allowing measured precipitation values (“ground truth”) at gauges to govern the magnitude. When absolutely necessary, the observed precipitation values at gauges are nudged up (or down) to force the SPAS results to be consistent with observed gauge values. Nudging gauge precipitation values helps to promote better consistency between the gauge value and the gridcell value, even though these two values sometimes should not be the same since they are sampling different area sizes. For reasons discussed in the "SPAS versus Gauge Precipitation" section, the gauge value and gridcell value can vary. Plus, SPAS is designed to toss observed individual hourly values that are grossly inconsistent with the radar data, hence driving a difference between the gauge and gridcell. In general, when the gauge and gridcell value differ by more than 15% and/or 0.50 inches, and the gauge data has been validated, then it is justified to nudge (artificially increase or decrease) the observed gauge value to "force" SPAS to derive a gridcell value equal to the observed value. Sometimes simply shifting the gauge location to an adjacent gridcell resolves the problems. Regardless, a large gauge versus gridcell difference is a "red flag" and sometimes the result of an erroneous gauge value or a mis-located gauge, but in some cases the difference can only be resolved by nudging the precipitation value.

Before final results are declared, a precipitation intensity check is conducted to ensure the spatial patterns and magnitudes of the maximum storm intensities at 1-, 6-, 12-, etc. hours are consistent with surrounding gauges and published reports. Any erroneous data are corrected and SPAS re-run. Considering all of the QA/QC checks in SPAS, it typically requires 5-15 basemap SPAS runs and, if radar data is available, another 5-15 radar-aided runs, to arrive at the final output.

Test Cases

To check the accuracy of the DAD software, three test cases were evaluated.

"Pyramidville" Storm

The first test was that of a theoretical storm with a pyramid shaped isohyetal pattern. This case was called the Pyramidville storm. It contained 361 hourly stations, each occupying a single grid cell. The configuration of the Pyramidville storm (see Figure G.15) allowed for uncomplicated and accurate calculation of the analytical DA truth independent of the DAD software. The main motivation of this case was to verify that the DAD software was properly computing the area sizes and average depths.

1. Storm center: 39°N 104°W
2. Duration: 10-hours
3. Maximum grid cell precipitation: 1.00"
4. Grid cell resolution: 0.06 sq.-miles (361 total cells)
5. Total storm size: 23.11 sq-miles
6. Distribution of precipitation:
 - Hour 1: Storm drops 0.10" at center (area 0.06 sq-miles)
 - Hour 2: Storm drops 0.10" over center grid cell AND over one cell width around hour 1 center
 - Hours 3-10:
 1. Storm drops 0.10" per hour at previously wet area, plus one cell width around previously wet area
 2. Area analyzed at every 0.10"
 3. Analysis resolution: 15-sec (~.25 square miles)

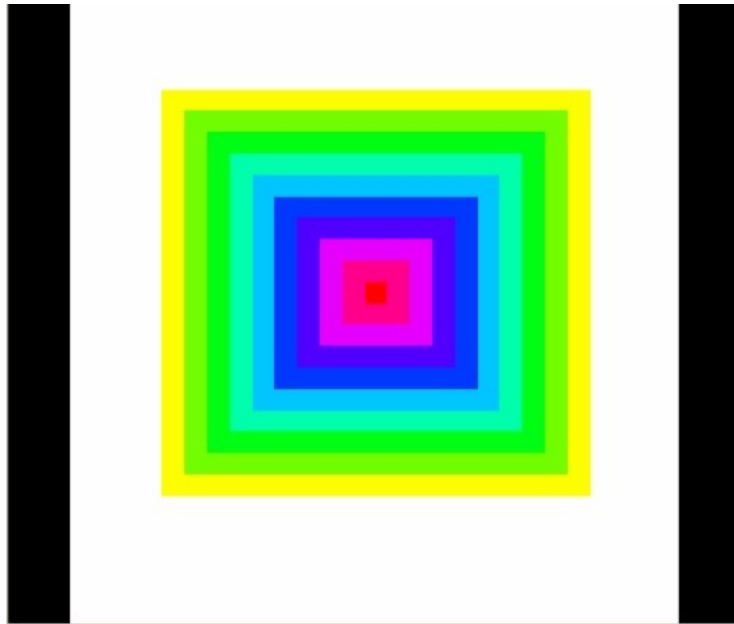


Figure G.15 "Pyramidville" Total precipitation. Center = 1.00", Outside edge = 0.10"

The analytical truth was calculated independent of the DAD software, and then compared to the DAD output. The DAD software results were equal to the truth, thus demonstrating that the DA estimates were properly calculated (Figure G.16).

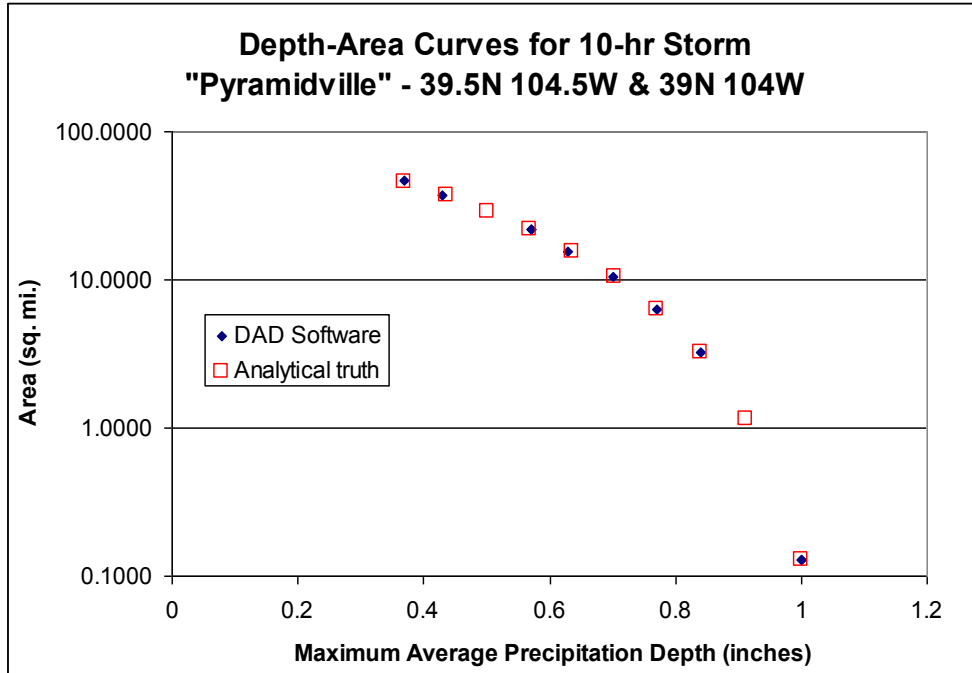


Figure G.16 10-hour DA results for “Pyramidville”; truth vs. output from DAD software

The Pyramidville storm was then changed such that the mass curve and spatial interpolation methods would be stressed. Test cases included:

- Two-centers, each center with 361 hourly stations
- A single center with 36 hourly stations, 0 daily stations
- A single center with 3 hourly stations and 33 daily stations

As expected, results began shifting from the ‘truth,’ but minimally and within the expected uncertainty.

Ritter, Iowa Storm, June 7, 1953

Ritter, Iowa was chosen as a test case for a number of reasons. The NWS had completed a storm analysis, with available DAD values for comparison. The storm occurred over relatively flat terrain, so orographics was not an issue. An extensive “bucket survey” provided a great number of additional observations from this event. Of the hundreds of additional reports, about 30 of the most accurate reports were included in the DAD analysis.

The DAD software results are very similar to the NWS DAD values (Table G.2).

Table G.2 The percent difference [(AWA-NWS)/NWS] between the AWA DA results and those published by the NWS for the 1953 Ritter, Iowa storm

%
Difference

Area (sq.mi.)	Duration (hours)				
		6	12	24	total
10		-15%	-7%	2%	2%
100		-7%	-6%	1%	1%
200		2%	0%	9%	9%
1000		-6%	-7%	4%	4%
5000		-13%	-8%	2%	2%
10000		-14%	-6%	0%	0%

Westfield, Massachusetts Storm, August 8, 1955

Westfield, Massachusetts was also chosen as a test case for a number of reasons. It is a probable maximum precipitation (PMP) driver for the northeastern United States. Also, the Westfield storm was analyzed by the NWS and the DAD values are available for comparison. Although this case proved to be more challenging than any of the others, the final results are very similar to those published by the NWS (Table G.3).

Table G.3 The percent difference [(AWA-NWS)/NWS] between the AWA DA results and those published by the NWS for the 1955 Westfield, Massachusetts storm

%
Difference

Area (sq. mi.)	Duration (hours)							
		6	12	24	36	48	60	total
10		2%	3%	0%	1%	-1%	0%	2%
100		-5%	2%	4%	-2%	-6%	-4%	-3%
200		-6%	1%	1%	-4%	-7%	-5%	-5%
1000		-4%	-2%	1%	-6%	-7%	-6%	-3%
5000		3%	2%	-3%	-3%	-5%	-5%	0%
10000		4%	9%	-5%	-4%	-7%	-5%	1%
20000		7%	12%	-6%	-3%	-4%	-3%	3%

The principal components of SPAS are: storm search, data extraction, quality control (QC), conversion of daily precipitation data into estimated hourly data, hourly and total storm precipitation grids/maps and a complete storm-centered DAD analysis.

OUTPUT

Armed with accurate, high-resolution precipitation grids, a variety of customized output can be created (see Figures G.17a-d). Among the most useful outputs are sub-hourly precipitation grids for input into hydrologic models. Sub-hourly (i.e. 5-minute) precipitation grids are created by applying the appropriate optimized hourly Z-R (scaled down to be applicable for instantaneous Z) to each of the individual 5-minute radar scans; 5-minutes is often the native scan rate of the radar in the US. Once the scaled Z-R is applied to each radar scan, the resulting precipitation is summed up. The proportion of each 5-minute precipitation to the total 1-hour radar-aided precipitation is calculated. Each 5-minute proportion (%) is then applied to the quality controlled, bias corrected 1-hour total precipitation (created above) to arrive at the final 5-minute precipitation for each scan. This technique ensures the sum of 5-minute precipitation equals that of the quality controlled, bias corrected 1-hour total precipitation derived initially.

Depth-area-duration (DAD) tables/plots, shown in Figure G.17d, are computed using a highly-computational extension to SPAS. DADs provide an objective three dimensional (magnitude, area size, and duration) perspective of a storms' precipitation. SPAS DADs are computed using the procedures outlined by the NWS Technical Paper 1 (1946).

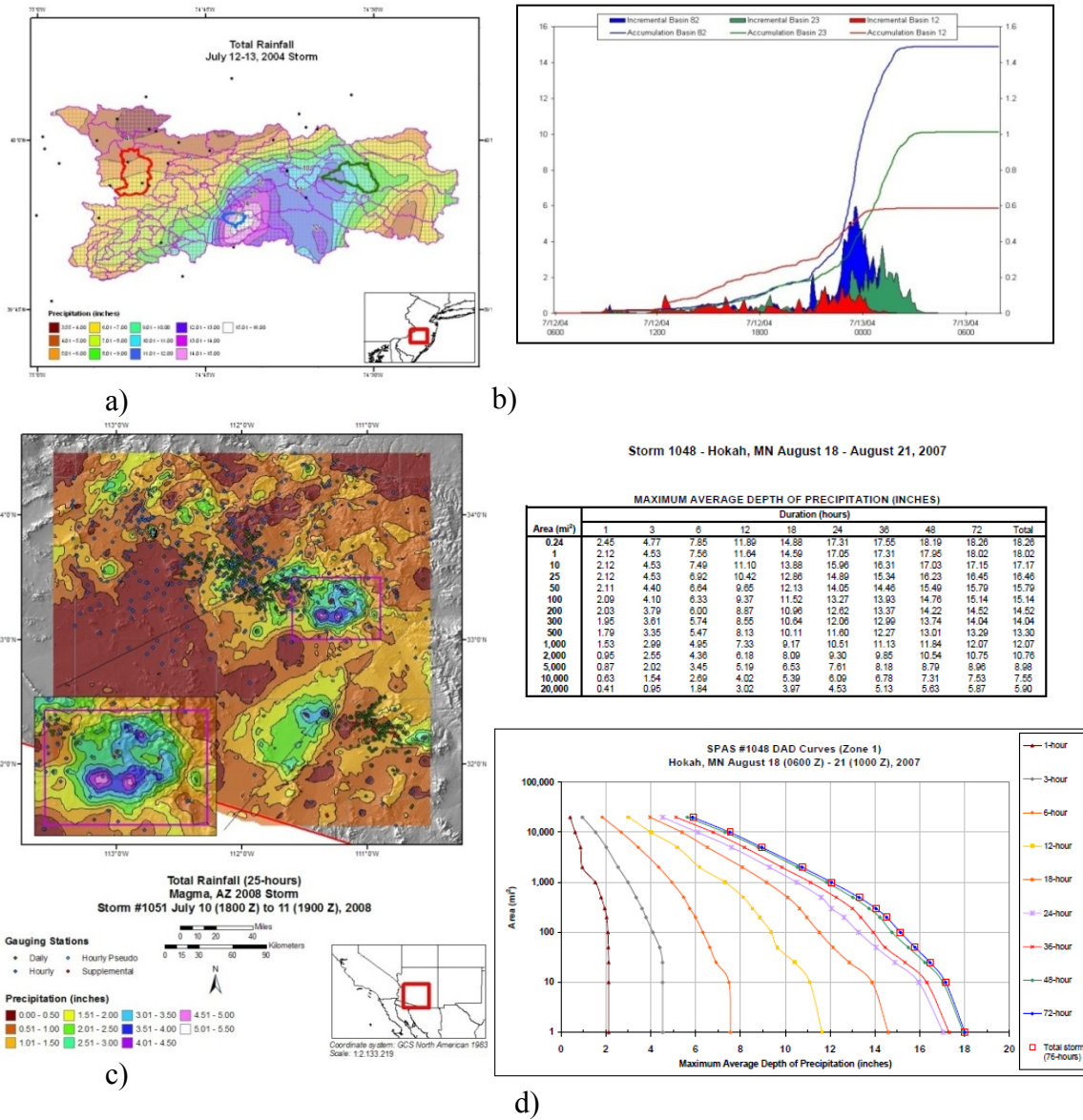


Figure G.17 Various examples of SPAS output, including (a) total storm map and its associated (b) basin average precipitation time series, (c) total storm precipitation map, (d) depth-area-duration (DAD) table and plot, and (e) precipitation gauge catalog with total storm statistics.

SUMMARY

Grounded on years of scientific research with a demonstrated reliability in post-storm analyses, SPAS is a hydro-meteorological tool that provides accurate precipitation analyses for a variety of applications. SPAS has the ability to compute precise and accurate results by using sophisticated timing algorithms, “basemaps”, a variety of

precipitation data and most importantly NEXRAD weather radar data (if available). The approach taken by SPAS relies on hourly, daily and supplemental precipitation gauge observations to provide quantification of the precipitation amounts while relying on basemaps and NEXRAD data (if available) to provide the spatial distribution of precipitation between precipitation gauge sites. By determining the most appropriate coefficients for the Z-R equation on an hourly basis, the approach anchors the precipitation amounts to accepted precipitation gauge data while using the NEXRAD data to distribute precipitation between precipitation gauges for each hour of the storm. Hourly Z-R coefficient computations address changes in the cloud microphysics and storm characteristics as the storm evolves. Areas suffering from limited or no radar coverage, are estimated using the spatial patterns and magnitudes of the independently created basemap precipitation grids. Although largely automated, SPAS is flexible enough to allow hydro-meteorologists to make important adjustments and adapt to any storm situation.

REFERENCES

- Baeck M.L., Smith J.A., 1998: “Precipitation Estimation by the WSR-88D for Heavy Precipitation Events”, *Weather and Forecasting*: Vol. 13, No. 2, pp. 416–436.
- Ciach, G.J., 2003: Local Random Errors in Tipping-Bucket Rain Gauge Measurements. *J. Atmos. Oceanic Technol.*, **20**, 752–759.
- Dickens, J., 2003: “On the Retrieval of Drop Size Distribution by Vertically Pointing Radar”, American Meteorological Society 32nd Radar Meteorology Conference, Albuquerque, NM, October 2005.
- Duchon, C.E., and G.R. Essenberg, 2001: Comparative Precipitation Observations from Pit and Above Ground Rain Gauges with and without Wind Shields, *Water Resources Research*, Vol. 37, N. 12, 3253-3263.
- Faulkner, E., T. Hampton, R.M. Rudolph, and Tomlinson, E.M., 2004: Technological Updates for PMP and PMF – Can They Provide Value for Dam Safety Improvements? Association of State Dam Safety Officials Annual Conference, Phoenix, Arizona, September 26- 30, 2004
- Guo, J. C. Y., Urbonas, B., and Stewart, K., 2001: Rain Catch under Wind and Vegetal Effects. *ASCE, Journal of Hydrologic Engineering*, Vol. 6, No. 1.
- Hunter, R.D. and R.K. Meentemeyer, 2005: Climatologically Aided Mapping of Daily Precipitation and Temperature, *Journal of Applied Meteorology*, October 2005, Vol. 44, pp. 1501-1510.
- Hunter, S.M., 1999: Determining WSR-88D Precipitation Algorithm Performance Using The Stage III Precipitation Processing System, Next Generation Weather Radar Program, WSR-88D Operational Support Facility, Norman, OK.
- Lakshmanan, V. and M. Valente, 2004: Quality control of radar reflectivity data using satellite data and surface observations, 20th Int’l Conf. on Inter. Inf. Proc. Sys. (IIPS) for Meteor., Ocean., and Hydr., Amer. Meteor. Soc., Seattle, CD-ROM, 12.2.
- Martner, B.E, and V. Dubovskiy, 2005: Z-R Relations from Raindrop Disdrometers: Sensitivity To Regression Methods And DSD Data Refinements, 32nd Radar Meteorology Conference, Albuquerque, NM, October, 2005
- Tokay, A., P.G. Bashor, and V.L. McDowell, 2010: Comparison of Rain Gauge Measurements in the Mid-Atlantic Region. *J. Hydrometeor.*, **11**, 553-565.
- Tomlinson, E.M., W.D. Kappel, T.W. Parzybok, B. Rappolt, 2006: Use of NEXRAD Weather Radar Data with the Storm Precipitation Analysis System (SPAS) to Provide

High Spatial Resolution Hourly Precipitation Analyses for Runoff Model Calibration and Validation, ASDSO Annual Conference, Boston, MA.

Tomlinson, E.M. and T.W. Parzybok, 2004: Storm Precipitation Analysis System (SPAS), proceedings of Association of Dam Safety Officials Annual Conference, Technical Session II, Phoenix, Arizona.

_____, R.A. Williams, and T.W. Parzybok, September 2003: Site-Specific Probable Maximum Precipitation (PMP) Study for the Great Sacandaga Lake / Stewarts Bridge Drainage Basin, Prepared for Reliant Energy Corporation, Liverpool, New York.

_____, R.A. Williams, and T.W. Parzybok, September 2003: Site-Specific Probable Maximum Precipitation (PMP) Study for the Cherry Creek Drainage Basin, Prepared for the Colorado Water Conservation Board, Denver, CO.

_____, Kappel W.D., Parzybok, T.W., Hultstrand, D., Muhlestein, G., and B. Rappolt, May 2008: Site-Specific Probable Maximum Precipitation (PMP) Study for the Wanahoo Drainage Basin, Prepared for Olsson Associates, Omaha, Nebraska.

_____, Kappel W.D., Parzybok, T.W., Hultstrand, D., Muhlestein, G., and B. Rappolt, June 2008: Site-Specific Probable Maximum Precipitation (PMP) Study for the Blenheim Gilboa Drainage Basin, Prepared for New York Power Authority, White Plains, NY.

_____, Kappel W.D., and T.W. Parzybok, February 2008: Site-Specific Probable Maximum Precipitation (PMP) Study for the Magma FRS Drainage Basin, Prepared for AMEC, Tucson, Arizona.

_____, Kappel W.D., Parzybok, T.W., Hultstrand, D., Muhlestein, G., and P. Sutter, December 2008: Statewide Probable Maximum Precipitation (PMP) Study for the state of Nebraska, Prepared for Nebraska Dam Safety, Omaha, Nebraska.

_____, Kappel, W.D., and Tye W. Parzybok, July 2009: Site-Specific Probable Maximum Precipitation (PMP) Study for the Scoggins Dam Drainage Basin, Oregon.

_____, Kappel, W.D., and Tye W. Parzybok, February 2009: Site-Specific Probable Maximum Precipitation (PMP) Study for the Tuxedo Lake Drainage Basin, New York.

_____, Kappel, W.D., and Tye W. Parzybok, February 2010: Site-Specific Probable Maximum Precipitation (PMP) Study for the Magma FRS Drainage Basin, Arizona.

_____, Kappel W.D., Parzybok, T.W., Hultstrand, D.M., Muhlestein, G.A., March 2011: Site-Specific Probable Maximum Precipitation Study for the Tarrant

Regional Water District, Prepared for Tarrant Regional Water District, Fort Worth, Texas.

_____, Kappel, W.D., Hultstrand, D.M., Muhlestein, G.A., and T. W. Parzybok, November 2011: Site-Specific Probable Maximum Precipitation (PMP) Study for the Lewis River basin, Washington State.

_____, Kappel, W.D., Hultstrand, D.M., Muhlestein, G.A., and T. W. Parzybok, December 2011: Site-Specific Probable Maximum Precipitation (PMP) Study for the Brassua Dam basin, Maine.

U.S. Weather Bureau, 1946: Manual for Depth-Area-Duration analysis of storm precipitation. *Cooperative Studies Technical Paper No. 1*, U.S. Department of Commerce, Weather Bureau, Washington, D.C., 73pp.

Appendix H

Smethport, PA 1942 Extreme Rainfall Event Transposition Limitations Memo



PO Box 680
Monument, Co 80132
(719) 488-9117

<http://appliedweatherassociates.com>

July 25, 2011

Memo for Record

To: Ohio PMP Review Board

Subject: **Discussion and Recommendation Regarding the Transposition Limits of the Smethport 1942 Extreme Rainfall**

Introduction

Applied Weather Associates (AWA) has thoroughly investigated the Smethport July 1942 Mesoscale Convective Complex (MCC) which produced world record level rainfalls at durations of 4 to 12 hours in north central Pennsylvania. This storm was extensively investigated by the Weather Bureau (now the NWS), USGS, West Penn Power Company and the United States Engineer Office to collect both official and unofficial rainfall and stream flow measurements and erosion observations throughout the region. Vast amounts of data was collected and analyzed. This data has led to a high level of confidence in the storm patterns and timing, even without the help of NEXRAD. The spatial distribution and magnitude of this storm was highly influenced by the local terrain, as elevations rise and fall abruptly in the region, helping to focus the heaviest areas of precipitation and also helping to channel low level winds and moisture transport to favored areas. This memo will discuss whether this storm is transpositionable to any location within the state of Ohio, and if so what those limits would be. In order to determine the transposition limits of the storm the following aspects will be discussed in relation to what may be expected in Ohio: an investigation of the storm dynamics, general synoptic situation, interactions with topography, similarities and differences with conditions that are found in Ohio, and AWA's recommendation.

Overview

AWA has conducted extensive evaluations of the Smethport storm over the last several years. These include analyzing all available rainfall data, various reports and analysis from several agencies, analysis of the highest rainfall totals, exposure and accuracy of observations, and the synoptic and mesoscale environments. Included in these analyses were understanding of the interaction of the unique topography of the storm location and its interaction with the storm development and propagation. This is explicitly relevant for the current PMP study within Ohio and whether the storm could have occurred in the same manner in Ohio. By definition, in order for the storm

to be considered transpositionable, both meteorological and topographic environment must be homogenous at the two locations being considered. If either of these scenarios is violated, then the storm in question cannot be transpositioned to the other location.

Smethport Storm Event Background

The extreme rainfall which occurred in the Smethport area of north central Pennsylvania (Figure 1) was by all accounts an extraordinary amount of rainfall. The most extreme rainfall amounts were limited to individual rainfall cells embedded within the larger region of heavy rainfall. Rainfall occurred the evening of July 17th through the afternoon of July 18th, 1942. Thirteen separate centers reported 20 inches or more of rainfall in 12 hours or less, with 34.5 inches being the largest amount reported at Smethport, PA. This established a new world record rainfall amount for that time period. This storm resulted from recurrent thunderstorm activity associated with an atmospheric flow pattern that had been responsible for several previous flood events from Missouri (e.g., East St Louis, July 8, 1942) through Ohio, Kentucky, and Pennsylvania.

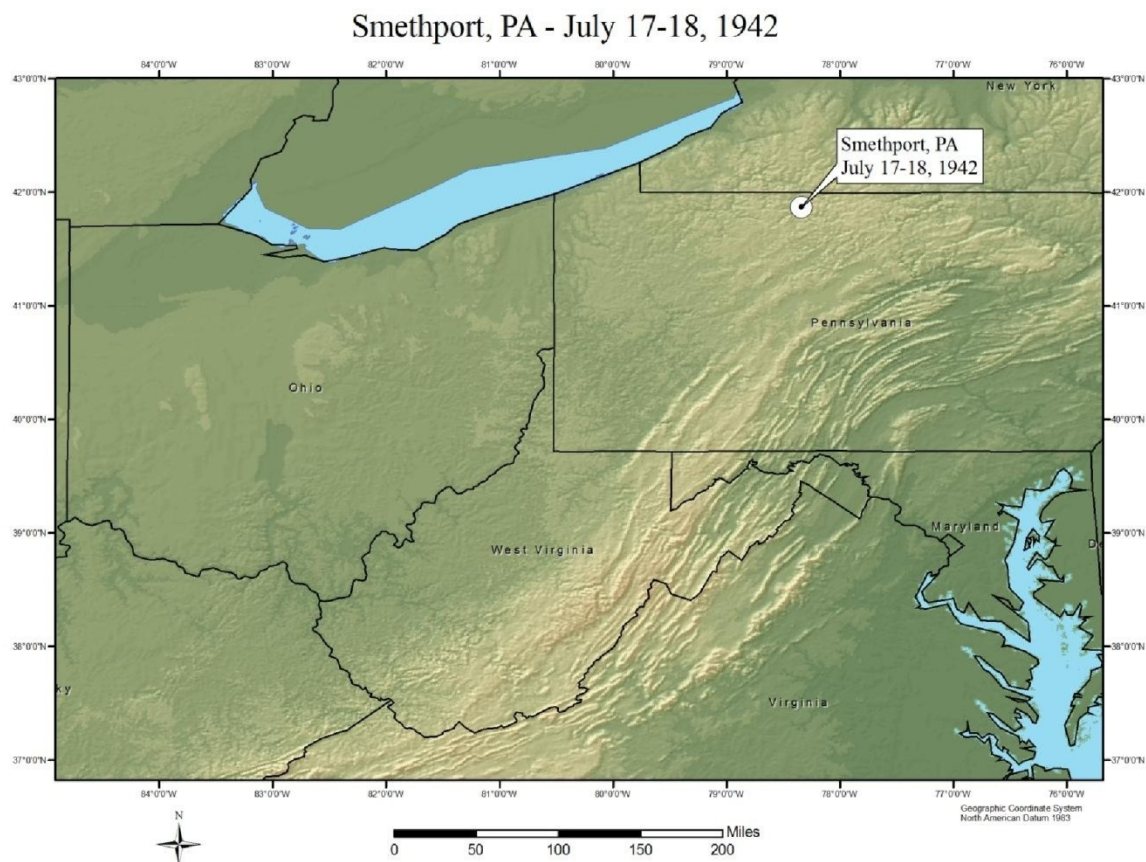


Figure 1. Regional location of Smethport, PA in relation to the state of Ohio

Recently re-analysis of the event shows that none of the highest rainfall amounts were recorded in standard rain gauges and therefore some of the magnitudes may be in

question. However, for purposes of this memo, the exact amount of rainfall is not in question; instead the processes which led to the heavy rainfall and whether they could occur in Ohio are being investigated.

The NWS used this storm in the development of the PMP values in HMR 51, utilizing the USACE storm studies analysis (OR 9-23). Also, as part of their analysis, the NWS produced explicit transposition limits for the storm. Unfortunately, the methods and data used to derive the transposition limits displayed in Figure 2 is not documented and therefore can't be verified and validated. Further, for some reason they made two versions, an original which was then re-drawn and adjusted. These are very low resolution, hand drawn maps which do not properly take into account the highly variable topography of the region affected. For purposes of this investigation, these are only used a reference and not as guidance.

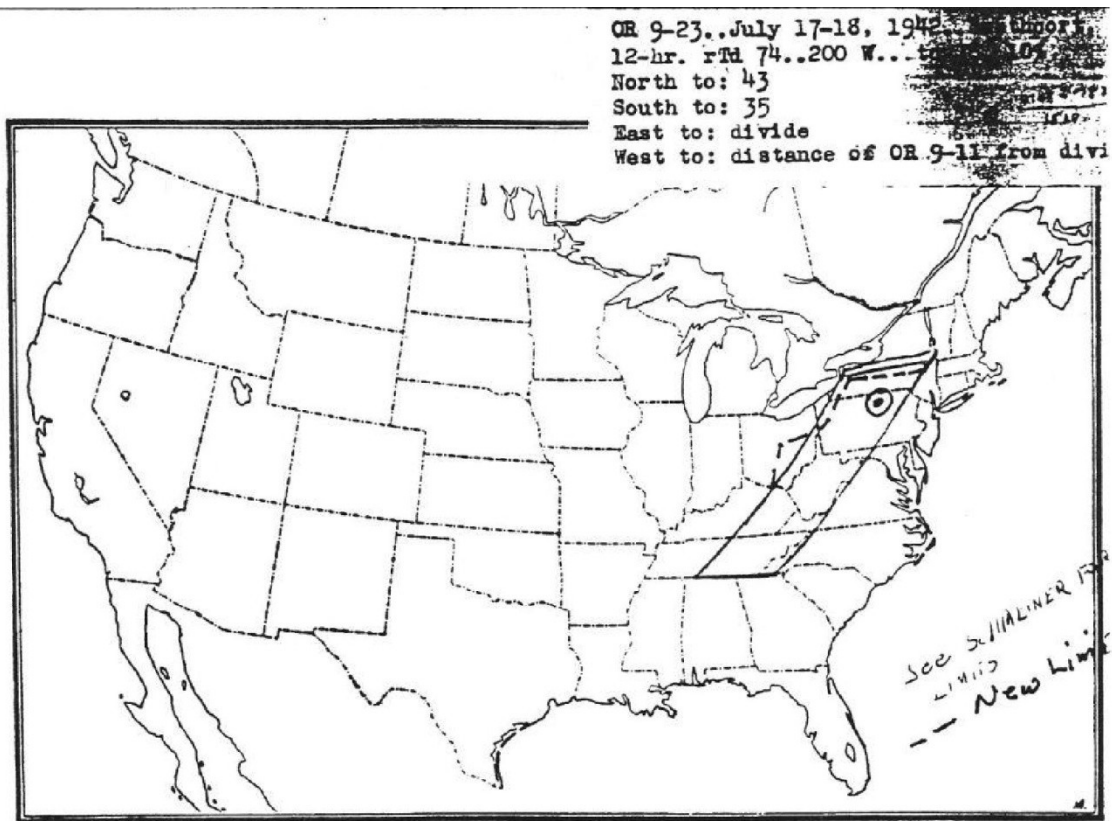


Figure 2. Smethport transposition limits produced by the NWS. Note there are two versions on this map for unknown reasons

Synoptic Pattern Associated with the Storm

The weather pattern of July 17-18 was a stagnant type characterized by a warm anticyclone centered over the Southeastern United States and the Atlantic Ocean. This pattern circulated maritime tropical moist air northward from the Gulf of Mexico over the upper Midwest, then eastward into New York and southeastward into Pennsylvania. A

quasi-stationary front extended eastward from Minnesota through the Great Lakes and then southward through eastern New York and New Jersey. This front advanced slowly northeastward during July 18th.

Both atmospheric dynamics and orographic lift of the very moist air south of the front contributed to the initiation of the thunderstorm cells. There was a regenerating influence of the locally formed dense, cold air mass in the vicinity of the heavy rain. The cooled surface air layers were due to persisting moderate to heavy precipitation, evaporative cooling, hail melting and cold rain conduction. These cold air masses acted as mini-cold fronts initiating additional thunderstorm cells. Winds over the region were from the northwest with no southerly component observed.

The slow moving frontal zone became pronounced about sunset on July 17th initiating heavy rainfall from thunderstorms over southern New York then spreading southward into Pennsylvania during the early morning hours. The thunderstorms moved southeastward steered by the northwest wind flow aloft. However, thunderstorms also developed and propagated southwestward. During the pre-dawn hours of July 18th, the rainfall spread northeastward along the frontal boundary. About sunrise, the rainfall region moved southwestward, bringing a wave of heavy rainfall. By the afternoon hours, temperatures cooled dramatically and the rainfall diminished. This could account for the "propagation" of the storm system towards the southwest while individual cells moved towards the southeast in the prevailing flow. This is also supported by the observation that thunderstorms "spread fanwise" during the early morning hours of July 18, 1942.

There were three successive periods of downpours with the first and the last being the most intense. The greatest rainfall fell in a region containing no official rain gages. The heaviest rainfall was in the Allegheny Basin above Eldred, where storm totals of 35.5" and 34.5" were reported. The main orientation of the rainfall pattern was northwest to southeast consistent with the northwesterly winds aloft and anchored to the underlying topography. Great variations in intensity within relatively short distances occurred during the storm.

Analysis Relating to the Transpositioning to Ohio

Extensive discussions have occurred as part of this PMP study regarding this event and its potential transpositionability to Ohio with the Review Board and internally within AWA. It has been determined that the general synoptic patterns associated with the storm's development could occur (and have occurred) in the same way over any portion of Ohio as occurred during the actual storm event. The storm type was a mesoscale convective complex (MCC). The MCC storm type has been extensively studied over the last 30 years (see Maddox 1980, 1981 for example) and is recognized as important rainfall producers over small area sizes (less than 500-square miles) and short durations (less than 12-hours). This storm type occurs frequently from April through October from the foothills of the Rockies through the east coast of the United States, including all of Ohio.

Therefore, consideration of the meteorological portion of the transposition definition is satisfied with this storm.

Extensive analysis was then completed on the interaction of the highly variable topography in and around the Smethport region with the storm environment and its effects on rainfall production, magnitude, and spatial distributions. Guidance regarding transpositionability is given in HMR 51 Section 2.4.2,

“Topography is one of the more important controls on limits to storm transposition. If observed rainfall patterns show correspondence with underlying terrain features, or indicate triggering of rainfall by slopes, transposition should be limited to areas of similar terrain.”

And in HMR 51 Section 2.4.2, steps a and c,

“Transposition was not permitted across the generalized Appalachian Mountain ridge.”

“In regions of large elevation difference, transpositions were restricted to a narrow elevation band (usually within a 1000 ft of the elevation of the storm center).”

The Smethport storm’s spatial pattern of multiple centers was primarily attributed to two factors. The region where the most extreme rainfall occurred is within the western slopes of the Appalachian Mountains where topographic features influence boundary layer wind flows. Upslope regions initiate updrafts and lead to convective cloud development in highly unstable atmospheric conditions. Hence regions of upslope boundary layer winds are associated with enhanced cloud development and potentially extreme rainfall centers. Additionally, as presented in the Weather Bureau Smethport storm discussions (Weather Bureau, 1943), the outflow boundaries created by cold downdrafts from heavy rain cells initiated adjacent convection clouds acting as mini-frontal boundaries. These two factors, topography and outflow boundaries, were responsible for creating the thirteen separate heavy rainfall centers with individual storm rainfall totals of 20 inches or more.

AWA was able to utilize tools not available to the NWS (such as GIS) and updated understanding of orographics affects on rainfall production and distribution. A GIS projects was set up to explicitly analyze the topography of Ohio and Pennsylvania, specifically regarding the elevation changes and gradients in the two states. Figure 3 shows the variation in elevation across the two states and surrounding region using a 500 foot increment. Notice the large gradient around Smethport, PA and eastward as compared to Ohio, where this is almost no gradient evident across the state.

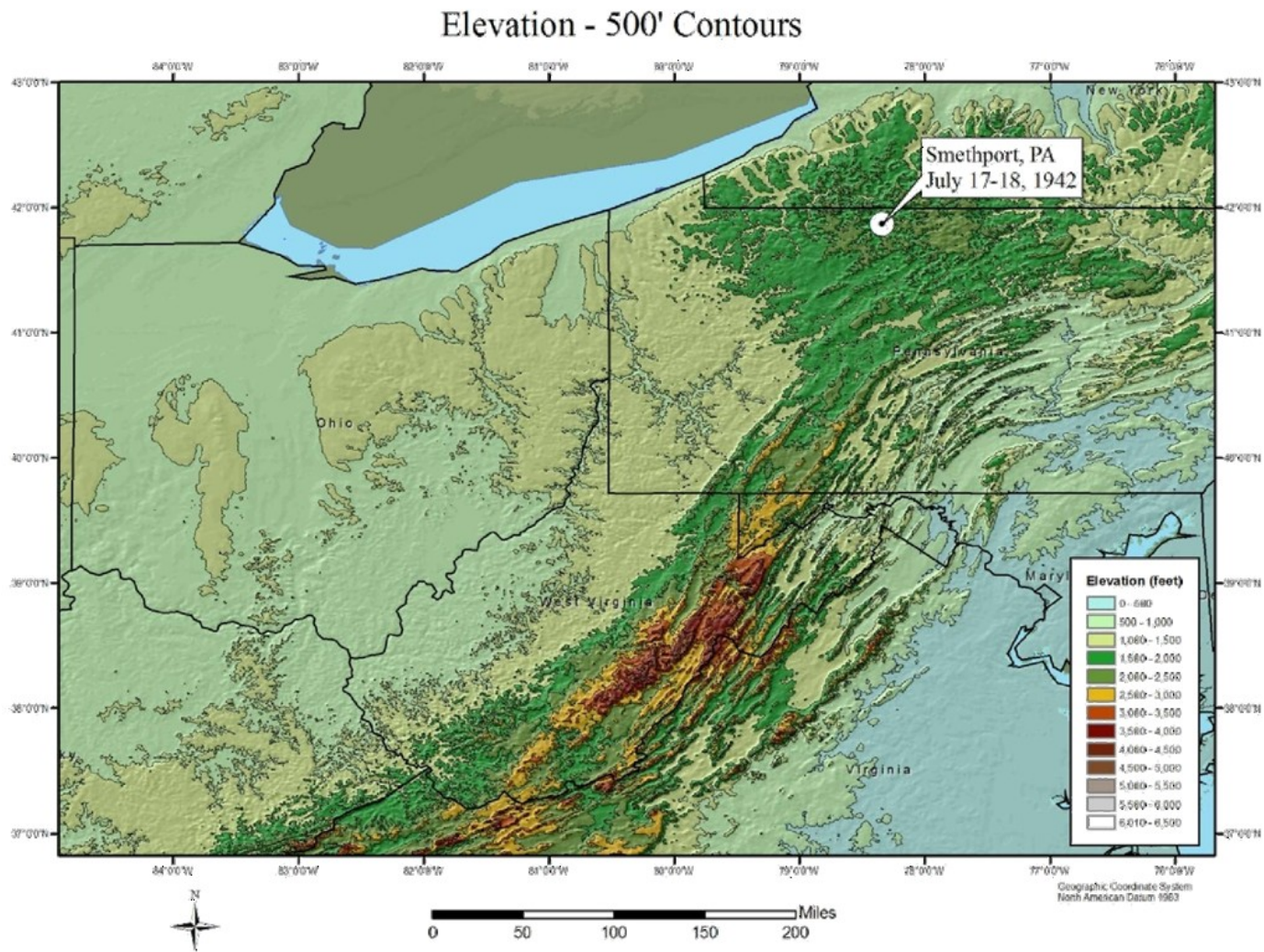


Figure 3. Elevation contours at 500 foot increments across Ohio, Pennsylvania, and West Virginia

In general, Pennsylvania has a much greater variation in elevation range across the state, and specifically around the Smethport region. Even more important is the gradient between the varying elevations. This shows an even greater difference between two states. Figure 4 shows the gradient in Ohio, Pennsylvania, and surrounding regions. Notice the amount of elevation change over very short distances around the Smethport region and along the Appalachian chain, while no locations in the state of Ohio is there a similar gradient. This is important because storm dynamics, and therefore rainfall production, are directly related to the amount of elevation change over distance, with a larger elevation change over a shorter distance leading to more efficient storm dynamics and higher rainfall production. Further, rainfall patterns are disrupted more effectively by a higher gradient. Therefore, rainfall patterns become anchored to specific terrain features, resulting in much higher amounts of rainfall occurring on the higher windward slope locations and much lower rainfall amounts occurring on the lower leeward slopes. This is evident in the Smethport storm by the location of the highest rainfall storm centers and how they are very closely tied to the terrain (Figure 5). Notice in most cases, the rainfall amount on and associated with a ridgeline is 2 to 3 times greater than an adjacent valley location. Further, the gradient between rainfall amounts is extreme, going from over 30 inches to less than 7 inches in less than a mile.

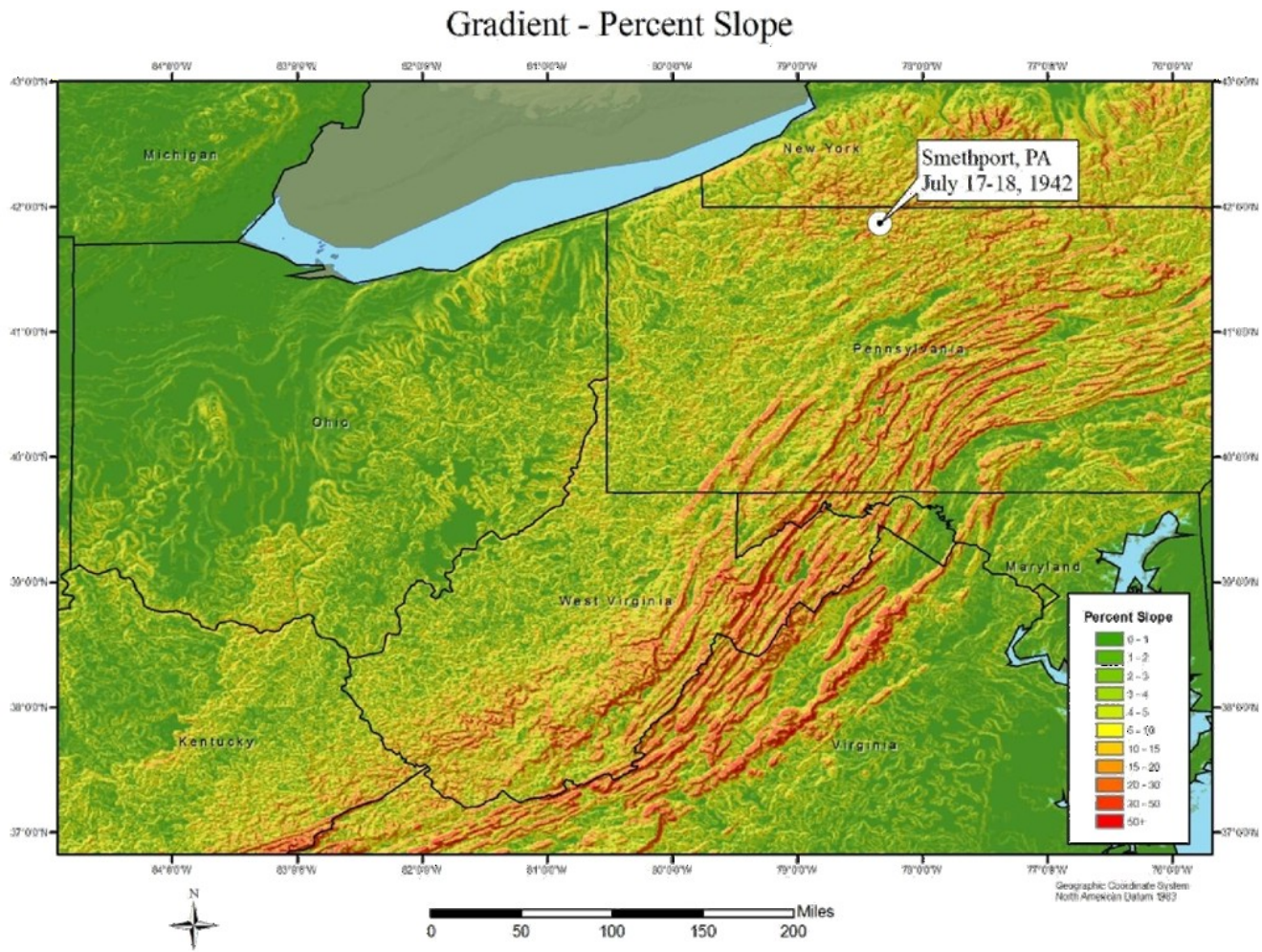


Figure 4. Elevation gradients across Ohio, Pennsylvania, and West Virginia. Red and orange shadings are higher gradients, yellows and greens are lower gradients.

Storm Isohyetal Patterns and Analysis

It should be noted however, that because there was no NEXRAD weather radar available to analyze the spatial characteristics of the rainfall in between rain gauge locations, exact spatial patterns are not possible to quantify. Instead, the spatial pattern is limited to the location of the rain gauge and bucket survey reports, which are generally located in lower elevations where people live, and the interpolation of the various parties who produced the total storm isohyetal patterns.

Much effort was put into the construction of a storm isohyetal maps with the primary analysis constructed by Mr. J.E. Stewart of West Penn Power Company and modified by the Weather Bureau, the Corps of Engineers and the USGS. A letter dated November 26, 1943 from Mr. William R. Hiatt, Acting Hydrologic Director at the Weather Bureau, includes the following paragraph:

“It should be noted that equally plausible interpretations of the unofficial rainfall reports could lead to different isohyetal values near the storm center. Material differences in resulting duration-depth data would become negligible for the larger areas but any duration-depth computations for the areas under 100 square miles should be classed as doubtful.”

In another letter from the Office of Hydrologic Director, dated June 22, 1943, Mr. Merrill Bernard states:

“...that unless we have actual measurements of rainfall or other definite information which could be used to evaluate the amount of rainfall we cannot estimate the amount from nearby records and be sure of any degree of accuracy.”

A letter from Mr. J.W. Mangan, District Engineer, USGS to Mr. Merrill Bernard at the Weather Bureau states that Mr. Stewart of West Penn Power Company is very satisfied that the 20 inch isohyetal is well fixed but above that magnitude there is considerable doubt.

There appears to be at least four versions of the isohyetal analysis. Mr. Stewart of West Penn Power Company produced the first based on precipitation records, topography, and relative erosion in small streams. This map was reviewed by the Weather Bureau and modified slightly to take into account the meteorological characteristics of the storm. The Corps of Engineers made an extensive hydrologic analysis of the storm. As a result of that analysis, it was concluded by the Corps of Engineers that the Weather Bureau map showed too much total precipitation over the storm area for the runoff observed. The Corps of Engineers prepared a new map that shows considerably less precipitation. The USGS map is basically the Weather Bureau map redrawn in such a manner that wherever an acceptable interpretation of the data could be made showing less precipitation than the Weather Bureau map, that one was used. The resulting map is quite similar to the one prepared by the Corps of Engineers. Figure 6 shows the isohyetal map from the USGS report.

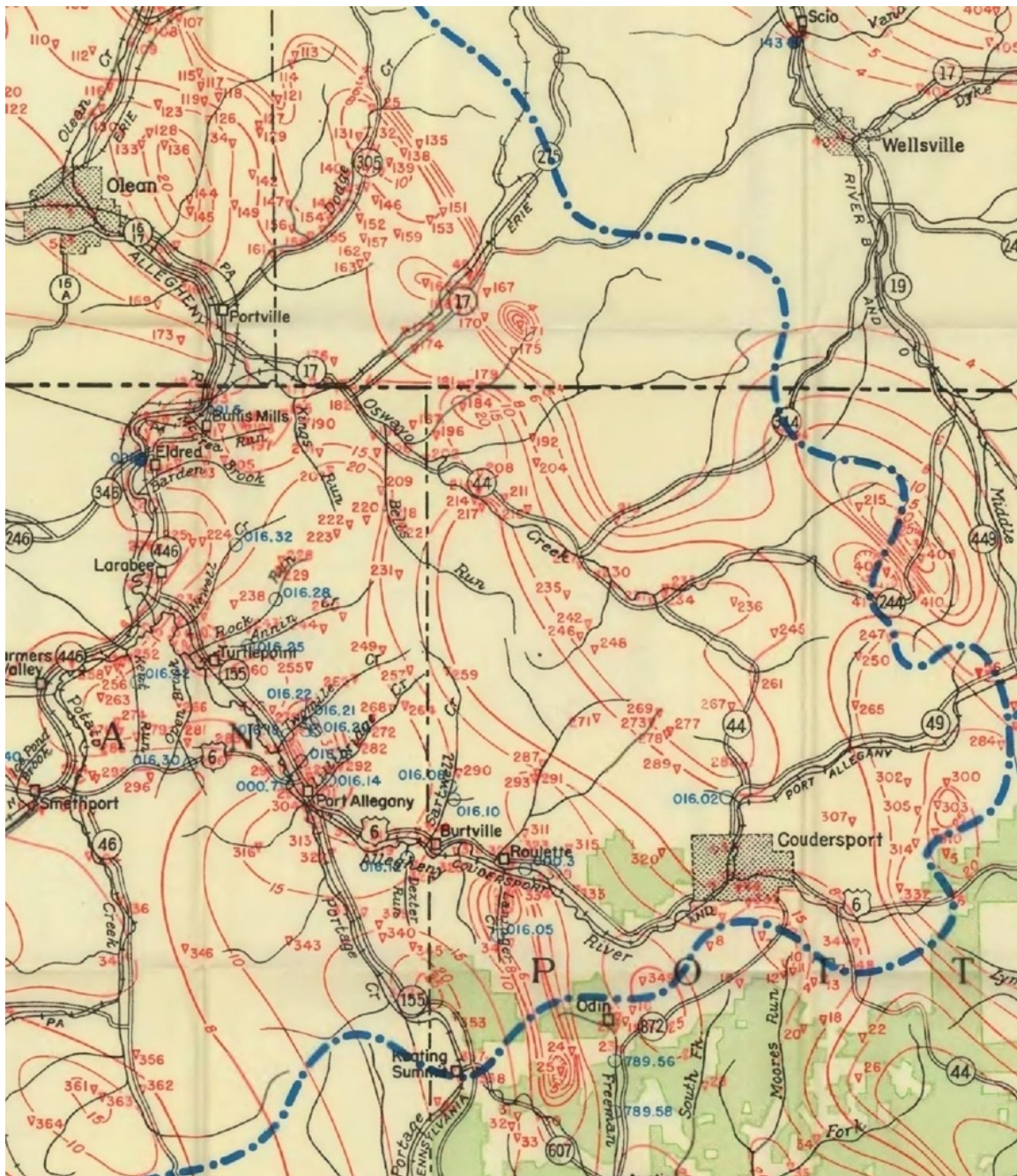


Figure 6. Isohyetal map from the USGS Report for the main part of the Smethport storm

Terrain Affects on Rainfall Patterns

Another important affect of the topography around the Smethport location that is not found in Ohio is the funneling affect it has on the low level winds and how that helped to focus the moisture in certain areas. Schwarz (1970) “suggests both terrain-

induced triggering and damming of moisture-laden low-level flow as possible mechanisms” (from Smith and Karr 1990) for increased rainfall production. This led to enhanced moisture convergence at the lowest levels and more efficient storm dynamics and rainfall production.

As part of the Ohio Review Board meeting held June 22-23, 2011 in Columbus, AWA, along with Review Board member Dr Barry Keim, performed field reconnaissance by driving west/northwest from Columbus to Russell Pointe and around Indian Lake. This route started at just over 700 feet in elevation along the Scioto River in downtown Columbus and took us over the highest point in the state of Ohio, Campbell Hill, at 1,549 feet approximately 50 miles to the west/northwest. Surprisingly, the terrain encountered was very benign, with very little noticeable gradient between the two locations and very little relief in the surrounding countryside. Most importantly, none of the terrain would be considered similar to what is found in and around the Smethport region. No terrain within Ohio would be considered as having an orographic influence on storm production and rainfall similar to Smethport and therefore no correlation to the terrain which triggered and anchored the Smethport storm is found in Ohio.

Finally, the authors of HMR 51 designated two “stippled” regions (HMR 51 Section 1.4.2) within the HMR 51 territory (Figure 7). These areas were considered to be affected by orographics and therefore not homogenous to the other regions covered by HMR 51. The stippled area covering the Appalachian Mountains encompasses the Smethport storm domain but does not encompass any part of Ohio. This adds further evidence that the topography in and around Smethport is different than what is found in Ohio. It should be noted that this conclusion was reached independently by the authors of HMR 51 separate from AWA’s findings.

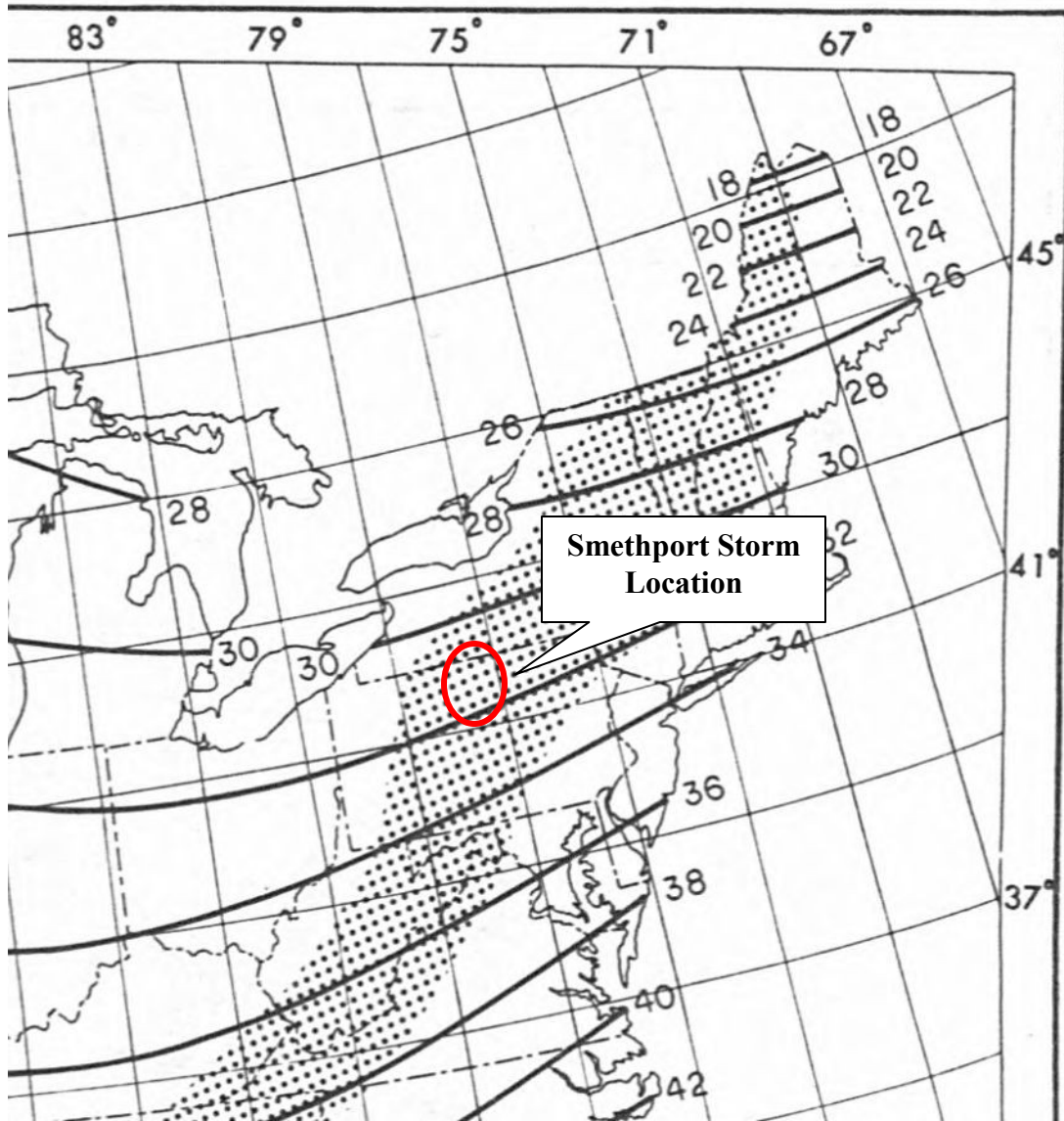


Figure 7 Stippled region of HMR 51 over the Appalachian Mountains with the Smethport storm location designated by the red oval.

Recommendation

It is the recommendation of AWA that the Smethport storm not be considered transpositionable to the state of Ohio based on the differences in topography between the storm location and any point within Ohio as discussed and detailed in this report. These explicit differences violate the principle of homogeneity required in the transposition process. Therefore, although the storm mechanism of an MCC is transpositionable, the amount of affect related directly to the difference in topography at Smethport versus Ohio can't be quantified or accounted for in the current process of PMP development thereby eliminating this storm from consideration of PMP development within Ohio.

References

Maddox, R.A., 1980: Mesoscale convective complexes. *Bull. Amer. Meteor. Soc.*, 61, 1374-1387.

_____, 1981: The structure and lifecycle of midlatitude mesoscale convective complexes. Ph.D. dissertation, Colorado State University, 171 pp.

Smith, J.A., and A.F. Karr, 1990: A statistical model of extreme storm rainfall, *Journal of Geophysical Research*, 95(D3), 2083-2092.